IntechOpen

Laboratory Unit Operations and Experimental Methods in Chemical Engineering

Edited by Omar M. Basha and Badie I. Morsi

LABORATORY UNIT OPERATIONS AND EXPERIMENTAL METHODS IN CHEMICAL ENGINEERING

Edited by **Omar M. Basha** and **Badie I. Morsi**

Laboratory Unit Operations and Experimental Methods in Chemical Engineering
http://dx.doi.org/10.5772/intechopen.72537
Edited by Omar M. Basha and Badie I. Morsi

Contributors

Enrique Hernández-Sánchez, Julio César Velázquez, Benjamin Oyegbile, Guven Akdogan, Meschac-Bill Kime, Bienvenu Mbuya, Brenda Prager, Syamsul Rizal Abd Shukor, Nor Irwin Basir, Zainal Ahmad, Emese Pálovics, Elemér Fogassy, Beáta Szolnoki, Zsolt Szeleczky, Miklós Bosits, R Anantharaj, R Achsah, M Danish John Paul, Juan Ortega Saavedra, Raul Rios, Adriel Sosa, Luis Fernandez

Notice

First published in London, United Kingdom, 2018 by IntechOpen
eBook (PDF) Published by IntechOpen, 2019
IntechOpen is the global imprint of INTECHOPEN LIMITED, registered in England and Wales, registration number: 11086078, The Shard, 25th floor, 32 London Bridge Street
London, SE19SG – United Kingdom
Printed in Croatia

British Library Cataloguing-in-Publication Data
A catalogue record for this book is available from the British Library

Additional hard and PDF copies can be obtained from orders@intechopen.com

Laboratory Unit Operations and Experimental Methods in Chemical Engineering
Edited by Omar M. Basha and Badie I. Morsi

p. cm.

Print ISBN 978-1-78984-055-1

Online ISBN 978-1-78984-056-8

eBook (PDF) ISBN 978-1-83881-700-8

Meet the editors

Dr. Omar M. Basha is an Assistant Professor at the Department of Chemical, Biological and Bioengineering at North Carolina A&T State University. He was previously a fellow at the National Energy Technology Laboratory in Pittsburgh. He obtained his Ph.D. in Chemical Engineering from the University of Pittsburgh, and his BS and MS degrees in Chemical Engineering from Texas A&M University at Qatar. His research work focuses on multiphase reactor design and scaleup, computational fluid dynamic modeling and carbon capture and sequestration.

Professor Badie I. Morsi joined the Chemical and Petroleum Engineering Department, University of Pittsburgh, in 1982 and currently is Director of the Petroleum Engineering Program. Professor Morsi's research activities involve different aspects of chemical, environmental, and petroleum engineering. His recent research work focuses on the design and scaleup of multiphase reactors, and modeling and optimization of industrial processes with a focus on Fischer–Tropsch Synthesis.

Contents

Preface

Chemical engineering is a dynamic and ever-growing profession, which is reflected by the variety of scales and topics covered by this book, ranging from education to material science. The purpose of this book is to create a platform for the exchange of different experimental techniques, approaches and lessons, in addition to new ideas and strategies in teaching laboratory unit operations to undergraduate chemical engineering students. It is recommended for instructors and students of chemical engineering and natural sciences who are interested in learning about different experimental setups and techniques, covering a wide range of scales, which can be applied to many areas of chemical engineering. Fundamental knowledge of thermodynamics and energy and material balance principles is assumed.

The first section in this book explores new studies in the pedagogy of laboratory unit operations to chemical engineering undergraduate students. The second section presents applications of various experimental methods and techniques to different areas of interest in chemical engineering, such as kinetic growth of metallic layers, preparation and separation of enantiomeric mixtures, and hydrodynamic characterization of stirred tanks, among others.

It is hoped that this book will also appeal to academic and practicing professionals of many disciplines.

Finally, we would like to thank the authors for their noteworthy contributions and Ms. Maja Bozicevic and the rest of the IntechOpen team for their invaluable efforts in the preparation of this book.

Dr. Omar M. Basha
Department of Chemical, Biological and Bio Engineering
North Carolina A&T State University, USA

Professor Badie I. Morsi
Department of Chemical and Petroleum Engineering
University of Pittsburgh, USA

Section 1

Pedagogies of Laboratory Unit Operations

Chapter 1

Utilizing a Differentiation Framework, Piagetian Theories and Bloom's Taxonomy to Foster Experiential Learning Activities in Chemical Engineering

Brenda Hutton-Prager

Additional information is available at the end of the chapter

http://dx.doi.org/10.5772/intechopen.75646

Abstract

This chapter will explore the development of laboratory experiments and analysis for undergraduate chemical engineering students, by utilizing a differentiation framework specifically adapted for university-level education. The differentiation framework explores the relationship between Piagetian and post-Piagetian *thinking skills* with differentiated *learning skills*, demonstrating links with Bloom's taxonomy and experiential learning theories. Experimental activities developed within such a framework will allow *all* students to participate fully in the learning experience intended, as they will be given opportunities to reflect on the learning, and put this new learning into action, *within* their current thinking operational level. This chapter provides an in-depth look into the educational framework proposed, and then shows examples of how it is used in the development of experimental activities. Educators following this advice will greatly enhance the educational outcomes of the experimental activities conducted.

Keywords: personalized learning, differentiation framework, Bloom's taxonomy, Piagetian and post-formal thinking, experiential learning

1. Introduction

There is no lack of pedagogical theories aimed at the K-12 education sector, many of which can be utilized together in order to provide an excellent education for children. Some of these theories are being employed in lower classmen with higher education to improve the educational outcomes of young adult learners [1–5]. Malcolm Knowles [6] popularized the term

"andragogy," which refers to adult learning theories. These ideas became widespread in the 1960s, and typically referred to informal education for later year adults, who could draw on their life experiences as part of their learning. Formal education such as that experienced at university, community college or trade school, did not adopt such principles. These young adult learners can benefit from teaching and learning methods used in the high schools, but with extensions or adaptations to meet their undergraduate needs. Many have typically not gained sufficient "life experience" to benefit from andragogical teaching methodology as defined, and hence fall into an "in-between" educational group, where teaching methods need to be developed more formally.

This chapter outlines some key adaptations of pedagogical methods suitable in post-secondary education, followed by applications of these methods in chemical engineering undergraduate laboratory classes. It is anticipated that these methods would be useful for all Science, Technology, Engineering, and Mathematics (STEM) undergraduate and graduate education.

2. Development of an educational framework for STEM education

2.1. Piagetian and post-Piagetian (pP) learning theories

Piaget's theory, or Piagetian theory, has had a huge impact on the educational beliefs of educators around the world, and has largely dictated the "expected" intellectual development of children as they progress from birth to adulthood [7]. While this theory is still well accepted in many educational domains, the connections with biological progression of childhood development have come under scrutiny. It is well documented that students acquire new knowledge in a series of progressive stages (matching Piagetian stages), except that this development occurs at vastly different rates between students, with factors such as level of maturity, experience, culture, and individual ability strongly influencing these rates [8]. Due to these different rates of progression, it has been well observed that as many as 50% of freshmen students in higher education have yet to complete the final stage of Piagetian acquirement of knowledge [7].

Briefly, the four stages outlined by Piaget are (a) the sensorimotor stage for infants (0–2 years); (b) the pre-operational stage (2–7 years); (c) the concrete operational stage (7–11 years); and (d) the formal operational stage (12–15 years) [7–9]. The sensorimotor stage sees infants acquiring knowledge using their sensory skills such as touch, sight, or feelings, and is present with the infant right up until the time speech begins. The pre-operational stage occurs when young children use the additional skill of language to bring further meaning to their knowledge development. While language is used to describe various situations, there is often an over-exaggeration and little logic to the verbal explanations, and others opinions have little impact on the learner, although they may be copied. At the concrete operational stage, children are able to expand their thought processes and overall intellect by incorporating logic, comparing objects, and understanding concrete ideas [8]. In the final stage of Piaget's theory, the learner can deal with more abstract ideas, construct their own thought patterns, and evaluate information provided;

http://dx.doi.org/10.5772/intechopen.75646

however, while they can evaluate and make sense of information, typically only one single answer will be considered "correct" [8, 10].

More recently, Piagetian theory has been extended to include further thought patterns, commonly known as post-Piagetian (pP) or post-formal ideas. In a study by Wu and Chiou [10], post-formal thinking was linked to creativity, and also the need for creativity in science (and likely STEM) fields to pursue and generate original thought. Although formal operational thinking is required for performing systematic tasks—a necessity in STEM fields—it does not allow for creativity, as formal thinkers believe there is only one correct answer [10]. Therefore, successful STEM researchers need to display both formal and creative thinking. Post-formal or pP levels of development are said to include two further stages: (e) relativistic thinking; and (f) dialectical thinking. In relativistic thinking, the learner begins to observe contradictions with potential solutions, and ultimately accepts that more than one solution is plausible given different ways of viewing a particular situation. This acceptance of other perspectives enables more novel solutions to ultimately be found. In dialectical thinking, the learner is open to new knowledge, and in fact *expects* to change their current thought pattern as new knowledge is found or presented. This is known as an "evolution of knowledge" thought pattern, and essentially can only evolve *from* contradictions of thought. Dialectical thinking enables the learner to synthesize new thought, and is essential for the creative process. Researchers operating at this level are typically more creative [10]. A final stage in thinking skill suggested here is (g) creative or independent thinking, where post-formal thinking has become an independent process, and the learner no longer relies upon guidance to come up with individual thought. This helps distinguish the educator demonstrating and encouraging development of thinking patterns (e) and (f) to research students versus those who have since mastered the "art" of thinking. The ultimate goal of a successful PhD student is one who is equipped with sufficient thinking intellect to be independent, and hence thinking stage (g) is included in the current discussion. These last three stages can equally be applied to professionals in their respective fields who have gained expert-level competence and independence of thought.

Given seven progressive stages of thinking skill development and acquirement, influenced by many outside factors influencing the rate of development, a typical class will consist of students operating at varying thinking levels. As such, it is important to run all classes, even in higher education settings, in a differentiated fashion to meet the needs of all students.

2.2. Differentiated or personalized learning theories

Carol Tomlinson has made the differentiated teaching and learning pedagogy famous, particularly in the K-12 educational sector [11–13], also more recently known as personalized learning. The ultimate goals of differentiated teaching is to promote growth in learning of *all* students from their starting point, ultimately promoting independence of learning within their particular stage of intellectual thinking development. With the explosion of the computer age, many automated tools are being developed to provide drill practice for students at their level of competency, gradually increasing or decreasing the level of difficulty as required. This is one of many tools at an educator's disposal to utilize in the classroom. Others include providing

differentiated homework sheets; group work to conduct more open-ended problems; inquiry-based learning tasks; experiential learning tasks; active learning; and many more. Each of these tasks, if carefully constructed, provides opportunities for learners to actively engage with the material, promoting depth of learning within their zone of proximal development (ZPD) [14], all the while challenging them to the next level of thinking.

This method of teaching (and learning) is quite popular at the K-12 level, despite some inevitable critics [15]. However, it is yet to gain popularity and commonality in higher and graduate level education. Much of this is to do with the fact that the original Piagetian theory concluded formal operational thinking by age 15, and hence there was no need for differentiated learning in higher education settings, since *all* students would be performing at the same intellectual level of thinking. More recent post-formal thinking levels, and an acceptance of different rates of thinking development in all learners, strongly dictate the necessity to continue differentiated learning into the higher education sector.

2.2.1. Differentiated learning in K-12 education

Differentiated learning is described by a number of key characteristics by several researchers in the field [16–23], and these have been further summarized into five key differentiation principles, DP1–DP5 below [24]:

1. Understand student need and preferred learning modes.
2. Focus on key concepts and provide multiple approaches to learning.
3. Provide challenging learning experiences within each student's ZPD.
4. Foster collaboration between students and their faculty.
5. Create independent learners and ownership of learning.

For concrete operational thinkers, the educator would likely recap prior core knowledge before beginning a new topic, and identify the types of activities that students prefer to assist their learning (DP1). When teaching the key concepts of the topic, the educator would incorporate variety in the activities, but would provide strong guidance and instructional teaching regardless of activity being undertaken (DP2). Problem-solving and critical thinking would be explicitly demonstrated to the students to enable them to follow similar patterns when solving problems on their own (DP3). Group activities would feature strongly in the learning, however in the early stages, students would learn "how to work in groups" more so than relying specifically on group tasks to promote further learning (DP4). Finally, the educator would provide tasks that competent learners within this thinking category could successfully complete unaided, but the vast majority of tasks would be those following pre-specified steps.

By contrast, for formal operational thinkers, the educator would create opportunities for learners to be more responsible for their own learning. For example, while he/she would still identify the existing knowledge of the learners, review of the core knowledge would be up to the student (DP1) and, although the key concepts would still be taught in multiple ways,

http://dx.doi.org/10.5772/intechopen.75646

there would be less dependence on the instructional approach, providing more freedom for students to explore abstract problems (DP2). Challenging tasks would rely on students' prior mastery of problem-solving skills, concentrating more on developing adaptations of these skills to non-routine problems (DP3). Collaborative tasks with other students would see the students now begin to rely on each other to add to existing knowledge, having now mastered the key functioning of a team (DP4). Independence would be demonstrated when learners rely on their own problem-solving skills, and those of their peers, to independently work problems and make sense of more abstract ones as well (DP5).

A detailed study by Valiandes [22] was conducted in 13 Cypriot primary schools, covering 479 fourth-grade students (average age 9 years) and 24 teachers. The students were functional at the pre-operational and concrete operational thinking stages of Piaget. An important aspect of this study was the in-depth support given to the teachers to adequately train them in differentiated teaching strategies. Students were tested on literacy skills, and post-test results were significantly better for students participating in differentiated learning than the control group, which had largely instructional-based learning. Typical observations of differentiated instruction included noting the time spent by the teacher (a) commenting on student general behavior; (b) providing additional examples; (c) direct teaching/asking questions; and (d) providing student guidelines for work. Other observations included identifying the degree of activity variation; providing personalized support to students; providing learning opportunities to students of all readiness levels; time for students to reflect on basic knowledge and skills, or prerequisite knowledge; prioritizing order of activities; accomplishing lesson objectives; and providing differentiated homework. Many of these observations fit well into the DP in the concrete operational level. As a result of this in-depth study, differentiated practices were described as [22]:

> *"instruction planning based on constructivism learning theory, the hierarchical order of learning activities (DP1), the maximization of students' active participation in the learning process, the reduction of teachers' talking time during teaching (DP2), the variation of activities, the opportunity for students to work at their own pace, the personalized support that students receive (DP3), the differentiation of activities according to students' interests and learning profile (DP4), and the continuous evaluation of students' achievement with a simultaneous and ongoing evaluation of the effectiveness of the learning process (DP5)."*

The above quote has been interlaced with the identification of the five DPs as explained earlier, to demonstrate that these principles broadly cover many descriptions of differentiated practices. This example shows both the effectiveness of differentiated instruction at (mostly) the concrete operational level, as well as the importance of fully equipping teachers with the appropriate skills in delivering such instruction.

2.2.2. Differentiated learning in higher education

Educators of lower classmen in the higher education sector may encounter significant numbers of students operating in the concrete or formal operational levels, and hence differentiating the instruction would follow a similar pattern to those outlined above in Section 2.2.1. This is adequately demonstrated by a few reported studies of freshmen level mathematics

classes [25, 26]. In the study by Chamberlin and Powers [25], freshmen mathematics students taking "number and operations" were studied. Data were initially gathered on the students to judge their interests and preferred learning modes (DP1). Graduated activities were then implemented, each aimed at differing levels of intellectual readiness based on an analysis of the students' pre-requisite core knowledge. These activities included class extension activities, student work groups, student choice in activities, direct instructional modification as required, differentiated homework sheets, and formative/summative testing (DP2–DP4). Analysis of the pre- and post-testing indicated that students receiving differentiated instruction improved by 1.7 points out of 8, while the control group improved by only 0.3 points. It was concluded that the differentiated learning was successful, and mastery of required skills and independence in performance was observed (DP5) at the thinking operational levels of the students. The range of activities particularly identifies students working in the concrete and formal operation stages.

What might a differentiated classroom look like for upper classmen, or learners intellectually ready to undertake relativistic and/or dialectical thinking? In these two stages, the learner would gradually take on a more active role in their learning skill development through the five DPs. While these principles remain similar, the learner would become more active in participating and directing the learning, with the educator playing a guidance role. In relativistic thinking stages, the educator may still outline the required pre-requisite knowledge but would expect the student to revise accordingly. The educator would still deliver key concepts in multiple ways, but the learner would also be expected to experiment with different modes of learning, in order to maximize knowledge retention. In DP3–DP4, the activities presented to the students would begin at lower level (concrete thinking) to confirm knowledge of new concepts, but would progress to include abstract and ill-defined problems that present different solution paths.

In the dialectical thinking stage, the learner would take an even more active role in understanding his/her needs at the beginning of a new topic, and deciphering the key concepts of that topic. This level of learning/instruction within a formal institution would be seen in graduate level classes, advanced students in lower level classes, or research studies. As such, the activities in DP3 and DP4 would be learner-initiated (possibly at the initial direction of the educator), where learners would delve in depth into the chosen topic and make sense of the apparent contradictions presented. Students may eventually come to the realization of new knowledge as a result of these apparent anomalies.

In the final creative thinking stage, the learner has essentially mastered all previous stages of intellectual thinking development and can pursue a new field of interest at depth, and with the ability to creatively synthesize new knowledge. This would typically be seen with an advanced PhD student and/or experienced researchers, as well as expert industry professionals.

The extension of differentiated teaching and learning to the later stages of post-formal thinking is graphically displayed in Appendix A. The horizontal axis describes a progression in *differentiated learning skills* (DP1–DP5), while the vertical axis describes a progression in *thinking skills* (Piagetian and pP thinking stages). This arrangement shows the differentiation

framework as it commonly stands in K-12 education (concrete and formal operations only), and then extended for later-year learners (post-formal thinking). Note that sensorimotor and pre-operational levels have been left blank, given that the focus is on higher educational training. Next to DP5 for each thinking level is a description of characteristics a learner will display once they have achieved independence with learning *at that thinking level*. This figure is to be interpreted as a continuum for both thinking and learning skills, and the characteristics described will alert the educator that the learner is ready to progress to the next level of intellectual thinking. The ages and approximate school year levels next to Piagetian and pP thinking stages are intended as a guide only, and are *very fluid*, with a particular reminder of the many outside influences that affect the rate of progression through these stages. This is true also for progressing through the various learning stages within each thinking level. Finally, the vertical axis to the right of the figure *loosely* assigns the different levels of Bloom's taxonomy, which also covers different thinking stages from lower to higher order thinking.

To the best of the author's knowledge, Appendix A is believed to be the first attempt by linking intellectual thinking skills at the higher and graduate education levels with a differentiation framework. Extensions to this level have not typically been considered to this depth. Several school systems provide differentiated curricula in all mainstream classes to grade 10, and then assume a more "one-size-fits-all" approach beyond this level (e.g., [27]). This is despite the general acceptance that Piagetian rates of progression are fluid, and competence in formal operational thinking by age 16 is no longer expected in *all* students. Hence, Appendix A is an attempt to provide additional differentiation assistance from grade 10.

2.3. Bloom's taxonomy

Bloom's taxonomy was originally published in 1956, and later developed and modified in 2002 by Krathwohl [28]. This most common form of Bloom's taxonomy is the cognitive domain, represented by lower order thinking (LOT) and higher order thinking (HOT) activities. However, two other domains have also been developed, which include the affective domain (interests, attitudes, and values) and the psychomotor domain (motor skills).

The cognitive domain can be used in a number of ways by the educator, and indeed learners, to fully master a topic of interest. In Appendix A, it can be seen that the six main cognitive stages of Bloom's taxonomy (LOT: remember, understand, and apply; and HOT: analyze, evaluate, and create) are loosely matched with the Piagetian and pP developmental thinking skills. In this way, the broad matching of categories indicates that it takes many years to move through the LOT and HOT cognitive domains suggested by Bloom, showing that progressive intellectual development is required to access higher levels of Bloom's taxonomy. This taxonomy is progressive in a similar manner as Piagetian thinking skills, and demonstrates that one must be comfortable with LOT before accessing HOT.

On a much smaller scale, an educator may commonly use this taxonomy for a particular topic or even a single class being presented to learners. Tasks will be organized such that early activities require students to remember and understand new terminology and concepts, and later ones will provide opportunity in applying these concepts to progressively more difficult

tasks. The depth of LOT and HOT will vary depending on the intellectual thinking level of the learner (Piagetian and pP), and hence the ability to "create" new knowledge for any given topic will be limited by the depth of thinking capability of the learner.

Fully independent learners operating in the creative domain of post-formal thinking will have developed their own methods of learning a new topic to expert level, based on a culmination of all previous learning they have experienced to that point. Even at this fully independent thinking stage, a learner to a new topic of interest will still need to progress through LOT and HOT in order to become sufficiently competent in a new field. These learners will have the skills to generate *actual* new knowledge, as opposed to learners operating at lower thinking skill levels, who will create new knowledge *for them* in their overall development. This is a key difference between a researcher or industry expert generating new knowledge and a learner becoming competent in their field.

The five broad DP also to some degree have links with Bloom's LOT and HOT. For example, in DP1 and DP2, the teaching and learning focus is on understanding existing knowledge and learning concepts of a new topic. In DP3 and DP4, the focus shifts to applying this newly gained knowledge to progressively more difficult tasks, which require some degree of the analysis and evaluation of the assigned problem. Finally, in DP5, independence of the learner within their current thinking skill category is reached when they are able to become fully competent with the range of tasks required, creating new knowledge *for them*.

To recap, Bloom's taxonomy can be used as a tool to (a) demonstrate life-long learning; (b) frame the teaching of a given topic; and (c) frame the learning of a given topic for more independent learners.

3. Developing experimental activities within the educational framework for chemical engineering

Within the framework, previously discussed are many opportunities for the educator to develop and deliver a variety of learning activities. While there are many activities available in an educator's "toolkit" for various situations, only experiential learning will be explored here, which governs the nature of experimental tasks and other experience-based non-experimental learning activities for the class. This learning theory, together with the educational framework discussed, will be demonstrated in the development of experiential activities for chemical engineering undergraduates.

3.1. Experiential learning theory

Kolb's experiential learning was progressed to its current form from significant earlier works of Dewey, Lewin, and Piaget [29]. Its prime motivation is the acquirement of knowledge through experience. The four modes of learning are (a) concrete experience; (b) reflective observation; (c) abstract conceptualization or thinking; and (d) active experimentation, or acting on one's new knowledge [29]. These are often summarized into: experience; reflect; think;

http://dx.doi.org/10.5772/intechopen.75646

and act. This curiosity-driven learning increases engagement and interest of students, helping them to achieve learning independence. Similarities can be observed with the Piagetian and pP thinking stages, where the earlier ones are concerned with experience (touch, visual, smell, etc.); the intermediate stages develop reflection and thinking about observations; and the final stages promote action of a learner to discover new information for her/himself.

As an activity in an educator's toolkit, this theory can be shown as a small in-class thinking task to explain an observation; as a longer-term real-life assignment or design project; or as a formal experimental class. Such activities could form the instruction over DP2–DP4, depending on depth and time constraints. To avoid confusion, an *experimental class* is a subset of *experiential learning*, and not all experiential activities need to include experiments.

3.2. Developing an experimental activity in chemical engineering

Following the differentiation framework and interactions with Piagetian and pP theories, as well as Bloom's taxonomy, the educator must start at DP1 by "knowing the student needs." Knowing these needs will determine which Piagetian thinking skills primarily make up the laboratory class. For lower classmen, the students would typically be operating over a range of concrete, formal, and relativistic, while for upper classmen, the latter two would be more common, perhaps with some operating at dialectical thinking stage. However, each class is unique, and this must be determined by the educators running the theory classes, and discussed with the educators running the practical classes (as is most usually the case).

Having decided on two or three thinking skill levels that best represent the class, the educator will then develop the practical class on a particular unit operation with key learning objectives in mind, mostly within the DP2–DP4 range. Within this range, the level of difficulty of the tasks increases, from providing conceptual knowledge of the experiment through to applying this knowledge, and then analyzing and evaluating the resulting data. This is akin to the middle part of a Bloom's taxonomy cycle. DP5, where students practice independence, may be incorporated by a final task that requires the students to come up with a part or all of an extended investigation from their experimental task. This will build on their knowledge gained within the previous DPs, and will equip them with independent skills *within* their thinking skill range. When developing the experimental class, the educator should also keep in mind the experiential learning cycle just described, allowing adequate opportunity for reflection and cognitive thinking after an observation, followed by tasks that allow the students to actively use their newly gained knowledge.

A common method to incorporate different levels of thinking operational ability is to include choice between the required tasks. Those operating at higher thinking levels will typically choose the tasks that satisfy their need and hunger for learning, while those at lower levels will choose tasks more suitable for them. Rarely do students choose "the easy way out," as discovered by Hutton-Prager and O'Haver [30], and the vast majority of students genuinely engage with material by challenging themselves.

A planning template is shown in **Table 1**, demonstrating how the educational framework and pedagogies can be used to develop a meaningful laboratory class. The final format to the

DP	Theories	Description
1	Differentiation framework	The educator must first determine the key learning objectives for the laboratory class, including the "bare minimum" acceptable levels of knowledge to be gained.
		She/he then considers the prior knowledge of the students coming into the laboratory class.
		What thinking level (Piagetian, pP) are the students operating at? The educator confers with other professors who know the students well.
2	Differentiation framework; LOT from Bloom's taxonomy	A short and concise theoretical base of the unit operation intended for the experimental study is provided, including references to more detailed discussions. This will assist students learning this for the first time and those who need a brief review.
3–4	Differentiation framework; LOT from Bloom's taxonomy	As most laboratory classes are done in groups, DP3 and DP4 will be considered together.
		Regardless of thinking operational level within the class, it is good to begin with some concrete tasks to confirm one's knowledge, and become competent in operating the equipment. A precise procedure* on how to routinely operate the equipment is provided.
	Progressively challenging tasks covering Piagetian and pP thinking levels; "experience" and "reflect" from experiential learning	A variety of tasks are designed for the students to collect data/observations for subsequent analysis, and the precise instructions are gradually reduced as the students gain competence running the unit operation. These data collection tasks need to align with the key learning objectives, and will allow students to fully explore the capabilities or function of the unit operation.
	HOT from Bloom's taxonomy; "reflect" and "think" from experiential learning	Utilizing the collected data, written response tasks are provided that require students to analyze and evaluate the information, drawing on their knowledge and the theory behind the unit operation. Many of these tasks are open-ended to ensure reflection/in-depth thinking by the students.
5	HOT from Bloom's taxonomy; "act" from experiential learning	Within the ability levels of the learners, an extension to the investigation is provided, where the students are required to come up with their own procedure to investigate a new phenomenon on the unit operation. An applied response task to this investigation is also included.

*Precise procedure required for safety reasons; use DP5 to allow students freedom in coming up with a new experimental task instead.

Table 1. Planning template to assist in coming up with a well-rounded experimental task, meeting all the required learning objectives.

students would be a handout (or part of an experimental booklet) detailing the unit operation name, theory, tasks, and questions. Report write-up differs between colleges, and specific information on how this is to be done needs to be conveyed to the students. It is common to follow the format of a typical research publication.

3.2.1. Dissecting unit operation experimental activities into educational outcomes

There are some dedicated educational researchers looking into developing meaningful experimental activities that promote long-term retention and learning by the students (for example,

see [31–34]). Frequently, experiments are labeled as "cookbook" experiments, where students follow a detailed set of instructions and describe what they observe [33]. While this does have obvious advantages from a safety and time viewpoint, on its own, it does not provide sufficient opportunity for students to practice HOT questions and reflective activities as per experiential learning principles. However, as a differentiated activity, some students may *require* a more "cookbook" style experiment to assist progression of their learning, but this would still be incorporated with other opportunities to extend thinking. It is important to take into account the students' thinking levels when developing experimental tasks.

Some more "innovative" experiments presented at the American Society of Engineering Education (ASEE) annual conference in 2016, have been reviewed as per the template described in **Table 1**, and their results appear in **Table 2**. The reader is encouraged to read the full publications, as only a brief summary is presented here. This summary is based only on the conference presentation materials, and not the actual laboratory information presented to the students.

DP	Theories	Experiment 1: Mechanical properties of foods [34]	Experiment 2: Unsteady state conduction [34]	Experiment 3: Air conditioner experiment—thermodynamics cycle [32]
1	Differentiation framework	Detailed objectives provided	Detailed objectives provided	Does not appear to have been provided.
2	Differentiation framework; LOT from Bloom's taxonomy	Fundamental physical properties of food in unit operations covered in classes preceding experimental activity.	Fourier's Law of conduction previously developed in classes.	Pre-lab worksheet completed with instructor guided demonstration of equipment, discussing equipment, concepts and how to collect data.
3–4	Differentiation framework; LOT from Bloom's taxonomy.	Operating procedure provided	Operating procedure provided	No procedures provided, in lieu of the previous week's demonstration of the equipment.
	Progressively challenging tasks; "experience" and "reflect" from experiential learning	Experiment was designed in three parts, progressively becoming more difficult.	Difficult to assess—does not appear to progress tasks.	Spreadsheet assignment done individually, asking for specific calculations and tables to be created in Excel.
	HOT from Bloom's taxonomy; "reflect" and "think" from experiential learning	Good assessment questions which are open-ended and require students to think and reflect.	Assessment tasks require calculations but they do not appear to provide depth beyond calculation procedures.	Target audience given to each group. Team devised experimental plan based on their audience, and collected relevant data.
5	HOT from Bloom's taxonomy; "act" from experiential learning	None provided, but difficult to determine from information provided.	None provided.	A3 lab report poster required for submission; website creation to explain new concepts learned.

Table 2. Summary of three experimental tasks, dissected into the proposed framework.

This small sample of experiments demonstrates many of the tasks required as per the planning template (**Table 1**). Two of the three experimental tasks provided detailed objectives. It could not be determined from the information provided whether or not student ability or operational thinking levels were taken into account. Based on the description of tasks performed, Experiment 1 would suit formal operational thinkers; Experiment 2 would be better suited for concrete—formal operational thinkers; and Experiment 3 would be an excellent task for formal—relativistic thinkers. The first two experiments lack the creativity and HOT tasks (even at the suitable thinking levels), while the third experiment lacks some initial tasks at the LOT level to assist students in building their knowledge. The pre-laboratory worksheet and Excel task may be sufficient, but this will depend on the operational thinking levels of the students performing this task. The creative tasks discussed in Experiment 3 were pleasing to see, and fully met the requirements of HOT and experiential learning in a fun and engaging way for the students.

These same experiments could be written for students performing at different thinking skill development levels, and activities within each of the learning skill (DP) categories would hence vary to accommodate the different thinking levels. If Experiment 2 was used at the concrete operational development level, DP3–DP4 would need to be populated with additional experimental tasks and at least one open-ended question. There would also need to be a task included in which students could "act" on their new knowledge and participate in HOT at their operational thinking level. If this same experiment was developed for formal and/or relativistic thinkers, then there would be more challenging activities included within DP3–DP4 exploring different aspects of Fourier's law; many more open-ended questions; and full exploratory tasks with no direction provided by the instructor. However, this would need to be preceded by some concrete activities to prepare the students in competency of equipment operation, both from a safety viewpoint as well as providing groundwork in which they can build knowledge. This was well-demonstrated in Experiment 3.

By stark contrast, the more common "cookbook" experiments [33] would typically provide objectives (DP1); sometimes a background theory (DP2); a step-by-step procedure to be followed *exactly*; a set of basic analysis and closed questions relating to the observations (partial requirement of DP3–DP4); and no extended task from the learning gained (no DP5). This setup lacks student engagement and does not extend the theoretical learning provided in class into practical settings [33].

3.2.2. Example of a freshman design project developed within the educational framework

Hutton-Prager has previously described a Freshman design project implemented in ChE101: Introduction to Chemical Engineering at the University of Mississippi (UM) [30, 35], as part of the development of differentiated teaching and learning. Each semester, this four-week program requires students to investigate the full-scale processing of a candy bar. It begins with student groups making the candy bar in a food laboratory, and observing the intricacies required to successfully prepare the bar. Data and observations are collected and subsequently analyzed, along with a detailed investigation of the scale-up process. **Table 3** demonstrates how this project meets the requirements of the experimental planning template (**Table 1**), covering all aspects of DP1–DP5, Bloom's taxonomy and experiential learning.

DP	Theories	Description
1	Differentiation framework	The educator, having spent most of the semester with the students, has determined that most students are operating in the concrete and formal operations stages. The key objectives of the freshman design project are: • Provide a real-life example from the food industry where chemical engineers may be employed. • Understand the process conditions required for control in a full-scale process. • Perform calculations of flow rate, pressure, and temperature. • Identify unit operations within the candy-bar process. • Gain an appreciation of what is required for scale-up of a "recipe" to bulk production of candy bars. • Learn how to draw flow charts of the process. • Consider economic aspects of the candy-bar process.
2	Differentiation framework; LOT from Bloom's taxonomy	The project statement provided to the students details a real-life scenario of a student on an internship, involved in doing some plant trials to scale-up a new candy bar for potential sale. All the learning leading up to this design project is on developing skill in conducting pressure, temperature, and flow rate calculations.
3–4	Differentiation framework; LOT from Bloom's taxonomy	A recipe is provided to the students that carefully details the exact steps to be taken to make a small-scale version of the candy bar (likened to a plant trial in the scenario). Discussions before the practical session require students to think about how they will log their temperature vs. time data in the various sections of the candy-bar preparation, and come up with their own observation sheets.
	Progressively challenging tasks covering Piagetian and pP thinking levels; "experience" and "reflect" from experiential learning	Students are encouraged to come up with their own methods for the chocolate coating of the candy bar. They are advised before the experimental trial to research into the most suitable methods for chocolate coating. During the laboratory class, students identify different unit operations and think about how these stages would need to be modified if being prepared on a much larger scale. As an example, they quickly realize that manually stirring the mixture over a hot plate will require substantial modifications on a large scale.
	HOT from Bloom's taxonomy; "reflect" and "think" from experiential learning	In the subsequent weeks after the experimental session, students work their way through a guided template report, in which they are required to graph their temperature vs. time data; perform statistical calculations on the data; explain their observations; and explain the chemistry behind the candy-bar process. The choice of candy bar *always* involves a caramelization step or a bicarbonate soda reaction step, which requires thinking/reflection by the students to scientifically explain the observations from the experimental trial. This is framed by an executive summary; background on the candy-bar company; conclusions; and recommendations on whether to go to full-scale production. The *actual* answer is irrelevant; it is the analysis/evaluation of the trial in coming to a recommendation that is important.
5	HOT from Bloom's taxonomy; "act" from experiential learning	Students are asked to explore scale-up of their process. They identify the unit operations of the process; decide on an order for continuous candy bar preparation; draw a block-flow diagram representing the full-scale process; choose a unit operation to explore its detailed design; perform example calculations of flow rate, average molecular weight, etc.; and consider some economic impacts on the final sale of the candy bar. They submit their written report with a "supervisor" target audience, and produce a 5-min verbal presentation discussing their experimental trial, the results, and their recommendations.

Table 3. Description of the freshman design project implemented in ChE101: Introduction to Chemical Engineering, at University of Mississippi.

This design project covers all four stages of experiential learning (experience, reflect, think, and act); the five differentiation principles; and both LOT and HOT from Bloom's taxonomy. Bare minimums have been built into the written report, where students must demonstrate their skill in the required calculations and explanations of observations. In DP5 where students explore the scale-up process, they have a choice in which unit operation to investigate. Depending on operational thinking level, students may choose an "easier" unit operation that requires less explanation than others, and will not be penalized. There is no upper limit to the depth in which students explore this project. The final requirement of the verbal presentation provides opportunities for students to learn oral communication skills, and importantly promotes independence as they explain their project in a realistic scenario.

4. Non-experimental experiential activities

It is worth completing this discussion with a brief explanation of experiential activities that can be performed in a theory class. Remembering that experiential learning requires reflecting, thinking, and acting after an experience, a common activity employed by an educator is a thinking experiment. This requires the students to imagine a particular unit operation, and think about how it might work. Others might include practical demonstrations, real-life scenarios, or "story-telling" particularly in the form of analogies, which enables the learners to access the complexities of a topic using more familiar situations.

The author has previously introduced a very successful thinking experiment into ChE417: Separation Processes, at UM on fixed bed adsorbers. This is preceded by a theory lesson outlining the basic terminology of adsorption processes, typical adsorbents, and applications, followed by the various adsorption isotherms commonly discussed in the literature. This helps to build knowledge and creates an "experience" (although theoretical) of how adsorbers work and their typical applications. The thinking experiment begins in the following class, where the students are asked to think about how the concentration of solute in the fluid would vary as it travels over the length of a fixed bed adsorber. They draw their thoughts on a concentration vs. length graph. This is followed by a class discussion on mass transfer zones, and then students are asked to think about whether a narrow or wide mass transfer zone is better, with justification. They then need to discuss in groups what types of factors might affect the length and the rate of movement of this mass transfer zone, and are challenged to come up with at least 10 different factors. The thinking experiment continues where students are asked to draw on a concentration vs. time graph what the breakthrough situation may look like. With further discussion, they come to the realization that integrating such a curve will represent the amount of solute adsorbed for a given time. This exercise is highly engaging for the students, and enables them to fully "experience" the workings of a fixed bed adsorber, with considerable reflection and cognitive developmental opportunities. Acting on this new knowledge is subsequently gained with calculation questions for fixed bed adsorber design.

This straightforward example of presenting content in a highly engaging way demonstrates how a unit operations "experiment" can still be conducted effectively within a theory class. This type of teaching and learning is particularly suited to smaller colleges where equipment and funding may be minimal. Studies have shown that experiential learning activities such as the one described are only marginally less successful than an actual experimental program [36]. If the experimental programs are not carefully developed as outlined earlier in this chapter, then the net gain of experiential learning *via* experiment is reduced, and active learning activities within a theory class can be equally or more beneficial.

5. Conclusions

A differentiation framework for higher education has been introduced and discussed, which extends the framework commonly used in K-12 education systems. This framework has been built on existing ideas of post-Piagetian thinking levels, and has mapped each thinking level to five broad differentiation principles. The framework has also been linked to Bloom's taxonomy of lower and higher order thinking skills.

Using this differentiation framework and experiential learning theories, a model for experimental classes in undergraduate chemical engineering unit operations has been developed. This model has been demonstrated using some pre-existing experimental activities described at ASEE 2016 [32, 34]. Its full capacity has been shown with a freshman chemical engineering design project currently operational at the University of Mississippi, providing examples of how all aspects of a differentiated activity can be developed, meeting the requirements of both thinking and learning skill development.

Acknowledgements

This work has been developed at the University of Mississippi, and is not funded externally.

Conflict of interest

The author has no conflict of interest.

A. Appendix

A differentiation framework of learning skills, matched to operational thinking ability level, described by Piagetian and post-Piagetian theories.

PIAGET AND POST-PIAGET THINKING SKILLS AND DEVELOPMENT				DP1	DP2	DP3
	graduate education, education for life	22 years and above	Independent / Creative Thinker	When learners first encounter a new topic, they will revise any prior learning as required to progress with the new learning. They will identify and learn any new terminology, and fully understand what the terminology means. As they progress through the depth of learning a new topic, they will frequently check their progress to ensure they are gaining and maintaining long-term knowledge.	Learners will identify key concepts required in the new topic, and set about understanding them using the mode of learning that suits them best. Given that they have an appreciation for several different modes of learning, they may choose a few different ones in order to assist with their knowledge development. They will likely have in mind, or discover, some key applications of the topic they are investigating.	Learners will expand their conceptual knowledge by going into depth on specific areas of interest within the broad topic. They will likely start with concrete problems to confirm their knowledge, and then progress through more abstract cases, developing opinions and conclusions based on the information they have sought. They will suggest detailed experimental / computational programs to test new theories and/or justify potential contradictions in the literature.
	undergrad to graduate education	19 years and above	Dialectical Thinker	Learners will identify core pre-requisite knowledge of a new field of work, possibly in conjunction with an advisor / educator. They will be guided by the educator regarding how/where to find suitable information on their topic of interest, and the advisor will check in regularly to gauge the learner's development with the new content.	The learner and advisor will jointly decide on the key concepts required of the new topic, and the learner will employ his/her most favored learning modes in order to start developing detailed knowledge of the content area. They will familiarize themselves with likely applications to maintain interest.	Learners will study in depth specific areas of their chosen field as they expand their ZPD. They will begin with a concrete understanding of the facts, and progress through formal and relativistic problems. Contradictory information presented will force them to create new knowledge as they make sense of these differences. They will be able to carry out research programs, with some advisor guidance, and use new information to confirm different beliefs prevalent in the literature.
	senior high school to upper classmen university	17 years and above	Relativistic Knowledge	The educator outlines prior core knowledge required for the course, and expects the students to revise this content if needed. Formative testing will be maintained throughout the course, and the educator will gain an understanding of preferred learning modes, but will also expect students to adapt to other modes of learning delivered. Students will be able to 'convert' any learning mode delivered into their preferred mode.	The educator identifies the key concepts of a topic, and determines 'bare minimum' acceptable competencies. The educator then chooses multiple ways of delivering the learning to promote engagement and interest. Students also experiment with these different methods of delivery and investigate their own in order to promote learning.	The educator provides challenging tasks for each student within their ZPD, while encouraging students to their next level of understanding. Activities include concrete, operational and relativistic tasks to progress skill development through different thinking levels. Relativistic tasks will involve abstract and ill-defined problems, requiring students to evaluate the material and make informed assumptions to successfully solve the problem.
	middle school to lower classmen university	12-22 years	Formal Operations	The educator determines the entry-level ability of the students; what learning modes maximise their understanding; and what prior core knowledge is required. Regular formative testing throughout the semester informs the educator of academic progress and potential issues that require adressing.	The educator identifies the key concepts of a topic, and determines 'bare minimum' acceptable competencies. The educator then chooses multiple ways of delivering the learning in ways that match preferred learning modes. Repetition of the learning with different approaches will also enhance engagement, interest and relevence.	The educator develops critical thinking and problem-solving skills through carefully planned activities, which require students to think beyond standard solution methods in order to successfully solve problems. The educator provides tasks that expand the student's current ZPD. Concrete tasks will be assigned to familiarize the student with content, followed by more abstract problems to develop critical thinking.
	primary to high school	7-12 years	Concrete Operations	The educator recaps prior core knowledge before starting a new topic, and conducts formative and summative testing throughout the semester. The educator will ask what types of activities the students prefer most, and include these in the curriculum.	The educator identifies key concepts of a topic, and determines 'bare minimum' acceptable competencies. Content is delivered several different ways to engage students and maintain interest; however, strong guidance will feature in all ways employed. Specific instructions will be included during 'lecturing', working problems, creating posters, etc. Experiential learning will be overlaced with specificity in task description.	The educator will introduce the methods of problem-solving and critical thinking to the students, with specific instructions on 'how to problem-solve'. To prepare the more advanced students for operational thinking, the educator can provide tasks that require deviations from the standard set of instructions.
	kinder to low primary	2-7 years	Pre-operational stage			
	pre-kinder	0 - 2 years	Sensorimotor stage			
				Understand student needs and preferred learning modes	Focus on key concepts and provide multiple approaches to learning	Provide challenging learning experiences within each student's ZPD
				DIFFERENTIATED LEARNING SKILLS FRAMEWORK FOR THE EDUCATOR		
				Awareness of strengths / weaknesses; preferred mode of learning; and converting between modes	Identify key concepts and utilize several learning approaches to increase knowledge base	Challenge oneself with learning activities from lower to higher thinking skills to expand ZPD
				DIFFERENTIATED LEARNING SKILLS FRAMEWORK FOR THE STUDENT		

http://dx.doi.org/10.5772/intechopen.75646

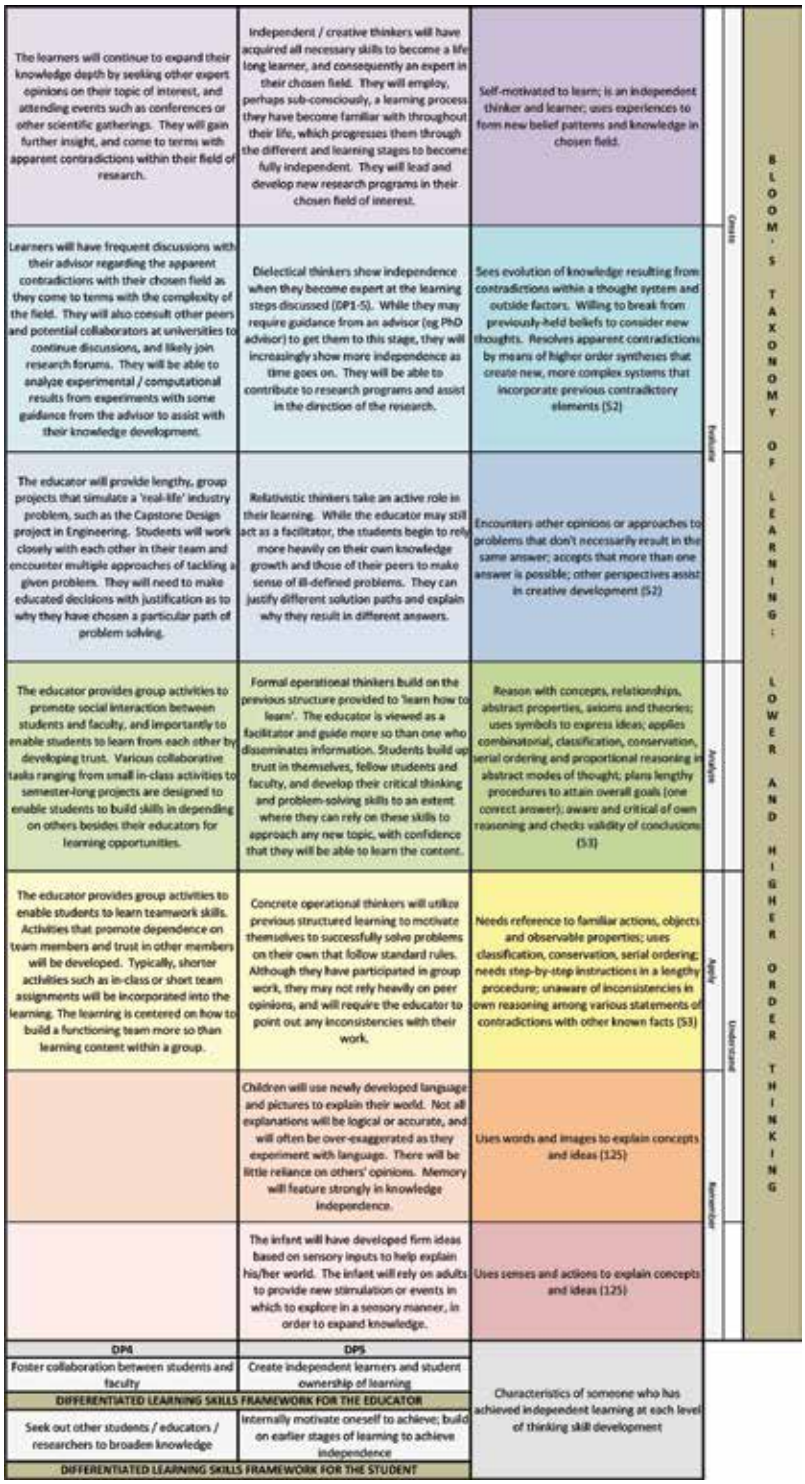

Author details

Brenda Hutton-Prager[1,2]*

*Address all correspondence to: bhprager@olemiss.edu

1 University of Mississippi, University, MS, USA

2 American Institute of Chemical Engineers (AIChE), American Coatings Association (ACA), American Chemistry Society (ACS), Australian College of Educators (ACE), Registered Teacher – Victoria Institute of Teaching (VIT), Australia

References

[1] Farrell S, Cavanagh E. Biodiesel production, characterization, and performance: A hands-on project for first-year students. Education for Chemical Engineers. Apr 2014;**9**(2): e21-e31

[2] Golter PB, Thiessen DB, Van Wie BJ. Adoption of a non-lecture pedagogy in chemical engineering: Insights gained from observing an adopter. Journal of STEM Education. 2012;**13**(5):52-61

[3] Gómez Puente SM, van Eijck M, Jochems W. Towards characterising design-based learning in engineering education: A review of the literature. European Journal of Engineering Education. 2011 May;**36**(2):137-149

[4] Han JH, Finkelstein A. Understanding the effects of professors' pedagogical development with clicker assessment and feedback technologies and the impact on students' engagement and learning in higher education. Computers in Education. Jul 2013;**65**:64-76

[5] Mantri A. Working towards a scalable model of problem-based learning instruction in undergraduate engineering education. European Journal of Engineering Education. May 4, 2014;**39**(3):282-299

[6] Smith MK. Malcolm Knowles, informal adult education, self-direction and andragogy. Encyclopedia of Informal Education [Internet]. 2002. Available from: www.infed.org/thinkers/et-knowl.htm

[7] Tomlinson-Keasey CA. Chapter 1: Piaget's theory and college teaching. In: Essays from and about the ADAPT Program. 1978:29. http://digitalcommons.unl.edu/adaptessays/29

[8] Ojose B. Applying Piaget's theory of cognitive development to mathematics instruction. Mathematical Education. 2008;**18**(1):26-30

[9] Lefmann T, Combs-Orme T. Early brain development for social work practice: Integrating neuroscience with Piaget's theory of cognitive development. Journal of Human Behavior in the Social Environment. Jul 2013;**23**(5):640-647

[10] Wu P-L, Chiou W-B. Postformal thinking and creativity among late adolescents: A post-Piagetian approach. Adolescence. 2008;**43**(170):237-251

[11] Wu EH. The path leading to differentiation: An interview with Carol Tomlinson. Journal of Advanced Academics. May 2013;**24**(2):125-133

[12] Tomlinson CA. The Differentiated Classroom: Responding to the Needs of all Learners. Alexandria, VA: Association for Supervision and Curriculum Development; 1999. 132 p

[13] Tomlinson CA. To the contrary: Differentiation does work. Education Week Spotlight on Differentiated Instruction. Jan 2016:16-17

[14] Murphy C, Scantlebury K, Milne C. Using Vygotsky's zone of proximal development to propose and test an explanatory model for conceptualising coteaching in preservice science teacher education. Asia-Pacific Journal of Teacher Education. Aug 8, 2015;**43**(4):281-295

[15] Delisle JR. Differentiation doesn't work. Education Week Spotlight on Differentiated Instruction. Jan 2016:15

[16] Bullock J. Differentiated instruction, one size does not fit all. Education Week Spotlight on Differentiated Instruction. Jan 2016:9-11

[17] Davis MR. District's ambitious effort fuels personalized learning. Education Week Spotlight on Differentiated Instruction. Jan 2016:12-15

[18] Herold B. Literacy gets a personalized makeover. Education Week Spotlight on Differentiated Instruction. Jan 2016:2-4

[19] Manning S, Stanford B, Reeves S. Valuing the advanced learner: Differentiating up. Clearing House: A Journal of Educational Strategies, Issues and Ideas May 24, 2010; **83**(4):145-149

[20] Rock ML, Gregg M, Ellis E, Gable RA. REACH: A framework for differentiating classroom instruction. Preventing School Failure: Alternative Education for Children and Youth. Jan 2008;**52**(2):31-47

[21] Sparks SD. Differentiated instruction: A primer. Education Week Spotlight on Differentiated Instruction. Jan 2016:7-8

[22] Valiandes S. Evaluating the impact of differentiated instruction on literacy and reading in mixed ability classrooms: Quality and equity dimensions of education effectiveness. Studies in Educational Evaluation. Jun 2015;**45**:17-26

[23] Watts-Taffe S, Barbara Laster BP, Broach L, Marinak B, McDonald Connor C, Walker-Dalhouse D. Differentiated instruction: Making informed teacher decisions. The Reading Teacher. Dec 2012;**66**(4):303-314

[24] Prager BH. An Analysis of the Current VCE mathematics Study Design and Comparison with other Equivalent Designs with respect to the Principles of Differentiation. Victoria, Australia: The University of Melbourne; 2013

[25] Chamberlin M, Powers R. The promise of differentiated instruction for enhancing the mathematical understandings of college students. Teaching Mathematics and Its Applications. Sep 1, 2010;**29**(3):113-139

[26] Konstantinou-Katzi P, Tsolaki E, Meletiou-Mavrotheris M, Koutselini M. Differentiation of teaching and learning mathematics: An action research study in tertiary education. International Journal of Mathematical Education in Science and Technology. Apr 15, 2013;**44**(3):332-349

[27] Victorian Curriculum and Assessment Authority. The Victorian Curriculum F-10 [Internet]. Victoria State Government; Available from: http://victoriancurriculum.vcaa.vic.edu.au/

[28] Krathwohl DR. A revision of Bloom's taxonomy: An overview. Theory Into Practice. 2002;**41**(4):212-218

[29] Kolb DA. Chapter 2: The process of experiential learning. In: Experiential Learning: Experience as the Source of Learning and Development. Englewood Cliffs, NJ: Prentice Hall; 1984. pp. 20-38

[30] Hutton-Prager BH, O'Haver J. Work in progress – Implementing a differentiation framework into freshman engineering classes. In: 8th Annual First Year Engineering Experience Conference. Columbus, Ohio. 2016. (Session T2D)

[31] Anderson LS, Ferri JK, Cramer AD. Flipped Laboratories in Chemical & Biomolecular Engineering. In: ASEE 123rd Annual Conference & Exposition. New Orleans, LA; 2016. (Paper ID#16947)

[32] Garrison LA, Garrison TJ. A Laboratory Structured to Encourage Thoughtful, Task-Based Experimentation. In: ASEE 123rd Annual Conference & Exposition. New Orleans, LA; 2016

[33] Habibi M, Fearing C, Muslu M. Pros and Cons of Laboratory Methods used in Engineering Education. In: ASEE 123rd Annual Conference & Exposition. New Orleans, LA; 2016. (Paper ID #15975)

[34] Piergiovanni PR, Jarboe JH. Experiments for A Unit Operations in Food Engineering Course. In: ASEE 123rd Annual Conference & Exposition. New Orleans, LA; 2016. (Paper ID #15686)

[35] Hutton-Prager B. Design of differentiated curricula in freshman chemical engineering courses. In: AIChE Annual Meeting, San Francisco, California, USA; 2016. (Paper ID #454066, Session 293f)

[36] Vigeant MA, Prince MJ, Nottis KEK, Koretsky M, Ekstedt T. Hands-on, Screens-on, and Brains-on Activities for Important Concepts in Heat Transfer. In: New Orleans, LA; 2016. (Paper ID #14724)

Chapter 2

Experiential Learning via Open-Ended Laboratory Initiatives

Nor Irwin Basir, Zainal Ahmad and
Syamsul Rizal Abd Shukor

Additional information is available at the end of the chapter

http://dx.doi.org/10.5772/intechopen.77015

Abstract

Conceptual mapping of existing knowledge on previous subject learned with the new knowledge can be accentuated using experiential learning methodologies. Open-ended laboratory (OEL) initiative exemplifies the intended outcome of experiential learning cycle where the learners encounter new experiences via laboratory experiments, reflecting the observation made interconnecting the inconsistencies between experience and understanding. This provides a solid basis for the learners to create or modify existing abstract concept of the experiments undertaken. These experiences will be put into context where the learners actively and adaptively experimenting and integrating previous knowledge with the new knowledge and put into practice by developing appropriate experimental procedures in order to achieve the set objectives given for a particular problem statement. This chapter illustrates the concept of open-ended laboratory (problem based), describing the transition of traditional laboratory (TL) to problem-based learning experience via experiential learning methodologies. The methodologies in developing the OEL in a chemical engineering laboratory course and their implementation in a process control laboratory setup were also outlined. The transition of traditional to problem-based findings and course outcomes attainments were investigated and measured using appropriate tools. The challenges and difficulties in implementing OEL were described and analyzed with data obtained from the experiences of conducting OEL in the School of Chemical Engineering, Universiti Sains Malaysia.

Keywords: experiential learning, concepts, implementation, assessment, open-ended laboratory

1. Introduction

Chemical engineering laboratory course has always been a core module in any chemical engineering curriculum around the globe. Some universities have even started the course as early as sophomore year toward their final year to reinforce chemical engineering fundamentals and apply the knowledge and skills gained from courses to actual chemical engineering experiments. This guided and prescriptive laboratory course is no longer adequate within the context of synergies between twenty-first century learning skills and the establishment of outcome-based education.

In the advent of Industrial Revolution 4.0 and the challenges to produce learners equipped with the essential twenty-first century skills, chemical engineering laboratory course has become one of the essential tools for innovative teaching and learning processes beyond the boundaries of conventional setting. It is a platform that engages learners in multidimensions of cognitive, psychomotor, affective skills where knowledge is being applied in a practical manner thus making it the most suitable stage to increase the experiential learning of the learners.

Experiential learning provides a solid platform for stimulating the learners' intuitiveness to be more systematic, inquiry-based with specific end in mind. Thus, providing opportunities for the learners to be more engaging intellectually, creative, and taking initiative while making decision and be accountable for the outcomes attained at the end of the exercise. Conceptual mapping of existing knowledge on previous subject learned with the new knowledge can be accentuated using experiential learning methodologies. Experiential learning philosophy relies in the learning through experience where learners can reflect on their actions to gain understanding on the consequences of that action and arrange the understanding into a generalization of principles of accumulated knowledge which can be obtained via open-ended laboratory (OEL) exercise.

2. Concept of open-ended laboratory

OEL initiative exemplifies the intended outcome of experiential learning cycle where the learners encounter new experiences via designing and conducting laboratory experiments, reflecting on the made observation and interconnecting the inconsistencies between experience and understanding. These features provide a solid basis for the learners to create or modify existing abstract concept of the experiments undertaken. These experiences will be put into context where the learners actively and adaptively experimenting and integrating previous knowledge with the new knowledge and put into practice by developing appropriate experimental procedures in order to achieve the set objectives given for a particular problem statement [1].

In contrast with the OEL initiatives, the traditional laboratory (TL) approach lies in the concept of information assimilation process where information is transmitted through a symbolic medium, assimilated by the learner, and generalized before actually being applied. Therefore,

most TL approach is carried out following theoretical-based lectures attended by the learners before a meaningful TL can be conceived [2]. This resulted in a laboratory procedures consisted of detailed set of instructions for the experimental set up by the instructors in closed manner with the expectation of the learners should obtain and foolproof the experimental results that would support the theory learned in the class. Though this approach would be optimal on the side of the instructors in establishing the theories learned in the classroom but it also creates a *faux accent* on the learner's sides as it skips many important steps in designing an experiment and reduced the efficacy of a laboratory experimental sessions in teaching important laboratory skills to learners, thus, placing it to only a step higher than a mere laboratory demonstration to the learners. In practice, learners not just lost the opportunity to develop skills in designing an experiment but usually mislaid the logic of the experiment as well as they put more psychomotor efforts to manipulate and following instructions when executing the experiments rather than invest time to develop higher thinking order cognitive skills involving the experimental setup.

OEL works in tandem with the experiential learning process where learners conceived the conceptual and practical of the undertaken action with the understanding that it involves consequences in a particular circumstance and finally being able to reflectively generalizing the principle across a range of circumstances. OEL would bring the learners' learning experience nearer to the real professional life situation of practicing scientist and engineers as most engineering laboratory procedures are developed and manipulated through experience and knowledge accumulated from scientific literatures rather than handed in the form of standardized procedures as in testing laboratory works. It is important to note that neither OEL nor TL should be seen as competitive to each other but rather the two learning processes are complementary to each other. The keyword here is to strike a balance between both approaches as both are necessary for optimal learning since the emphasis between depth and breadth of laboratory skills varies greatly in both approaches. The TL has the advantages of greatly reducing the time and effort necessary to cover many new laboratory techniques, whereas OEL increases intrinsic motivation among learners as they connect the skills to real-world context and will definitely assist the knowledge retention for years to come.

Departing from TL toward OEL, one will find that there are varying degrees in the level of laboratory openness. **Table 1** shows the gross representation in level of laboratory openness. Level 0 would represent a fully laboratory demonstrations while level 5 for undertaking a full laboratory research project. Levels 1 and 2 are where the TL dominates and OEL be more dominant in Levels 3 and 4. In practice, the time for delivery at the upper level will definitely take more time than the lower level as learners require time to define the needs of open nature of elements in that level compared to time taken to understand the nature of a given elements. Al level 4, OEL elements intensify the time taken to complete tasks the learners need to develop in the laboratory procedures and dissecting the problem analysis of the experiment. A typical profile of the laboratory based on the level of openness is given in **Table 2**.

It is advisable for learners to undergo a series of progressive openness from lower levels so that the learners could acquire many useful laboratory skills that would be of help when going to the next level and finally acquire research and investigation skills that would be useful to carry out in a laboratory research project. One could see that if learners are not being

Level	Experimental theme	Problem statement	Experimental methodology	Expected results	Expected discussion
0	Given	Given	Given	Given	Given
1	Given	Given	Given	Given	Open
2	Given	Given	Given	Open	Open
3	Given	Given	Open	Open	Open
4	Given	Open	Open	Open	Open
5	Open	Open	Open	Open	Open

Table 1. Level of openness in laboratory.

Level	Typical profile
0	In laboratory demonstrations, learners are given all information pertaining to the experiment including the objectives, procedures, results, and its corresponding discussion which sometimes some of it in a form a fill in the blanks statements to emphasis the theory to the learners.
1	In traditional laboratory courses, learners are supplied with the laboratory manual containing all relevant information such as operating procedures and learners needed to digest before conducting the laboratory experiment. There are questions left for the learners for discussion or it is left open but hints of theory involved is given so that the expected results from experiment can be anticipated by the learners. Learners also supplied with the data sheets to guide them in data collection.
2	In traditional laboratory courses, learners are supplied with the laboratory manual containing many relevant information such as operating procedures and learners needed to digest before conducting the laboratory experiment. Learners need to plan and arrange the format for data collection as the data sheets to guide in data collection not given. Discussion on the experiment is left open for learners to evaluate based on the results.
3	In open-ended laboratory courses, learners are supplied with the clear objectives and problem statement of the experiment. However, the laboratory procedures to achieve the objectives are not given or coarsely given. Learners need to develop the procedures through literature or operating manual of the equipment. Learners also need to identify the various parameters and data that need to be collected. Discussion on the experiment is left open for learners to evaluate based on the results.
4	In open-ended laboratory courses, learners are supplied only with the clear objectives of the experiment. Learners to analyze the ill-defined problem with the help from literature review and come up with the problem statement. Learners develop the methodology and laboratory procedures to achieve the objectives through literature or operating manual of the equipment. Learners also need to identify the various parameters and data that need to be collected. Discussion on the experiment is left open for learners to evaluate based on the results.
5	In free laboratory research project, learners decided to carry out from an ill-defined experimental theme usually in the form of final year research project that takes at least the whole semester to complete.

Table 2. Typical profile based on level of openness of the laboratory.

exposed to OEL and only used to participate in TL, it is going to be a steep learning curve for the side of learners to be able to do a full laboratory research project in a later stage. In this perspective, OEL act as the scaffolding for the full research project.

http://dx.doi.org/10.5772/intechopen.77015

The delivery of OEL has many models which the instructors would have to see as which models would give the best fit to the learning processes organization as different learning institutions have different strength and capability. The factors to weigh, in addition to selecting the level of laboratory openness, would be the degree of independence given to the learners in OEL for decision-making. As OEL would be more open than TL, the questions arise on the role of instructors in assisting learners in determining the scope of the problem statements, selected experimental procedures, selected parameters, and data collection. OEL initiatives would take a longer period of time not just by the learners but also by the instructors as the role of laboratory instructors are now redefined to include supervision.

3. Open-ended laboratory in undergraduate program in the School of Chemical Engineering, Universiti Sains Malaysia

A case study of OEL practiced in the School of Chemical Engineering, Universiti Sains Malaysia is presented in this section. OEL initiative has been introduced to the laboratory courses offered by the School since academic session 2013/2014 and has been the standard practice until now. The implementation of OEL has been adapted from the OEL approach reported in [3, 4]. The laboratory courses involved three courses: EKC291, EKC394, and EKC493 that would be taken by students at their second, third to fourth year, respectively. Each laboratory course is a two credit hours course which means about 4 h of laboratory session per teaching week. The level of laboratory openness in OEL approach is made increasing with the students' incremental years of study. The laboratory courses are a mix between OEL and TL approaches. The students were divided into groups of three/four, and each team is given one OEL project during the semester, while another eight laboratory works are meant for TL. Prior to the introduction of OEL in the laboratory courses, students would have been required to conduct about 12 experiments in TL approach. The School believes that 1 OEL + 8 TL format in three laboratory courses would be best compromise to both develop generic laboratory skills by the students and give students opportunity to delve into a wide variety of experimental topics.

The OEL were running for 4 weeks with one supervisor to craft the question or the problem statement, monitor and marking the group and individual performance of the student. Each group was given 3 h duration of in-lab sessions and 2 h duration of out-lab sessions in each week. The distributions of in-lab and out-lab sessions were shown in **Tables 3–6**. In-lab and out-lab sessions were spread between week 1 and week 4 where the student can have a mixture of session in each week. In-lab session means the students can carry the laboratory work during laboratory session where it normally starts in week 3 after the students have familiarized with the experimental rig and came up with the appropriate standard operating procedure (SOP) of the experiment, while an out-lab session is the discussion handled outside or during the laboratory session which do not involved directly with the laboratory experiment.

In addition, students were briefed on the safety on the laboratory prior to the OEL Lab in the first week. This safety briefing is carried out by the school safety officer. In week 1, the supervisor will hand in in-lab and out-lab activity to the student as shown in **Table 3** and the

In-lab session (3 h)	Out-lab session (2 h)
• Understanding the problem with facilitator's guidance • Brainstorming, giving ideas to solve problem • Identifying available resources and tools • Identifying what you know and what you need to know in solving the problem • Facilitator marks individual in-lab activities	• Get more resources to help understand the problem • Divide work among group members • Report findings to group • Agree on a solution

Table 3. In-lab and out-lab activity for week 1.

In-lab session (3 h)	Out-lab session (2 h)
• Present solution to facilitator • Facilitator comments on solution, making sure the group is on the right track • Group begins to design experiment • Group confirms the experiment layout • Facilitator monitors and marks individual in-lab activities	• Group conducts some simulation work to reconfirm design (if necessary) • Group verifies availability of equipment and tools to conduct experiment • Group prepares schematic or flow diagrams for experiment

Table 4. In-lab and out-lab activity for week 2.

In-lab session (3 h)	Out-lab session (2 h)
• Group begins to conduct experiment • Facilitator monitors and marks individual in-lab activities • Group obtain results from experimental work	• Group starts preparing comprehensive report • Planning for presentation session

Table 5. In-lab and out-lab activity for week 3.

In-lab session (3 h)	Out-lab session (2 h)
• Report writing • (Facilitator monitors and marks individual in-lab activities)	• Continuation of report writing and submission not later than Thursday of the week.

Table 6. In-lab and out-lab activity for week 4.

examples of the scenario/problem statement in **Figures 1** and **2**. The tasks can be given out as a role-playing case study or as in a problem scenario case study.

The supervisor will act as the facilitator to guide the student in understanding the given problem, propose the SOP and run the experiment accordingly to get the expected experimental outcomes. In week 2, the students need to propose the solution and the SOP to the

supervisor where the supervisor will then evaluate and assess the proposed solution and ensure that the propose solution and SOP able to guide the team to get the expected outcome of the problem as shown in **Table 4**. In weeks 3 and 4 (see **Tables 5** and **6**), the team will

Memo: Technical Manager to Technical Team

Subject: Cooling Tower performance

I received a complaint from Operation Department about the performance of our cooling tower where the additional heat exchanger in the cooling water circuit makes the existing cooling tower seem not be able to cool down the cooling water return (CWR) to the design values. In the complaint, it is reported that the additional heat exchanger in the system increased the heat load of the cooling tower.

Therefore, I would like your team to investigate the claim by the Operation team and please rectify the problem. if the complaint in the report is true. Please check the performance of the existing tower using the min temperature of the CW inlet at ambient temperature then after additional heat exchanger in the CW circuit the cooling water inlet temperature may increase up to max of ΔT 10 15 C. The criteria you may need to have a look are:

1. Air velocity through the tower

2. Driving force

3. Performance/efficiency

Figure 1. Sample of role-playing memos as task given in OEL.

Problem Scenario:

The School has bought 3 control valves with different characteristics from supplier A to replace the old control valves in the existing engineering laboratory. The School's management place an order for the valves based on the specification information given in the catalogue.

Using the existing rig in the Laboratory, the laboratory manager asked your team to check whether the delivered control valves are actually following the design specifications given in the catalogue or in reality differ from the original specifications. The technical instructor requires your team to outline the procedures to determine the control valve characteristic in the report. (Please refer to specifications given in the catalogue, in particular, the inherent characteristic of the control valve)

After the study, the engineering laboratory technician as the person in charge would like to seek your opinion about the suitability of the control valves because the person in charge are not sure which control valve would be better for low flow with quick response application. The person in charge would like to know about the controllability of the valves in the region of high flow as well, as he/she intended to install one of the control valve in a boiler system which needs a fast response to reduce the pressure in the steam header.

Since the flow is unstable at times, the pressure tend to oscillate quite heavily, therefore the laboratory manager would like you to determine whether this scenario has a significant effect to the control valve performance. Please outline the procedures or state the justifications in the report when deciding the correct control valves and report all important parameters in the performance study.

Figure 2. Sample of problem scenario given as task in OEL.

conduct the experiment and monitored by the supervisor and also laboratory technicians, analyze the result, preparing the comprehensive report, and also the viva voce session.

4. Assessment methods for open-ended laboratory

The assessment method covers not only the comprehensive report submitted but also other components of assessments as shown in **Table 7**. Many assessments methods employed by

Details	Marks
Peer and self-assessment	10
Supervisor evaluation on student participation (quizzes, assessment rubrics, etc.)	15
Comprehensive report	50
Seminar presentation/viva 45 min	20
Attendance	5

Table 7. Assessment method in OEL.

Bil	Item
1	Title page
2	Abstract/summary
3	Table of content
4	Introduction
5	Application in industry
6	Objectives
7	Methodology-procedure and experimental setup
8	Result and discussion
9	Conclusions
10	Acknowledgment
11	Abbreviation/nomenclatures
12	References (at least 10 from technical articles/books)
13	Appendices
14	25–30 pages max (excluding title page and appendices)

Table 8. Format of comprehensive report for OEL.

the School were adapted from references [5–7]. Based on the assessment, the students' teamwork, psychomotor/lab handling skill, and presentation skill were taken into account. In each assessment, for example, the comprehensive report, the rubrics are given based on the rating for each attribute. The contents of the comprehensive report are shown in **Table 8**.

5. Reflections in open-ended laboratory initiatives

In OEL, the students will utilize their fundamental knowledge of chemical engineering that they had learned in Years 1 and 2 and apply in Year 3 in Chemical Engineering Laboratory III. The students need to set what are the objectives of that particular experiment and also what is the goal that they want to obtain or achieve in that particular given problem. In addition, they need to discuss and propose to their supervisor the design steps on the experiment, how to set up the procedures for the experiment and the most important thing is they need to present it to the supervisor to attain his agreement on the proposed procedures. In this activity, the students will cogitate and use their higher order thinking skill to design and propose the procedures to the supervisor. Thus, the data that need to be collected also need to be determined by the students. Some experiment like in TL, there a lot of data need to be taken into account; however in OEL, only data that related to the design of experiment or goal need to be collected. Skill of presenting the result like using graph or flowchart or how to organize the data are very important in this stage as well as skill to analyze the data using any statistical tool, if needed. The results and the goals of the experiment need to be justified whether it is achieved or the result deviated from the theory. In this stage, the student uses their own ability to propose the solution and set the goal for the experiment. However, if the student were not able to obtain or achieve the goals, the student can apply different strategies or methods, subject to supervisor's approval in the attempt to get the expected result. This activity indicates that the students have the capability to analyze the result properly and propose a new solution that may solve the problem hence obtaining the goal of the experiment.

The feedbacks on OEL from the student were carried out as part of the question asked in the exit survey by the exiting students. The response obtained from the students are shown in **Figure 3** and summarized in **Table 9**. The students were asked the question how effective OEL in strengthening students' laboratory skills with 5-point Likert scale-type response with least effective, less effective, average, very effective, and highly effective. It is shown that the students' tendency is favorable toward OEL and has been improving from the first year of OEL's inception to the laboratory courses in 2014. This can be seen from mean rating scale of 3.50 out of 5.00 in 2014 and increasing to 4.00 and 4.08 in 2015 and 2016, respectively, before settling at rating scale of 3.75 in 2017 (see **Table 9**). The accepted minimum response as a performance indicator to indicate support on the OEL initiative was set at response at scale 4 (very effective) and above. Response started in 2014 with highly divided at 48:52 (yes:no) ratio and later improved in the subsequent years presumably by better supervision and guidance by the laboratory instructors on the students groups as the laboratory instructors gained more experience. In the qualitative response section in exit survey, most students generally comment that

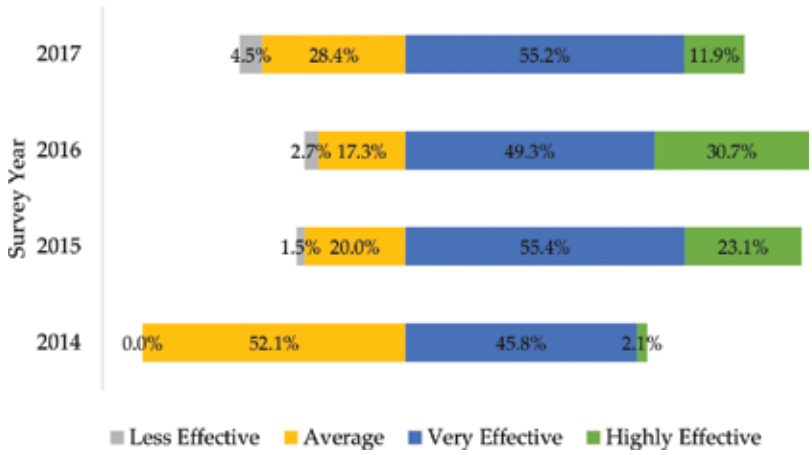

Figure 3. Exit survey response of students on how effective OEL in strengthening students' laboratory problem-solving skills.

Year	Sample size, n	Mean, μ	Standard deviation, σ	Mode and median
2014	48	3.50	±0.30	3 (Average)
2015	65	4.00	±0.50	4 (Very effective)
2016	75	4.08	±0.59	4 (Very effective)
2017	67	3.75	±0.53	4 (Very effective)

Table 9. Analysis of exit survey response on effectiveness of OEL in strengthening laboratory problem-solving skills.

the OEL did make the students to be more creative in solving the given problem, excite their HOTS and also increased their attainment toward lifelong learning. Other skills like teamwork and presentation skill were also seen to improve and in turn would provide the necessary skills for the students' survival in the ever-challenging working environment in industry.

Reflecting through the OEL initiatives as compared to TL approach has shifted the norm of laboratory practices among the students. Given ample time to design their experimental work, the students learn the importance of coming to the laboratory prepared and developed the logic of experimental work. This initiative promotes intrinsic motivation of the students and creates a mind shift from passive laboratory user to an active participant. Knowing responsibly the hardwork required in OEL, prepares the students a real-life research project environment where delicate balance of compromise between the theoretical experimental setup that can be carried out in laboratory to the constraints of time, cost, and safety. Students are also compelled to learn independently from literature and sought guidance from their supervisor and found to be involved in peer to peer learning as they tried to solve the problems.

Supervisors of the OEL project need to invest time to supervise the OEL groups as our experience shows that while few of the OEL groups tend to seek shortcuts and find the easiest way to complete the project, the reality is many of the OEL groups tend to choose the most exciting

path. However, due to the constraints in resources and time, many of the chosen exciting paths taken by the OEL groups are not practical. It was the experience of the supervisors that can help the students to take into considerations the practical aspects of the project to enable them to complete the OEL project within the time frame. Creative students will find the given autonomy, and fewer restrictions on the implementation of OEL project will increase their intrinsic motivations as they themselves (to certain extent) define the direction of the OEL project. The creativity in solving OEL project usually would translate well into the good assessment grades by the OEL supervisor as students make an impression by giving fresh ideas and unorthodox approaches.

Nonetheless, not all students would be pleased on the introduction of OEL initiatives, as a handful of students were found to be frustrated, as the results of OEL do not necessarily be one correct answer. Students also feel that the increased interaction with the laboratory teammates and the technicians as well as the progress of the OEL project sometimes depends on factors beyond individual control that can contribute to their frustration. The OEL initiative also found to create many logistic and laboratory safety issues. In TL, each piece of equipment had one specific role with particular standard operating procedures, whereas in OEL, students are required to use different raw materials and operating parameters in order to meet the needs of their problems and thus, creates additional load to the laboratory technician to monitor the experimental work by the students. The laboratory technicians also need to upgrade their know-how and knowledge, especially the safe operating limit of equipment and limit of its flexibility in adapting to new experiments.

It is important for the course or program owner to note that the considerations for selecting and embedding OEL in laboratory courses depend on the learning outcomes. It is the laboratory course's intended learning outcomes that dictate the pedagogy and assessment for laboratory courses. This is the crux of constructive alignment in the philosophy of outcome-based education. Adopting TL approach would be sufficient if the intended learning outcomes in the laboratory course simply concentrate on students' ability to skillfully conduct experiments on certain topics; however if the intended learning outcomes of the laboratory course would be the ability of the students to design an experiment on a given topic and at higher level the program intended outcome aspires to increase the experiential learning of the students then the TL approach would be less adequate and it warrants a better delivery method to achieve the intended learning and program outcomes such as OEL.

6. Conclusions

Analysis for the reflection activity showed that there are mixtures on the students' perception on OEL. Some of the students see the OEL initiatives did help them to have a deeper understanding on the fundamental concept of chemical engineering like mass transfer and heat transfer. On the other hand, there are a handful of students who perceive this OEL as a burden to them like creating their own experimental procedures. A higher percentage of the students agreed that OEL activities provide them better laboratory skills than TL. OEL initiatives nevertheless increase the experiential learning of the students as they equip and prepare them better in their research-based final-year project (FYP) and facing the real environment in industry.

Acknowledgements

The authors would like to acknowledge Dr. Derek Chan and Dr. Khairiah as a coordinator of Chemical Engineering Laboratory II (EKC 394) and Dr. Vel Murugan for Chemical Engineering Laboratory III (EKC 493) for fruitful discussion on OEL implementation in the School of Chemical Engineering USM.

Author details

Nor Irwin Basir*, Zainal Ahmad and Syamsul Rizal Abd Shukor

*Address all correspondence to: chirwin@usm.my

School of Chemical Engineering, Universiti Sains Malaysia, Penang, Malaysia

References

[1] Wankat PC, Oreovicz FS. Teaching Engineering. 2nd ed. Vol. 2015. Purdue University Press. p. 482

[2] Porter MC. Curriculum development and implementation for physiological chemistry laboratory (CHEM 3402): An open-ended laboratory approach [Thesis]. Texas Tech University; 1996

[3] Azli NA, Tan CW, Ramli N. Implementation model of a problem-based laboratory (PBlab) established for a bachelor of engineering (electrical) program at Universiti Teknologi Malaysia. In: Proceedings of RCEE & RHEd2010, 7-9 June 2010; Kuching, Sarawak; 2010. pp. 1-5

[4] Rahman NA, Kofli NT, Takriff MS, Abdullah SRS. Comparative study between open ended laboratory and traditional laboratory. In: Proceedings of 2011 IEEE Global Engineering Education Conference (EDUCON), 4-6 April 2010; Amman, Jordan; 2010. pp. 40-44

[5] Kofli NT, Rahman NA. The open ended laboratory for measurement of communication skill for chemical/biochemical engineering students. Procedia - Social and Behavioral Sciences. 2011;**18**:65-70

[6] Kofli NT, Badar SN, Rahman NA, Mastar MS, Abdullah SRS. Open ended laboratory (OEL) assignment as tool imparting generic skills for engineering students. Asian Social Science. 2012;**8**:146-152

[7] Rahman NA, Kofli NT. Effect of peers assessment and short report in year III laboratory course. International Education Studies. 2013;**6**:23-27

Section 2

Application of Experimental Methods in Research

Chapter 3

Kinetics of Growth of Iron Boride Layers on a Low-Carbon Steel Surface

Enrique Hernández-Sánchez and
Julio Cesar Velázquez

Additional information is available at the end of the chapter

http://dx.doi.org/10.5772/intechopen.73592

Abstract

This chapter describes the boriding process and the parameters that govern it. It also describes the features of the obtained layers and the main applications of materials treated with this hardening process. The kinetics of growth of the Fe_2B face is described using a mathematical model, in which the evolution of the growth of the boride layers is assumed to be controlled by the boron diffusion by means of a dimensional analysis of Fick's second law. The evolution of the growth of the Fe_2B face on a low-carbon steel surface is illustrated by contour diagrams that involve the main variables of the process (time and exposure temperature). This type of diagrams allows the optimization of the process as a function of the treatment parameters.

Keywords: boriding, iron boride, kinetics, surface layers, low carbon steel

1. Introduction

Boriding is a thermochemical treatment by which it is possible to obtain extremely hard layers. Through boriding, it is possible to enhance the wear resistance and corrosion resistance of acid and/or alkaline media.

Through boron diffusion in the surface of a metal or alloy, a dense zone of borides of the base metal with high mechanical properties is expected to appear.

The relatively small size of the boron atom (8.7×10^{-2} nm) allows it to diffuse in a high variety of metals, such as iron alloys, nickel, nickel alloys, cobalt alloys, titanium and titanium alloys [1].

Boron reacts with metals to form intermetallic compounds that enhance surface hardness and increase wear resistance [2].

The formation of iron borides during the boriding of steel alloys, consists of two main reactions. First, nucleation of the iron boride particles on the surface of the substrate takes place; then, a diffusive process occurs where the layer starts to grow on the metallic surface.

The thickness of the achieved layers is highly dependent on the temperature at which the process is realized and on the exposure time. During the diffusion process and the subsequent absorption of boron atoms, the formation of interstitial solid solutions, which can be single-or double-face Fe_2B or Fe_2B/FeB, occurs.

The formation of the FeB and Fe_2B faces can be explained by the low solid solubility of atomic boron in steel. When this value is not exceeded, the boron can only be present in the iron matrix as a solid solution. However, when the limit of solubility is reached, the Fe_2B face is formed and grows with a flat front during the boriding process if enough active boron is provided [2].

During the diffusion process, borides are formed in grain boundaries. Also, as the transportation of boron atoms through the grain boundaries increases, the formation of a flat front can be disturbed and the Fe_2B face will have an irregular morphology similar to a saw-toothed shape.

Nevertheless, although the Fe_2B face is formed with a saw-toothed morphology, one should note that, once a continuous face of Fe_2B is formed, it will act as a diffusion barrier, this is because of some properties of this boride, such as a high melting point and high stability at high temperatures, which are characteristics of the compounds known as inhibiters of diffusion. Therefore, it is expected that the Fe_2B face could be a barrier for boron or iron diffusion.

On the other hand, to obtain the uninterrupted growth of the Fe_2B face, a continuous flux of boron or iron is necessary, depending on the side of the Fe_2B/Fe interface on which the diffusion occurs. Likewise, by assuming that the growth of the Fe_2B boride occurs from the surface to the interior of the substrate (that is, in the Fe/Fe_2B interface) and that the boron flux has to pass through the previously formed diffusion barrier of Fe_2B, the Fe-B relation will not have the required proportion to continue forming the Fe_2B-type boride. The proportion of boron will be lower because the active boron is accumulated at the back at the Fe_2B face. This sequence of events could explain why FeB is generally the outermost face in steels exposed to boriding for long periods of time and high temperatures where the diffusion speed is higher.

In that sense, a metallic matrix with a high concentration of alloy elements could enhance the formation of a double-face FeB/Fe_2B as a consequence of the growth of a continuous Fe_2B face, which will act as a diffusion barrier.

1.1. Mechanical, physical, and chemical properties of iron borides

The structure of borides is determined by the size of the boron atom and the size of the atoms of the material in which it is diffused, as well as its strong tendency to mix with them. Boron is highly soluble in materials with a small atomic volume, such as iron and its alloys. Depending

on the characteristics of the substrate and boron's potential to be employed during the treatment, it is possible to generate single-face (Fe_2B) or double-face (FeB/Fe_2B) layers on the surface, which will be hard layers with a saw-toothed morphology.

According to Matuschka [3], the chemical composition of iron borides can be obtained from the Fe/B faces, as shown in **Figure 1.**

The FeB face has 16.2% boron by weight and has an orthorhombic crystalline structure, with lattice parameters a = 0.4053 nm, b = 0.5495 nm, and c = 0.2946 nm. On the other hand, the Fe_2B face contains approximately 8.83% boron by weight with a tetragonal crystalline structure and lattice parameters a = 0.5978 nm, and c = 0.4249 nm.

Both intermetallic compounds have a preferential crystallographic direction of growth [001] because the atomic density is higher in that direction.

The nature of the layer formed depends on the boron potential that surrounds the sample.

It has been established that for low-to-medium boron potentials, preferential growth of the Fe_2B face [4] is expected. The formation of the FeB face requires a high boron potential, in addition to the influence of the alloying elements content in the steel, especially chromium, nickel, vanadium, tungsten and molybdenum [5].

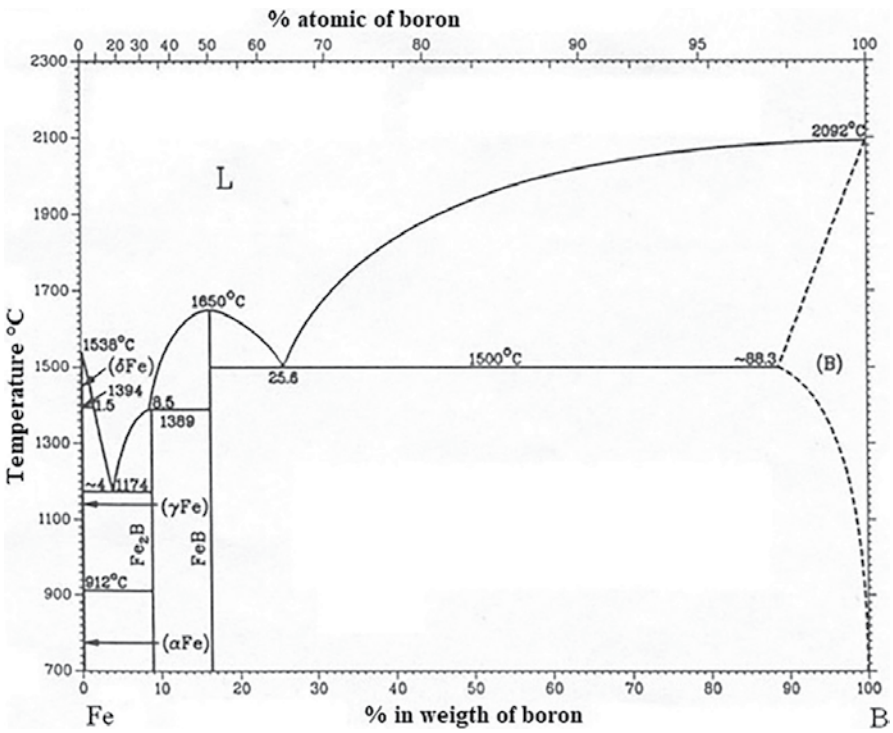

Figure 1. Iron-boron faces diagram [3].

The presence of oxygen during the treatment favors the formation of porosity in the borides because oxygen reacts with the carbon of the boriding agent (B_4C) and forms CO and a boron oxide, which obstructs the boriding process; thus, the formation of boron oxides consumes the active boron as B_2O_3 [6].

The porosity of the boride layers represents points of stress concentration, which indicates degradation of the mechanical properties of the layers **Table 1** shows some chemical and mechanical properties of the iron borides.

Properties	**FeB**	**Fe_2B**
Density (g/cm^3)	6.75	7.43
Thermal expansion coefficient (ppm/K)	23 in the range of 200–873 K	7.65–9.2 in the range of 373–1073 K
Hardness (HV)	1900–2200	1800–2000
Young's modulus (GPa)	590	285–295
Fatigue resistance		It can increase in 33% in layers up to 40 μm in thickness (185 a 245 N/mm^2)

Table 1. Some chemical and mechanical properties of the iron borides.

1.2. Influence of the alloying elements on the growth of borides

The morphology of the growth front of the iron borides is determined mainly by the alloying elements in the substrate and not by the preferential crystalline growth of the layers in the [001] direction, as was initially proposed [3, 7]. A saw-toothed front is observed mainly in pure iron and low-to-medium carbon steels. However, in high-carbon-content steels, the thickness of the layers tends to decrease because carbon atoms do not diffuse on the boriding faces and tend to be pushed into the matrix of the substrate, thereby forming a diffusion zone just below the layer.

Elements like nickel and chromium in concentrations of up to 9% and 6% by weight, respectively, favor the formation of iron borides with flat growth fronts.

Segregation of the alloying elements occurs from the substrate to the boride layers by forming intermetallic compounds with active boron. The atoms of the alloying elements diffuse in the layer substitutionally and tend to concentrate in the tips of boride columns, causing a reduction in the active boron flow in this zone; this is why iron-boron reactions lose importance and the size of the columns decreases progressively.

Figure 2 shows three microphotographs of iron boride layers obtained from three ferrous substrates, where different morphologies of the growth fronts as a function of the alloying elements of each material can be observed.

1.3. Applications of the boriding process

The use of boriding as a surface-hardening process greatly improves the mechanical, physical and chemical properties of the surface of materials exposed to it.

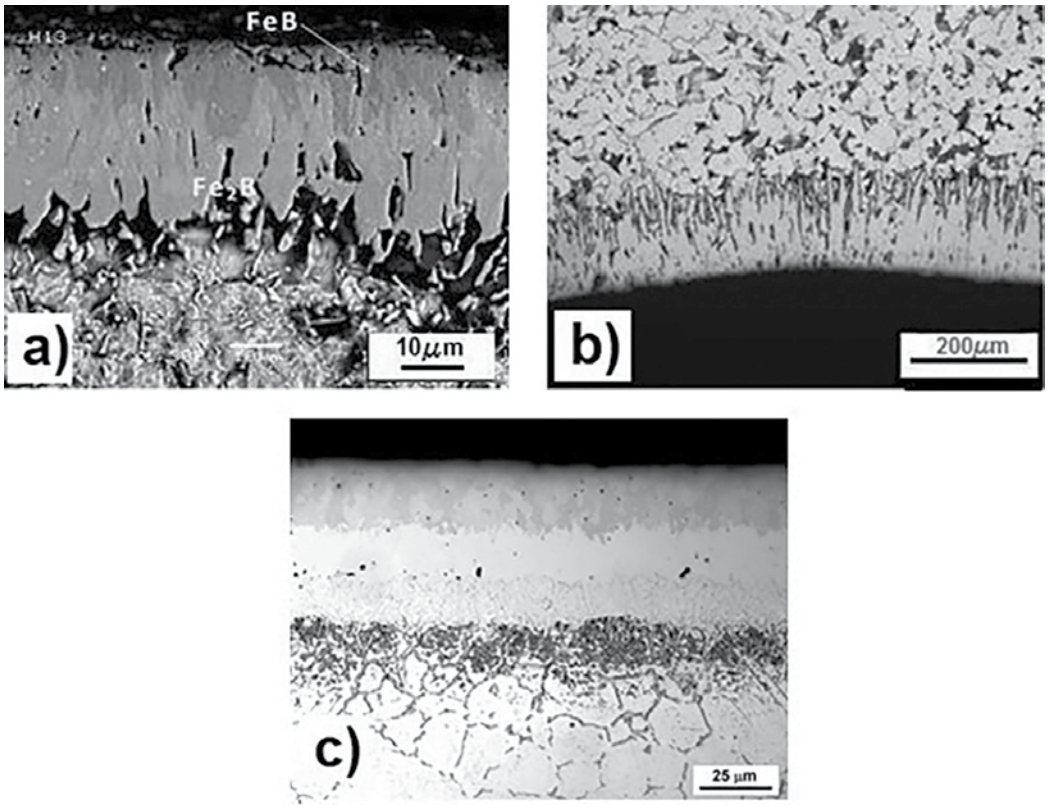

Figure 2. Morphology of the boride layers of different ferrous alloys: a) AISI H13, b) AISI 1018 and c) AISI 316.

Table 2 shows some materials exposed to boriding and their properties before and after the process.

Steel	Surface layer	Hardness (HV) Before and after treatment		Ref
(AISI)		Before	After	
5140	Fe_2B	253	1198–1739	[1]
4340	FeB-Fe_2B	300	1077–1632	[1]
D2	FeB-Fe_2B	660	1500–2140	[1]
1018	Fe_2B	126	1800–1843	[2]
9840	FeB-Fe_2B	265	1600	[9]
1018	Fe_2B	120	1700	[9]
4140	FeB-Fe_2B	290	1446–1739	[12]

Table 2. Materials exposed to boriding and the resulting properties.

In industrial applications, a single Fe_2B face is more desirable than a double FeB/Fe_2B-type face layer because of the formation of cracks in the interface of growth, which are caused by the

difference in the thermal expansion coefficients of the two faces. Additionally, the substrate generates residual stresses of compression and tension during the growth of borides.

1.4. Kinetics of growth of iron borides

1.4.1. Influence of experimental conditions on the formation of the iron boride layers

In order to control the boriding process and achieve its automatization, it is essential to know the kinetic parameters that govern it [8]. Some mathematical models have been developed to establish the variables that affect the kinetics of the boride layer formation process and thus generate a layer thickness according to the needs of the operation [9].

The thickness of the resulting layer has to be determined as a function of the base material. According to the industrial application, a layer thickness in the range of 15 to 20 μm (thin layers) is employed as protection against adhesive wear (stamping die, extrusion tools, etc.). For erosion-corrosion protection, it is recommended to work with relatively high-thickness layers (50 to 250 μm) formed on low-alloy steels. In the case of high-alloy steels, the optimum layer thickness is between 25 and 76 μm [10].

In this chapter, the evolution of boron diffusion on Fe_2B is described by considering the experimental data of layer growth, obtained during the application of the powder-pack boriding process to a low-carbon steel. Additionally, the kinetic growth of the Fe_2B layer can be analyzed by the estimation of its thickness as a function of the processing time in the examined temperature range.

1.4.2. Diffusion model

During the boriding process, the layer thickness increases as the treatment temperature and time increase, maintaining a parabolic relation between the thickness of the layer and the time of treatment [11].

From experimental layer thickness data, it is possible to determine the parabolic growth constants. It is necessary to assume that the rate of growth is controlled by boron diffusion by means of a dimensional analysis of the second law of Fick

$$\frac{\partial C}{\partial t} = D\frac{\partial^2 C}{\partial X^2} \tag{1}$$

In general, the deduction of Fick's second law is very complex; nevertheless, a solution can be considered as:

$$C_{(x,t)} = A + Berf\left(\frac{x}{2\sqrt{Dt}}\right) \tag{2}$$

The expression of Eq. (2) considers a case where the boron concentration profile in the Fe_2B face is a lineal function, as shown in **Figure 3**.

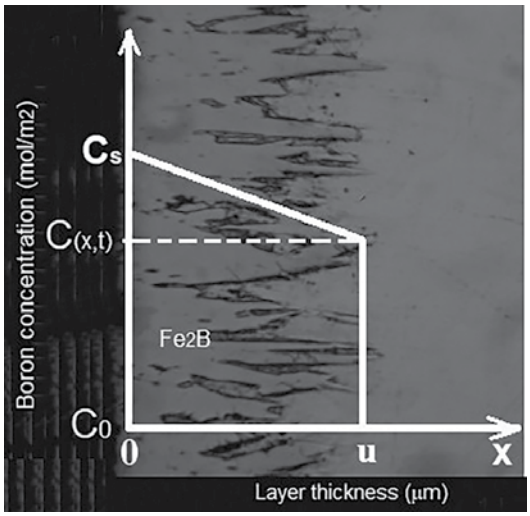

Figure 3. Schematic representation of the boron concentration profile on the Fe_2B layer.

The initial and boundary conditions for the interval $0 \leq x \leq u$ can be established from the concentration profile, as shown in **Figure 3**.

The initial conditions are:

$$x = 0, C_{(x,t)} = C_s \tag{3}$$

Thus, the substitution of x y $C_{(x,t)}$ in Eq. (2) results in:

$$C_s = A + B(0), \quad A = C_s \tag{4}$$

The boundary conditions are established as:

$$x = u; C_{(x,t)} = C_0 \tag{5}$$

Then, by substituting Eq. (5) in Eq. (2), it can be established that:

$$C_0 = C_s + Berf\left(\frac{u}{2\sqrt{Dt}}\right) \tag{6}$$

Then, extracting B from Eq. (6) results in:

$$B = \left(\frac{C_0 - C_s}{erf\left(\frac{u}{2\sqrt{Dt}}\right)}\right) \tag{7}$$

Replacing A and B in Eq. (4) results in:

$$C_{(x,t)} = C_s + \left(\frac{C_0 - C_s}{erf\left(\frac{u}{2\sqrt{Dt}}\right)}\right) \text{erf}\frac{x}{2\sqrt{Dt}} \tag{8}$$

On the other hand, it is well known that:

$$\lim_{u\to 0} erf\left(\frac{u}{2\sqrt{Dt}}\right) \Rightarrow 0 \tag{9}$$

$$\lim_{u\to \infty} erf\left(\frac{u}{2\sqrt{Dt}}\right) \Rightarrow 1 \tag{10}$$

Finally, the boron concentration in the Fe_2B layer is expressed as follows:

$$C_{(x,t)} = C_s + (C_0 - C_s) erf\left(\frac{x}{2\sqrt{Dt}}\right) \tag{11}$$

When the layer thickness (x) is extracted from Eq. (11), it can be rewritten as:

$$x^2 = \left[2\sqrt{D}\, erf^{-1}\left(\frac{C_{(x,t)} - C_s}{C_0 - C_s}\right)\right]^2 t \tag{12}$$

where:

$C_{(x,t)}$ is the boron concentration at a distance x at a time t (mol/m^3).

C_s is the boron concentration at the surface of the sample (mol/m^3).

C_0 is the boron concentration at the substrate (mol/m^3).

x is the thickness of the layer [μm].

t is the treatment time [s].

D is the boron diffusion coefficient in the Fe_2B layer [m^2/s].

erf is the Gauss error function [11].

Consequently, for a distance x at any time t, the relation between the boron concentrations and the diffusion coefficient remains constant, as shown in Eq. (13). Therefore, Eq. (12) takes the form of Eq. (14).

$$K = \left[2\sqrt{D}\, erf^{-1}\left(\frac{C_{(x,t)} - C_s}{C_0 - C_s}\right)\right]^2 \tag{13}$$

K is the constant of parabolic growth [m^2 s^{-1}], expressed by Eq. (13).

$$x^2 = Kt \tag{14}$$

x is the layer thickness [m] and K depends on the boron diffusion coefficient in the Fe_2B layer and the boron concentration gradients through the thickness of the Fe_2B layer, and t is the treatment time [s].

Considering that for the treatment conditions (time and temperature), the square of the layer thickness changes linearly with time, the relation between the constant of parabolic growth (K), the activation energy, and the temperature of the process can be expressed as an Arrhenius model:

$$K = K_o \exp\left(-\frac{Q}{RT}\right) \tag{15}$$

where K_o is a pre-exponential factor that depends on the boron potential of the boron source surrounding the substrate during the thermochemical treatment [$m^2\ s^{-1}$] and R is the universal constant of ideal gases [8.3144 J mol^{-1} K^{-1}].

The activation energy needed to make the diffusion process occur in the Fe_2B layer can be estimated by plotting Eq. (15) in logarithmic form, as follows:

$$\ln K = \ln K_o - \left(\frac{Q}{RT}\right) \tag{16}$$

Figure 4 shows the graph $\ln K$ *vs* $1/T$, where the resulting straight line can be observed.

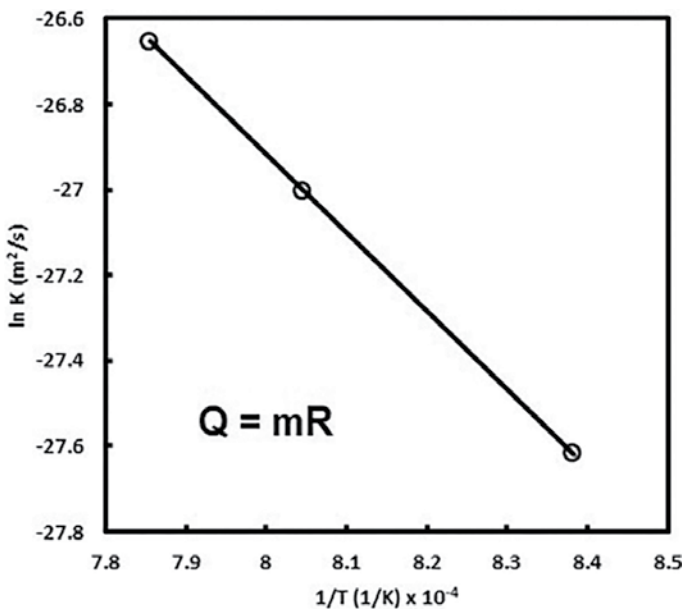

Figure 4. Graph $\ln K$ *vs* $1/T$.

Finally, after the constant of parabolic growth (K) and the pre-exponential factor (K_0) have been determined for the specific range of experimental conditions (temperature and time), Eq. (14) can be transformed to:

$$x = \sqrt{K_0 - \exp\left(\frac{-Q}{RT}\right)t} \tag{17}$$

Eq. (17) describes the relation between the layer thickness and the experimental parameters of time and temperature. According to Eq. (17), the behavior of the layer thickness as a function of the treatment conditions can be described by means of contour diagrams [12], based on the previously established empirical relations, between the process parameters and the thickness of the boride layers. These contour diagrams are especially useful when the aim is to optimize the boriding process, since the experimental parameters can be estimated as a function of the desired layer thickness.

Figure 5 shows a contour diagram that shows the experimental conditions of time and temperature as a function of the layer thickness.

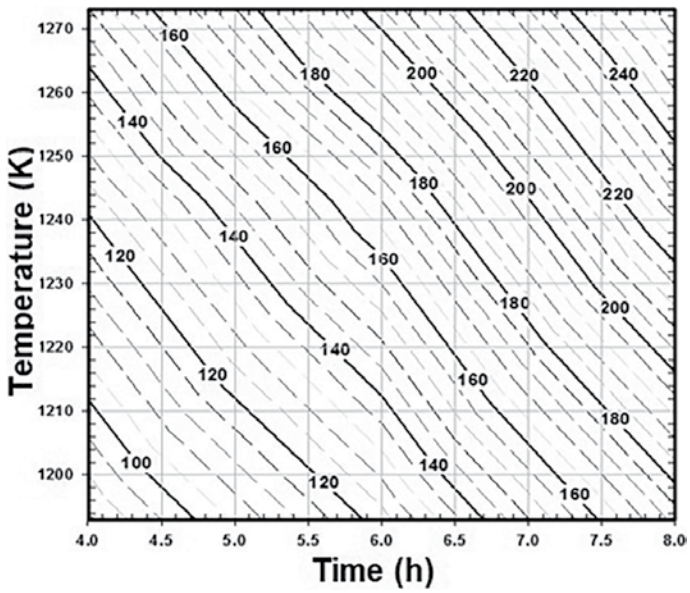

Figure 5. Contour diagram that describes the behavior of the iron boride layers as a function of the experimental conditions.

The contour diagram can be an excellent tool for determining the best treatment conditions for the generation of the determined layer thickness after the analysis of the experimental results.

1.4.3. Experimental considerations

Before to the experimental process it is necessary to observe certain considerations in order to obtain the best results. The next issues are the steps to follow during the powder-pack boriding process:

1.4.3.1. Establishment of treatment conditions

Boriding process takes place in a range of temperatures from 800 to 1100°C and exposure times between 1 and 12 h, depending on the chemical composition of the substrate. The treatment

conditions are the main features that determine the characteristics of the layers such as thickness, hardness and Young's modulus.

1.4.3.2. Selection and preparation of the material

Boriding process can be applied to a several metallic materials, nevertheless, it is very important to consider that resulting layers will be affected by the chemical composition of the substrate. Also the dimensions of the samples have to be considered according to the internal dimensions of the furnace.

Samples should be metallographically prepared in order to allow the correct diffusion of the boron. The metallographic process consists on grind the samples by means of SiC emery paper from 60 to 600 mesh to obtain a good final roughness after the boriding process. Samples should be clean preferably by sonication to remove any impurity.

1.4.3.3. Packaging of the samples

Samples should be packaged in a SS container as shown in **Figure 6**, it is very important to make sure that the samples are perfectly covered with the powder mixture to avoid the oxidation. The powder mixture can be of different composition but the most commonly used is CSi 90% wt., B_4C 5% wt., and KBF_4 5% wt.

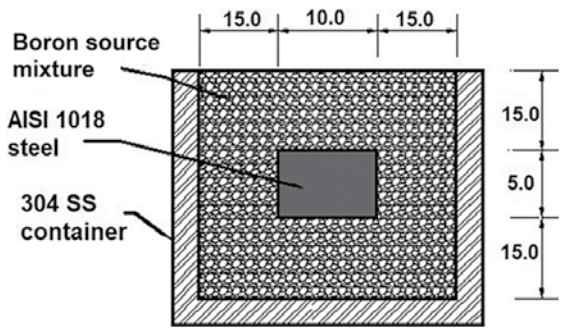

Figure 6. Schematic representation of the location of the samples inside the boriding mixture (dimensions in millimeters).

1.4.3.4. Furnace requirements

For the application of the powder-pack boriding it is no necessary a special furnace, so that, it is enough a conventional furnace with temperature control. The temperature of the furnace has to be set according to the pre-established value and let that the furnace is to stabilize.

1.4.3.5. Thermochemical treatment

Once the temperature in the furnace is stable, the SS container with the samples is set into it and after the temperature stabilizes again, the process starts.

After the process time, the SS container with the samples is removed from the furnace and cooled to room temperature in quiet air. Then, samples are cleaned with scotch fiber to remove impurities.

1.5. Application example

1.5.1. Treatment conditions

In this application example, three temperatures (1173, 1223, and 1273 K) and three exposure times (1.5, 3, and 5 h) for each temperature were considered, as treatment conditions.

Experimental conditions are the main features that determine the layer's properties such as thickness, hardness and Young's modulus.

1.5.2. Sample material

Cylindrical samples of AISI 1018 (structural Steel) with 10 mm diameter and 5 mm length were considered as the samples for the experiments. Their chemical composition was as follows: 0.15–0.20%wt. C, 0.6–0.90%wt. Mn, 0.04%wt. P max., 0.15–0.30%wt. Si and 0.05%wt. S max. The hardness of annealed AISI 1018 is 126 HB; nevertheless, after boriding a surface layer, high hardness can be expected (2000 HV).

1.5.3. Thermochemical treatment of powder-pack boriding

Powder-pack boriding was considered as a good alternative to generate hard layers, because it is a low-cost process and the resulting layers are of reasonable quality. The process consists of packing the samples in a powder mixture rich in boron inside of a stainless steel box.

The powder-pack method offers some advantages over others techniques because it does not require the presence of an inert atmosphere, so that it can be carried out in a conventional furnace. The powder mixture generally consists of 5%wt. B_4C which acts as a boron donor, 5% wt. KBF_4 which acts as an activator and 90%wt. SiC which acts as a diluent [13].

The samples´ location inside of the SS box is of great importance because the amount of boron that diffuses to the samples depends on the amount of boron in the source surrounding the samples [13]. In addition, an insufficient amount of boriding agent can facilitate the presence of oxygen, which would allow the formation of iron oxides on the surface of the material. A boriding agent thickness of 10 mm around the samples is considered enough to protect them from oxidation during the process because of the absence of an inert atmosphere.

The chemical reaction that takes place during the boriding process is as follows:

$$B_4C + 3SiC + 3O_2 \xrightarrow[SiF_4]{BF_3} 2Si + SiO_2 + 4CO \tag{18}$$

It is clear that KFB_4 aggregated as an activator does not interfere in the chemical reaction, so that it does not contribute free boron during the thermochemical process.

1.5.4. Physical characterization of the hardened steels

Figure 7 shows the process diagram of the physical characterization of the Fe_2B layers obtained on the surface of the ASISI 1018 steel.

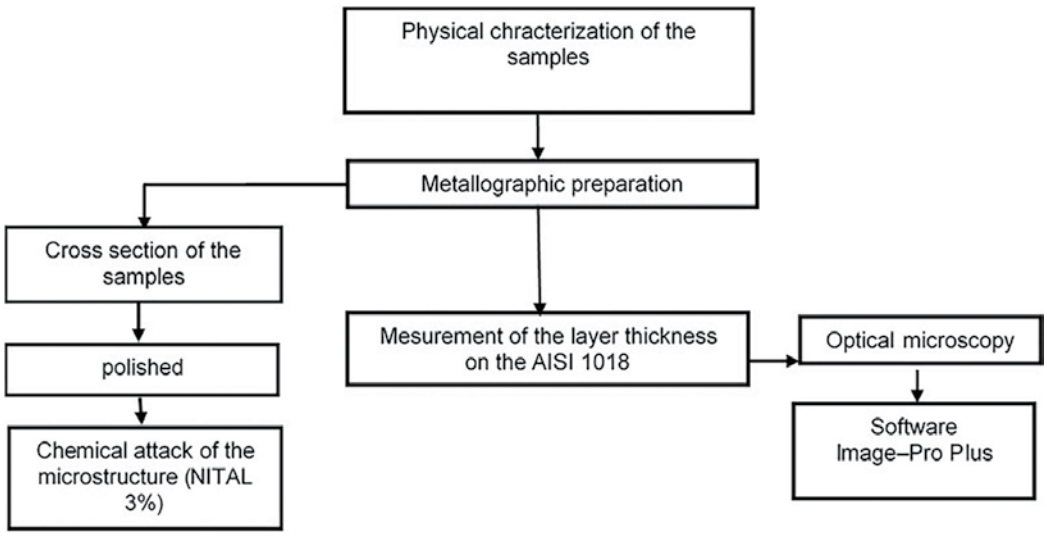

Figure 7. Flux diagram of the physical characterization of the AISI 1018 steel.

1.5.5. Layers thickness measurement

The measurement of the layer thickness was realized through the digitization of microscopy images by means of specialized software of image analysis.

Figure 8 shows the methodology used for the measurement of the layer thickness of the Fe_2B layers. At least 50 measurements are recommended for each picture in order to achieve a reliable value of the thickness.

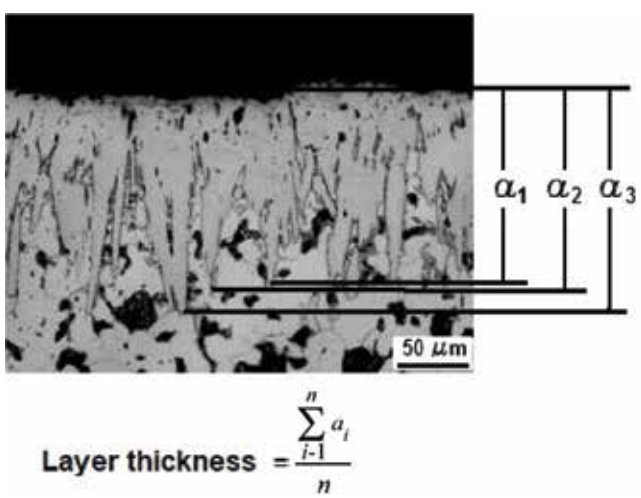

Figure 8. Methodology for the layer thickness measurement.

1.6. Results and discussion

1.6.1. Layer thickness

The layer thickness was obtained by the methodology described in **Figure 8**. Each numerical value of layer thickness was the result of the average of at least 50 measurements and the results are shown in **Table 3**.

Temperature. (K)	1.5 h	3 h	5 h
1173	32.51 ± 3.92	58.57 ± 6.27	73.96 ± 6.24
1223	45.37 ± 5.11	67.05 ± 10.28	86.02 ± 7.23
1273	48.55 ± 4.22	76.82 ± 6.67	97.84 ± 10.01

Table 3. Layers thickness of Fe_2B (μm) obtained for the different treatment conditions of time and temperature.

Figure 9 shows the evolution of the layer thickness as a function of the temperature and treatment time, according to Eq. (14).

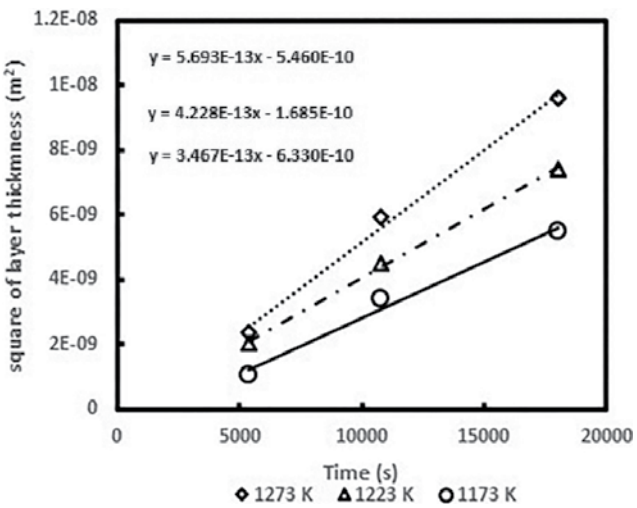

Figure 9. Evolution of the layer growth as a function of the different treatment conditions.

According to the results, the growth of the layers is described by a parabolic function (Eq. 14). The slopes of the lines obtained from **Figure 9** represent the constants of parabolic growth K, which indicates a controlled growth [1, 8, 14, 15].

Table 4 shows the values of the parabolic growth constant K, which were obtained from the slopes of the straight lines shown in **Figure 9**.

Temperature (K)	K (m^2 s^{-1})	1/T	Ln K	K_0	Q (KJ/mol)
1173	3.47E-13	8.53E-04	−2.87E + 01	1.8383E-10	61.3719122
1223	4.23E-13	8.18E-04	−2.85E + 01		
1273	5.69E-13	7.86E-04	−2.82E + 01		

Table 4. Constant of parabolic growth (K) and parameters for calculation of activation energy.

1.6.2. Estimation of the activation energy

Interstitial diffusion occurs when the atoms move from an interstitial position to another unoccupied neighbor but without permanently displacing any of the atoms in the crystalline network of the solvent. In general, less energy is required to displace an interstitial atom from the surrounding places. Consequently, the activation energy necessary for the process is smaller for interstitial diffusion than for vacancy or substitutional diffusion.

The activation energy necessary to make the process occur can be obtained by applying an Arrhenius-type expression (Eq. 16), as shown in **Figure 10**. As one can observe, from the plotting of the Eq. 16 (**Figure 10**), the slope of the straight line resulting of the graph can be used for the calculation of the activation energy as follows:

$$m = \frac{Q}{R} \tag{19}$$

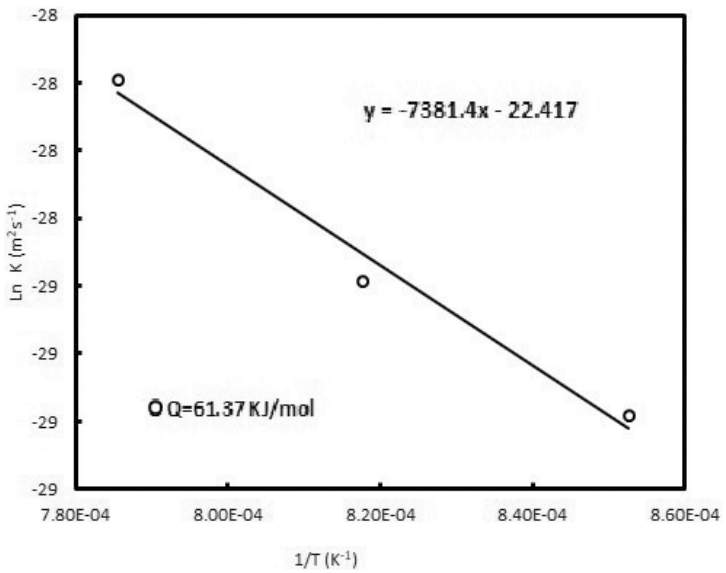

Figure 10. Behavior of the constant of parabolic growth as a function of the treatment temperature.

According to Eq. (19), activation energy can be estimated as:

$$Q = m*R$$

Then, by substituting the values of m and R:

$$Q = (7381.4)(8.3144)$$

The estimated activation energy value for the formation of the Fe_2B layer on the AISI 1018 steel surface was 61.37 KJ/mol. This value was compared with those obtained by different studies for different boriding steels (**Table 5**).

Material	Boriding method	Faces in the layer	Layer morphology	Activation energy, kJ/mol	Reference
AISI W1	B_4C powder	FeB, Fe_2B	Flat	171.2	[16]
AISI 5140	Salt bath	FeB, Fe_2B, CrB, Cr_2B	Saw-toothed	223	[1]
AISI 4340			Saw-toothed	234	
AISI D2			Flat	170	
AISI H13	B_4C paste	FeB, Fe_2B, CrB, Cr_2B	Flat	186.2	[17]
AISI 4140	Salt bath	FeB, Fe_2B, CrB	Saw-toothed	218.4	[12]
AISI 1018	B_4C paste	Fe_2B	Saw-toothed	161.82	[11]
AISI 1018	B_4C Powder	Fe_2B	Saw-toothed	61.37	Present work

Table 5. Values of the activation energy obtained for different steels exposed to boriding.

As can be seen in **Table 5**, the activation energy is also a function of the chemical composition of the substrate exposed to boriding, so that it increases as the alloying elements in the substrate increase.

The pre-exponential factor (K_0) can be also achieved from the **Figure 10** as shown in **Table 4**.

According to the results obtained from the **Figure 10**, Eq. (17) can be re-written as:

$$x = \sqrt{1.84E - 10 \exp\left(-\frac{61371.9122}{8.3144T}\right)(t)} \tag{20}$$

Eq. (20) can be used to estimate the layer thickness as a function of the experimental conditions of time and temperature.

Table 6 compares the experimental values of the layer thickness and those estimated by Eq. (20) after determining the activation energy Q and the pre-exponential constant K_0 values for the treatment conditions.

Temperature. (K)	1.5 h		3 h		5 h	
	Experimental	By model	Experimental	By model	Experimental	By model
1173	32.51 ± 3.92	39.98	58.57 ± 6.27	56.55	73.96 ± 6.24	73.01
1223	45.37 ± 5.11	45.61	67.05 ± 10.28	64.5	86.02 ± 7.23	83.26
1273	48.55 ± 4.22	51.48	76.82 ± 6.67	72.8	97.84 ± 10.01	93.99

Table 6. Comparison between the experimental values of layer thickness (μm) and those obtained by applying the Eq. 20.

Table 6 shows a good agreement between the experimental values and those obtained from Eq. (20). These results indicate that it is possible to optimize the boriding process in industrial applications.

1.6.3. Contour diagram

Based on Eq. (20), it is possible to generate a contour diagram that represents the evolution of the layer thickness as a function of the experimental parameters, as shown in **Figure 11**.

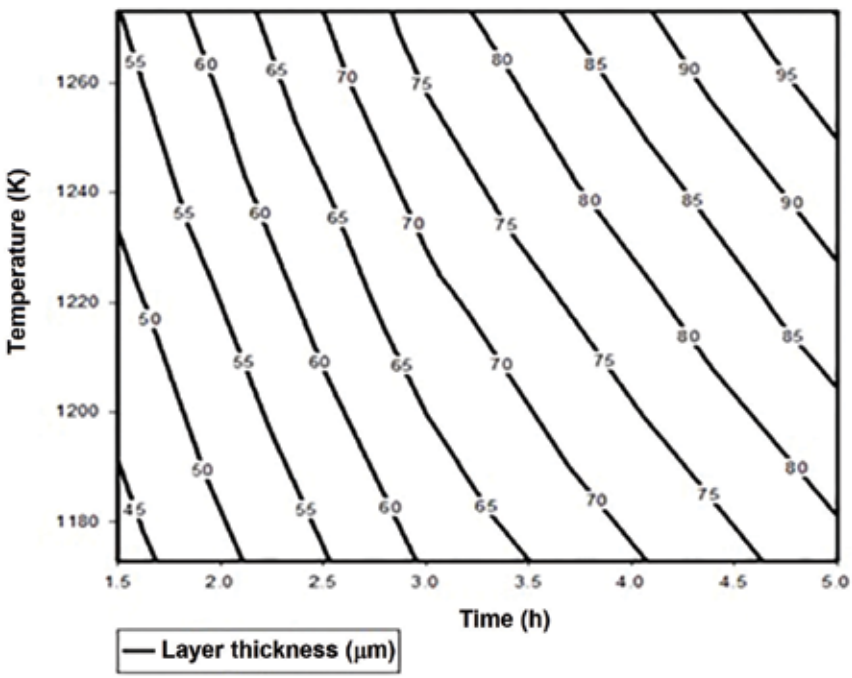

Figure 11. Contour diagram for the estimation of the layer thickness as a function of the experimental conditions.

Contour diagrams like these are especially useful in industrial applications, where representative process schemas are required to estimate quickly and reliably the desired layer thicknesses for a particular application.

1.7. Conclusions

According to the results, it is possible to observe that the layer thickness increases as the temperature and the treatment time increases, so the layer growth can be controlled.

The behavior of the parabolic growth constant as a function of the treatment temperature was established to determine the activation energy required for the formation of the boride layer on the surface of the AISI 1018 steel. Likewise, the boriding mixture used for the formation of the surface layer was enough to supply the required boron at different treatment conditions of time and temperature.

Finally, the growth of the Fe_2B layers on the surface of the AISI 1018 steel was represented by a contour diagram that establishes the time and temperature conditions of the boriding process, which helps to ensure the optimization of the process for superficially hardened low-carbon steels.

Author details

Enrique Hernández-Sánchez[1]* and Julio Cesar Velázquez[2]

*Address all correspondence to: enriquehs266@yahoo.com.mx

1 Instituto Politécnico Nacional-UPIBI, México City, México

2 Departamento de Ingeniería Química Industrial, ESIQIE, Instituto Politécnico Nacional, México City, México

References

[1] Sen S, Sen U, Bindal C. An approach of kinetic study of borided steels. Surface and Coatings Technology. 2005;**191**(2–3):274-285. DOI: http://doi.org/10.1016/j.surfcoat.2004.03.049

[2] Hernández Sánchez E. CARACTERIZACIÓN DE ACEROS BORURADOS AISI H13 [Thesis]. México: Instituto Politécnico Nacional. SEPI-ESIME; 2008. p. 145

[3] Von Matuschka AG. Boronizing. 1st ed. Germany: Carl Hanser Verlag; 1980. p. 97

[4] Campos Silva IE. Cinética de Difusión en el Proceso termoquímico de Borurización en aceros estructurales, de Baja Aleación, Herramientas e Inoxidables [thesis]. México: Universidad Autónoma Metropolitana; 1994. p. 165

[5] Campos I, Ramírez G, Figueroa U, Martínrz J, Morales O. Evaluation of boron mobilty on the faces FeB, Fe_2B and diffusion zone in AISI 1045, and M2 steels. Applied Surface Science. 2007;**253**(7):3469-3475. DOI: https://doi.org/10.1016/j.assusc.2006.07.046

[6] Palombarini G, Sambogna G, Carbucicchio M. Pole of Oxygen in iron boriding using boron carbide. Journal of Materials Science Letters. 1993:741-742. DOI: 10.1007/BF00626705

[7] Fisher C, Schaaber R. Proceeding of heat treatment. The Metals society. 1976;**76**:27-30

[8] Campos I, Oseguera J, Figueroa U, García JA, Bautista O, Kelemenis G. Kinetic study of boron diffusion in the pasts boriding process. Materials Science and Engineering. 2003; **352**(1–2):261-265. DOI: https://doi.org/10.1016/S0921-5093(02)00910-3

[9] Melendez E, Campos I, Rocha E, Barron MA. Structutal and Strength Characterization. Materials Science and Engineering: A. 1997;**234-236**:900-903. DOI: https://doi.org/10.1016/S0921-5093(97)00389-4

[10] Campos Silva I, Ortiz Domínguez M, Cimenoglu H, Escobar Galindo R, Keddam M, Elias Espinosa M, López Perrusquia N. Diffusion model for growth of Fe_2B layer pure iron. Surface Engineering. 2009;**27**(3):189-195. DOI: 10.1179/026708410X12550773057820

[11] Villa Velázquez Mendoza C. Estudio del Agrietamiento Tipo Palmqvist y Evaluación de Esfuerzos Residuales en Aceros Borurados AISI 1018 [thesis]. México: Instituto Politécnico Nacional-ESIME; 2009. p. 209

[12] Sen S, Sen U, Bindal C. The growth kinetic of borides formed on boronized AISI 4140 steel. Vacuum. 2005;**77**(2):195-202. https://doi.org/10.1016/j.vacuum.2004.09.005

[13] Vipin J and Sundararajan G. Influence of the pack thickness. Surface and Coatings Technology. 2002;**149**(1):21-26. https://doi.org/10.1016/S0257-8972(01)01385-8

[14] Campos I, Ramírez G, Figueroa U, Villa VC. Paste boriding process evaluation of boron mobility on borided steels. Surface Engineerin. 2007;**23**(3):216-222. http://dx.doi.org/10.1179/174329407X174416

[15] Campos-Silva I, Ortíz-Domínguez M, López Perrusquia N, Escobar-Galindo R, Gómez-Vargas OA, Hernández-Sánchez E. Determination of boron diffusion coefficients in borided tool steels. Defect and Diffusion Forum. 2009;**283-286**:681-686. DOI: 10.4028/www.scientific.net/DDF.283-286.681

[16] Genel K, Ozbek I, Bindal C. Kinetics of boriding of AISI W1 steel. Materials Science and Engineering: A. 2003;**347**(1–2):311-314. https://doi.org/10.1016/S0921-5093(02)00607-X

[17] Genel K. Boriding kinetics of H13 steel. Vacuum. 2006;**80**(5):451-457. DOI: 10.1016/j.vacuum.2005.07.013

Chapter 4

Hydrodynamic Characterization of Physicochemical Process in Stirred Tanks and Agglomeration Reactors

Benjamin Oyegbile and Guven Akdogan

Additional information is available at the end of the chapter

http://dx.doi.org/ 10.5772/intechopen.77014

Abstract

A short review of the state of the art in experimental and computational fluid dynamics (CFD) characterization of micro-hydrodynamics and physicochemical processes in stirred tanks and agglomeration reactors is presented. Results of experimental and computational studies focusing on classical mixing tanks as well as other innovative reactors with various industrial applications are briefly reviewed. The hydrodynamic characterization techniques as well as the influence of the fluid dynamics on the efficiency of the physicochemical processes have been highlighted including some of the limitations of the reported modeling approach and solution strategy. Finally, the need for specialized CFD codes tailored to the specific needs of fluid-particle reactor design and optimization is advocated to advance research in this field.

Keywords: physicochemical, hydrodynamics, wet agglomeration, stirred tanks, CFD

1. Introduction

Hydrodynamic and physicochemical interactions play an important role in many industrial unit processes and hence its importance in many engineering applications of fluid flow. Fluid flow investigations in a wide range of process conditions as well as complex biological, physical and chemical processes have been the subject of many scientific publications over the past two decades. Several studies on bench, pilot and industrial scales have been conducted on a wide variety of hydrodynamic conditions and different reactor geometric designs. In many of these studies, the aim is to provide an insight into the fluid flow and process dynamics in terms of the spatial and temporal evolution within the flow device, and in some cases, performance testing of newly designed flow units and processing techniques with potential applications on

industrial scale. Regardless of the focus of these studies, it is quite apparent that valuable information can be obtained from the basic study of fluid flow dynamics in process units especially from design and optimization perspective.

A quick survey of the studies in this field shows that many innovative process reactors have been successfully tested on different scales for a wide variety of technical applications ranging from fine particle separation and water purification to cell culture preparation [1–6]. Experimental data, which are collected in these studies for numerical validation purposes, are often used to characterize the hydrodynamic behaviour as well as to quantify the fluid parameters of interest such as the flow velocity profile, vorticity, turbulent kinetic energy and its rate of dissipation, turbulent intensity, and so on. While there is a large body of scientific literature focusing on the hydrodynamics and physicochemical processes in stirred tank reactors, the aim of the present communication is to briefly summarize developments in this field especially in the application of the knowledge of the fluid dynamics to fluid-particle reactor design, development and optimization.

2. Design and formulation of mixing tank problems

2.1. Design parameters and process optimization

In fluid engineering problems, research has shown that it is possible to optimize all influencing process parameters in an evolutionary manner right from the conceptual design to the final performance testing phase. This will entail the integration of the fluid flow investigation with the process reactor conceptual design and system optimization [1]. Nowadays, this multistage process design and optimization work flow shown in **Figure 1** can be fully automated through the use of computational platform. In formulating and developing a numerical solution strategy to a particular physical problem involving fluid-particle interactions, a sound theoretical

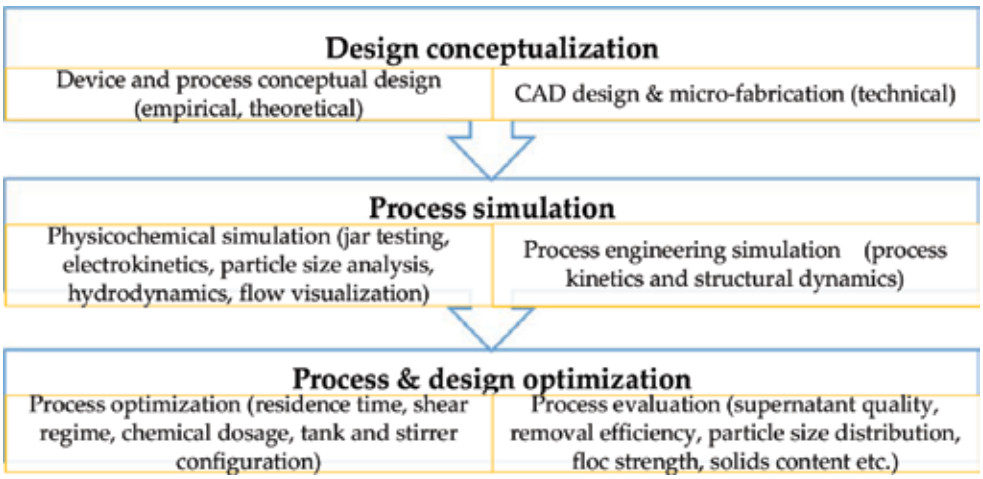

Figure 1. Reactor design and process optimization parameters in mixing tank applications.

http://dx.doi.org/ 10.5772/intechopen.77014

understanding and analysis of the problem is often required. This will assist in the selection of appropriate experimental data collection methods and mathematical models that sufficiently encapsulate the physics of the problem. A number of numerical approaches and solution strategies discussed in the subsequent sections have been developed for a multitude of fluid flow scenarios. Therefore, it is important to evaluate each circumstance individually and form an opinion regarding which model would provide the best fit for a particular fluid engineering problem. It has been suggested that the robustness of any mathematical model is a function of the numerical code being used and the flow scenario being modeled [7].

2.2. Fluid dynamics and governing equations

The interactions of different phases in fluid flow occur on different scales of the fluid motion as depicted in **Figure 2**. Fluid dynamics is primarily focused on the macroscopic phenomena of the fluid flow in which the fluid is treated as a continuum. For instance, a fluid element is composed of many molecules, and the fluid dynamics represent the behaviour of the numerous molecules within the system. This concept with certain assumptions forms the basis of the derivation of fluid conservation equations of mass and momentum also known as the Navier-Stokes equation using a fluid control volume [8, 9]. The general form of the governing equations of mass and momentum conservation in any fluid flow system can be written as follows (Eqs. (1) and (2)):

$$\frac{\partial \rho}{\partial t} + \nabla \cdot \left(\rho \vec{v}\right) = S_m \tag{1}$$

$$\frac{\partial}{\partial t}\left(\rho \vec{v}\right) + \nabla \cdot \left(\rho \vec{v} \vec{v}\right) = -\nabla p + \nabla \cdot \left(\overline{\overline{\tau}}\right) + \rho \vec{g} + \vec{F} \tag{2}$$

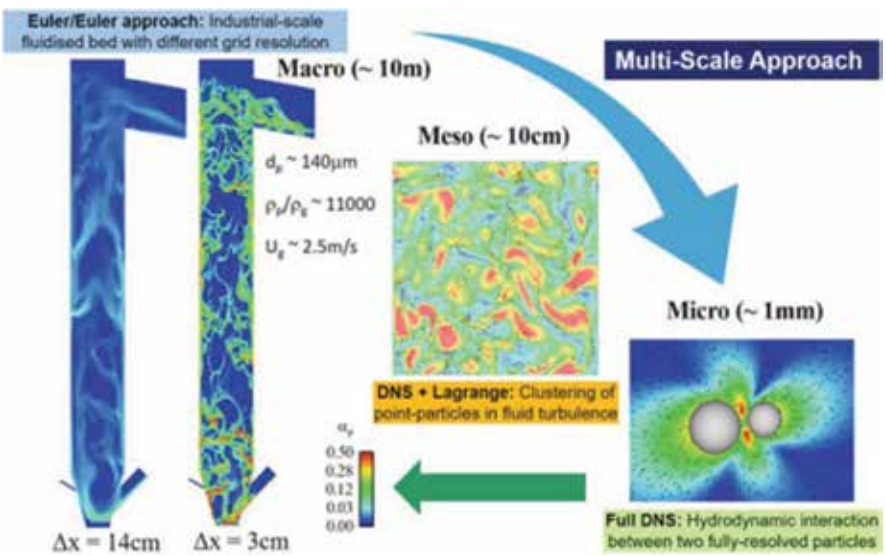

Figure 2. Multiscale modeling approach to fluid-particle interactions (reproduced from [14] with permissions © 2017 Springer).

where ϱ is the density, p is the static pressure, $\vec{v}$ is the velocity component, S_m is the source term that represent the mass added to the continuous phase from the disperse phase or any user define source, $\bar{\tau}$ represents the stress tensor due to viscous stress, $\varrho\vec{g}$ is the gravitational force and $\vec{F}$ represent the exerted body forces [10–13].

2.3. Modeling approach and solution strategies

In modeling complex single and multiphase flows in mixing tanks and process reactors, there exist two common numerical solution strategies, namely Eulerian-Eulerian and Eulerian-Lagrangian modeling approach, depending on the scale of the fluid flow as shown schematically in **Figure 3**. In the former, the fluid domain is treated as an interpenetrating continuum, while in the latter, the discrete or distinct particles of the dispersed phase are tracked in the Lagrangian reference frame. In addition to the flow field, information on the particle population such as the mean size, mass or volume fraction, and number density can be obtained using either of the two approaches [10]. Several variants of these two classes exist such as the Eulerian granular model based on the kinetic theory of granular flow (KTGF), disperse phase model (DPM), discrete element model (DEM) and the macroscopic particle model (MPM). In the case of Eulerian-Eulerian approach, the species distribution of the discrete phase may be accounted for using the population balance model (PBM), while the Eulerian-Lagrangian models can directly compute the particle size distribution while taking into account different collision and interaction mechanisms using DEM [15–18].

2.3.1. Treatment of flow domain and turbulent flow conditions

Turbulence modeling forms an integral part of the numerical analysis of complex fluid flows since most engineering fluid flows entail certain form of instability. Several closure models

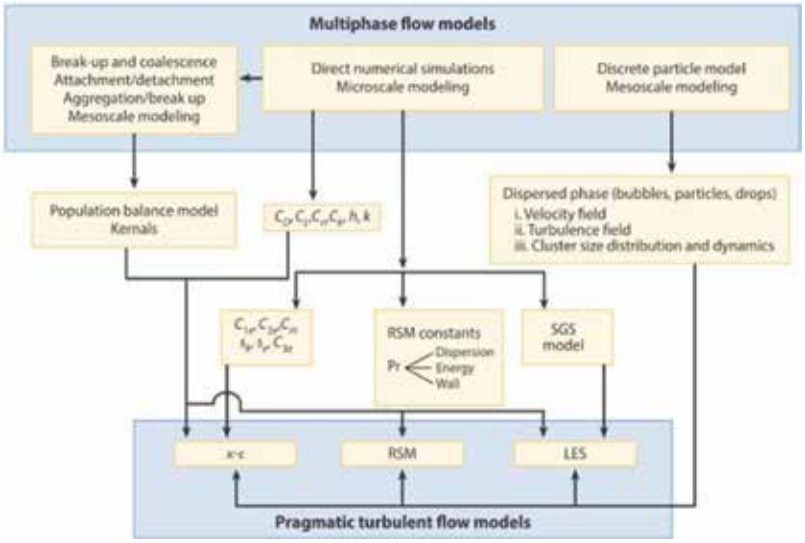

Figure 3. Parametric relationships between different modeling strategies (reproduced from [19] with permissions © 2015 Annual Reviews).

have been developed for resolving turbulence parameters in steady-state Reynolds Averaged Navier-Stokes (RANS) equations. The two equation eddy viscosity models such as k-ε and k-ω have been found to perform reasonably well in the modeling of rotating flows in process reactors with the only drawback being the assumption of local isotropic turbulence. The underlying theoretical assumptions underpinning the use of these models can be found in the following reference texts [12, 13]. Since the reactors encountered in most of the practical physicochemical processes contain moving or rotating parts, it is therefore necessary to take this into consideration in the preparation of the computational grid. The most common strategy for steady-state calculations include the single reference frame (SRF), multiple reference frame (MRF) or frozen rotor approach, mixing plane model (MPM) and snapshot approach, while the sliding or dynamic mesh is frequently used in transient calculations of fluid flow. For detailed information on the practical applications of the above-mentioned methods, readers are referred to the following reference texts [20, 21].

2.3.2. Model coupling for multiphase flow problems

Modeling complex physicochemical processes involving fluid flow sometimes necessitates the integration of the existing mathematical models in order to appropriately describe the physics of the problem. This can be achieved through the use of specially developed or customized in-house numerical codes or a modification of the existing ones with several software package vendors offering a platform for software improvement through the use of Application Programming Interface API or Application Customization Toolkit ACT. Such flexibility allows engineers and researchers to extend the capability and versatility of the existing numerical codes. Many software vendors go a step further in this respect by actively encouraging the development of scalable apps that extend the capability of their core software; an excellent example is the mixing tank template released by ANSYS Inc. for the automation of mixing tank simulation process. However, there exist several other flexible options for numerical code development using the open source platform, and the readers are advised to consider available options for their specific problem.

3. Experimental analysis of physicochemical processes

Several analytical and instrumental techniques have been developed for the study of complex hydrodynamic-mediated processes found in particle-laden flow—flocculation, wet agglomeration, sedimentation, floatation, fluidization and crystallization that often occur in a wide range of process conditions. These techniques shown in **Figure 4** are used either in the quantification of the hydrodynamics of the carrier and dispersed phase, or in the determination of the spatial and temporal evolution of the discrete phase properties such as the change in the particle size and distribution. In the case of the hydrodynamic interactions of the carrier and dispersed phase, a number of laser-based fluid flow techniques such as particle image velocimetry (PIV), particle tracking velocimetry (PTV), laser Doppler anaemometry (LDA), laser Doppler velocimetry (LDV), and more recently, radioactive tracking techniques such as positron emission particle tracking (PEPT) and computer-aided radioactive particle tracking (CARPT) have gained wider acceptance in the scientific community and in industry due to

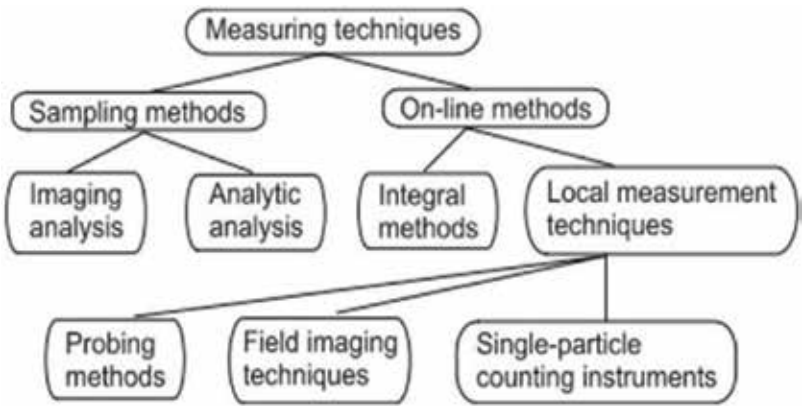

Figure 4. Experimental measurement techniques for multiphase particulate flow (reproduced from [18] with permissions © 2012 CRC Press).

their ease of use and non-intrusive nature [20–22]. These techniques provide valuable insight into the salient macroscale fluid flow characteristics such as the instantaneous and time-averaged hydrodynamic behaviour of the continuous phase, as well as the influence of the dispersed phase on the fluid flow. This is achieved by coupling the flow field measurements with the particulate phase properties and motion [21]. The experimental data set is subsequently used in the validation of numerical simulation results [18, 23].

The dominant and widely used macroscale experimental fluid flow characterization techniques are the laser velocimetry and radioactive particle tracking techniques such as the PIV or PTV, LDV or LDA with the PIV reported to be a more efficient technique [24]. These on-line methods facilitate the determination of the properties of multiphase particle-laden flow especially at low concentration. These local methods are quite superior to other similar techniques such as optical fiber probing and light scattering due to their non-intrusive nature with little or no interference on the flow while providing time series and time-averaged fluid flow characteristics with a high spatial resolution [18]. The workings of typical field imaging technique such as PIV consist of the tracer particles, laser source for flow illumination and high capacity cameras—complementary metal-oxide semiconductor (CMOS) or charge-coupled device (CCD) for the fluid flow image recording. The captured images are thereafter post-processed and correlated to obtain the hydrodynamic parameters of interest. **Table 1** provides a list of recent publications on the experimental analysis of physicochemical processes in stirred tanks. These studies demonstrated the importance of robust and reliable experimental data for complex fluid flow analysis and numerical model validation. Recent advances in experimental techniques have led to the emergence of radioactive particle tracing measurement techniques which aim to improve the ease of data collection, data accuracy and reliability.

In order to correlate the hydrodynamic and process conditions with the suspension or dispersion properties especially the change in the species concentration—spatial and temporal evolution of the particle size distribution, a number of laboratory measurement techniques are widely adopted [25]. The choice will depend to a large extent on the concentration and size distribution of the disperse phase and the nature of the flow. Regardless of the chosen analytical approach, such a correlation will facilitate an assessment of the treatment process

Reactor configuration	Stirrer configuration	Experimental technique	Technical application	Tracer particles
Cylindrical tank	Rotating disc	2D PIV	Mixing/agglomeration	Silver-coated and hollow glass spheres [1]
Cylindrical tank	Hydrofoil impellers	PEPT	Mixing	Radioactive particles [26]
Cylindrical tank	Rushton turbine	PIV	Mixing	Polymeric and glass particles [27]
Cylindrical tank	Hollow blade semi-elliptic disc turbine	TRPIV, PIV	Mixing	Neutrally buoyant glass beads [24]
Cylindrical tank	Pitched-blade turbine impeller	FPIV	Mixing	Soda-lime glass beads [28]
Cylindrical tank	Rushton turbine	CARPT	Mixing	Radioactive particles [29]
Cylindrical tank	Rushton turbine	LDA	Mixing	Hollow glass spheres [30]
Cylindrical tank	Kenics static mixer	PEPT	Mixing	Radioactive particles [31]
Cylindrical tank	Pitched-blade turbine	PEPT	Mixing	Radioactive particles [32]
Cylindrical tank	Pitched-blade turbine	PIV	Mixing	Silica glass spheres [23]
Square tank	Hydro foil impeller	PIV, image analysis	Mixing/agglomeration	In situ agglomerated flocs [33]
Cylindrical tank	Six-blade Rushton turbine	3V3	Mixing	Opt image polycrystalline particles [34]
Cylindrical tank	Rushton turbine, pitched-blade turbine	PEPT	Mixing	Monosized silica gel particles [35]
Cylindrical tank	Six-blade Rushton turbine	PEPT, LDA	Mixing	Ion-exchange resin particles [36]
Cylindrical tank	Rotor-stator mixer	PIV	Mixing	Polyamide particles [37]

Table 1. Selected studies on the experimental analysis of physical and chemical processes in stirred tanks.

and the reactor performance under a particular process condition. For instance, the conventional physicochemical simulation tests such as the cylinder, Imhoff cone and jar tests can be combined with parametric analytical techniques such as the Buchner-funnel or pressure filtration test, capillary suction time (CST) test, electrokinetic charge analysis using colloidal titrations (i.e. zeta and streaming potential), laser light scattering or laser diffraction, microscopy, image analysis, photometric dispersion analysis (PDA), fiber optic sensor and HNMR spectroscopy. These techniques have been successfully employed to characterize the physicochemical process in bench, pilot and full-scale studies [38–41]. A careful consideration of the limitations of each of these approaches will ensure proper selection of an appropriate method.

In most of the physicochemical processes involving particulate flow either as a colloidal dispersion or granular suspension, the species attributes—mean size, particle concentration and distribution and fractal properties of the resulting agglomerates—are the primary parameters of interest [21]. In this case, an appropriate physicochemical simulation such as a jar or cylinder test is often followed by a parametric analysis to characterize the process performance as a function of species attributes. Several other parameters may be of interest depending on the type of reactor and the required solid-liquid separation method. Such parameters may include aggregate mean size, shape and distribution, aggregate volume concentration, aggregate strength, sludge volume index, silting index, residual supernatant turbidity, absorbance or optical density, electrical conductivity, viscosity, zeta or streaming potential, specific resistance to filtration, capillary suction time, and so on [38, 39]. In the case of chemical optimization, a parametric dose-response curve will give reasonably accurate information on the required chemical dose for a particular process condition [42–45]. **Table 2** and **Figure 5** show a typical correlation of the agglomerate test properties with the process condition—shear rate. However, regardless of the choice of parametric test, an examination of the supernatant, sediment, filtrate and residue will yield some valuable information on the reactor performance under specific process conditions. Such assessment is carried out either by direct *in situ* measurements such as in particle counting, *ex situ* analysis in which the samples are extracted for measurements or by other indirect parametric indicators. A detailed discussion on the practical applications of different dispersed phase measurement techniques is available elsewhere [40, 41].

Considering the wide range of options available to select from, optimizing a given physicochemical condition for a particular process reactor under laboratory conditions is a daunting task. Therefore, in optimizing the design and process parameters for a particular reactor, a statistical correlation of these parameters from a data set is often required, depending on the available time and complexity of the problem, to obtain accurate information on the optimum design and process conditions. A number of statistical methods such as the design of experiment and response surface methodology can be applied to a large set of experimental data to obtain the desired optimization points. This will facilitate an understanding of the influence of different process conditions on the reactor performance which will assist in the selection of optimized operating conditions.

Test parameters	**Agitation speed**	
	145 rpm	**165 rpm**
Mean agglomerate diameter, mm	3.8330	3.9182
Mean agglomerate compressive strength, Nm m^{-2}	0.4298	0.4351
Mean strain rate, s^{-1}	0.3639	0.4088
Mean maximum compressive force, N	4.9476	5.2303

Table 2. Agglomerate characteristics test properties as a function of the reactor agitation speed in a wet agglomeration process.

http://dx.doi.org/ 10.5772/intechopen.77014

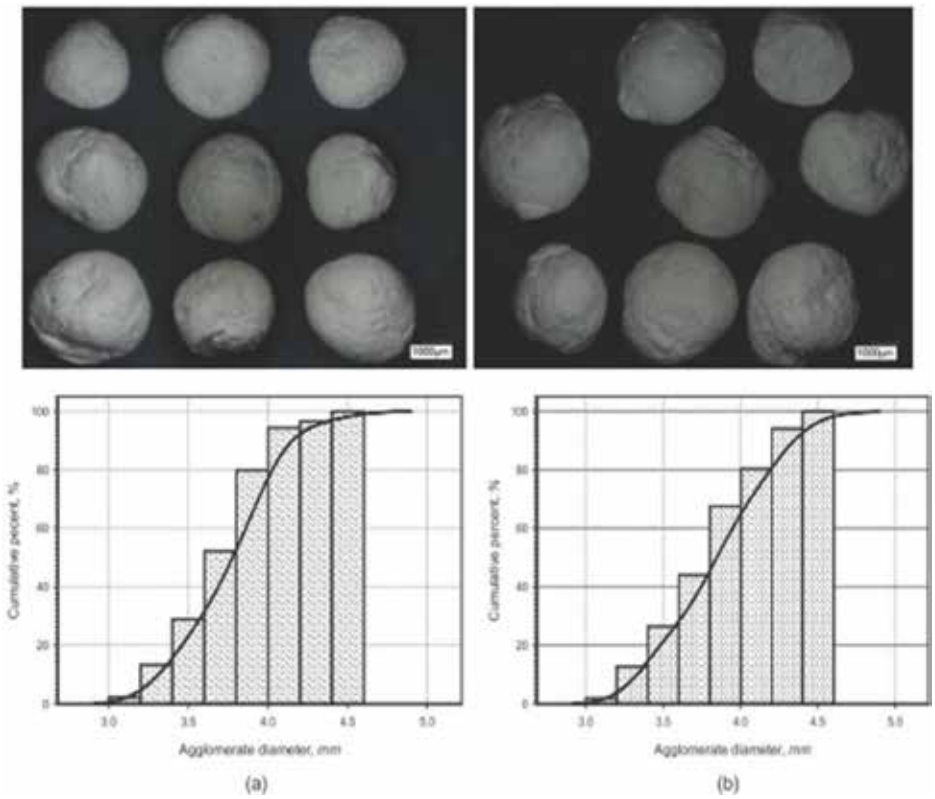

Figure 5. A parametric correlation of agglomerate properties with the process condition—shear rate (a) 145 rpm and (b) 165 rpm.

4. Modeling physicochemical processes in stirred tank reactor

The use of computational fluid dynamics (CFD) as a research tool to investigate complex fluid-particle interactions has been growing in popularity both in academia and in the industry [46]. CFD provides a powerful alternative and a more robust platform for engineers in the design of equipment and processes involving fluid flow and heat transfer when compared to the classical experimental approach. Nowadays, numerical simulations complement the experimental and analytical techniques and are increasingly being performed in many fluid engineering applications ranging from chemical and mineral processing to civil and environmental process engineering [46]. However, it is worth pointing out that the continual development of reliable empirical, mathematical and computational models relies on a robust and detailed experimental data.

Tables 3 and **4** provide a list of recent experimentally validated numerical studies focusing on the physicochemical analysis of fluid-particle reactors. The former is focused on the analysis of the mixing phenomena in stirred tanks while the latter deals with the technical application of mixing

for several industrial processes. The modeling approach in most of these studies is applicable to mixing tanks and process reactors of various geometric designs. Joshi et al. [47, 48] provide a comprehensive review of CFD applications in a single phase mixing tank hydrodynamic analysis focusing on axial and radial flow impellers in a multitude of flow scenarios. Their two-part study, which is one of the most detailed and comprehensive reviews in this field, summarizes developments in mixing tank modeling by bringing together the results of scientific investigations spanning several decades. Similar reviews focusing on turbulent multiphase flows and multiphase

Reactor configuration	Fluid agitator/ application	Experimental validation method	Numerical code/ modeling approach	Turbulence models
Cylindrical tank	Grid disc impeller	LDA	CFX/MRF	k-ε [53]
Cylindrical tank	Grid disc impeller, solid disc, propeller	LDA	CFX/MRF	k-ε [52]
Cylindrical tank	Rushton turbine, flotation impeller	2D PIV	Fluent/MRF	k-ε [54]
Cylindrical tank	Rushton disc impeller	LDA	Fluent/snapshot	k-ε [55]
Cylindrical tank	Rushton turbine	LDA	Fluent/MRF	k-ε, DES [56]
Cylindrical tank	Foil impeller, Rushton turbine	Image analysis	PHOENICS/MRF	k-ε [57]
Cylindrical Tank	Pitched-blade turbine	PEPT	CFX/MRF	k-ε [58]
Cylindrical tank	Rushton turbine	LDV	Fluent/MRF	k-ε [59, 60]
Cylindrical tank	Rushton turbine	PLIF	Fluent/MRF	k-ε [61]
Square tank	Rushton turbine	Power consumption measurements	Fluent/MRF	RSM [62]
Cylindrical tank	Pitched-blade turbine	2D PIV	Fluent/sliding mesh	k-ε [63]
Cylindrical tank	Rushton turbine	CARPT	Fluent/MRF	k-ε [64]
Cylindrical tank	Rushton turbine	Solids concentration measurements	CFX/MRF	k-ε [65]
Cylindrical tank	Pfaudler retreat curve impeller	2D PIV, laser granulometry, nephelometry	Fluent/sliding mesh	k-ε [66]
Square tank	Rotating cylinder	LDA	Fluent/MRF	k-ε [67]
Cylindrical tank	Rushton turbine, pitched blade turbine	RPT, LDA	Fluent/MRF	k-ε [68]
Cylindrical tank	Rushton turbine	LDV	Fluent/MRF	k-ε, LES [69]
Cylindrical tank	Flat blade turbine, pitched blade turbine, Rushton turbine	LDV	Fluent/MRF	k-ε [70]
Cylindrical tank	Rushton turbine	LDV	Fluent/MRF	RSM [71]
Cylindrical tank	Rushton turbine, disc turbine, elliptical blade disc turbine	SPIV	Fluent/sliding mesh	k-ε, LES [72]

Reactor configuration	Fluid agitator/ application	Experimental validation method	Numerical code/ modeling approach	Turbulence models
Cylindrical tank	Rushton turbine	2D PIV, LDA	Fluent/sliding mesh	DES [73]
Cylindrical tank	Double Rushton turbine	LDA	CFX/MRF	k-ε [74]
Cylindrical tank	Rushton turbine	Mixing time, power consumption, solids concentration measurements	CFX/MRF/sliding grid	k-ε [75]
Cylindrical tank	Rushton turbine	Particle size analysis, conductometry	Fluent/MRF	k-ε [76]
Cylindrical tank	Pitched-blade turbine, double disc impeller	PIV, critical impeller speed measurements	Fluent/MRF	k-ε [77]
Cylindrical tank	Rushton turbine	LDV	Fluent/MRF	k-ε [78]
Cylindrical tank	Pitched-blade turbine	PEPT	Fluent/MRF	k-ω, k-ε, RSM [79]
Cylindrical tank	Rigid, rigid-flexible and punched rigid-flexible impeller	Solids concentration measurements	Fluent/MRF	k-ε [80]
Cylindrical tank	Flat blade impeller, angle pitch impeller	DPIV	Fluent/MRF	k-ε [81]
Cylindrical tank	Rotor-stator mixer	PIV	Fluent/MRF/sliding mesh	k-ε, k-ω [82]
Cylindrical tank	Rotor-stator mixer	LDA	Fluent/sliding mesh	k-ε [83]

Table 3. Selected studies on CFD characterization of single phase and multiphase flows in classical stirred tank reactors.

reactor modelling, and which provide a more comprehensive discussion on the subject matter are available elsewhere [19, 49–51].

Regardless of the specific focus of each study, most of the studies differ only in terms of stirrer-vessel configurations, experimental validation methods and the choice of modeling approach. In terms of the stirrer-vessel configuration, there is a wide variety of flow inducers available for fluid flow investigation, each with different power demands and flow patterns. In addition to well-established impeller designs employed in most of the studies—Rushton turbine, pitched-blade turbine, propeller, and so on, a few innovative designs have been used with good results [52]. The turbulence models of choice in most of the investigations are the two equation eddy viscosity models such as k-ε and k-ω, and RSM models which are quite efficient in handling rotating flows in stirred tanks and multiphase reactors. The dominant modeling approaches for rotating flow problems are the MRF and sliding mesh. The former is suitable for steady-state problems while the latter is employed for transient calculations. Despite the technical limitations of some of the experimental flow measurement techniques, reasonable agreement was obtained in most of the studies between the experimental data and numerical simulation. In a few of the studies, the model predictions were not quite robust enough when compared to the experimental data set partly due to the complexity of the flow scenario being modeled.

Reactor configuration	Fluid agitator/application	Experimental validation method	Numerical code/modeling approach	Turbulence models
Cylindrical flocculator	Paddle mixer/flocculation	LDA, 2D PIV	CFX/MRF	k-ε, RSM [84]
Rectangular flocculator	Axial impeller/water purification	2D PIV	Fluent/MRF	k-ε [85]
Cylindrical sedimentation tank	Axial impeller/water purification	Laser diffraction	CFX/MRF	k-ε [86]
Cylindrical Jar testing device	Paddle stirrer/flocculation	LDA	Fluent/MRF	k-ε, k-ω, RSM [7, 87, 88]
Cylindrical flocculation reactor	Rushton turbine/ bio-flocculation	LDV	Fluent/MRF	k-ε [89]
Cylindrical stirred tank	Pitched turbine blade/silica particle deagglomeration	Laser diffraction/ PIDS	Fluent/MRF	k-ε [90]
Cylindrical stirred bioreactor	Marine impeller/cell cultivation	Tracer and dynamic method	Fluent/MRF	k-ε [91]
Cylindrical tank	R1342-type impeller/ flocculation	Image analysis	Fluent/MRF	k-ε [92]
Cylindrical tank	Rushton impeller/cell culture	Optical sensor	CFX/MRF	k-ε [93]
Cylindrical bioreactor	Rushton, scaba and paddle impellers/cell culture	Optical density	Fluent/MRF	k-ε [94]
Cylindrical tank	Turbine, anchor and oblique impellers/autoclave	Tracer injection	Fluent/MRF	k-ε [95]
Cylindrical bioreactor	Marine impeller/recombinant protein synthesis	PIV	Fluent/MRF	k-ε [91, 96]
Cylindrical tube reactor	Impeller/bacterial inactivation	2D PIV	CFX/MRF	RSM [2]
Cylindrical bioreactor	Rushton turbine/anaerobic digestion	Gas chromatography	Fluent/MRF	k-ε [97]
Cylindrical tank	Turbine impeller/ polymerization	Droplet size measurements	Fluent/MRF	k-ε [98]
Cylindrical tank	Rushton impeller/cell cultivation	Dynamic method	Fluent/MRF	k-ε [99]
Cylindrical tank	Rushton turbine/cell inactivation	PIV	Fluent/MRF	k-ε [100]
Cylindrical tank	Rushton turbine and propellers/cell culture	Dynamic method	Fluent/MRF	RSM [101]
Cylindrical crystallizer	Rushton impeller/ precipitation	X-ray/laser diffraction	Fluent/MRF	k-ε [102]
Cylindrical Photobioreactor	Rotating cylinder/algal culture	Optical density	Fluent/SRF	k-ω [103, 104]

Table 4. Selected studies on CFD characterization of hydrodynamics and physicochemical processes in field-assisted process reactors.

5. Conclusions and future perspectives

A review of recent advances in the experimental analysis and numerical modeling of physicochemical processes in stirred tanks and agglomeration reactors have been presented. This review briefly summarizes important findings and major contributions from numerous publications in this field. This short review of the developments in this field clearly shows that significant progress has been made over the past decade in the understanding of complex physicochemical phenomena that are vital for many industrial and environmental processes, especially from experimental and theoretical perspective. However, there is still a gap in knowledge especially in the suitability of the existing mathematical models to accurately predict the reactor performance in a wide range of existing and emerging processes. This clearly calls for a numerical code programming and development to form an integral part of the engineering training and curriculum in future. The successful design, development and optimization of agglomeration units depend on the robustness of the experimental data, mathematical models and simulation tools. This short review is by no means an exhaustive one, and readers are advised to consult other multitudes of scientific publications on the subject matter. In conclusion, numerical modeling along with robust experimental data will continue to be highly indispensable well into the foreseeable future.

Acknowledgements

The authors would like to acknowledge the financial support from the National Research Foundation (NRF) and The World Academy of Sciences (TWAS) under the funding instrument number UID: 105553.

Author details

Benjamin Oyegbile* and Guven Akdogan

*Address all correspondence to: oyegbile@sun.ac.za

Department of Process Engineering, Stellenbosch University, Stellenbosch, South Africa

References

[1] Oyegbile B, Hoff M, Adonadaga M, Oyegbile B. Experimental analysis of the hydrodynamics, flow pattern and wet agglomeration in rotor-stator vortex separators. Journal of Environmental Chemical Engineering. 2017;**5**:2115-2127. DOI: 10.1016/j.jece.2017.04.016

[2] Thomas SF, Rooks P, Rudin F, Cagney N, Balabani S, Atkinson S, et al. Swirl flow bioreactor containing dendritic copper-containing alginate beads: A potential rapid method for the eradication of *Escherichia coli* from waste water streams. Journal of Water Process Engineering. 2015;**5**:6-14. DOI: 10.1016/j.jwpe.2014.10.010

[3] Sievers M, Stoll SM, Schroeder C, Niedermeiser M, Onyeche TI. Sludge dewatering and aggregate formation effects through Taylor vortex assisted flocculation. Separation Science and Technology. 2008;**43**:1595-1609. DOI: 10.1080/01496390801973888

[4] Wang X, Jin P, Yuan H, Wang E, Tambo N. Pilot study of a fluidized-pellet-bed technique for simultaneous solid/liquid separation and sludge thickening in a sewage treatment plant. Water Science and Technology. 2004;**49**:81-88

[5] Dionysiou DD, Balasubramanian G, Suidan (M) MT, Khodadoust AP, Baudin I, Laîné J-M. Rotating disk photocatalytic reactor: Development, characterization, and evaluation for the destruction of organic pollutants in water. Water Research. 2000;**34**:2927-2940. DOI: 10.1016/S0043-1354(00)00022-1

[6] Loraine G, Chahine G, Hsiao C-T, Choi J-K, Aley P. Disinfection of gram-negative and gram-positive bacteria using DynaJets® hydrodynamic cavitating jets. Ultrasonics Sonochemistry. 2012;**19**:710-717. DOI: 10.1016/j.ultsonch.2011.10.011

[7] Bridgeman J, Jefferson B, Parsons SA. Computational fluid dynamics modelling of flocculation in water treatment: A review. Engineering Applications of Computational Fluid Mechanics. 2009;**3**:220-241. DOI: 10.1080/19942060.2009.11015267

[8] Krüger T, Kusumaatmaja H, Kuzmin A, Shardt O, Silva G, Viggen EM. The Lattice Boltzmann Method: Principles and Practice. Basel: Springer; 2017

[9] Jahanshaloo L, Pouryazdanpanah E, Sidik NAC. A review on the application of the lattice Boltzmann method for turbulent flow simulation. Numerical Heat Transfer, Part A: Applications. 2013;**64**:938-953. DOI: 10.1080/10407782.2013.807690

[10] Lian G, Moore S, Heeney L. Population balance and computational fluid dynamics modelling of ice crystallisation in a scraped surface freezer. Chemical Engineering Science. 2006;**61**:7819-7826. DOI: 10.1016/j.ces.2006.08.075

[11] Das S, Bai H, Wu C, Kao J-H, Barney B, Kidd M, et al. Improving the performance of industrial clarifiers using three-dimensional computational fluid dynamics. Engineering Applications of Computational Fluid Mechanics. 2016;**10**:130-144. DOI: 10.1080/19942060.2015.1121518

[12] ANSYS, Inc. ANSYS Fluent Theory Guide 18.2 2017

[13] ANSYS, Inc. ANSYS Fluent User's Guide 18.2 2017

[14] Sommerfeld M. Numerical methods for dispersed multiphase flows. In: Bodnár T, Galdi GP, Nečasová Š, editors. Part. Flows. Heidelberg: Springer; 2017. pp. 327-396

[15] Jeldres RI, Fawell PD, Florio BJ. Population balance modelling to describe the particle aggregation process: A review. Powder Technology. 2017;**326**:190-207. DOI: 10.1016/j.powtec.2017.12.033

[16] Hellesto A, Ghaffari M, Balakin B. A parametric study of cohesive particle agglomeration in a shear flow—Numerical simulations by the discrete element method. Journal of Dispersion Science and Technology. 2016;**38**:611-620. DOI: 10.1080/01932691.2016.1185015

[17] Schellander D. CFD Simulations of Particle Laden Flow: Particle Transport and Separation. Hamburg: Anchor Academic Publishing; 2014

[18] Crowe CT, Schwarzkopf JD, Sommerfeld M, Tsuji Y. Multiphase Flows with Droplets and Particles. 2nd ed. Boca Raton, FL: CRC Press; 2011

[19] Joshi JB, Nandakumar K. Computational modeling of multiphase reactors. Annual Review of Chemical and Biomolecular Engineering. 2015;**6**:347-378. DOI: 10.1146/annurev-chembioeng-061114-123229

[20] Johnson RW, editor. Handbook of Fluid Dynamics. 2nd ed. Boca Raton, FL: CRC Press; 2016

[21] Michaelides E, Crowe CT, Schwarzkopf JD, editors. Multiphase Flow Handbook. 2nd ed. Boca Raton, FL: CRC Press; 2016

[22] Mavros P. Flow visualization in stirred vessels: A review of experimental techniques. Chemical Engineering Research and Design. 2001;**79**:113-127. DOI: 10.1205/02638760151095926

[23] Li G, Gao Z, Li Z, Wang J, Derksen JJ. Particle-Resolved PIV experiments of solid-liquid mixing in a turbulent stirred tank. AICHE Journal. 2018;**64**:389-402. DOI: 10.1002/aic.15924

[24] Liu X, Bao Y, Li Z, Gao Z. Analysis of turbulence structure in the stirred tank with a deep hollow blade disc turbine by time-resolved PIV. Chinese Journal of Chemical Engineering. 2010;**18**:588-599. DOI: 10.1016/S1004-9541(10)60262-5

[25] Hasan BO. Breakage of drops and bubbles in a stirred tank: A review of experimental studies. Chinese Journal of Chemical Engineering. 2017;**25**:698-711. DOI: 10.1016/j.cjche.2017.03.008

[26] Fangary YS, Barigou M, Seville JPK, Parker DJ. A Langrangian study of solids suspension in a stirred vessel by positron emission particle tracking PEPT. Chemical Engineering and Technology. 2002;**25**:521-528. DOI: 10.1002/1521-4125(200205)25:5<521::AID-CEAT521>3.0.CO;2-C

[27] Montante G, Paglianti A, Magelli F. Analysis of dilute solid-liquid suspensions in turbulent stirred tanks. Chemical Engineering Research and Design. 2012;**90**:1448-1456. DOI: 10.1016/j.cherd.2012.01.009

[28] Unadkat H, Rielly CD, Hargrave GK, Nagy ZK. Application of fluorescent PIV and digital image analysis to measure turbulence properties of solid-liquid stirred suspensions. Chemical Engineering Research and Design. 2009;**87**:573-586. DOI: 10.1016/j.cherd.2008.11.011

[29] Rammohan A, Kemoun A, Al-Dahhan M, Dudukovic M. Characterization of single phase flows in stirred tanks via computer automated radioactive particle tracking (CARPT). Chemical Engineering Research and Design. 2001;**79**:831-844. DOI: 10.1205/02638760152721343

[30] Komrakova AE, Liu Z, Machado MB, Kresta SM. Development of a zone flow model for the confined impeller stirred tank (CIST) based on mean velocity and turbulence measurements. Chemical Engineering Research and Design. 2017;**125**:511-522. DOI: 10.1016/j.cherd.2017.07.025

[31] Rafiee M, Simmons MJH, Ingram A, Stitt HE. Development of positron emission particle tracking for studying laminar mixing in Kenics static mixer. Chemical Engineering Research and Design. 2013;**91**:2106-2113. DOI: 10.1016/j.cherd.2013.05.022

[32] Guida A, Nienow AW, Barigou M. PEPT measurements of solid–liquid flow field and spatial phase distribution in concentrated monodisperse stirred suspensions. Chemical Engineering Science. 2010;**65**:1905-1914. DOI: 10.1016/j.ces.2009.11.005

[33] Kilander J, Blomström S, Rasmuson A. Spatial and temporal evolution of floc size distribution in a stirred square tank investigated using PIV and image analysis. Chemical Engineering Science. 2006;**61**:7651-7667. DOI: 10.1016/j.ces.2006.09.001

[34] Sharp KV, Hill D, Troolin D, Walters G, Lai W. Volumetric three-component velocimetry measurements of the turbulent flow around a Rushton turbine. Experiments in Fluids. 2009;**48**:167-183. DOI: 10.1007/s00348-009-0711-9

[35] Fishwick R, Winterbottom M, Parker D, Fan X, Stitt H. The use of positron emission particle tracking in the study of multiphase stirred tank reactor hydrodynamics. Canadian Journal of Chemical Engineering. 2005;**83**:97-103. DOI: 10.1002/cjce.5450830117

[36] Chiti F, Bakalis S, Bujalski W, Barigou M, Eaglesham A, Nienow AW. Using positron emission particle tracking (PEPT) to study the turbulent flow in a baffled vessel agitated by a Rushton turbine: Improving data treatment and validation. Chemical Engineering Research and Design. 2011;**89**:1947-1960. DOI: 10.1016/j.cherd.2011.01.015

[37] Mortensen HH, Innings F, Håkansson A. The effect of stator design on flowrate and velocity fields in a rotor-stator mixer—An experimental investigation. Chemical Engineering Research and Design. 2017;**121**:245-254. DOI: 10.1016/j.cherd.2017.03.016

[38] Bache DH, Gregory R. Flocs in Water Treatment. London: IWA Publishing; 2007

[39] Bratby J. Coagulation and Flocculation in Water and Wastewater Treatment. 3rd ed. London: IWA Publishing; 2016

[40] Gregory J. Flocculation Measurement Techniques. In: Tadros T, editor. Encycl. Colloid Interface Sci. Heidelberg: Springer; 2013. pp. 492-52

[41] Gregory J. Monitoring particle aggregation processes. Advances in Colloid and Interface Science. 2009;**147-148**:109-123. DOI: 10.1016/j.cis.2008.09.003

[42] Bache DH, Zhao YQ. Optimising polymer use in alum sludge conditioning: An ad hoc test. Journal of Water Supply: Research and Technology—AQUA. 2001;**50**:29-38

[43] Oyegbile B, Ay P, Narra S. Optimization of physicochemical process for pre-treatment of fine suspension by flocculation prior to dewatering. Desalination and Water Treatment. 2016;**57**:2726-2736. DOI: 10.1080/19443994.2015.1043591

[44] Al Momani FA, Örmeci B. Optimization of polymer dose based on residual polymer concentration in dewatering supernatant. Water, Air, and Soil Pollution. 2014;**225**:1-11. DOI: 10.1007/s11270-014-2154-z

[45] Ramphal SR, Sibiya MS. Optimization of coagulation-flocculation parameters using a photometric dispersion analyser. Drinking Water Engineering and Science. 2014;**7**:73-82. DOI: 10.5194/dwes-7-73-2014

[46] Tu J, Yeoh GH, Liu C. Computational Fluid Dynamics: A Practical Approach. Oxford: Butterworth-Heinemann; 2013

[47] Joshi JB, Nere NK, Rane CV, Murthy BN, Mathpati CS, Patwardhan AW, et al. CFD simulation of stirred tanks: Comparison of turbulence models. Part I: Radial flow impellers. Canadian Journal of Chemical Engineering. 2011;**89**:23-82. DOI: 10.1002/cjce.20446

[48] Joshi JB, Nere NK, Rane CV, Murthy BN, Mathpati CS, Patwardhan AW, et al. CFD simulation of stirred tanks: Comparison of turbulence models (part II: Axial flow impellers, multiple impellers and multiphase dispersions). Canadian Journal of Chemical Engineering. 2011;**89**:754-816. DOI: 10.1002/cjce.20465

[49] Balachandar S, Eaton JK. Turbulent dispersed multiphase flow. Annual Review of Fluid Mechanics. 2009;**42**:111-133. DOI: 10.1146/annurev.fluid.010908.165243

[50] Tinoco H, Lindqvist H, Frid W. Numerical simulation of industrial flows. In: Angermann L, editor. Numer. Simul.—Ex. Appl. Comput. Fluid Dyn. Rijeka: InTech; 2001

[51] Pradip M. Computational fluid dynamics analysis of turbulent flow. In: Minin IV, Minin OV, editors. Comput. Fluid Dyn. Technol. Appl. Rijeka: InTech; 2011. pp. 255-92

[52] Buwa V, Dewan A, Nassar AF, Durst F. Fluid dynamics and mixing of single-phase flow in a stirred vessel with a grid disc impeller: Experimental and numerical investigations. Chemical Engineering Science. 2006;**61**:2815-2822. DOI: 10.1016/j.ces.2005.10.066

[53] Dewan A, Buwa V, Durst F. Performance optimizations of grid disc impellers for mixing of single-phase flows in a stirred vessel. Chemical Engineering Research and Design. 2006;**84**:691-702. DOI: 10.1205/cherd05044

[54] Basavarajappa M, Draper T, Toth P, Ring TA, Miskovic S. Numerical and experimental investigation of single phase flow characteristics in stirred tanks using Rushton turbine and flotation impeller. Minerals Engineering. 2015;**83**:156-167. DOI: 10.1016/j.mineng.2015.08.018

[55] Deshpande VR, Ranade VV. Simulation of flows in stirred vessels agitated by dual Rushton impellers using computational snapshot approach. Chemical Engineering Communications. 2003;**190**:236-253. DOI: 10.1080/00986440302144

[56] Yang FL. Turbulent flow and mixing performance of a novel six-blade grid disc impeller. Korean Journal of Chemical Engineering. 2015;**32**:816-825. DOI: 10.1007/s11814-014-0255-4

[57] Prat OP, Ducoste JJ. Simulation of flocculation in stirred vessels: Lagrangian versus Eulerian. Chemical Engineering Research and Design. 2007;**85**:207-219. DOI: 10.1205/cherd05001

[58] Liu L, Barigou M. Numerical modelling of velocity field and phase distribution in dense Monodisperse solid–liquid suspensions under different regimes of agitation: CFD and PEPT experiments. Chemical Engineering Science. 2013;**101**:837-850. DOI: 10.1016/j.ces.2013.05.066

[59] Karimi M, Akdogan G, Bradshaw SM. A computational fluid dynamics model for the flotation rate constant, part I: Model development. Minerals Engineering. 2014;**69**:214-222. DOI: 10.1016/j.mineng.2014.03.028

[60] Karimi M, Akdogan G, Bradshaw SM. A CFD-kinetic model for the flotation rate constant, part II: Model validation. Minerals Engineering. 2014;**69**:205-213. DOI: 10.1016/j.mineng.2014.05.014

[61] Coroneo M, Montante G, Paglianti A, Magelli F. CFD prediction of fluid flow and mixing in stirred tanks: Numerical issues about the RANS simulations. Computers and Chemical Engineering. 2011;**35**:1959-1968. DOI: 10.1016/j.compchemeng.2010.12.007

[62] Chtourou W, Ammar M, Driss Z, Abid MS. CFD prediction of the turbulent flow generated in stirred square tank by a Rushton turbine. Energy and Power Engineering. 2014;**6**:95-110. DOI: 10.4236/epe.2014.65010

[63] Ge C-Y, Wang J-J, Gu X-P, Feng L-F. CFD simulation and PIV measurement of the flow field generated by modified pitched blade turbine impellers. Chemical Engineering Research and Design. 2014;**92**:1027-1036. DOI: 10.1016/j.cherd.2013.08.024

[64] Wadnerka D, Utika RP, Tade MO, Pareek VK. CFD simulation of solid–liquid stirred tanks. Advanced Powder Technology. 2012;**23**:445-453. DOI: 10.1016/j.apt.2012.03.007

[65] Tamburini A, Cipollina A, Micale G, Brucato A, Ciofalo M. CFD simulations of dense solid–liquid suspensions in baffled stirred tanks: Prediction of suspension curves. Chemical Engineering Journal. 2011;**178**:324-341. DOI: 10.1016/j.cej.2011.10.016

[66] Calvo S, Delafosse A, Collignon M-L, Crine M, Toye D. Experimental characterisation and modelling of homogeneous solid suspension in an industrial stirred tank. Advances in Mechanical Engineering. 2013;**5**:1-9. DOI: 10.1155/2013/329264

[67] Escamilla-Ruíz IA, Sierra-Espinosa FZ, García JC, Valera-Medina A, Carrillo F. Experimental data and numerical predictions of a single-phase flow in a batch square stirred tank reactor with a rotating cylinder agitator. Heat and Mass Transfer. 2017;**53**:2933-2949. DOI: 10.1007/s00231-017-2030-7

[68] Bashiri H, Alizadeh E, Bertrand F, Chaouki J. Investigation of turbulent fluid flows in stirred tanks using a non-intrusive particle tracking technique. Chemical Engineering Science. 2016;**140**:233-251. DOI: 10.1016/j.ces.2015.10.005

[69] Zadghaffari R, Moghaddas JS, Revstedt J. Large-Eddy simulation of turbulent flow in a stirred tank driven by a Rushton turbine. Computers and Fluids. 2010;**39**:1183-1190. DOI: 10.1016/j.compfluid.2010.03.001

[70] Ammar M, Chtourou W, Driss Z, Abid MS. Numerical investigation of turbulent flow generated in baffled stirred vessels equipped with three different turbines in one and two-stage system. Energy. 2011;**36**:5081-5093. DOI: 10.1016/j.energy.2011.06.002

[71] Qi N, Wang H, Zhang K, Zhang H. Numerical simulation of fluid dynamics in the stirred tank by the SSG Reynolds stress model. Frontiers of Chemical Engineering in China. 2010;**4**:506-514. DOI: 10.1007/s11705-010-0508-7

[72] Li Z, Song G, Bao Y, Gao Z. Stereo-PIV experiments and large Eddy simulations of flow fields in stirred tanks with Rushton and curved-blade turbines. AICHE Journal. 2013;**59**:3986-4003. DOI: 10.1002/aic.14117

[73] Chara Z, Kysela B, Konfrst J, Fort I. Study of fluid flow in baffled vessels stirred by a Rushton standard impeller. Applied Mathematics and Computation. 2016;**272**:614-628. DOI: 10.1016/j.amc.2015.06.044

[74] Wang H, Jia X, Wang X, Zhou Z, Wen J, Zhang J. CFD modeling of hydrodynamic characteristics of a gas–liquid two-phase stirred tank. Applied Mathematical Modelling. 2014;**38**:63-92. DOI: 10.1016/j.apm.2013.05.032

[75] Tamburini A, Cipollina A, Micale G, Brucato A, Ciofalo M. Influence of drag and turbulence modelling on CFD predictions of solid liquid suspensions in stirred vessels. Chemical Engineering Research and Design. 2014;**92**:1045-1063. DOI: 10.1016/j.cherd.2013.10.020

[76] Wang L, Zhang Y, Li X, Zhang Y. Experimental investigation and CFD simulation of liquid–solid–solid dispersion in a stirred reactor. Chemical Engineering Science. 2010;**65**:5559-5572. DOI: 10.1016/j.ces.2010.08.002

[77] Murthy BN, Kasundra RB, Joshi JB. Hollow self-inducing impellers for gas–liquid–solid dispersion: Experimental and computational study. Chemical Engineering Journal. 2008;**141**:332-345. DOI: 10.1016/j.cej.2008.01.040

[78] Deglon DA, Meyer CJ. CFD Modelling of stirred tanks: Numerical considerations. Minerals Engineering. 2006;**19**:1059-1068. DOI: 10.1016/j.mineng.2006.04.001

[79] Wadnerkar D, Tade MO, Pareek VK, Utikar RP. CFD simulation of solid–liquid stirred tanks for low to dense solid loading systems. Particuology. 2016;**29**:16-33. DOI: 10.1016/j.partic.2016.01.012

[80] Gu D, Liu Z, Xie Z, Li J, Tao C, Wang Y. Numerical simulation of solid-liquid suspension in a stirred tank with a dual punched rigid-flexible impeller. Advanced Powder Technology. 2017;**28**:2723-2734. DOI: 10.1016/j.apt.2017.07.025

[81] Xinli W, Jie R, Xiangrui M. Simulation and Experiment Study of Flow Field and Dynamic Performance in Stirred Reactor, Hangzhou, China. 2007. pp. 1408-13. DOI: 10.1007/978-3-540-76694-0_265

[82] Mortensen HH, Arlov D, Innings F, Håkansson A. A validation of commonly used CFD methods applied to rotor stator mixers using PIV measurements of fluid velocity and turbulence. Chemical Engineering Science. 2018;**177**:340-353. DOI: 10.1016/j.ces.2017.11.037

[83] Utomo AT, Baker M, Pacek AW. Flow pattern, periodicity and energy dissipation in a batch rotor–stator mixer. Chemical Engineering Research and Design. 2008;**86**:1397-1409. DOI: 10.1016/j.cherd.2008.07.012

[84] Korpijärvi J, Laine E, Ahlstedt H. Using CFD in the study of mixing in coagulation and flocculation. In: Hahn HH, Hoffmann E, Odegaard H, editors. Chem. Water Wastewater Treat. VI. Heidelberg: Springer; 2000. pp. 89-99

[85] Essemiani K, De Traversay C. Optimisation of the flocculation process using computational fluid dynamics. In: Hahn H, Hoffman E, Odegaard H, editors. Chem. Water Wastewater Treat. VII. London: IWA Publishing; 2002. pp. 41-49

[86] Samaras K, Zouboulis A, Karapantsios T, Kostoglou M. A CFD-based simulation study of a large scale flocculation tank for potable water treatment. Chemical Engineering Journal. 2010;**162**:208-216. DOI: 10.1016/j.cej.2010.05.032

[87] Bridgeman J, Jefferson B, Parsons S. Assessing Floc strength using CFD to improve organics removal. Chemical Engineering Research and Design. 2008;**86**:941-950. DOI: 10.1016/j.cherd.2008.02.007

[88] Bridgeman J, Jefferson B, Parsons SA. The Development and Use of CFD Models for Water Treatment Processes. St. Julians: Malta; 2007

[89] Yang Z, Wu Z, Zeng G, Huang J, Xu H, Feng J, et al. Assessing the effect of flow fields on flocculation of kaolin suspension using microbial flocculant GA1. RSC Advances. 2014;**4**:40464-40473. DOI: 10.1039/C4RA04101A

[90] Özcan-Taşkın GN, Padron GA, Kubicki D. Comparative performance of in-line rotor-stators for deagglomeration processes. Chemical Engineering Science. 2016;**156**:186-196. DOI: 10.1016/j.ces.2016.09.023

[91] Kaiser SC, Eibl R, Eibl D. Engineering characteristics of a single-use stirred bioreactor at bench-scale the Mobius CellReady 3L bioreactor as a case study. Engineering in Life Sciences. 2011;**11**:359-368. DOI: 10.1002/elsc.201000171

[92] He W, Xue L, Gorczyca B, Nan J, Shi Z. Experimental and CFD studies of floc growth dependence on baffle width in square stirred-tank reactors for flocculation. Separation and Purification Technology. 2018;**190**:228-242. DOI: 10.1016/j.seppur.2017.08.063

[93] Zhang H, Zhang K, Fan S. CFD simulation coupled with population balance equations for aerated stirred bioreactors. Engineering in Life Sciences. 2009;**9**:421-430. DOI: 10.1002/elsc.200800074

[94] Azargoshasb H, Mousavi SM, Jamialahmadi O, SAS MSB. Experiments and a three-phase computational fluid dynamics (CFD) simulation coupled with population balance equations of a stirred tank bioreactor for high cell density cultivation. Canadian Journal of Chemical Engineering. 2016;**94**:20-32. DOI: 10.1002/cjce.22352

[95] Zheng H, Huang Z, Liao Z, Wang J, Yang Y, Wang Y. Computational fluid dynamics simulations and experimental validation of macromixing and flow characteristics in low-density polyethylene autoclave reactors. Industrial and Engineering Chemistry Research. 2014;**53**:14865-14875. DOI: 10.1021/ie502551c

[96] Odeleye AOO, Marsh DTJ, Osborne MD, Lye GJ, Micheletti M. On the fluid dynamics of a laboratory scale single-use stirred bioreactor. Chemical Engineering Science. 2014;**111**:299-312. DOI: 10.1016/j.ces.2014.02.032

[97] Azargoshasb H, Mousavi S, Amani T, Jafari A, Nosrati M. Three-phase CFD simulation coupled with population balance equations of anaerobic syntrophic acidogenesis and methanogenesis reactions in a continuous stirred bioreactor. Journal of Industrial and Engineering Chemistry. 2015;**27**:207-217. DOI: 10.1016/j.jiec.2014.12.037

[98] Xie L, Liu Q, Luo Z-H. A multiscale CFD-PBM coupled model for the kinetics and liquid–liquid dispersion behavior in a suspension polymerization stirred tank. Chemical Engineering Research and Design. 2018;**130**:1-17. DOI: 10.1016/j.cherd.2017.11.045

[99] Villiger TK, Neunstoecklin B, Karst D, Lucas E, Stettler M, Broly H, et al. Experimental and CFD physical characterization of animal cell bioreactors: From micro- to production scale. Biochemical Engineering Journal. 2017. DOI: 10.1016/j.bej.2017.12.004

[100] Liu Y, Wang Z-J, Xia J, Haringa C, Liu Y, Chu J, et al. Application of Euler-Lagrange CFD for quantitative evaluating the effect of shear force on *Carthamus tinctorius* L. cell in a stirred tank bioreactor. Biochemical Engineering Journal. 2016;**114**:209-217. DOI: 10.1016/j.bej.2016.07.006

[101] Sarkar J, Shekhawat LK, Loomba V, RAS. CFD of mixing of multi-phase flow in a bioreactor using population balance model. Biotechnology Progress. 2016;**32**:613-628. DOI: 10.1002/btpr.2242

[102] Ojaniemi U, Puranen J, Manninen M, Gorshkova E, Louhi-Kultanen M. Hydrodynamics and kinetics in semi-batch stirred tank precipitation of L-glutamic acid based on pH shift with mineral acids. Chemical Engineering Science. 2017;**178**:167-172. DOI: 10.1016/j.ces.2017.12.029

[103] Gao X, Kong B, Vigil RD. Comprehensive computational model for combining fluid hydrodynamics, light transport and biomass growth in a Taylor vortex algal photobioreactor: Lagrangian approach. Bioresource Technology. 2017;**224**:523-530. DOI: 10.1016/j.biortech.2016.10.080

[104] Gao X, Kong B, Ramezani M, Olsen MG, Vigil RD. An adaptive model for gas–liquid mass transfer in a Taylor vortex reactor. International Journal of Heat and Mass Transfer. 2015;**91**:433-445. DOI: 10.1016/j.ijheatmasstransfer.2015.07.125

Chapter 5

New Opportunities to Improve the Enantiomeric and Diastereomeric Separations

Emese Pálovics, Szeleczky Zsolt, Szolnoki Beáta,
Bosits Miklós and Fogassy Elemér

Additional information is available at the end of the chapter

http://dx.doi.org/10.5772/intechopen.78220

Abstract

The preparation of single enantiomers (ee ~100%) is one of the most important demands both for industrial practice and research. Actually, the resolution of the racemic compounds still remains the most common method for producing pure enantiomers on a large scale. To obtain the pure enantiomers, it is necessary to find the appropriate conditions and resolving agents. During the separation of diastereomeric mixtures, similar trends can be observed as in course of the distribution of enantiomeric mixtures between phases, because just the presence of one-third chiral compound (namely the resolving agent) is the difference. This chapter presents new observations and establishments about the new opportunities to optimize the separation of chiral mixtures, especially the diastereomeric mixtures.

Keywords: diastereomeric mixtures, pH, solvent, crystallization time, temperature, ultrasound irradiation

1. Introduction

In many cases, living organisms contain only one of the two enantiomers of chiral molecules, but often racemic compounds (1:1 mixture of the two enantiomers) are obtained in the chemical syntheses. The biological activity of enantiomers may be different or even opposite, so the enantiomeric separations are necessary and inevitable. Many methods described in the literature for the separation of enantiomers involve the formation of diastereomers followed by decomposition. These enantiomeric separation methods are discussed and systematized in several articles [1–10].

In most cases, the mixtures of diastereomers received by adequate resolving agents, or the mixtures of enantiomers isolated thereof, have to be separated. It is common in the separation methods, that the distribution of the mixtures between two phases is necessary, and the phase separation have to be applied [11–13].

Besides the effect of the applied solvents, the phase distribution of the mixtures is also determined by kinetic or thermodynamic control [14]. The phase distribution is also determined by the eutectic composition of the chiral molecules in the mixtures [15, 16].

Besides, the distribution between the phases is pH-dependent [17]. It seems that the effect of the kinetic control between two phases can be stabilized with the application of ultrasound [18]. The formation of solvates can also determine the distribution and the crystallization-based separation of diastereomers [19, 20]. By the incorporation of compounds of similar structure to the solvate-forming molecules, the fractionated crystallization can be successful in other solvents as well [21]. In the case of the crystallization of diastereomers, better separation can be reached, if the resolving agent is partially replaced by an achiral reagent of similar structure compared to the cases without replacement [22]. In the following, the most characteristic examples of the above-mentioned methods will be discussed.

2. pH dependence of the separation of diastereomeric mixtures

2.1. pH dependence in course of resolution of racemic acid with chiral base

A thermodynamic model has been elaborated [23] for the salt-salt resolution of racemic *cis*-permethric acid (**CPA**) with half-equivalent (*S*)-*N*-benzyl-2-aminobutanol ((*S*)-BAB) [24]. The amount of the base was systematically changed to investigate the pH dependence of the resolution. The calculated and measured *ee* and T curves are plotted in **Figure 1**. After the separation of the diastereomeric salt, by neutralizing the mother liquor with hydrochloric acid, the (*R*,*R*)-**CPA**·(*S*)-**BAB** diastereomer was precipitated.

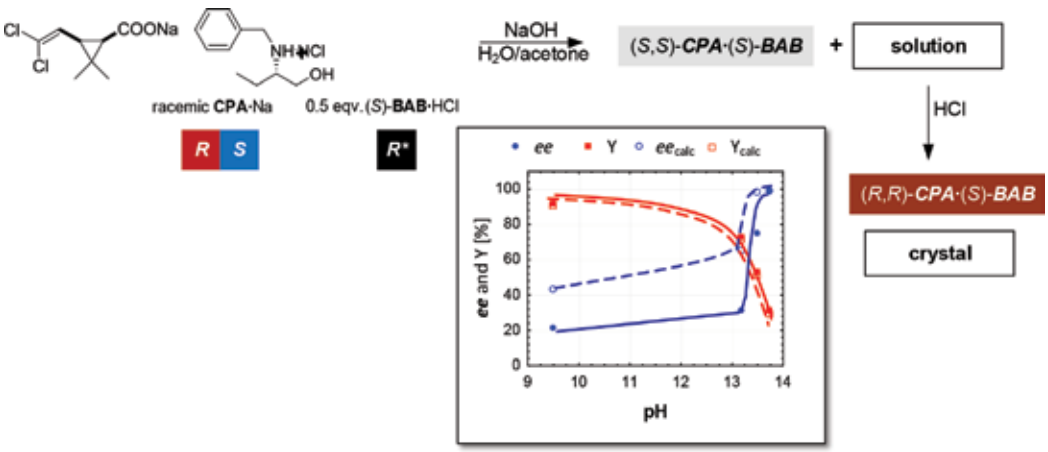

Figure 1. pH-dependent resolution of racemic cis-permethric acid with (*S*)-*N*-benzyl-2-aminobutanol.

http://dx.doi.org/10.5772/intechopen.78220

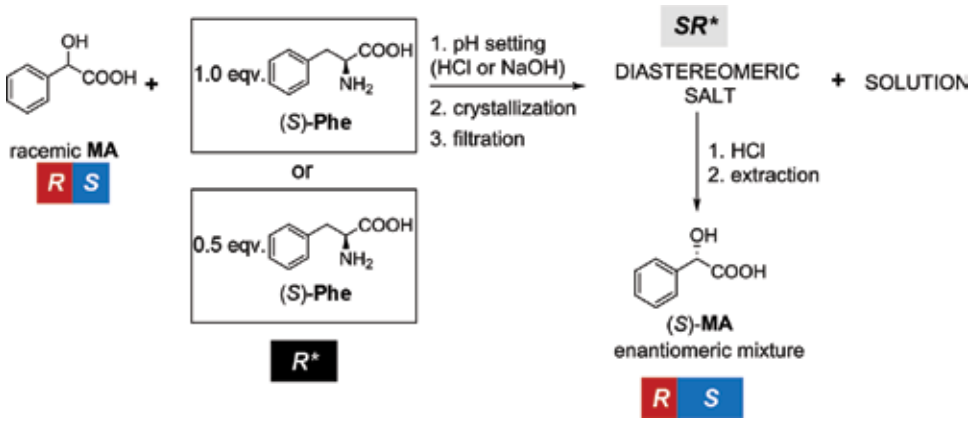

Scheme 1. pH dependence during the resolution of mandelic acid with (*S*)-Phe.

2.2. pH dependence during the resolution of racemic mandelic acid with (S)-phenylalanine

In the case of (*S*)-**Phe**, experiments were carried out both with equivalent and half-equivalent amount of resolving agent relative to racemic mandelic acid (**MA**). The adjusting of the pH was accomplished with NaOH and cc. HCl (**Scheme 1**) [17].

In the case of the application of 1.0 equivalent resolving agent, the enantiomeric purity (44–51%) and yield of the crystalline salt are almost the same between pH 1.3 and 2.3. This pH range matches well the pK_a value of the carboxyl group of **Phe** (1.83). The time of crystallization was 15 min in all cases (**Figures 2** and **3**).

The pH dependence of the diastereomeric salt was also investigated after 2 weeks, when the thermodynamic equilibrium was reached (**Figure 4**).

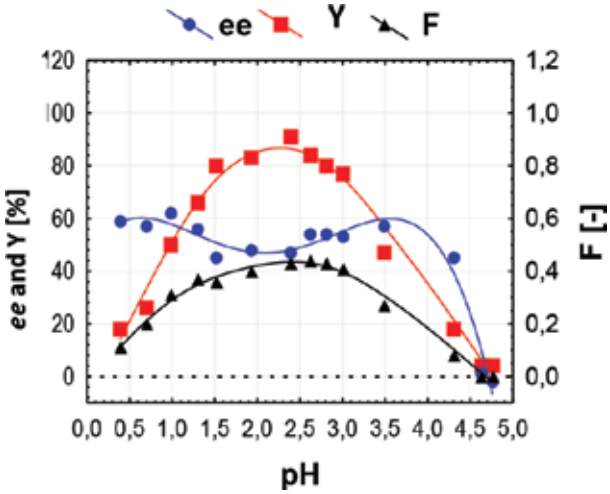

Figure 2. pH dependence in course of the resolution of mandelic acid with 1.0 equivalent (*S*)-**Phe.**

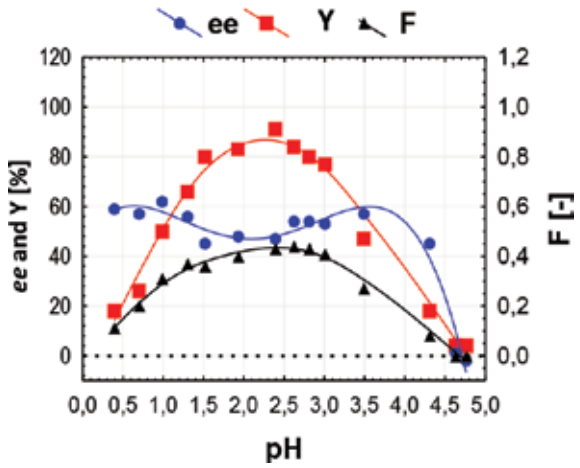

Figure 3. pH dependence in course of the resolution of mandelic acid with 0.5 equivalent (*S*)-**Phe.**

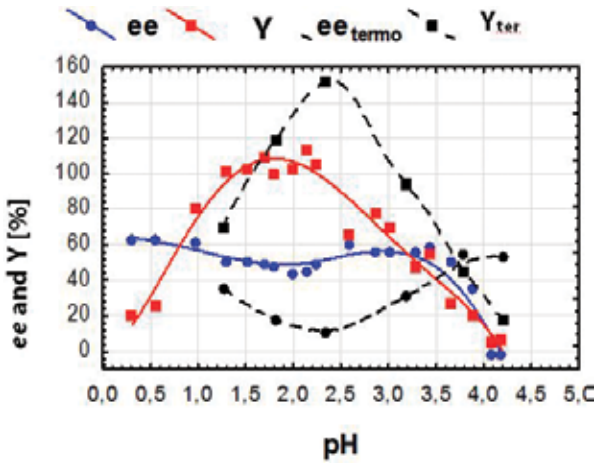

Figure 4. pH dependence in course of the resolution of mandelic acid with 1.0 equivalent (S)-Phe after 2 weeks of crystallization (the denotation thermo is applied for the results of the resolutions after 2 weeks of crystallization).

The purity of the enantiomeric mixtures separated from the crystalline phase became highly pH-dependent. At pH 1.2, the enantiomeric purity received during fast crystallization (*ee*: 52%) decreased to 36%, while at pH 2.3 from 49 to 11%. The optimum of the pH dependence can be reached in the case of kinetic control.

2.3. pH dependence in course of the resolution of racemic mandelic acid with (*R*)-pregabalin

The pH dependence of the resolution of racemic mandelic acid with (*R*)-pregabalin ((*R*)-**PG**) was carried out by kinetic control (crystallization time: 15 min) (**Scheme 2**).

The (*R*)-**MA** enantiomer mixtures can be received with almost identical enantiomeric purities (43–50%) and yields in the range of pH 3.0–4.4. The maximal value of the efficiency of the

http://dx.doi.org/10.5772/intechopen.78220

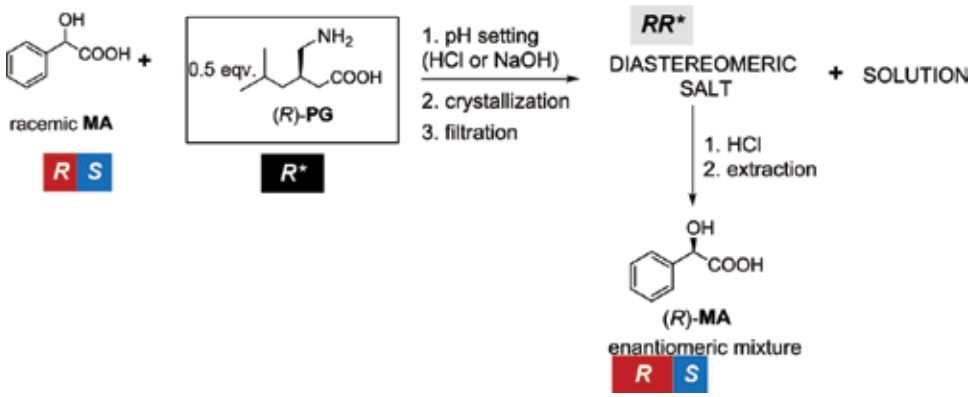

Scheme 2. pH dependence of the resolution of mandelic acid with (*R*)-PG.

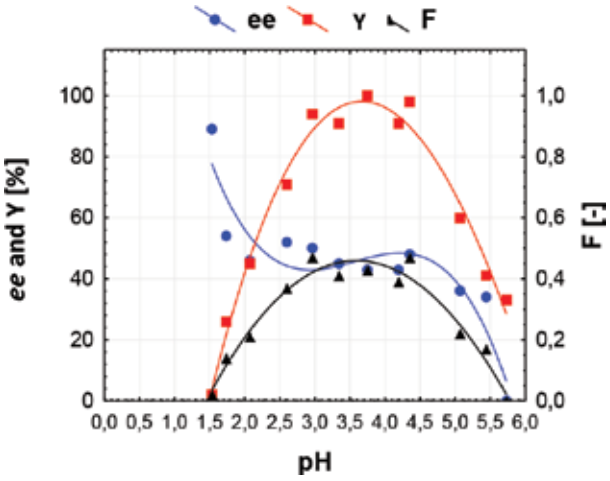

Figure 5. pH dependence in course of the resolution of mandelic acid with 0.5 equivalent (*R*)-**PG.**

resolution was reached in a pH range similar to the pK_a value of the carboxyl group of the resolving agent (**Figure 5**).

3. Role of eutectic compositions, crystallization time and solvent in case of diastereomer separation

3.1. Role of the solvent

The right choice of the solvent is crucial in course of the fractionated crystallization of diastereomers. The composition of the crystalline phase received during resolution is often changed in case of solvate or hydrate formation. The dominant configuration can also change, depending on the applied solvent. For example, by changing the solvent in case of resolution of racemic 6-fluoro-2-methyl-1,2,3,4-tetrahydroquinoline (FTHQ) with half-equivalent (*R*,*R*)-di-*p*-toluoyl-tartaric

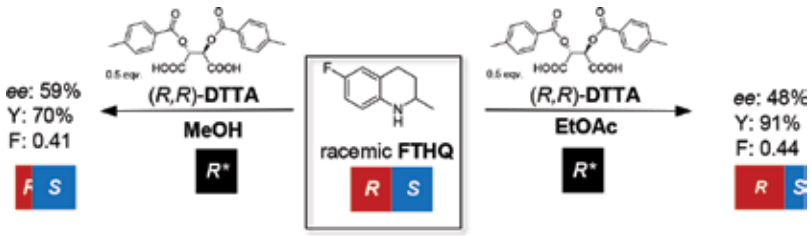

Scheme 3. Resolution of flumequine intermediate.

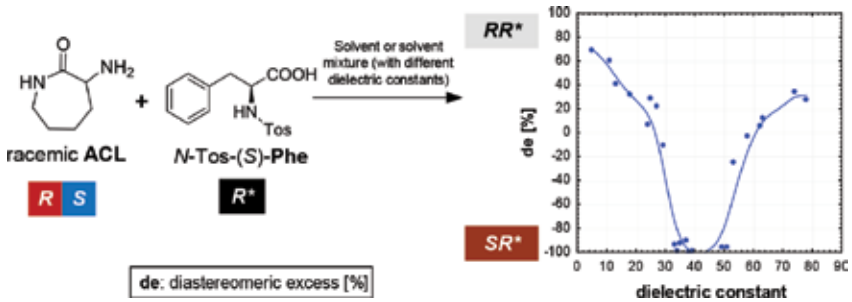

Figure 6. The first dielectric constant-dependent resolution was carried out by *Sakai*.

acid [(*R*,*R*)-DTTA)] resolving agent, the crystalline phase is enriched in different enantiomer, even without solvate formation [25]. When applying ethyl acetate as solvent, (*R*)-FTHQ with 48% enantiomeric excess, while with the application of methanol (*S*)-FTHQ with 59% enantiomeric excess can be separated from the filtrated diastereomer salt (**Scheme 3**).

Correlation was found between the composition of the diastereomeric salt and the dielectric constant of the solvent/mixture of solvents in course of the resolution of *α*-3-amino-ε-caprolactame (ACL) with *N*-tosyl-(*S*)-phenylalanine (*N*-Tos-(*S*)-**Phe**) [26]. In the ranges of 5–27 and 62–78 of the dielectric constant, the (*R*)-**ACL**·*N*-Tos-(*S*)-**Phe** diastereomer was in excess in the crystalline phase, while between the two ranges the (*S*)-**ACL**·*N*-Tos-(*S*)-**Phe** diastereomer was enriched (**Figure 6**).

According to the single-crystal studies, the dielectric constant of the solvent [27] also influences the hydrogen bonding system thus forming the chiral recognition process. This phenomenon was demonstrated *via* several other resolution experiments [28–32].

3.2. Role of the crystallization time

The effect of different crystallization times on the enantiomeric mixtures separated from the crystalline phase was investigated in course of the resolution of the racemic 6-fluoro-2-methyl-1,2,3,4-tetrahydroquinoline (**FTHQ**) with half-equivalent (*R*,*R*)-di-*p*-toluoyl-tartaric acid ((*R*,*R*)-**DTTA**)) [25]. When the mixture was filtrated after 5 min of crystallization, the solid phase composed mainly of the (*R*)-**FTHQ**·(*R*,*R*)-**DTTA** diastereomer, while after 3 weeks of crystallization, the (*S*)-**FTHQ**·(*R*,*R*)-**DTTA** diastereomer became the main component (**Scheme 4**). The kinetic control resulted in (*R*)-**FTHQ**·(*R*,*R*)-**DTTA** diastereomer, while the thermodynamic control gave (*S*)-**FTHQ**·(*R*,*R*)-**DTTA** diastereomer in the solid phase.

http://dx.doi.org/10.5772/intechopen.78220

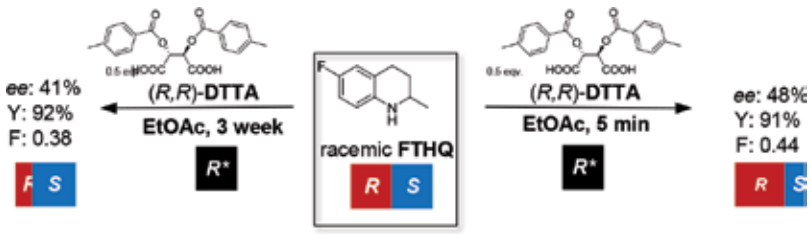

Scheme 4. Time dependence of the resolution of flumequine intermediate.

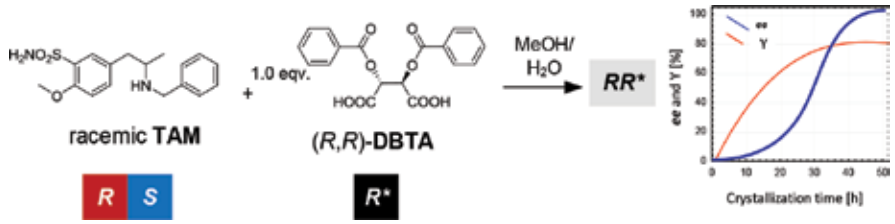

Figure 7. Time dependence of the resolution of tamsulosin intermediate.

By reacting the tamsulosin (**TAM**) intermediate with equivalent (*R,R*)-dibenzoyl-tartaric acid ((*R,R*)-**DBTA**), racemic enantiomer mixture could be separated from the crystalline phase; however, after 2 days of crystallization, the solid phase enriched in the required (*R*)-enantiomer (**Figure 7**) [33]. The thermodynamically preferred composition resulted in the best separation.

3.3. Effect of the eutectic composition of the enantiomeric mixtures of either the racemic compound or the resolving agent

In course of the fractionated crystallization of the mixtures of diastereomeric salts, the effects of the applied solvent and the crystallization time, and thus the enantiomeric ratio of the crystalline diastereomer, are determined by the eutectic compositions of the racemic compound or the resolving agent [11, 13]. At the same time, in the case of the organocatalysis, the eutectic composition of the catalyst determines the enantiomer purity of the product [34].

Consequently, in processes with the participation of chiral compounds, the enantiomer purity of the formed new chiral molecule is determined by the eutectic composition of the enantiomeric mixtures of the starting chiral compounds [12–14].

3.3.1. Effect of the eutectic composition of the resolving agent (ee_{EUres}) in course of kinetic control

At the resolutions of racemic mandelic acid (**MA**) and 2-chloro-mandelic acid (**CMA**) with (*R*)-pregabalin, the purity of the recoverable enantiomeric mixture (ee_{DIA}) is determined by the eutectic composition of the resolving agent (ee_{EUres}) in course of kinetic control 13.

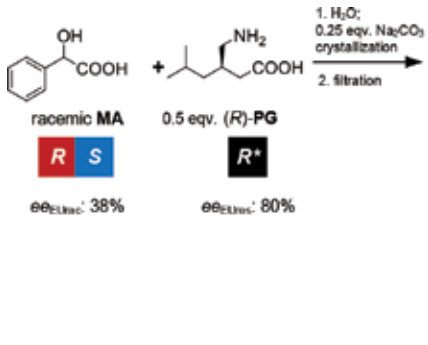

Exp.	time [h]	ee_{DIA} [%]	Y [%]	F [-]
1	0.25	80	56	0.45
2	24	71	60	0.43
3	168	62	69	0.43

Scheme 5. Time-dependent resolution of racemic mandelic acid with (*R*)-pregabalin.

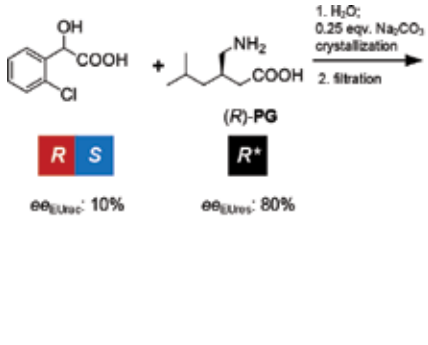

Exp.	time [h]	ee_{DIA} [%]	Y [%]	F [-]
1	0.25	92	53	0.49
2	24	65	79	0.51
3	168	29	124	0.36

Scheme 6. Time-dependent resolution of racemic 2-chloro-mandelic acid with (*R*)-pregabalin.

By plotting the ee_{DIA} enantiomeric purity values of the enantiomeric mixtures of mandelic acid (**MA**) and 2-chloro-mandelic acid (**CMA**), recovered from the crystallized diastereomeric salt after the resolution with pregabalin (**PG**) (**Schemes 5** and **6**, respectively), in the function of time, it can be clearly seen that in the case of both **MA** and **CMA,** by increasing the time of the crystallization, the enantiomeric purity decreases (**Figure 8**). The highest enantiomer purity was reached by immediate filtration after crystallization. Regarding the eutectic compositions of **MA**, **CMA** and **PG** (ee_{EUrac} and ee_{EUres}), it seems that in course of kinetic control, the eutectic composition of the resolving agent (**PG**) affects the enantiomer purity of the recoverable enantiomeric mixtures of **MA** and **CMA**.

3.3.2. Effect of the eutectic composition of eutectic composition of the resolving agent (ee_{EUres}) in course of thermodynamic control

The resolution of 2-chloro-mandelic acid (**CMA**) was carried out using (*S*)-phenylalanine ((*S*)-**Phe**) as resolving agent (**Schemes 7** and **8**) [13] was observed the effect of thermodynamic control. In this case the eutectic composition of the resolving agent (ee_{EUres}) had a great influence on the purity of the obtained enantiomeric mixture (ee_{DIA}).

http://dx.doi.org/10.5772/intechopen.78220

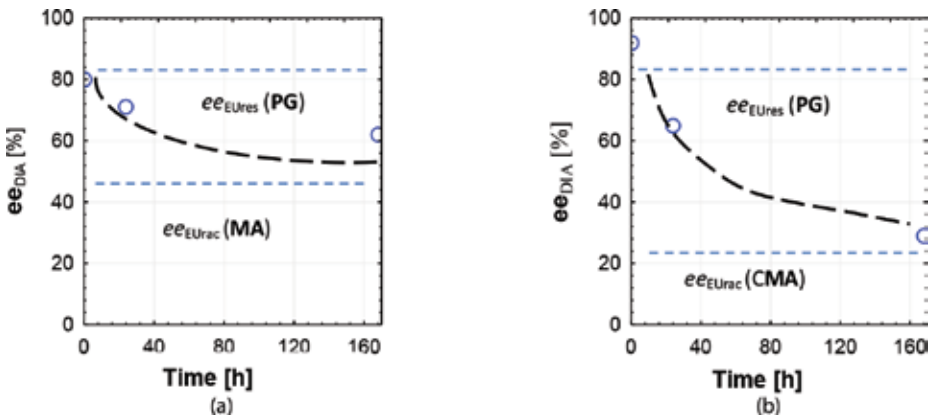

Figure 8. Effect of the crystallization time on the enantiomeric purity (ee_{DIA}) of the enantiomeric mixtures of **MA** (A) and **CMA** (B), recovered from the diastereomeric salt. The resolving agent was PG.

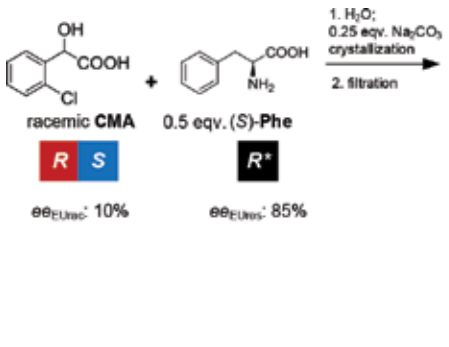

Exp.	time [h]	ee_{DIA} [%]	Y [%]	F [-]
1	0.25	14	21	0.03
2	64	23	35	0.08
3	168	46	17	0.08

Scheme 7. Resolution of racemic 2-chloro-mandelic acid with half-equivalent (*S*)-phenylalanine.

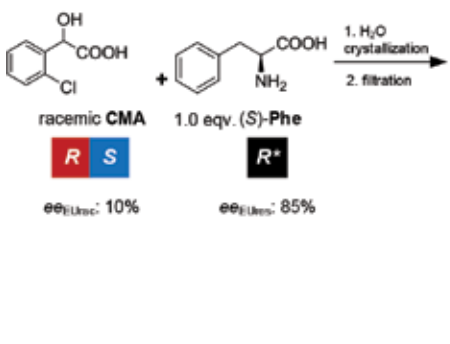

Exp.	time [h]	ee_{DIA} [%]	Y [%]	F [-]
1	0.25	11	72	0.08
2	64	41	37	0.14
3	168	45	47	0.21

Scheme 8. Resolution of racemic 2-chloro-mandelic acid with equivalent (*S*)-phenylalanine.

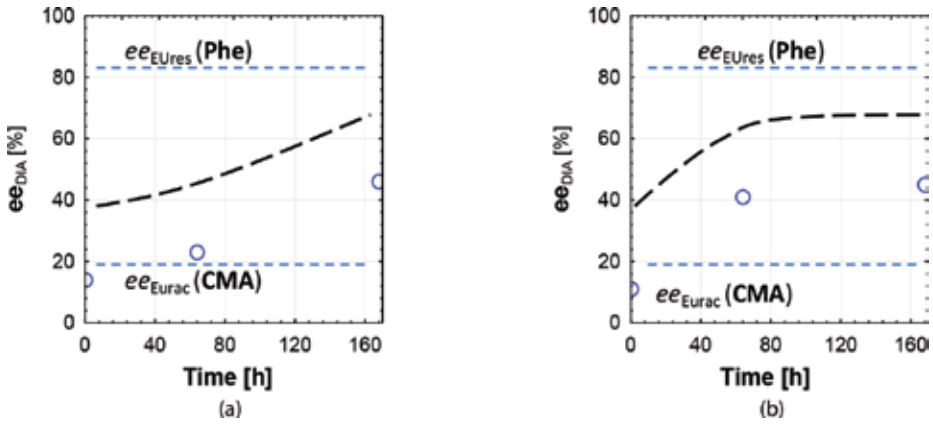

Figure 9. Effect of crystallization time on the enantiomer purity (ee_{DIA}) of **CMA** enantiomeric mixtures separated from the diastereomer salt after resolution with (*S*)-Phe, applying the methods of Pope-Peachey (a) and Pasteur (b).

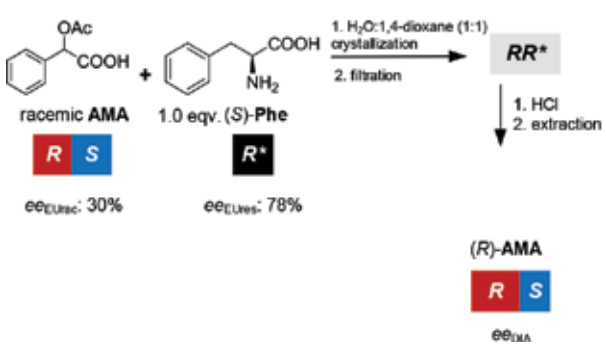

Exp.	time [h]	ee_{DIA} [%]	Y [%]	F [-]
1	0.25	56	79	0.44
2	72	87	39	0.34
3	168	88	36	0.32

Scheme 9. Time-dependent resolution of the racemic *O*-acetyl-mandelic acid with 1.0 equivalent (*S*)-phenylalanine.

By plotting the time dependence of the resolutions, increasing enantiomeric purities can be seen with increasing crystallization times (**Figure 9**).

As the eutectic compositions are known (ee_{EUrac}: 10% and ee_{EUres}: 85%), it can be stated that in course of thermodynamic control, the enantiomer purity of the recoverable (*S*)-**CMA** enantiomeric mixture is determined by the eutectic composition of the resolving agent (ee_{EUres}) [14].

The resolving agent was the determinant for thermodynamic control when the enantiomers of racemic *O*-acetylmandelic acid (**AMA**) were separated by (*S*)-phenylalanine ((*S*)-**Phe**). (**Scheme 9**) [14].

By increasing the time of the crystallization, the (*R*)-**AMA** content of the crystalline phase increases. The thermodynamic equilibrium is determined by the eutectic composition of the resolving agent (**Figure 10**) [14].

http://dx.doi.org/10.5772/intechopen.78220

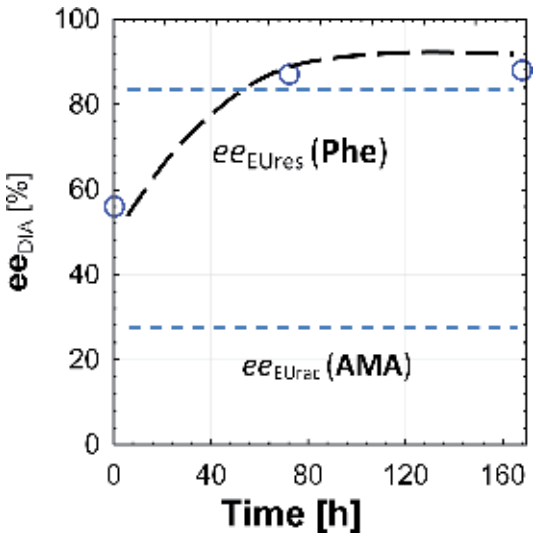

Figure 10. Effect of crystallization time on the enantiomer purity (ee_{DIA}) of enantiomeric mixtures of **AMA** separated from the diastereomer salt.

3.3.3. Effect of the eutectic composition of the racemic component (ee_{EUrac}) in course of thermodynamic control

The resolution of the racemic mandelic acid (**MA**) was carried out with (*S*)-phenylalanine [(*S*)-**Phe**] as resolving agent (**Scheme 10**). In this case, the purity of the recoverable enantiomeric mixture (ee_{DIA}) is determined by the eutectic composition of the racemic component (ee_{EUrac}) in course of thermodynamic control.

By plotting the enantiomer purity (ee_{DIA}) in the function of the crystallization time (**Figure 11**), it seems that in course of thermodynamic control, the enantiomer purity of the **MA** separated from the diastereomer salt decreases until the eutectic composition of the racemic mixture (ee_{EUrac}: 38%).

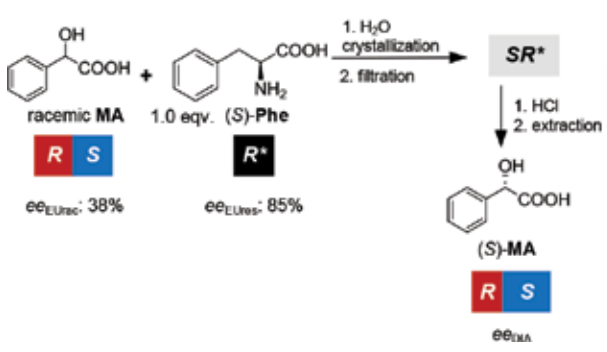

Exp.	time [h]	ee_{DIA} [%]	Y [%]	F [-]
1	0.25	61	52	0.32
2	24	52	48	0.25
3	168	38	66	0.25

Scheme 10. Resolution of racemic mandelic acid (**MA**) with 1.0 equivalent (*S*)-phenylalanine [(*S*)-**Phe].**

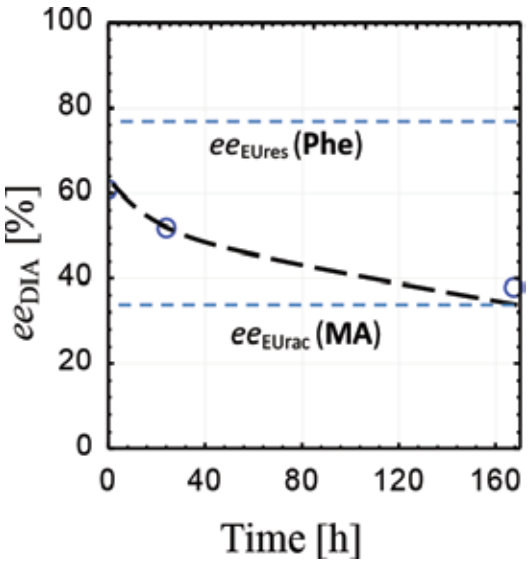

Figure 11. Effect of crystallization time on the enantiomer purity (ee_{DIA}) of the enantiomer mixtures of **MA** separated from the diastereomer salt.

4. Crystallization of diastereomers at different temperatures

The results of the resolutions based on salt formation can be influenced by changing the parameters. In order to reach higher purities, the temperature of the crystallization can be altered. The racemic mandelic acid has been resolved with (*R*)-pregabalin in water. The crystalline segregate was stirred for 168 hours at 26 and at 40°C. After filtration, the diastereomer salt was broken down, resulting in the enantiomeric mixtures of (*R*)-**MA** (**Scheme 11**).

The enantiomer purity of (*R*)-**MA** mixture was 81% at 26°C, while 93% enantiomeric excess was received at 40°C. The temperature-dependent solubility tests of the diastereomers have shown that by increasing the temperature, the difference in the solubility of the diastereomers may increase (**Figure 12**) [33, 35, 36].

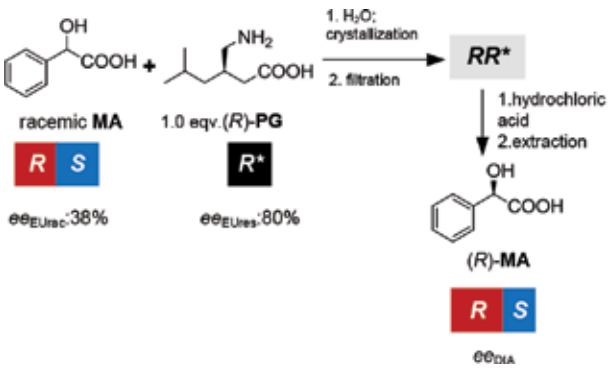

Exp.	time [h]	T [°C]	ee_{DIA} [%]	Y [%]	F [-]
1	168	26	81	84	0.68
2	168	40	93	50	0.47

Scheme 11. Resolution of mandelic acid with pregabalin enantiomer at different temperatures.

http://dx.doi.org/10.5772/intechopen.78220

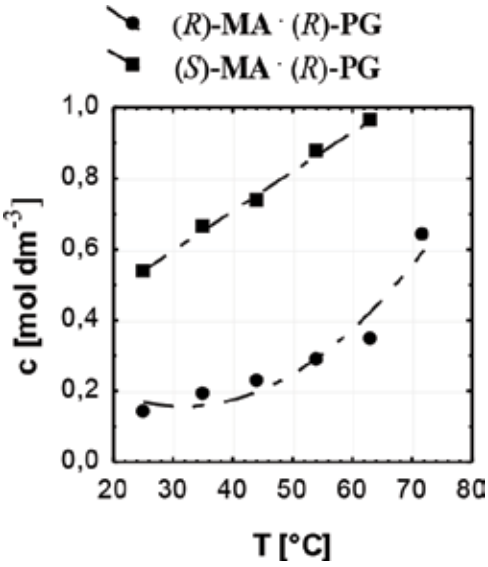

Figure 12. Temperature-dependent solubility of (*S*)-**MA**·(*R*)-**PG** and (*R*)-**MA**·(*R*)-**PG** diastereomers.

5. Effect of ultrasound on the composition of the diastereomeric salt

The resolution of the racemic etodolac (**ETO**) was carried out using cinchonidine (**CIN**) as resolving agent, with the application of seed and ultrasound. During the experiment, the ethanol solution was heated until complete dissolution of the components, followed by a crystallization of 4 hours at 0°C. During cooling, the reaction mixture was seeded with (*R*)-**ETO**.**CIN** diastereomer, which was then sonicated for 5 min, resulting in (*R*)-**ETO** enantiomer mixture of 99% enantiomer purity (**Scheme 12**). In the case of room temperature stirring, the product was received with low yield and low optical purity (~ee: 40%), which indicates the almost simultaneous crystallization of the two diastereomers [37].

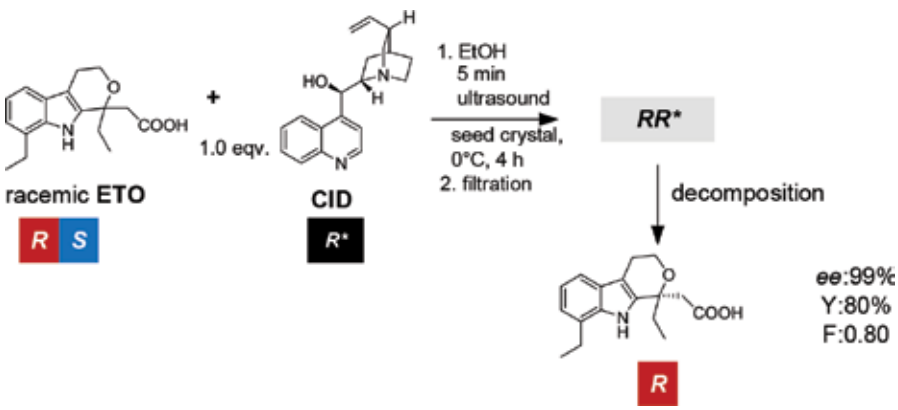

Scheme 12. Resolution of etodolac with the application of ultrasound.

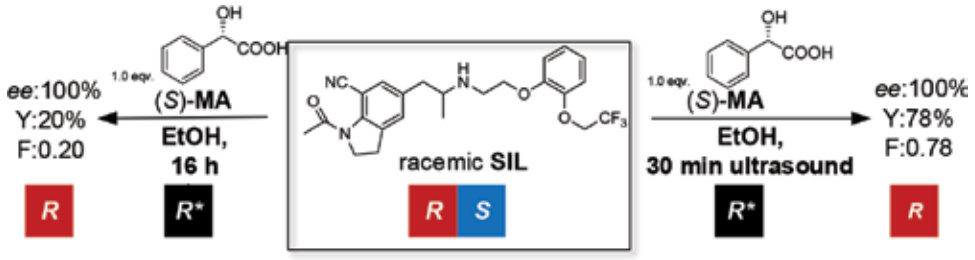

Scheme 13. Resolution of silodosin intermediate.

The resolution of the intermediate of silodosin (**SIL**) was carried out with (*S*)-mandelic acid (**MA**) during sonication (for 30 min) by Sun et al. They found a threefold increase in the yield. The ultrasound intensified the separation of the more stable diastereomer, ensuring fast crystallization in case of resolution based on salt formation (**Scheme 13**) [38].

The resolution of the racemic 2,3,5,6-tetrahydro-6-phenylimidazo[2,1-b]thiazole (**TET**) was carried out with (*R,R*)-dibenzoyl-tartaric acid ((*R,R*)-**DBTA**) in water/dichloromethane nonmiscible solvent mixture [36].

Comparative experiments were executed to determine the effect of the ultrasound treatment compared with conventional stirring. The racemic tetramisol was dissolved in the mixture of dichloromethane and water at 40°C. The resolving agent, 0.3 mol equivalent (*R,R*)-**DBTA**, was dissolved in dichloromethane at 40°C, and then the solutions were unified and cooled to 5°C. The speed of the magnetic stirrer was 500 rpm. The ultrasound treatment was carried out for 1, 5, 10, 15, 10 and 30 min, using a Bandelin Sonopuls HD 2200 apparatus, with 4.3, 6.5 and 11.0 W powers. After the appearance of the first crystal, the diastereomeric salt was allowed to crystallize for different times, that is for 1, 10, 20 and 30 min, followed by filtration. The diastereomeric salt was analyzed with chiral HPLC (**Figure 13**).

By filtrating the formed diastereomeric salt after 1 min of crystallization, (*S*)-tetramisol ((*S*)-**TET**) of 48% enantiomer purity could be separated with a yield of 91% (**Figure 14**).

By increasing the time of the crystallization, the enantiomer purity of the recoverable enantiomeric mixture decreases, while the yield increases. When the time of the crystallization was 30 min, the enantiomer purity decreased to 12%. The efficiency of resolution (F) values shows a significant decrease with increasing crystallization time (from 0.44 to 0.12). This is the beneficial effect of the kinetic control.

Immediate crystal precipitation was observed in the course of the application of ultrasound. When applying ultrasound of 4.3 W power, after 1 min an enantiomer purity of 39% and a yield of 84% were reached. By increasing the time of the sonication, the enantiomeric mixture of tetramisol could be separated from the diastereomeric salt with an *ee* between 54 and 64% and the yield was between 78 and 93%. The efficiency of resolution increased from 0.43 to 0.55 in course of sonication for 5–30 min (**Figure 15**). The use of ultrasound of 6.5 and 11.0 W power, respectively, resulted in almost the same *ee*, Y and F values after 30 min of sonication. Practically, the enantiomer purity was constant during the sonication.

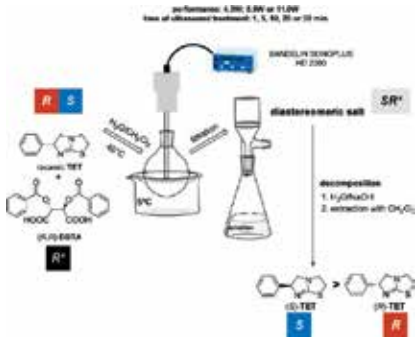

Figure 13. Schematic illustration of the experiments carried out with the application of ultrasound.

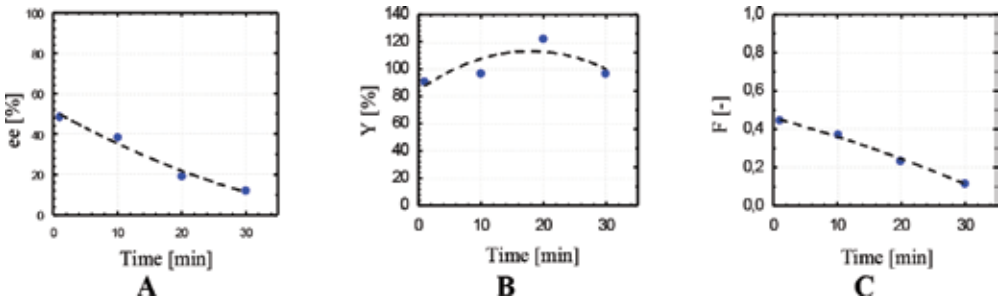

Figure 14. Enantiomer purity (A), yield (B) and efficiency of resolution value (C) of the enantiomeric mixture of tetramisol separated from the diastereomeric salt, in the function of the crystallization time, without the application of ultrasound (average values of three parallel experiments).

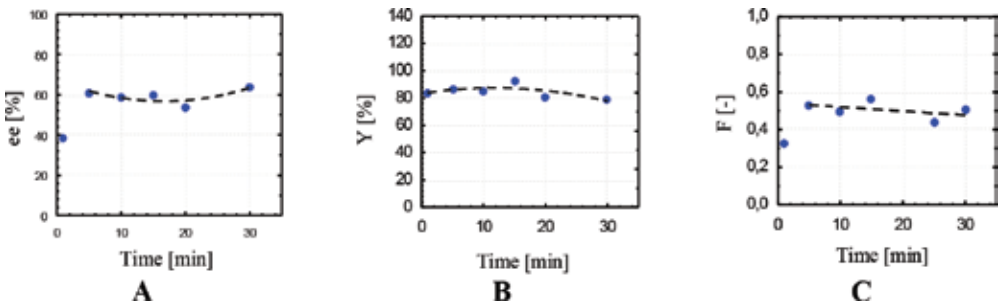

Figure 15. Enantiomer purity (A), yield (B) and efficiency of resolution value (C) of the enantiomeric mixture of tetramisol separated from the diastereomeric salt, in the function of the crystallization time, with the application of ultrasound of 4.3 W (average values of three parallel experiments).

6. Conclusion

One of the possibilities for the separation of mixtures of chiral compounds (for both enantiomers and diastereomers) is their non-linear distribution between two phases.

It is noteworthy that the result of the crystalline segregation can be essentially changed by the set of appropriate pH value. The recent recognition of the effect of the kinetic control

combined with ultrasound treatment, leading to a time-independent stabilization and amelioration of the result of the separation, is also remarkable.

The equilibriums can also be significantly affected by the formation of solvate molecules or with the built-in of non-solvent molecules of similar molecular architecture to the crystalline structure during the formation of the solid phase.

Acknowledgements

The authors thank the financial support of the Hungarian OTKA Foundation (K 124180 for E. Fogassy).

Author details

Emese Pálovics*, Szeleczky Zsolt, Szolnoki Beáta, Bosits Miklós and Fogassy Elemér

*Address all correspondence to: epalo@mail.bme.hu

Department of Organic Chemistry and Technology, Budapest University of Technology and Economics, Budapest, Hungary

References

[1] Newman P. Optical resolution procedures of chiral compounds 1-3. New York: Resolution Information Center. 1978-1984

[2] Wilen SH. Resolving agents and resolutions in organic cehemistry. In: Eliel EL, Allinger NL, editors. Topics in Stereochemistry. Vol. 107. New York: Wiley-Interscience; 1972

[3] Jaques J, Collet A, Wilen SH. Enantiomers, Racemates, and Resolutions, John Wiley & Sons, Inc., New York, Chichester, Brisbane, Toronto 1981

[4] Faigl F, Kozma D. Optical Resolution via Complex Formation with O,O′-Dibenzoyltartaric Acid, in Enantiomer Separation: Fundamentals and Practical Methods Chapter 3. (Edited by Toda, F.), Kluwer Academic Publishers, Dordrecht, Hollandia, 2004. p. 73

[5] Fogassy E, Nógrádi M, Pálovics E, Schindler J. Resolution of Enantiomers by Non-Conventional Methods Synthesis. 2005;**10**:1555

[6] Fogassy E, Nógrádi M, Kozma D, Egri G, Pálovics E, Kiss V. Optical resolution methods. Organic and Biomolecular Chemistry. 2006;**16**:3011

[7] Faigl F, Fogassy E, Nógrádi M, Pálovics E, Schindler J. Strategies in optical resolution (a practical guide). Tetrahedron: Asymmetry. 2008;**4**:519

[8] Sheldon RA. Chirotechnology: Industrial Synthesis of Optically Active Compounds. New York: Marcel Dekker; 1993

[9] Wilen SH, Collet A, Jaques J. Strategies in optical resolutions. Tetrahedron. 1977;**33**:2725

[10] Kobayashi Y, Kodama K, Saigo K. Supramolecular Architecture Consisting of an Enantiopure Amine and an Achiral Carboxylic Acid: Application to the Enantioseparation of Racemic Alcohols. Organic Letters. 2004;**17**:2941

[11] Pálovics E, Szeleczky Z, Faigl F, Fogassy E. In: Muntean SG, Tudose R, editors. Correlations between Separations of Enantiomeric- and Diastereomeric Mixtures, New Trends and Startegies in the Chemistry of Advanced Materials. 2013. pp. 74-79

[12] Pálovics E, Szeleczky Zs, Fődi B, Faigl F, Fogassy E. In How is the enantiomeric recognition influenced by the interactions of chiral systems? New trends and startegies in the chemistry of advanced materials with relevance in biological systems, technique and environmental protection. (Ed. Tudose R); 2015. pp. 14-16

[13] Pálovics E, Szeleczky Z, Fődi B, Faigl F, Fogassy E. Prediction of the efficiency of diastereomer separation on the basis of the behaviour of enantiomeric mixtures. RSC Advances. 2014;**4**:21254-21261

[14] Szeleczky Z, Bagi P, Pálovics E, Fogassy E. The effect of the eutectic composition on the outcome of kinetically and thermodynamically controlled resolutions that are based on the formation of diastereomers. Tetrahedron: Asymmetry. 2015;**26**:377-384

[15] Pálovics E, Schindler J, Faigl F, Fogassy E. Behavior of structurally similar molecules in the resolution processes. In: Carreira EM, Yamamoto H, editors. Comprehensive Chirality. Amsterdam: Elsevier; 2012. pp. 91-95

[16] Szeleczky Zs, Semsey S, Bagi P, Pálovics E, Faigl F, Fogassy E. Selecting resolving agents in respect of their eutectic compositions. Chirality: The pharmacological biological and chemical consequences of molecular asymmetry. 2016;**28**(3)**:**230-234

[17] Szeleczky ZS, Bagi P, Pálovics E, Faigl F, Fogassy E. The pH-dependency of diastereomeric salt resolutions with amphoteric resolving agents. Journal of Chemical Research-Synopses. 2016;**40**(**1**):21-25

[18] Szeleczky Zs, Kis-Mihály E, Semsey S, Pataki H, Bagi P, Pálovics E, Gy M, Gy P, Fogassy E, Madarász J. Effect of ultrasound-assisted crystallization in the diastereomeric salt resolution of tetramisole enantiomers in ternary system with O,O′-dibenzoyl-(2R,3R)-tartaric acid. Ultrasonics Sonochemistry. 2016;**32**:8-17

[19] Zhong N, Zhao X, Ma H, Chen Y. WO Patent 2007/0096661

[20] Jang SY, Kim S, Yun S, Bang HJ, Kim HK, Suh KH. Method for preparing (S)-(-)-amlodipine or a salt thereof and an intermediate used therein WO Patent 2008/100023. Chemical Abstracts. 2008;**149**:274860

[21] Bereczki L, Pálovics E, Bombicz P, Pokol G, Fogassy E, Marthi K. Optical resolution of N-formylphenylalanine succeeds by crystal growth rate differences diastereomeric salts. Tetrahedron:Asymmetry. 2007;**18**:260-264

[22] Szeleczky Z, Bagi P, Fődi B, Semsey S, Pálovics E, Faigl F, Fogassy E. Non-linear effects in the enantiomeric separation of mandelic acid using the mixtures of amphoteric resolving agents. Tetrahedron:Asymmetry. 2015;**26**:721-731

[23] Fogassy E, Faigl F, Ács M, Grofcsik A. Equilibrium-model of optical resolution via diastereomeric salt formation. Journal of Chemical Research. 1981;**11**:346-347

[24] Fogassy E, Faigl F, Ács M, Simon K, Kozsda É, Podányi B, Czugler M, Reck G. Structural studies on optical resolution via diasteroisomeric salt formation-enantiomer separation for cis-permethrinic acid[cis-2,2-dimethyl-3-(2,2-dichlorovinyl)-cyclo-propanecarboxylic acid]. Journal of the Chemical Society, Perkin Transactions. 1988;**2**:1385-1392

[25] Bálint J, Egri G, Kiss V, Gajáry A, Juvancz Z, Fogassy E. Unusual phenomena during the resolution of 6-fluoro-2-methyl-1,2,3,4-tetrahydroquinoline(FTHQ): thermodynamic-kinetic control. Tetrahedron: Asymmetry. 2002;**12**:3435-3439

[26] Sakai K, Sakurai R, Hirayama N. Chiral discrimination controlled by the solvent dielectric constant. Tetrahedron: Asymmetry. 2004;**15**:1073-1076

[27] Sakai K, Sakurai R, Akimoto T, Hirayama N. Molecular mechanism of dielectrically controlled optical resolution (DCR). Organic and Biomolecular Chemistry. 2005;**3**:360-365

[28] Shitara H, Shintani T, Kodama K, Hirose T. Solvent-Induced Reversed Stereoselectivity in Reciprocal Resolutions of Mandelic Acid and erythro-2-Amino-1,2-diphenylethanol. Journal of Organic Chemistry. 2013;**78**:9309-9316

[29] Sakurai R, Sakai K, Kodama K, Yamaura M. Dielectrically controlled resolution (DCR) of 3-aminopiperidine via diastereomeric salt formation with N-tosyl-(S)-phenylalanine. Tetrahedron: Asymmetry. 2012;**23**:221-224

[30] Sakai K, Sakurai R, Nohira H, Tanaka R, Hirayama N. Practical resolution of 1-phenyl-2-(4-methylphenyl)ethylamine using a single resolving agent controlled by the dielectric constant of the solvent. Tetrahedron: Asymmetry. 2004;**15**:3495-3500

[31] Kitamoto Y, Suzuki K, Morohashi N, Sakai K, Hattori T. Switching of the Diastereomer Deposited during the Crystallization of N-[(S)-1-Phenylethyl]-2′-carbamoyl-1,1′-binaphthalene-2-carboxylic Acid: Investigation of the Mechanism of Dielectrically Controlled Resolution. Journal of Organic Chemistry. 2013;**78**:597-605

[32] Kodama K, Kimura Y, Shitara H, Yasutake M, Sakurai R, Hirose T. Solvent-induced chirality control in the enantioseparation of 1-phenylethylamine via diastereomeric salt formation. Chirality. 2011;**23**:326-332

[33] Gizur T, Törley J, Fogassy E, Bálint J, Egri G, Demeter Á. Process for preparing tamsulosin hydrochloride. WO Patent 2004022532; Chemistry Abstract. 2004;**253341**:140

[34] Blackmond DG, Klussmann M. Spoilt for choice: assessing phase behavior models for the evolution of homochirality. Chemical Communications. 2007:3990-3996

[35] Nemák K, Ács M, Jászay ZM, Kozma D, Fogassy E. Study of the diastereomers formed formed between pipecolic acid N-alkylanilides and 2R,3R-tartaric acid or O,O′-dibenzoyl-2R,3R-tartaric acid. Do the tartaric acids form molecular complexes instead of salts during optical resolutions? Tetrahedron. 1996;**52**:1637-1642

[36] Szeleczky Zs. New recognition int he processes of diastereomeric salt resolution. PhD Thesis, Budapest University of Technology and economics, 2015, https://repozitorium.omikk.bme.hu/bitstream/handle/10890/1494/tezis_eng.pdf?sequence=4&isAllowed=y

[37] Ge L, Zhao Q, Yang K, Liu S, Xia F. Optical Resolution and Optimization of (R,S)-Propranolol Using Dehydroabietic Acid Via Diastereomeric Crystallization. Chirality. 2015;**27**:131-136

[38] Chou S, Tseng C, Chang L. Exploration of an Efficient Method for Optical Resolution of Etodolac. Journal of the Chinese Chemical Society. 2001;**48**:229-234

Chapter 6

Separation of Chiral Compounds: Enantiomeric and Diastereomeric Mixtures

Emese Pálovics, Szeleczky Zsolt, Szolnoki Beáta,
Bosits Miklós and Fogassy Elemér

Additional information is available at the end of the chapter

http://dx.doi.org/10.5772/intechopen.76478

Abstract

Despite the dramatic development of enantioselective synthesis and chromatographic separation methods, optical resolution still remains the cheapest and operationally simplest method for producing pure enantiomers on a larger scale. No extreme conditions or expensive reagents are required, and the eventually expensive resolving agents can be recovered. This chapter is based mainly on the authors' long experience in the resolution of industrially important molecules, and it presents new observations and establishments as well. Several methods for separation of chiral mixtures, enantiomeric and diastereomeric mixtures, are shown, and possibilities for predicting the efficiency of resolution based on the analysis of physico-chemical properties of the reactants are also described.

Keywords: enantiomeric mixtures, resolution, eutectic composition, helical structure

1. Introduction

Due to both practical and theoretical reasons, the properties and the possible preparation techniques of chiral compounds are investigated in ever widening fields of research, applying various examination methods [1, 2]. It is a great challenge for some researchers if the goal is to find a simple, inexpensive, economical and also patentable preparation of a given chiral compound (single enantiomer), for example according to the demands of the industrial production or drug discovery. Although nowadays several alternative synthetic pathways can be found for the preparation of a given single enantiomer, most probably in most cases the break-up of a certain racemic composition [3], leading to the synthesis of the final product,

followed by the purification of the mixture, is applied [1, 2, 4]. In most cases, mixtures of diastereomers received with appropriate resolving agents, or mixtures of enantiomers isolated thereof, have to be separated. It is common in the two separation methods, that the distribution of the mixtures between two phases, and the phase separation can be applied [4–6]. However, the phase distribution of the mixtures of chiral compounds is not linear, but the distributions follow the binary melting phase diagrams of the mixtures, or the ternary phase diagrams characteristic also for the applied solvent [7, 8].

Besides the effect of the applied solvents, the phase distribution of the mixtures is also determined by kinetic or thermodynamic control [9]. The phase distribution is also determined by the eutectic composition of the chiral molecules in the mixtures [10, 11]. The equilibrium of the supramolecular helical structures, which participate in the phase distribution, determines the formation of the phase equilibriums [12]. A remarkable consequence of the effect of the helical structures is that the mirror-image macroscopic enantiomers form not only mirror-image crystals, but by attaching together, mirror-image helical crystals are formed [13, 14]. At the same time, mainly one of the helicities can be attributed to a given enantiomer, most probably this is the reason behind the results of separations. In the followings, the most characteristic examples of the above-mentioned methods will be discussed.

2. Separation of enantiomeric mixtures without chiral reagent

2.1. Formation of macroscopically helical crystals

The enantiomeric mixtures form crystals of a given helicity corresponding to the major configuration (**Scheme 1**).

In case of purification of enantiomeric mixtures of threonine was observed, that the majority of crystals have a convolution corresponding to the helical structure of the excess, while the minor enantiomer, crystallized near the excess, have the opposite convolution. The ratio between the major and minor helical crystals is in good correlation with the eutectic composition

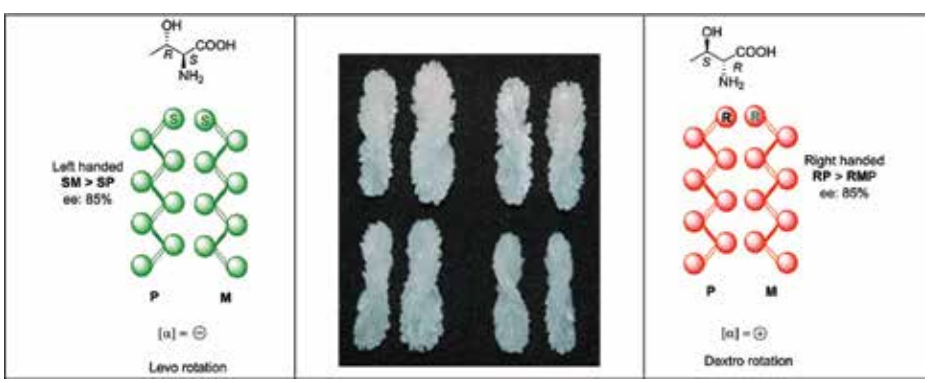

Scheme 1. Purification of enantiomeric mixtures of threonine from water ($ee_0 \neq 0$).

of the enantiomeric mixture of threonine. So the eutectic composition (ee_{Eu}) precipitates during evaporation, dominated by the helicity of the excess, along with the crystallization of the minor enantiomer as well.

Mirror-image crystals are formed from the supramolecular helical structures, which contain one of the enantiomer in excess. The helicity of the crystals is determined by the optical rotation of the enantiomer in excess [13, 14].

2.2. Particle-size-controlled crystallization

The ethanol solution of the conglomerate racemic *trans*-hydrobenzoin [15] (**THB**) was seeded with different amounts of (*S*,*S*)-**THB** and (*R*,*R*)-**THB** seeds of different particle size during a specified cooling program. After crystallization, the received crystals were separated to different ranges of particle size by sieving. Thus, enantiomeric mixtures of (*S*,*S*)-**THB** and (*R*,*R*)-**THB** of 83% and 87% enantiomeric excess were gained, respectively (**Scheme 2**) [16].

2.3. Gravity-based enantiomer separation

According to Soloshonok et al., the SDE (self disproportionation of enantiomers) appears in three main areas: gravitational field, phase transition, and the achiral chromatography [17]. Basically, the gravity-based SDE applies the differences in crystal density. The racemate enantiomeric mixture can be considered as the mechanical mixture of the racemic and enantiopure crystals, which can have different crystal densities. This difference can be applied for the separation of the racemic and enantiopure fraction. For example, from a enantiomeric mixture of phenylalanine (**Phe**) having 50% enantiomeric purity, two phases of 90 and 13% enantiomeric purity, respectively, could be separated after stirring in an inert solvent of appropriate density, set between the densities of the racemic and enantiopure crystals (**Scheme 3**) [18, 19].

Based on these results, separation of amino acid enantiomeric mixtures was carried out via density gradient ultracentrifugation, applying an iodinated gradient (*Nycodenz*) used in the isolation of nucleic acids and proteins. Recently, the density difference between the racemic and enantiopure Ibuprofen was utilized in an apparatus based on principle of magnetic levitation [20].

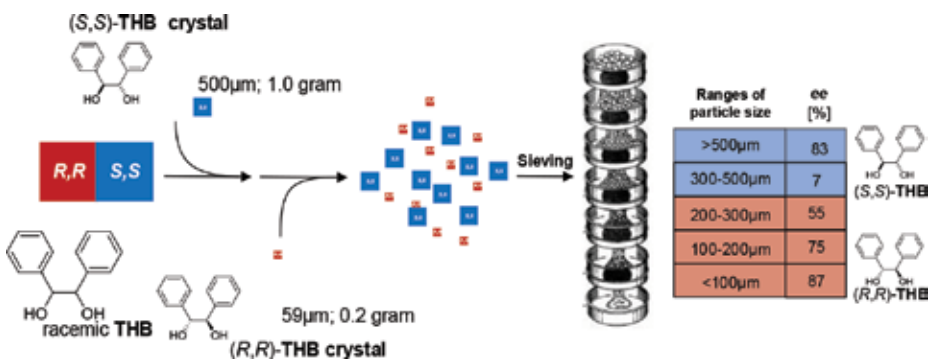

Scheme 2. Application of particle-size-controlled crystallization for resolution.

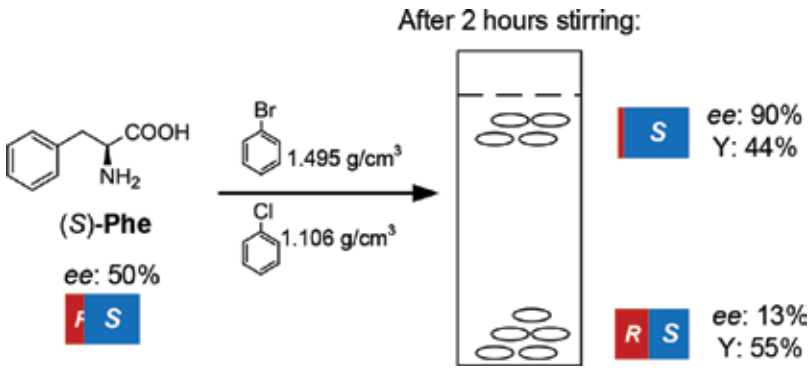

Scheme 3. Application of density difference for the purification of enantiomeric mixtures.

2.4. Distribution between phases, enantiomeric separation

In the case of phase transitions, the SDE phenomenon is not uniform, it highly depends on the type of the phase transition [17].

2.4.1. Fractionated crystallization

In the case of the recrystallization of enantiomeric mixtures, by plotting the enantiomeric purity of the solid phase in function of the starting enantiomeric purity, a curve similar to binary and ternary phase diagrams can be obtained (ee_0-*ee* curve) (**Scheme 4**). Regarding a racemate enantiomer mixture, by recrystallizing a mixture having lower purity than the eutectic composition, in any case increased purity will be gained in the solution/melt phase, while above the eutectic composition, the enantiomeric enrichment is expected in the solid phase [2]. The recrystallization is not successful in all the cases to reach enantiomeric enrichment, for example the recrystallization experiments of the enantiomer mixtures of *N*-formyl-phenylalanin (*N*-formyl-**Phe**) and *N*-acetyl-phenylalanin (*N*-Ac-**Phe**), were unsuccessful [21].

A possible mechanism of the recrystallization of racemate-type enantiomeric mixtures is described by Tamura [24–28].

2.4.2. Distribution between solid and gas phases, enantiomer separation

In the case of mandelic acid, the vapor phase has a eutectic composition, which is independent from the composition of the starting mixture and this composition will sublimate [29]. Independently from the preparation of the starting mixture, enantiomeric mixtures of mandelic acid of 30–54% enantiomeric purity were received as sublimates (**Scheme 5**), which approximates well the eutectic composition determined from the binary and ternary phase diagrams of mandelic acid (ee_{eu}: 32% [30, 31]). In the case of the sublimation of several racemate-type amino acids, the purities received in the sublimates [32–34] were identical to the eutectic compositions determined from the ternary phase diagrams [35].

http://dx.doi.org/10.5772/intechopen.76478

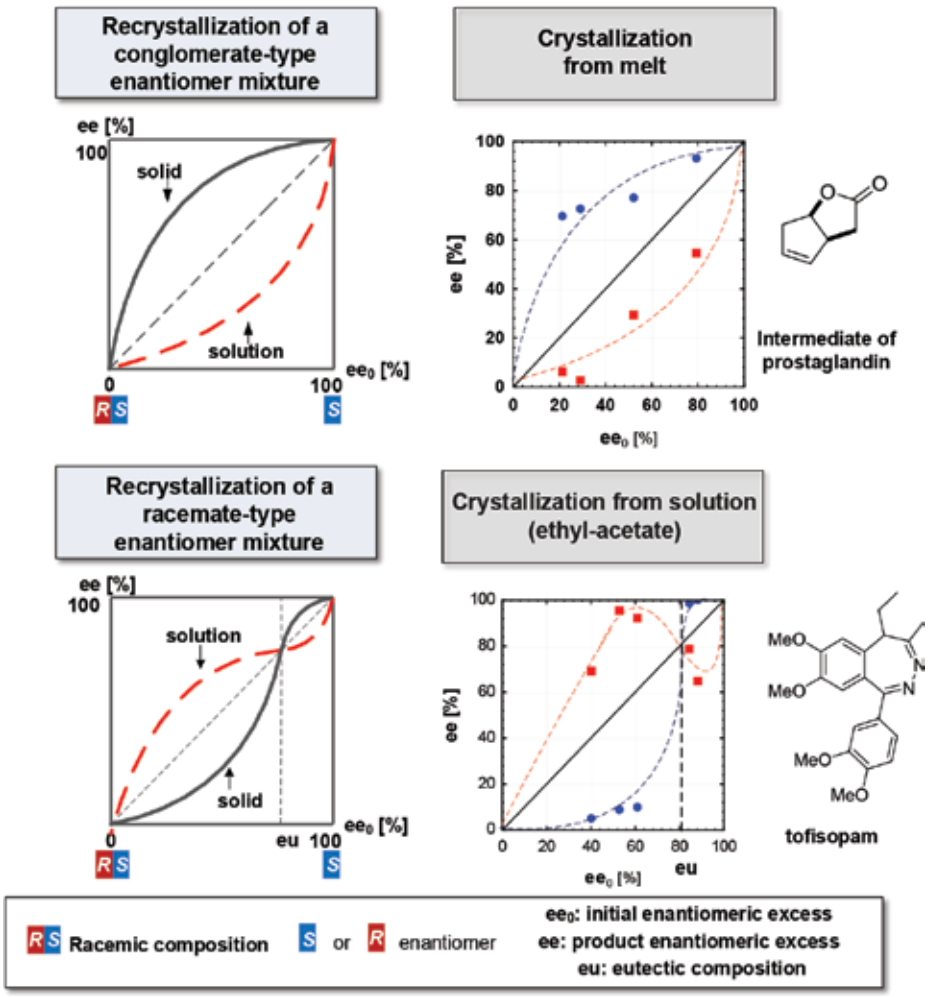

Scheme 4. Typical curve received from the recrystallization of a conglomerate-type enantiomer mixture (ee_0-ee diagram) and an example of ee_0-ee diagram for crystallization from melt [22] (upper diagrams); and a typical curve received from the recrystallization of a racemate-type enantiomer mixture (ee_0-ee diagram) and an example of ee_0-ee diagram for crystallization from solution (lower diagrams) [23].

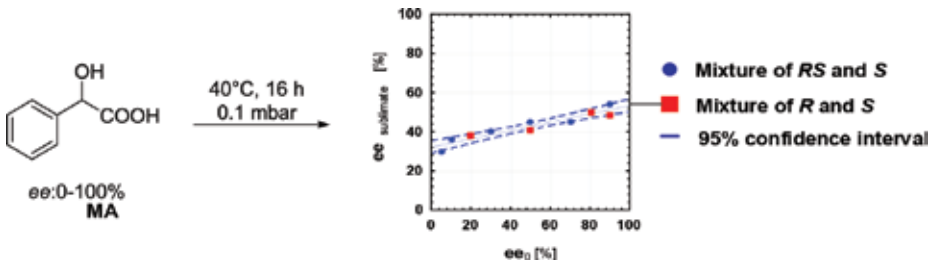

Scheme 5. Sublimation of enantiomer mixtures of mandelic acid (MA).

2.4.3. Distribution between liquid and gas phases, enantiomer separation

During the distillation of enantiomer mixtures of isopropyl-(*S*)-trifluorlactate (isopropyl-(*S*)-**TLAK**), the purity of the enantiomer mixtures gained in the distillate and in the residue was different from the starting composition (**Scheme 6**) [36, 37]. Another example for the enantiomer enrichment received by fractionated distillation is that an enantiomeric mixture of 91% enantiomer purity of *N*-trifluoracetyl-(*S*)-valine-methyl-ester (*N*-trifluoracetyl-**Val-Me**) could be further separated to two parts of 88.0 and 97.6% enantiomeric excess, respectively [38].

2.4.4. Separation of enantiomeric mixtures by achiral chromatography

The SDE phenomenon prevails in the case of enantiomeric enrichment by achiral chromatography. Applying achiral stationary phase and an appropriate eluent, the enantiomeric mixtures can be separated to a polar and a less polar phase, which have different enantiomer purity from the staring composition due to the formation of homo- and heterochiral associations. For example, an enantiomeric mixture of *N*-acetyl-1-phenylethylamin (*N*-Ac-**PhEA**) having 71% enantiomeric excess could be further separated on silica gel stationary phase to two fractions of 99 and a 28% *ee* values, respectively (**Scheme 7**) [39].

Such a separation was first described by Cundy and Crooks [40], but this method is applied by others as well, for the purification of enantiomeric mixtures [17, 41].

2.4.5. Separation of enantiomers by fractionated precipitation

After partial liberation of the achiral salt of the enantiomeric mixtures, the purity of the received enantiomeric mixture may be different from the starting composition. By the addition of base equivalent to the enantiomeric excess to the hydrochloric salt of the conglomerate *Tisercin* (Levomepromazine) (**TIS**) in every case the liberating enantiomeric mixture is purer than the starting composition (**Scheme 8**) [42, 43].

By the resolution of the racemic *cis*-permethric acid (**CPA**), a mixture enriched in (*S,S*)-enantiomer was received. Further purification of the **CPA** was carried out by precipitation from its *Na*-salt with hydrochloric acid (**Scheme 9**) [44].

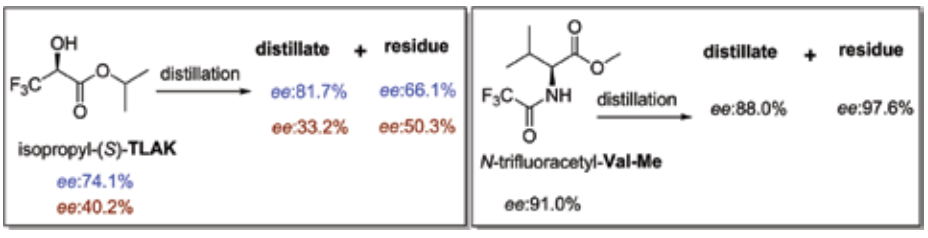

Scheme 6. Separation of enantiomer mixtures by distillation.

http://dx.doi.org/10.5772/intechopen.76478

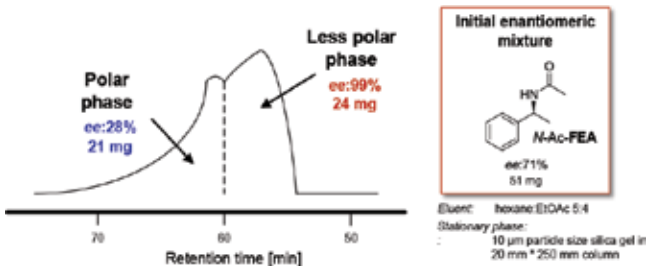

Scheme 7. Purification of enantiomeric mixture of *N*-acetyl-phenylethylamine applying achiral chromatography [45].

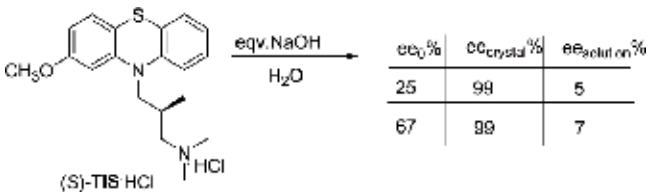

ee_0%	$ee_{crystal}$%	$ee_{solution}$%
25	99	5
67	99	7

Scheme 8. Fractionated precipitation of enantiomer mixture of Tisercin.

2.4.6. Kinetic control at the fractionated precipitation

In the case of the fractionated precipitation of the enantiomer mixtures of *N*-propionyl-phenylalanine (*N*-propionyl-**PhA**), the curve expected from the binary phase diagram is significantly different from the received one. The crystals of the enantiomeric excess catalyze (instead of the separation of a low enantiomeric excess, expected under thermodynamic control) the separation of much higher enantiomer purity. For example, in the case of a starting composition around ee_0: 20%, in the first fraction one of the enantiomers is enriched, while the second fraction will be enriched in the other one (**Scheme 10**) [21].

2.4.7. Precipitation and extraction

With the combination of precipitation and extraction, for example by liberating a part of the enantiomer mixture in the mixture of water and a water-immiscible solvent, the free enantiomer will stay in the organic phase, while the salt in the water [45].

2.4.8. Precipitation and distillation

The purification of enantiomer mixtures can also be carried out by the transformation of the racemic percentage of the enantiomer mixture into solid phase as salt, followed by the distillation of the free enantiomeric excess [46, 47]. This method was applied in the case of enantiomer mixtures of salts of 1-phenylethyl-amine (**PhEA**) composed with nonequivalent amounts of dicarboxylic acids. By plotting enantiomer purity of the distillate and the residue in the function of the starting enantiomer purity, a diagram similar to the ee_0-*ee* curve, received in

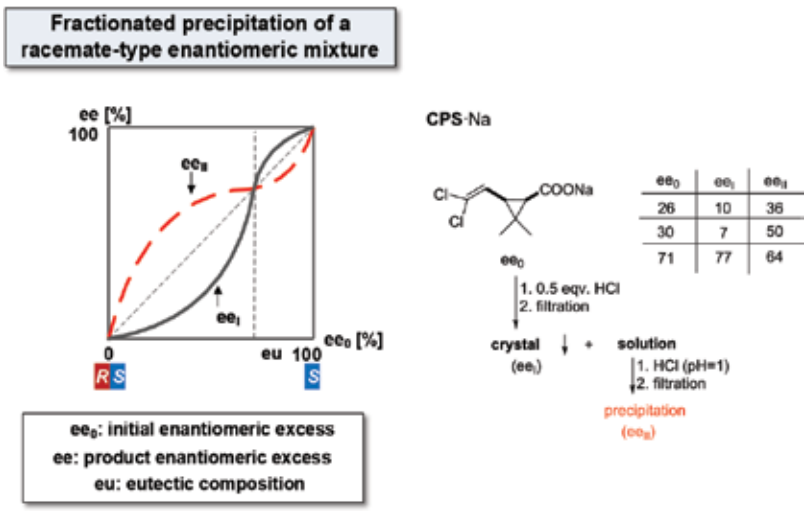

Scheme 9. Fractionated precipitation of *cis*-permethric acid.

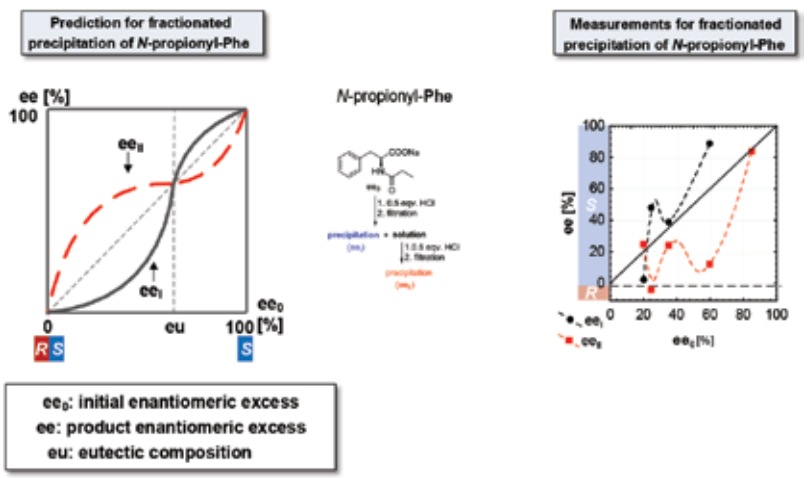

Scheme 10. Fractionated precipitation of N-propionyl-phenylalanine.

course of recrystallizations, can be obtained, and also, the joins are in accordance with the eutectic composition of the ternary phase diagram [48].

2.4.9. Precipitation of neutral salts of dicarboxylic acid

The racemic amlodipine with the chiral dicarboxylic tartaric acid crystallizes as the neutral salt of the racemic compound from solvents, without the presence of solvates or solvate-like molecules. Consequently, in the case of enantiomeric mixtures with achiral dicarboxylic acids, the crystallization of the neutral salt of the racemic percentage seemed to be logical.

http://dx.doi.org/10.5772/intechopen.76478

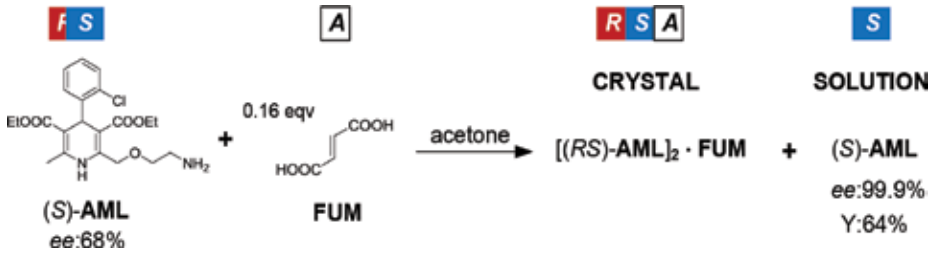

Scheme 11. Purification of enantiomeric mixture of amlodipine.

To the enantiomeric mixture of AML in solution (in acetone), achiral fumaric acid (**FUM**) was given in equal amount to the racemic percentage. The mixture was dissolved by heating. After cooling, the fumaric acid salt of the racemic percentage was filtered out, while the residue was evaporated, resulting in enantiopure (*S*)-**AML** and (*R*)-**AML** base, respectively. From a starting **AML** enantiomeric mixture of *ee*: 68%, reacted with 0.16 equivalent fumaric acid (equivalent to the racemic percentage), after the filtration of the precipitated crystalline neutral fumaric acid salt, (*S*)-**AML** of *ee*: 99.9% enantiomeric excess can be separated from the mother liquor (**Scheme 11**).

3. Separation of diastereomeric mixtures (recent results)

3.1. Chiral salt of helical supramolecular structure as resolving agent (separation of diastereomeric molecular complex)

The salt of a chiral amine of supramolecular helical (double helix) structure and an achiral acid precipitates from the solvent (methanol) containing racemic alcohol as well, in the form of supramolecular helical crystals, which are composed of chiral amine, acid and one enantiomer of the racemic alcohol (**Scheme 12**) [49].

According to Kinbara, the most suitable resolving agent of a racemic molecule can be selected by the design of a stable hydrogen bond system [50]. Saigo et al. concluded after the analysis of several single crystals of pairs of diastereomeric salts, that the formed CH/π interactions play a significant role in the solubility difference of the diastereomers, which clearly influences the chiral recognition and thus the result of the separation [51, 52].

Others estimated well by quantum chemical computations the difference between the lattice energies of the pairs of diastereomeric salts, without preliminary knowledge on the crystal structure [53, 54]. However, it is confessed by the authors that these calculations need to be upgraded in order to be safely applicable in the search of resolving agents.

The conclusions drawn from the preparative results can facilitate the choice of the resolving agent. For example, it is already trivial, that very good separations can be reached with the application of a resolving agent of similar molecular structure (structurally related) to the racemic compound [10, 21, 55–58].

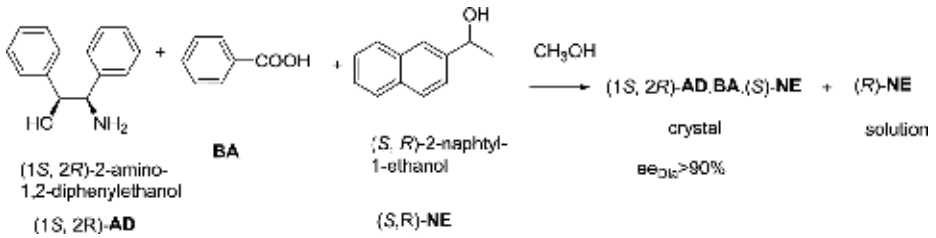

Scheme 12. The salt of chiral base and achiral acid crystallizes with the appropriate enantiomer of racemic alcohol.

3.2. Ratio of the molecules composing the diastereomer

Another approach construes the importance of the ratio of molecular lengths of the racemic molecule and the resolving agent instead of the structural similarity. According to Sakai, the author of the "space-filler concept," the crystal-lattice of the less soluble diastereomer salt is influenced by the structural properties of the constituents of the salt (i.e., the enantiomer and the resolving agent), such as the molecular size. Sakai et al. investigated the relative molecular length of the racemic molecule and the resolving agent in course of resolutions of 1-aryl-alkyl-amines with 2-hydroxycarboxylic acids and vice versa (**Scheme 13**). Based on the results of 20 resolutions, the best separations of the racemic mixtures can be reached with the application of a resolving agent of similar molecular length [59].

Other researchers considered the longest carbon-chain as the length of a molecule (**Scheme 14**). Based on the average of the results of 21 resolutions (*ee*, F), almost linear correlation was found between the difference of the molecular length of structurally related racemic mixtures and resolving agents, and the result of the resolution (**Schemes 15** and **16**) [10].

Besides the abovementioned 21 resolutions [10], carried out with structurally related resolving agents, the results of 28 additional resolutions [8, 18, 60–74] applying structurally non-related resolving agents were systematized (most of them were industrialized).

Based on the results of 49 resolutions, by plotting the average enantiomeric excess and efficiency of resolution values in function of the difference of molecular length, respectively, the following diagrams are received (**Schemes 17** and **18**). Accordingly, higher enantiomeric excess can be reached in case of higher difference of molecular length of the racemic compound and the resolving agent [75].

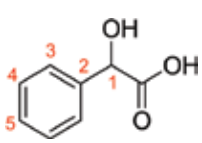

Scheme 13. Calculation of molecular length according to Sakai.

http://dx.doi.org/10.5772/intechopen.76478

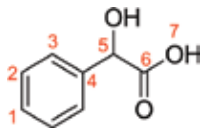

Scheme 14. Calculation method of molecular length used by other researchers.

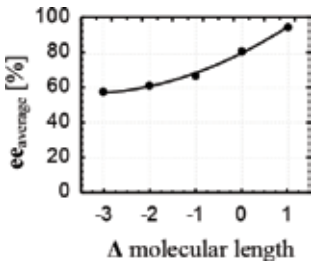

Scheme 15. Average of enantiomeric excess values of enantiomeric mixtures separated from diastereomeric salt in function of the difference of molecular length.

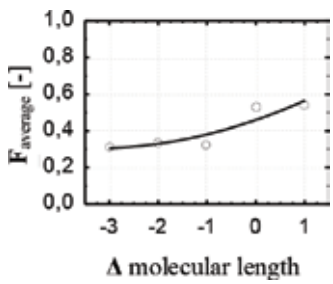

Scheme 16. Average of efficiency of resolution values of enantiomeric mixtures separated from diastereomeric salt in function of the difference of molecular length.

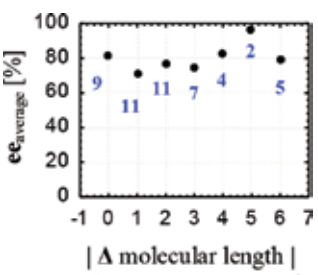

Scheme 17. $ee_{average}$ values of 49 resolutions in function of the difference of molecular lengths (blue numbers represent the number of samples).

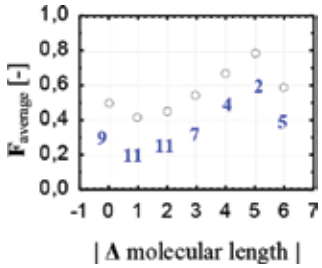

Scheme 18. $F_{average}$ values of 49 resolutions in function of the difference of molecular lengths (blue numbers represent the number of samples).

4. Amino acids and their mixtures as resolving agents

4.1. Amino acid resolving agents

1-Aminoindane was successfully resolved with the application of nearly 0.5 equivalent aspartic acid (**Asp**) and the (*R*)-enantiomer was separated (**Scheme 19**) [76].

For the resolution of racemic acids basic amino acids were also applied, for example (*S*)-lysine (**Lys**) (**Scheme 20**) [77, 78].

4.2. Mixtures of amino acids as resolving agents

With the application of equivalent amount of (*S*)-**Phe**, (*S,S*)-**AP** and (*S*)-**PG** resolving agents or their mixtures in course of the resolution of racemic mandelic acid (**Scheme 21**), the most effective resolving agent was the (*S*)-**PG**. In the case of resolutions carried out using the mixtures of resolving agents in 1:1 ratio, the most effective combination was the mixture of (*S*)-**Phe** and (*S*)-**PG.**

Among the half-equivalent resolving agents, (*S*)-**Phe** was the most effective, while from the half-equivalent resolving agent combinations, the mixture of (*S*)-**Phe** and (*S,S*)-**AP** was the most effective [8].

The racemic mandelic acid (**MA**) cannot be resolved from water with the application of (*S*)-**Ala**, however, a diastereomeric salt of *ee*: 23% enantiomeric excess was received using (*S*)-**Phe** as resolving agent. Applying mixtures of the two resolving agents in different ratios, (*S*)-**MA** of significantly increased enantiomeric excess could be separated from the precipitated diastereomeric mixture when the resolving agent consisted of 0.35 mol (*S*)-**Phe** and 0.65 mol (*S*)-**Ala** [8]. This is the application of the Dutch resolution method in the case of amino acid mixture resolving agents (**Scheme 22**).

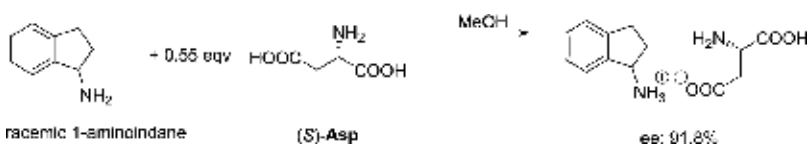

Scheme 19. Resolution of Rasagilin intermediate with (*S*)-aspartic acid.

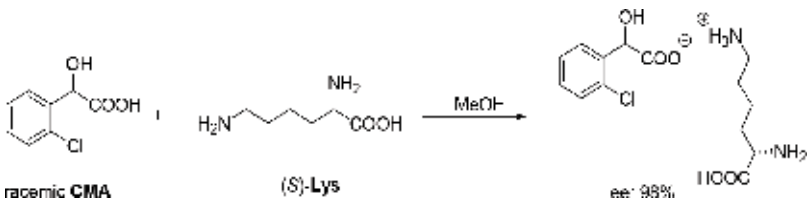

Scheme 20. Resolution of 2-chloro-mandelic acid with (S)-lysine.

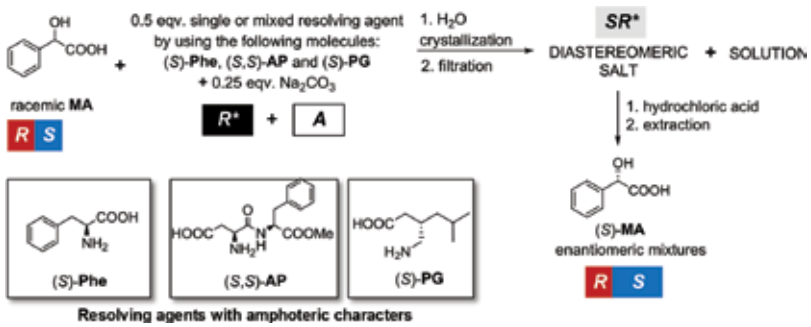

Scheme 21. Resolution of mandelic acid with the application of mixtures of resolving agents according to the Pope-Peachey half-equivalent method.

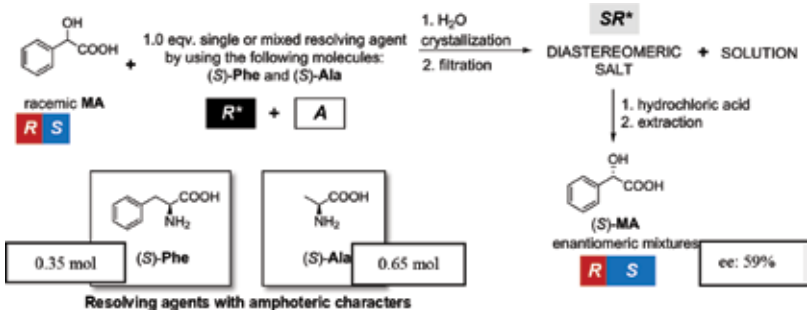

Scheme 22. Resolution of mandelic acid with the mixture of (*S*)-**Phe** and (*S*)-**Ala** resolving agents.

5. Presence, role, and effect on the diastereomer separation of achiral additive

5.1. Achiral additive structurally related to the racemic compound

After the resolution of *N*-acetyl phenylalanine (*N*-acetyl-**Phe**) with 1.0 equivalent (*R*)-1-phenylethylamine ((*R*)-**PhEA**), (*S*)-*N*-acetyl phenylalanine of 5% enantiomer purity could be separated from the diastereomeric salt. However, when equivalent amount of the structurally related phenoxy acetic acid (**PhOAA**) was given to the racemic *N*-acetyl-phenylalanine and this mixture was resolved with 2 equivalents of (*R*)-1-phenylethylamine, (*S*)-*N*-acetyl-phenylalanine of 88% enantiomeric excess was enriched in the diastereomeric salt (**Scheme 23**) [79].

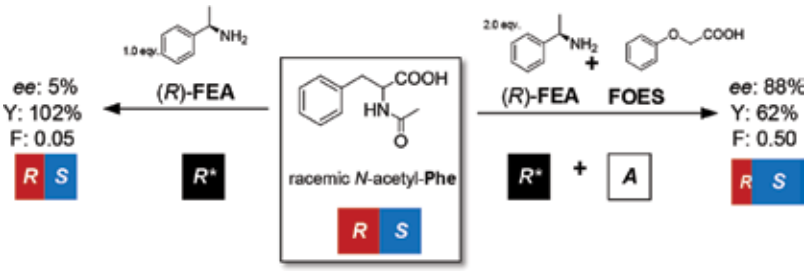

Scheme 23. Resolution of *N*-acetyl-phenylalanine in the presence of phenoxy acetic acid.

5.2. Achiral additive structurally related to the resolving agent

With the application of achiral additives, which are structurally related to the resolving agent, the efficiency of the enantiomer separations was significantly improved.

By changing the half of the phenylglycine methyl ester (**PhG-Me**) enantiomer resolving agent to the structurally related benzylamine (**BA**) in course of the resolution of *N*-acetyl phenylglycine (*N*-Ac-**PhG**), the enantiomer purity of the diastereomer salt of *N*-Ac-**PhG** increased by 54%, compared to the results of the 1 equivalent **PhG-Me** resolving agent (**Scheme 24**). Also in the case of 1-phenyl-ethyl amine (**PhEA**) resolving agent, by exchanging the half of **PhEA** to benzylamine, both the enantiomer purity and the efficiency of resolution values increased [79].

The resolution of racemic ibuprofen (IBU) with (*R*)-1-phenylethylamine ((*R*)-PhEA) and benzylamine (BA) as structurally related achiral additive was investigated. The unreacted enantiomer mixture of IBU was removed by $scCO_2$ extraction from the received diastereomeric salt. The addition of the achiral benzylamine resulted in higher efficiency of resolution (F_{SCS}) values compared to the experiments without additive (**Scheme 25**) [80].

5.3. Additive of similar structure to the polar part of the resolving agent

Racemic 1-phenylethylamine (**PhEA**) was resolved with *N*-glutaryl-1-phenylethylamine (**PhEA-GA**) applying urea and its derivatives and thiourea additives of neutral character, which show structural similarity with a part of the resolving agent. Although the enantiomer purity of the **PhEA** received from the diastereomeric salt decreased (from *ee*: 62% to *ee*: 51–54%), the increased yields led to higher efficiency of resolution values (from F: 0.36 to F: 0.37–0.49) in all cases (**Scheme 26**). The urea was

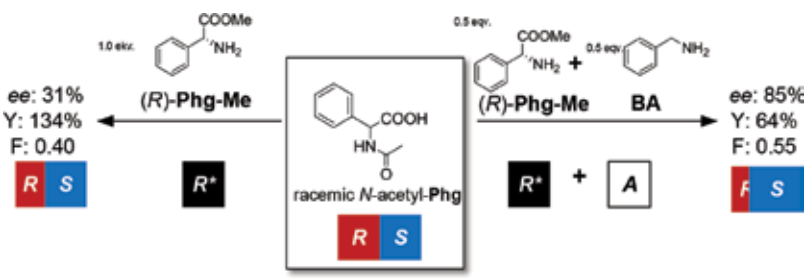

Scheme 24. Resolution of N-acetyl-phenylglycine with 1-phenylethylamine and with benzylamine as achiral additive.

http://dx.doi.org/10.5772/intechopen.76478

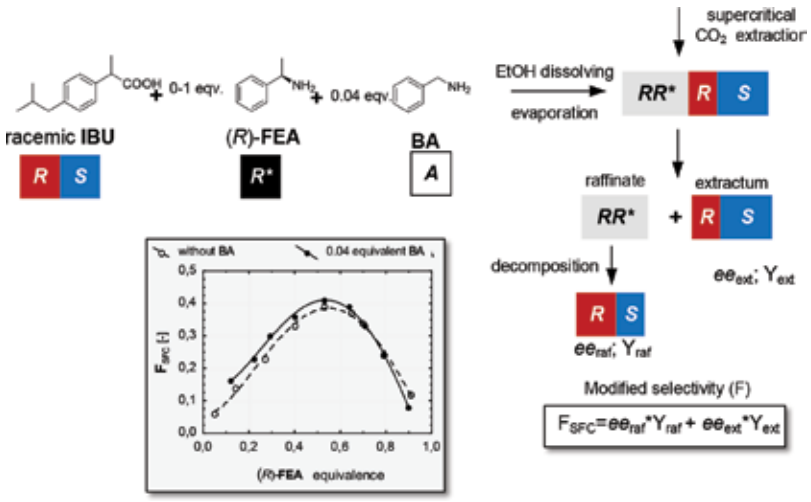

Scheme 25. Effect of benzylamine on the resolution of racemic ibuprofen by $scCO_2$ extraction.

proven to be present in the solid phase; therefore the process of the crystallization was investigated by polarization microscopy. According to the results, the nucleation of the diastereomer salt of (*S*)-**PhEA**·(*R*)-**PhEA-GA** starts on the surface of the initially appearing needle-like urea crystals [81].

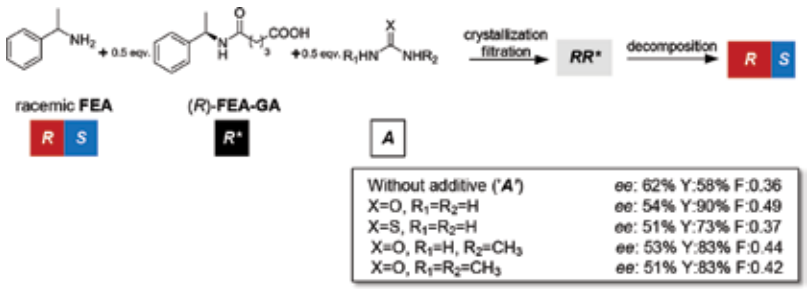

Scheme 26. Resolution of racemic 1-phenylethylamine in the presence of urea and its derivatives.

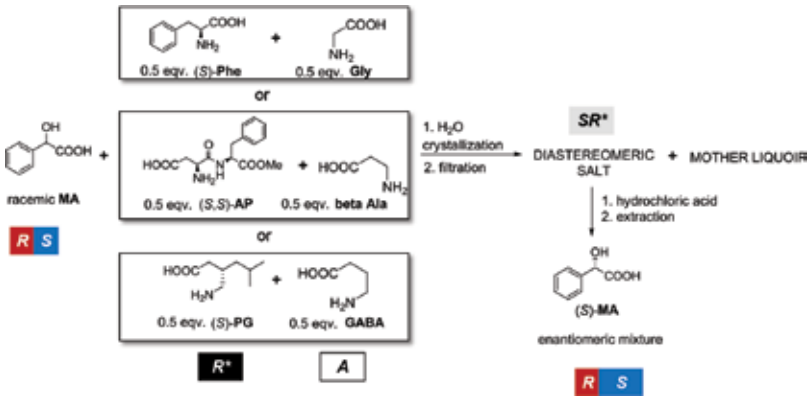

Scheme 27. Resolution of mandelic acid with the application of amphoteric achiral additives.

5.4. Application of achiral additives structurally related to amino acids [19]

The resolution of racemic mandelic acid (**MA**) was carried out with mixtures of amphoteric resolving agents and structurally similar achiral compounds in 1:1 ratio, namely with the mixtures of (*S*)-**Phe** and **Gly**, (*S,S*)-**AP** and β-**Ala**, and (*S*)-**PG** and **GABA**, respectively (**Scheme 27**).

The results were compared to experiments carried out with the application of solely half-equivalent resolving agent. In the case of (*S*)-**Phe**, the addition of achiral glycine resulted in Δ*ee* = 15%, in the case of aspartame ((*S,S*)-**AP**), the achiral β-Ala led to Δ*ee* = 38%; while the combination of (*S*)-pregabalin ((*S*)-**PG**) and γ-aminobutyric acid (**GABA**) led to an increase of Δ*ee* = 9% in enantiomeric purity.

6. Effect of solvate forming solvents and molecules having similar structure on the results of diastereomer separation

In the case of resolution of amlodipine with (*S,S*)-tartaric acid ((*S,S*)-**TA**) from dimethyl-sulfoxide solvent, the dimethyl-sulfoxide solvate of (*S*)-amlodipine-hemi-(*S,S*)-tartrate salt crystallizes with high purity (**Scheme 28I**) [82]. The diastereomer salt enriched in (*S*)-amlodipine precipitates also from *N,N*-dimethylacetamide (**DMA**) solvent (**Scheme 28II**) [83] from 2-butanone solvent, the diastereomer salt of (S)-amlodipine crystallized applying (R,R)-tartaric acid as resolving agent

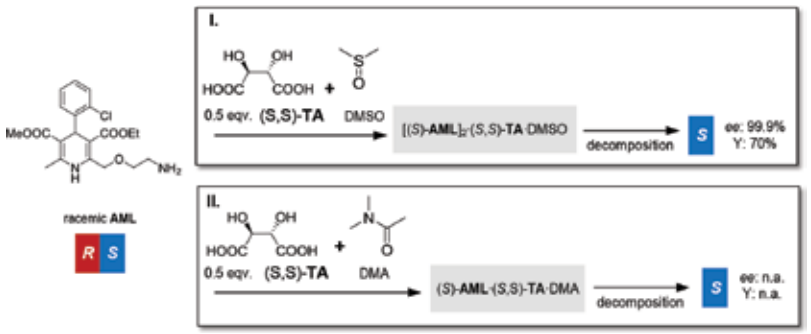

Scheme 28. Resolutions of amlodipine with (*S,S*)-tartaric acid.

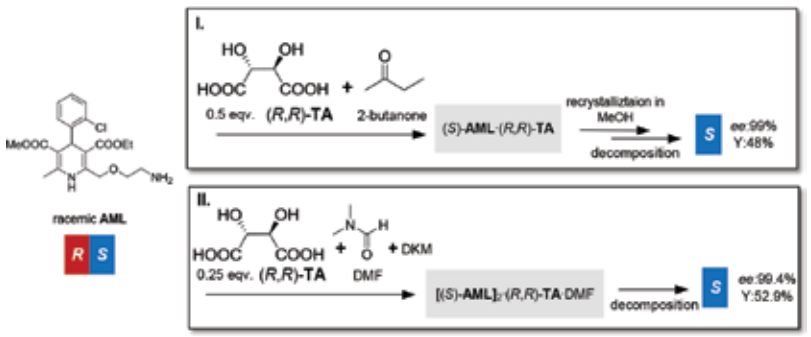

Scheme 29. Resolution of amlodipine with (*R,R*)-tartaric acid.

http://dx.doi.org/10.5772/intechopen.76478

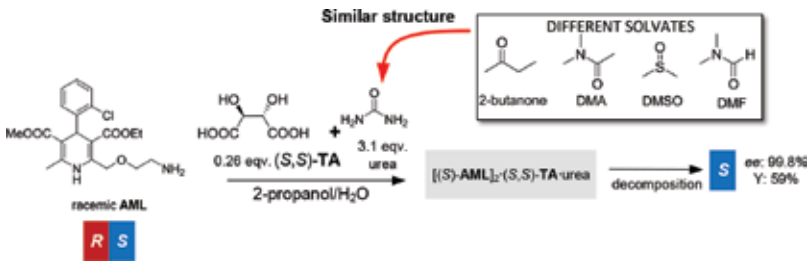

Scheme 30. Resolution of amlodipine with (*S*,*S*)-tartaric acid in the presence of urea.

(**Scheme 29I**) [84]. From the mixture of N,N-dimethylformamide and cosolvents, the DMF solvate of ((S)-**AML**)$_2$·(R,R)-**TA** crystallized, with high enantiomeric purity (**Scheme 29II**) [85].

With the addition of urea, which has similar structure to the different solvates, to the resolving agent (*S*,*S*)-tartaric acid, from the mixture of 2-propanol and water enantiopure *S*-amlodipine can be received with good yield (**Scheme 30**) [86]. The reason of the selection of urea as additive is not explained by the inventors, but the structural similarity is easily recognizable, thus this patent can be considered as the first published form of the application of achiral additive having similar structure as the solvate.

7. Conclusion

One of the possibilities for the separation of mixtures of chiral compounds (enantiomers, diastereomers) is their nonlinear distribution between two phases. The phase-distribution depends on the starting mixture, which follows well the curves of the binary and ternary phase diagrams. The equilibrium processes between the supramolecular associates, formed from the chiral molecules, as well as the solubility equilibriums and the catalytic interactions of the formed crystals lead to the phase distribution of the mixtures. Most probably the helical structure of the associates, resulting in another mirror-image relation, determines their phase-distribution.

In the case of enantiomeric mixtures, the macroscopic manifestation of the helical associates is the formation of crystals of helical structure, related to the configuration of the enantiomer in excess. The phase-distribution is determined by the eutectic composition of one of the present chiral molecules through the effects of the solvent and the time-dependence of the phase equilibriums. The equilibriums can be affected by the partial replacement of the chiral compounds by structurally related chiral or achiral molecules.

It has a more beneficial effect, if the molecules composing the diastereomer have different size and bond lengths.

Acknowledgements

The authors thank the financial support of the Hungarian OTKA Foundation (K 124180 for E. Fogassy).

Author details

Emese Pálovics*, Szeleczky Zsolt, Szolnoki Beáta, Bosits Miklós and Fogassy Elemér

*Address all correspondence to: epalo@mail.bme.hu

Department of Organic Chemistry and Technology, Budapest University of Technology and Economics, Budapest, Hungary

References

[1] Fogassy E, Nógrádi M, Kozma D, Egri G, Pálovics E, Kiss V. Optical resolution methods. Organic & Biomolecular Chemistry. 2006;**16**:3011-3030

[2] Faigl F, Fogassy E, Nógrádi M, Pálovics E, Schindler J. Separation of non-racemic mixtures of enantiomers: An essential part of optical resolution. Organic & Biomolecular Chemistry. 2010;**8**:947-959

[3] Fogassy E, Nógrádi M, Pálovics E, Schindler J. Resolution of Enantiomers by Non-Conventional Methods. Synthesis. 2005:1555-1568

[4] Pálovics E, Szeleczky Z, Faigl F, Fogassy E. Correlations between separations of enantiomeric-and diastereomeric mixtures. In: Muntean SG, Tudose R, editors. New Trends and Startegies in the Chemistry of Advanced Materials. Romana, Timisoara: Acad; 2013. p. 74, ISSN.: 2065-0760

[5] Pálovics E, Szeleczky Zs, Fődi B, Faigl F, Fogassy E. How is the enantiomeric recognition influenced by the interactions of chiral systems? In: Tudose R, editor. New Trends and Startegies in the Chemistry of Advanced Materials with Relevance in Biological Systems,Technique and Environmental Protection. Romana, Timisoara: Acad; 2015. pp. 14-16

[6] Pálovics E, Szeleczky Z, Fődi B, Faigl F, Fogassy E. Prediction of the efficiency of diastereoisomer separation on the basis of the behaviour of enantiomeric mixtures. RSC Advances. 2014;**4**:21254-21261

[7] Pálovics E, Szeleczky Z, Bagi P, Faigl F, Fogassy E. Regularities between Separations of Enantiomeric and Diastereoisomeric Mixtures. Prediction of the Efficiency of Diastereomeric/ Enantiomeric Separations on the Basis of Behaviour of Enantiomeric Mixtures. Periodica Polytechnica Chemical Engineering. 2015;**59**:26-37. DOI: https://doi.org/10.3311/PPch.7328

[8] Szeleczky Z, Bagi P, Pálovics E, Fogassy E. The effect of SDE on the separation of diastereomeric salts: A case study for the resolution of mandelic acid derivatives with Pregabalin. Tetrahedron: Asymmetry. 2014;**5**:1095-1099

[9] Szeleczky Z, Bagi P, Pálovics E, Fogassy E. The effect of the eutectic composition on the outcome of kinetically and thermodynamically controlled resolutions that are based on the formation of diastereomers. Tetrahedron: Asymmetry. 2015;**26**:377-384

[10] Pálovics E, Schindler J, Faigl F, Fogassy E. Behavior of structurally similar molecules in the resolution processes. In: Carreira EM, Yamamoto H, editors. Comprehensive Chirality. Amsterdam: Elsevier; 2012. pp. 91-95

[11] Szeleczky Zs, Semsey S, Bagi P, Pálovics E, Faigl F, Fogassy E. Selecting resolving agents in respect of their eutectic compositions. Chirality: The Pharmacological Biological and Chemical Consequences of Molecular Asymmetry. 2016;**28**(3):230-234

[12] Pálovics E, Szeleczky Zs, Fogassy E. How is the enantiomeric recognition influenced by the interactions of chiral systems? In: Tudose R, editor. New Trends and Startegies in the Chemistry of Advanced Materials with Relevance in Biological Systems, Technique and Environmental Protection. Romana, Timisoara: Acad; 2016. pp. 14-16

[13] Viedma C. Selective Chiral Symmetry Breaking during Crystallization: Parity Violation or Cryptochiral Environment in Control? Crystal Growth & Design. 2007;**7**:553-556. DOI: 10.1021/cg060698d

[14] Viedma C, McBride M, Kahr B, Cintas P. Enantiomer-Specific Oriented Attachment: Formation of Macroscopic Homochiral Crystal Aggregates from a Racemic System. Angewandte Chemie International Edition. 2013;**52**:10545-10548. https://doi.org/10.1002/anie.201303915

[15] Collet A, Brienne MJ, Jacques J. Chemical Reviews. 1980;**80**:215-230

[16] Maillard D, Koller G, Wakaresko E. Process of isolating enantiomer components from enantiomer mixtures by particle-size-controlled crystallization. WO Patent 2010012746; Chemical Abstracts. 2010;**152**:223340

[17] Sorochinsky AE, Soloshonok VA. Self-disproportionation of Enantiomers of Enantiomerically Enriched Compounds. In: Shurid V, editor. Topics in Current Chemistry. Cham, Heidelberg, New York, Dordrecht, London: Springer; 2013;**341**:301-339. DOI: 10.1007/128_2013_434

[18] Fogassy E, Kozma D, Kassai C. Enantiomer resolution by flotation. Hungarian Patent 75951. Chemical Abstracts. 1997;**127**:318552

[19] Kozma D, Kassai C, Fogassy E. Enantiomeric enrichment by the use of density differences between racemic compounds and optically active enantiomers. Tetrahedron Letters. 1995;**36**:3245-3246

[20] Yang X, Wong SY, Bwambok DK, Atkinson MBJ, Zhang X, Whitesides GM, Myerson AS. Separation and enrichment of enantiopure from racemic compounds using magnetic levitation. Chemical Communications. 2014;**50**:7548-7551

[21] Pálovics E. Structurally related compounds with common skeleton in the resolution processes [Phd thesis]. In: Budapest: Budapest University of Technology and Economics. 2008

[22] Ács M, Pokol G, Faigl F, Fogassy E. The role of binary phase-diagrams in separations of stereoisomeric mixtures. Journal of Thermal Analysis and Calorimetry. 1988;**33**:1241-1245

[23] Fogassy E, Ács M, Tóth G, Simon K, Láng T, Ladányi L, Párkányi L. Clarification of anomalous chiroptical bihavior and determination of the absolute-configuration of

1-(3,4-dimethoxyphenyl)-4-methyl-5-ethyl-7,8-dimethoxy-5h-2,3-benzodiazepine. Journal of Molecular Structure. 1986;**147**:143-154

[24] Tamura R, Fujimoto D, Lepp Z, Misaki K, Miura H, Takahashi H, Ushio T, Nakai T, Hirotsu K. Mechanism of Preferential Enrichment, an Unusual Enantiomeric Resolution Phenomenon Caused by Polymorphic Transition during Crystallization of Mixed Crystals Composed of Two Enantiomers. Journal of the American Chemical Society. 2002;**124**:13139-13153

[25] Iwama S, Horiguchi M, Sato H, Uchida Y, Takahashi H, Tsue H, Tamura R. Observation of the preferential enrichment phenomenon for essential α-amino acids with a racemic crystal structure. Crystal Growth & Design. 2010;**10**:2668-2675

[26] Iwama S, Kuyama K, Mori Y, Manoj K, Gonnade RG, Suzuki K, Hughes CE, Williams PA, Harris KDM, Veesler S, Takahashi H, Tsue H, Tamura R. Highly Efficient Chiral Resolution of dl-Arginine by Cocrystal Formation Followed by Recrystallization under Preferential-Enrichment Conditions. Chemistry—A European Journal. 2014;**20**:10343-10350

[27] Gonnade RG, Iwama S, Mori Y, Takahashi H, Tsue H, Tamura R. Observation of Efficient Preferential Enrichment Phenomenon for a Cocrystal of (dl)-Phenylalanine and Fumaric Acid under Nonequilibrium Crystallization Conditions. Crystal Growth & Design. 2011;**11**:607-615

[28] Manoj K, Takahashi H, Morita Y, Gonnade RG, Iwama S, Tsue H, Tamura R. Preferential Enrichment of DL-Leucine Using Cocrystal Formation With Oxalic Acid Under Nonequilibrium Crystallization Conditions. Chirality. 2015;**27**:405-410

[29] Bellec A, Guillemin J-C. Attempts to explain the self-disproportionation observed in the partial sublimation of enantiomerically enriched carboxylic acids. Journal of Fluorine Chemistry. 2010;**131**:545-548

[30] Lorenz H, Seidel-Morgenstern A. A contribution to the mandelic acid phase diagram. Thermochimica Acta. 2004;**415**:55-61

[31] Seidel-Morgenstern A, von Langermann J, Tam LM, Lorenz H, Seidel-Morgenstern A. Kombination von Biokatalyse und Kristallisation zur Darstellung enantiomeren-reiner Mandelsäurederivate. Chemie Ingenieur Technik. 2010;**82**:93-100. doi.org/10.1002/cite.200900157

[32] Blackmond DG, Klussmann M. Spoilt for choice: assessing phase behavior models for the evolution of homochirality. Chemical Communications. 2007:3990-3996

[33] Fletcher SP, Jagt RBC, Feringa BL. An astrophysically-relevant mechanism for amino acid enantiomer enrichment. Chemical Communications. 2007:2578-2580

[34] Perry RH, Wu C, Nefliu M, Cooks RG. Serine sublimes with spontaneous chiral amplification. Chemical Communications. 2007:1071-1073

[35] Klussmann M, Iwamura H, Mathew SP, Wells DH, Pandya U, Armstrong A, Blackmond DG. Thermodynamic control of asymmetric amplification in amino acid catalysis. Nature. 2006;**441**:621-623

[36] Katagiri T, Yoda C, Furuhashi K, Ueki K, Kubota T. Separation of an enantiomorph and its racemate by distillation: strong chiral recognizing ability of trifluorolactates. Chemistry Letters. 1996;**25**:115-116

[37] Katagiri T, Takahashi S, Tsuboi A, Suzaki M, Uneyama K. Discrimination of enantiomeric excess of optically active trifluorolactate by distillation: Evidence for a multicenter hydrogen bonding network in the liquid state. Journal of Fluorine Chemistry. 2010;**131**:517-520

[38] Koppenhoefer B, Trettin U. Is it possible to affect the enantiomeric composition by a simple distillation process? Fresenius' Zeitschrift für Analytische Chemie. 1989;**333**:750-750

[39] Nakamura T, Tateishi K, Tsukagoshi S, Hashimoto S, Watanabe S, Soloshonok VA, Aceña JL, Kitagawa O. Self-disproportionation of enantiomers of non-racemic chiral amine derivatives through achiral chromatography. Tetrahedron. 2012;**68**:4013-4017

[40] Cundy KC, Crooks PA. Unexpected pehnomenon in the high-performance liquid chromatographic anlaysis of racemic 14C-labelled nicotine: Separation of enantiomers in a totally achiral system. Journal of Chromatography A. 1983;**281**:17-33. https://doi.org/10.1016/S0021-9673(01)87863-8

[41] Soloshonok VA. Remarkable Amplification of the Self-Disproportionation of Enantiomers on Achiral-Phase Chromatography Columns. Angewandte Chemie International Edition. 2006;**45**:766-769. https://doi.org/10.1002/ange.200503373

[42] Jacob RM, Regnier GL. Verfahren zur Herstellung von Phentiazin derivaten German Patent 1045407. Chemical Abstracts. 1961;**55**

[43] Jacob RM, Regnier GL. German Patent Verfahren zur Herstellung von Phentiazinderivaten 1040034. Chemical Abstracts. 1961;**55**:18035

[44] Fogassy E, Faigl F, Ács M, Simon K, Kozsda É, Podányi B, Czugler M, Reck G. Structural studies on optical resolution via diasteroisomeric salt formation-enantiomer separation for cis-permethrinic acid[cis-2,2-dimethyl-3-(2,2-dichlorovinyl)-cyclo-propanecarboxylic acid]. Journal of the Chemical Society, Perkin Transactions. 1988;**2**:1385-1392

[45] Fogassy E, Faigl F, Ács M. Selective reactions of enantiomeric-mixtures. Tetrahedron Letters. 1981;**22**:3093-3096

[46] Kozma D, Madarász Z, Ács M, Fogassy E. A new method for enantiomer enrichment: Distillation to separate the free and complexed enantiomers after partial salt formation. Chirality. 1995;**7**:381-382. doi.org/10.1002/chir.530070512

[47] Kozma D, Simon H, Pokol G, Fogassy E. Enantiomeric enrichment of partially resolved N-methyl-amphetamine. Journal of Thermal Analysis and Calorimetry. 2002;**69**:409-416

[48] Kozma D, Simon H, Kassai C, Madarász Z, Fogassy E. Investigation of the physicochemical basis of enantiomeric enrichment: The example of α-phenylethylamine with achiral dicarboxylic acids Chirality. 2001;**13**:29-33. doi.org/10.1002/1520-636X(2001)13:1<29::AID-CHIR6>3.0.CO;2-P

[49] Kobayashi Y, Kodama K, Saigo K. Supramolecular Architecture Consisting of an Enantiopure Amine and an Achiral Carboxylic Acid: Application to the Enantioseparation of Racemic Alcohols. Organic Letters. 2004;**6**(17):2941-2944. DOI: 10.1021/ol048948b

[50] Kinbara K. Design of Resolving Agents Based on Crystal Engineering. Synlett. 2005:732-743. DOI: 10.1055/s-2005-864794

[51] Saigo K, Kobayashi Y. The role of CH/π interaction in the stabilization of less-soluble diastereomeric salt crystals. Chemical Record. 2007;**7**:47-56. doi.org/10.1002/tcr.20100

[52] Kobayashi Y, Kokubo Y, Aisaka T, Saigo K. Hydrogen-bonding sheets in crystals for chirality recognition: synthesis and application of (2S,3S)-2,3-dihydroxy- and (2S,3S)-2,3-dibenzyloxy-1,4-bis(hydroxyamino)butanes. Tetrahedron: Asymmetry. 2008;**19**:2536-2541. doi.org/10.1016/j.tetasy.2008.11.006

[53] Leusen FJJ. Crystal Structure Prediction of Diastereomeric Salts: A Step toward Rationalization of Racemate Resolution. Crystal Growth & Design. 2003;**3**:189-192. DOI: 10.1021/cg020034d

[54] Karamertzanis PG, Anandamanoharan PR, Fernandes P, Cains PW, Vickers M, Tocher DA, Florence AJ, Price SL. Toward the Computational Design of Diastereomeric Resolving Agents: An Experimental and Computational Study of 1-Phenylethylammonium-2-phenylacetate Derivatives. Journal of Physical Chemistry B. 2007;**111**:5326-5336. DOI: 10.1021/jp068530q

[55] Gizur T, Péteri I, Harsányi K, Fogassy E. Resolution of racemic 1,3-disubstituted propanols by (R,R)-di-(4-toluoyl)-tartaric acid: Similar conditions for similar structures. Tetrahedron: Asymmetry. 1996;**7**:1589. doi.org/10.1016/0957-4166(96)00188-7

[56] Bálint J, Marthi K, Ács M, Egri G, Fogassy E. Preparative methods for enantiomeric enrichment of non-racemic enantiomeric mixtures. Enantiomer. 1997;**2**:27-35

[57] Guangyou Z, Yuquing L, Zhaohui W, Nohira H, Hirose T. Resolution of β-aminoalcohols and 1,2-diamines using fractional crystallization of diastereomeric salts of dehydroabietic acid. Tetrahedron: Asymmetry.2003;**14**:3297-3300. doi.org/10.1016/j.tetasy.2003.08.033

[58] Faigl F, Schindler J, Fogassy E. Advantages of structural similaritiesof the reactants in optical resolution processes. In: Sakai K, Hirayama N, Tamura R, editors. Novel Optical Resolution Technologies, Vol. 269. Berlin Heidelberg: Springer; 2007. pp. 133-157

[59] Sakai K, Sakurai R, Nohira H. New resolution technologies controlled by chiral discrimination mechanisms. In: Sakai K, Hirayama N, Tamura R, editors. Novel Optical Resolution Technologies, Vol. 269. Berlin Heidelberg: Springer; 2007. pp. 199-231

[60] Kozma D, Fogassy E. Preparative methods for enantiomeric enrichment of non-racemic enantiomeric mixtures. Enantiomer. 1997;**2**:51-59

[61] Fogassy E, Ács M, Felméri J, Aracs J. Problems of optical resolution of asparagine and aspartic-acid. Periodica Polytechnica Chemical Engineering. 1976;**20**:248

[62] Fogassy E, Ács M, Gizur T, Harsányi K, Aracs J, Berki K, Tőke L, Jászay Z. Optical resolution of threo-2-hydroxy-3-(2-aminophenylthio)-3-(4-methoxyphenyl)-propionic acid. WO Patent 9100270. Chemical Abstracts. 1991;**115**:28893

[63] Nagy L, Fogassy E, Tőke L, Ács M, Árvai L, Szabó G. Resolution of alkali metal salts and lactones of racemic cis-2-hydroxycyclopent-4en-1-ylacetic acid with optically-active α-phenylethylamine. Hungarian Patent 177583. Chemical Abstracts. 1982;**96**:6258

[64] Fogassy E, Ács M. Process for producing 2-(4-hydroxyphenoxy)propionic acid enantiomers from enantiomer mixtures. Hungarian Patent 60226. Chemical Abstracts. 1993;**118**:59420

[65] Fogassy E, Simay A, Bergmann J, Faigl F, Birkás E, Mozsolits K, Szinnyei É, Török Z, Zolyomi G, Ács M. Chemical Abstracts. 1989;**111**:96797

[66] Fogassy E, Faigl F, Ács M. Diastereomer salts of phenylalanine and N-acyl derivatives for the separation of optically active phenylalanine and N-acyl derivatives WO Patent 8503932. Chemical Abstracts. 1986;**104**:168835

[67] Nagy L, Fogassy E, Faigl F, Kozsda É, Csíz L, Czudor I. Producing enantiomers of insecticidal cis- or trans-cyclopropanecarboxylic acid esters Hungarian Patent 46649. Chemical Abstracts. 1989;**111**:553257

[68] Fogassy E. Optically active 3-methoxy-10-(2-methyl-3 dimethylaminopropyl)phenothiazine Hungarian Patent 152208. Chemical Abstracts. 1965;**63**:72057

[69] Fogassy E, Ács M, Faigl F. Process for preparing optically active alpha-/formylamino/-beta-phenyl-propionic acids Hungarian Patent 193201. Chemical Abstracts. 1986;**104**:168835

[70] Bálint J, Egri G, Vass G, Schindler J, Gajáry A, Friesz A, Fogassy E. Resolution of the flumequine intermediate 6-fluoro-2-methyl-1,2,3,4-tetrahydroquinoline. Tetrahedron: Asymmetry.2000;**11**:809-813. doi.org/10.1016/S0957-4166(99)00527-3

[71] Tóth G, Fogassy E, Ács M, Tőke L, Láng T. Racematspaltung von (±)-5-äthyl-1-(3,4-dimethoxyphenyl)-6,7-dimethoxy-4-methyl-5H-2,3-benzodiazepin und anomales chiroptisches verhalten der enantiomeren. Journal of Heterocyclic Chemistry. 1983;**20**:709. doi.org/10.1002/jhet.5570200340

[72] Nemák K, Ács M, Jászay ZM, Kozma D, Fogassy E. Study of the diastereoisomers formed between (N-alkyl)-pipecolic acid-anilides and 2R,3R-tartaric acid or O,O′-dibenzoyl-2R,3R-tartaric acid. Do the tartaric acids form molecular-complexes, instead of salts during optical resolutions? Tetrahedron. 1996;**52**:1637-1642. doi.org/10.1016/0040-4020(95)00992-2

[73] Nemák K, Kozma D, Fogassy E. Study of the mechanism of optical resolutions via diastereoisomeric salt formation. The role of the crystallization temperature in optical resolution of pipecolic acid xylidides. Molecular Crystals and Liquid Crystals A. 1996;**276-277**:31-36. doi.org/10.1080/10587259608039357

[74] Nemák K, Ács M, Kozma D, Fogassy E. Racemic compound formation-conglomerate formation Part 4. Optical resolution and determination of the melting phase diagrams of 2′,6′-pipecoloxylidide and four 1-alkyl-2′,6′-pipecoloxylidides. Journal of Thermal Analysis and Calorimetry. 1997;**48**:691-696

[75] Szeleczky Z, Semsey S, Bagi P, Fődi B, Pálovics E, Faigl F, Fogassy E. The Role of Differences in Molecule Length in Diastereomeric Salt Resolutions. Separation Science and Technology. 2016:1-6

[76] Dymácek B. Process of resolution of 1-aminoindan WO Patent 2012116752. Chemical Abstracts. 2012;**157**:437939

[77] Bálint J, Csatáriné Nagy M, Dombrády Z, Fogassy E, Gajáry A, Suba C. Processes for optical resolution of racemic 2-hydroxy-2-(2-chlorophenyl)acetic acid, and racemization of (S)-(+)-2-hydroxy-2-(2-chlorophenyl)acetic acid, for production of (R)-(-)-2-hydroxy-2-(2-chlorophenyl)acetic acid, an intermediate for clopidogrel. WO Patent 2003000636. Chemical Abstracts. 2003;**138**:73080

[78] Bousquet A, Musolino A. US Patent 9918110. Chemical Abstracts. 1999;**130**:296510

[79] Pálovics E, Schindler J, Faigl F, Fogassy E. The influence of molecular structure and crystallization time on the efficiency of diastereoisomeric salt forming resolutions. Tetrahedron: Asymmetry. 2010;**21**:2429-2434. doi.org/10.1016/j.tetasy.2010.09.005

[80] Molnár P, Bombicz P, Varga C, Bereczki L, Székely E, Pokol G, Fogassy E, Simándi B. Influence of benzylamine on the resolution of ibuprofen with (+)-(R)-phenylethylamine via supercritical fluid extraction. Chirality. 2009;**21**:628-636. doi.org/10.1002/chir.20655

[81] Schindler J, Egressy M, Bereczki L, Pokol G, Fogassy E, Marthi K. Enhanced efficiency due to the use of achiral additives in the optical resolution of 1-phenylethylamine by its glutaric acid derivative. Chirality. 2007;**19**:239-244. doi.org/10.1002/chir.20377

[82] Lee J, Lee MS, Yang WK, Lee J-C, Choi C-J, Kim HK, Chang Y-K. Lee G. (S)-(-)-amlodipine camsylate or hydrate thereof and pharmaceutical composition comprising same WO Patent 2008010659. Chemical Abstracts. 2008;**148**:175751

[83] Grogan D, Bush L. Compositions comprising (S)-amlodipine and an angiotensin receptor blocker and methods of their use WO Patent 2005070462. Chemical Abstracts. 2005;**143**:179633

[84] Zhong N, Zhao X, Ma H. Chen. Y. A Method for the Enantiomoeric Separation of Optical Active Amlodipine WO Patent 2005054196. Chemical Abstracts. 2005;**143**:43779

[85] Gharpure MM, Bhawal BM, Ranade PV, Deshmukh RD, Mehta SR. Process for producing enantiomer of amlodipine in high optical purity WO Patent 2006043148. Chemical Abstracts. 2006;**144**:432695

[86] Jang SY, Kim S, Yun S, Bang HJ, Kim HK, Suh KH. Method for preparing (S)-(-)-amlodipine or a salt thereof and an intermediate used therein WO Patent 2008/100023. Chemical Abstracts. 2008;**149**:274860

Chapter 7

Evaluation of Solution Thermodynamic Properties of Mixed Ionic Liquids at Different Temperatures (293.15–343.15) K

Achsah Rajendran Startha Christabel,
Danish John Paul Mark Reji and
Anantharaj Ramalingam

Additional information is available at the end of the chapter

http://dx.doi.org/10.5772/intechopen.77016

Abstract

The solution thermodynamic properties of mixed ionic liquids such as density, excess molar volume, partial molar volume and apparent molar volume are highly influential on the design of an effective separation unit and in the optimization of operating parameters like pressure, temperature and concentration for the separation processes. Therefore, it could be better to do a prior experimental study on of the solution thermodynamic properties of mixed ionic liquids at different temperatures for the whole mole fractions rather than doing separation characterization studies like selectivity, efficiency, distribution coefficient and performance index. In addition, the recovery and regeneration of ionic liquids also challenge researchers and separation scientists in several fields of applications. Therefore, in this chapter, density of pure 1-butyl-3-methyl imidazolium bis(trifluoromethylsulfonyl) imide {[BIMIM][NtF_2]}, 1-ethyl-3-methylimidazolium ethyl sulfate {[EMIM][ESO_4]}, 1-ethyl-3-methylimidazolium hydrogen sulfate {[EMIM][HSO_4]} and 1-butyl-3-methylimidazolium acetate {[BMIM][OAc]} and its binary mixtures have been measured at T (293.15–343.15) K. From the measured densities, isobaric expansivity, excess molar volume, partial molar volume, excess partial molar volume, and apparent molar volume have been calculated. Results were discussed in terms of physical interaction, chemical interaction and structural orientation at molecular level and their temperature and composition dependency.

Keywords: mixed ionic liquid, density, isobaric expansivity and excess property

1. Introduction

Ionic liquid is a green solvent. It is composed of organic cations and inorganic or organic anions; they can have liquid state near ambient temperature. Since this green solvent has unique properties when compared to conventional solvents such as larger temperature range of liquid state [1], high thermal stability, high ionic conductivity negligible vapor pressures, nonflammability and high solvating capacity (i.e., solubility), for polar or nonpolar organic, inorganic and organometallic compounds [2, 3]. It is well known that the solvation capacity of green solvent is influenced by the hydrogen bonded structure and interaction between the individual ions (cation or anion) with other substances. On the other hand, the green solvent is an organic salt and its microscopic structure is usually composed of a large cation with low order of molecular symmetry. Hence, the unstable lattice structure lowers the melting point to well below the room temperature [4]. Therefore, the green solvent has the capabilities as environmental-friendly solvent in many green chemical processes [5] such as, biocatalytical transformation, isomerization, used in multiphase homogeneous catalysis [6], synthesis, catalysis, liquid-liquid extraction and supercritical extraction, and also used as thermal fluids, lubricants, and working fluids in electrochemical devices such as batteries, capacitors and solar cells [7].

But there is no systematic study on application of green solvent at different temperature and compositions. On the other hand, the solution thermodynamic properties of pure ionic liquids and its mixtures are of interest from the point of both basic and applied research [7]. Also, a detailed knowledge of the solution thermodynamic properties of mixed green solvents are important in relating the microscopic and macroscopic behavior. In this context, There is no data generated by experimental or theoretical approach. Moreover, the complete design of new green chemical processes and new green products based on green solvents and mixed green solvents can only be achieved when their solution thermodynamic properties such as molar volume, excess molar volume, partial molar volume, excess partial molar volume, and apparent molar volume are adequately characterized. But there is no data on solution thermodynamic properties of mixed green solvents at different temperature for an entire mole fractions range. Therefore, it is very important to accumulate a sufficiently large data bank not only for green processes and product design but also for the development of correlation for these properties. In addition, a better understanding of the behavior of mixed green solvent demands the knowledge of density and its temperature and composition dependence. Obtaining knowledge on the solution thermodynamic properties is extremely important to improve their selection and performance.

2. Experimental methods

2.1. Chemicals

Green solvents like 1-butyl-3-methyl imidazolium bis(trifluoromethylsulfonyl) imide {[BIMIM][NtF_2]}, 1-ethyl-3-methylimidazolium ethyl sulfate {[EMIM][ESO_4]}, 1-ethyl-3-methylimidazolium hydrogen sulfate {[EMIM][HSO_4]} and 1-butyl-3-methylimidazolium acetate {[BMIM][OAc]} were supplied by Aldrich Chemistry, Germany with purity greater than 98%. All the green solvents (i.e., ionic liquids) were used without further purifications.

http://dx.doi.org/10.5772/intechopen.77016

2.2. Sample preparation

The binary mixture was prepared by transferring a known amount of the pure liquids via syringe into stoppered bottles and was properly sealed with parafilm tape to prevent evaporation and addition of moisture to the mixtures, using a Mettler AX-205 Delta Range balance with a precision of $\pm 10^{-5}$ g. The estimated uncertainty on the composition measurement was $\pm 10^{-4}$ g mole fraction. The stoppered bottles were placed inside a water-shaker bath set at atmospheric pressure, and allowed to shake for more than 6 h at 300 rpm in thermostatic shaker bath. Spring clamps were used to hold the flasks on the tray. The binary mixture was then allowed to settle for minimum of 12 h so that equilibrium is attained. The sample is taken from vial with a syringe to measure the density at temperature from 293.15 to 343.15 K with 5 K interval.

2.3. Density measurement

Density was measured using an Anton Paar DMA 4100 M with the oscillating U-tube method. In this method, the sample is introduced into a U-shaped borosilicate glass tube that is being excited to vibrate at its characteristic frequency. The characteristic frequency changes depending on the density of the sample. Through a precise determination of the characteristic frequency a mathematical conversion, the density of the sample can be measured. The density is calculated from the quotient of the period of oscillations of the U-tube and the reference oscillator [8]:

$$\rho = K_A^* Q^{2*} f_1 - K_B^* f_2 \tag{1}$$

where; K_A and K_B are apparatus constants, respectively, Q is the oscillation period of the reference oscillator. f_1 and f_2 are correction factors for temperature, viscosity, and nonlinearity.

3. Theory

When two liquid chemical species mixed with each other, the total weight of the mixture is equal to the sum of masses of the individual chemical species. But it is not true in case of volume. When two miscible liquids are mixed with each other, volume of the mixtures may not equal to the sum of the volume of the individual chemical species [9]. Ideal binary liquid mixture does not have volume changes. Hence, the binary liquid mixture has deviation from ideality due to the molecular interactions between solute-solvent or two components in the mixtures. In addition, the binary liquid mixture volume either increase or decrease as the function of composition of component i in the mixture. This difference in the volume of the mixture can be taken as a criterion and measure of molecular interactions at molecular level by means of isobaric expansivity, excess molar volume, partial molar volume, excess partial molar volume and apparent molar volume (**Figure 1**).

Isobaric expansivity is inversely proportional to the volume of component "i" in the mixture and its product with the rate of change of volume with respect to temperature at constant pressure. Hence the isobaric expansivity is defined as;

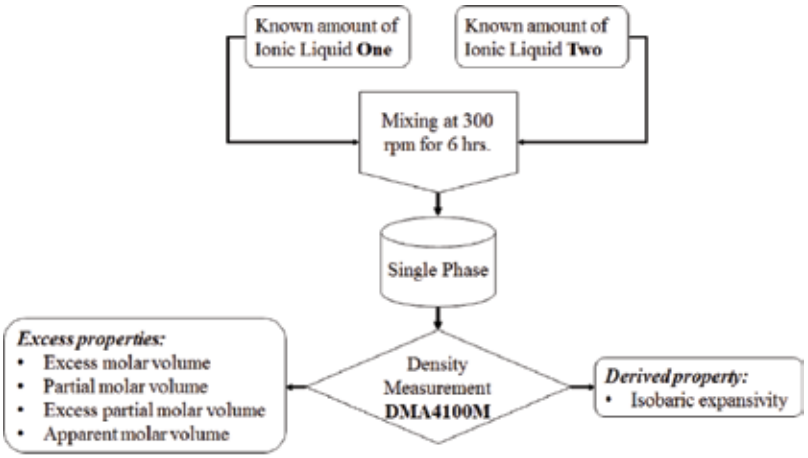

Figure 1. Illustrating the density measurement of binary mixtures using Anton Paar DMA 4100 M.

$$\alpha = \frac{1}{V}\left[\frac{\partial V}{\partial T}\right]_P = -\frac{1}{\rho}\left[\frac{\partial \rho}{\partial T}\right]_P = -\left[\frac{\partial \ln \rho}{\partial T}\right]_P \tag{2}$$

where; α is the isobaric expansivity, v is the volume of the fluid, ϱ is the density of the fluid, T is the temperature, P is the pressure.

The excess molar volume is the good estimator of unlike interaction in the binary mixture as a function of concentration of component "i" at constant temperature and pressure. The excess molar volume (cm^3/mole) is defined as [1, 13];

$$V_m^E = V_m^{real} - \sum_{i=1,2} V_m^{ideal} \tag{3}$$

$$= V_m^{real} - x_1 V_1^0 - x_2 V_2^0 \tag{4}$$

$$= \frac{x_1 M_1 + x_2 M_2}{\rho_{mix}} - \left[\frac{x_1 M_1}{\rho_1} + \frac{x_2 M_2}{\rho_2}\right] \tag{5}$$

where; V_m^E is the excess molar volume, V_m^{real} is the molar volume of real fluid, V_m^{ideal} is the molar volume of ideal, V_1^0 and V_2^0 are the molar volume of component 1 and 2, respectively. x_1 and x_2 are the mole fraction of component 1 and 2 in the binary mixture. M_1 and M_2 are the molecular weight of component 1 & 2. ρ_{mix}, ρ_1 & ρ_2 are the densities of binary mixture, component 1 and component 2, respectively.

Partial molar volume is the thermodynamic quantity and it is used to measure the change s in extensive properties of the binary mixture as the function of composition at constant temperature and pressure. In addition, the partial molar volume is a potential tool to estimate the solute-solvent interaction in the binary mixture at molecular level. The partial molar volume is used to measure the incremental volume by addition of co-solvent in the binary

mixtures. Hence, the partial molar volume is not necessarily the same as the molar volume of the pure component as it depends on how the molecules interact, structural rearrangement, and the geometrical fitting of the molecules [13]. The partial molar volume (cm^3/mole) can be evaluated using the following equations;

$$\overline{V}_1 = V_m^E + V_1^0 + x_2 \left(\frac{\partial V_m^E}{\partial x_1}\right)_{P,T} \tag{6}$$

$$\overline{V}_2 = V_m^E + V_2^0 - x_1 \left(\frac{\partial V_m^E}{\partial x_1}\right)_{P,T} \tag{7}$$

where; $\overline{v}_i$ and $\overline{v}_2$ are the partial molar volume of component 1 and 2, respectively.

Excess partial molar volume is the property of binary mixtures which is useful to characterize the non-ideal behavior of real mixtures. Excess partial molar volume is the different between the partial molar volume of a component "i" in a real mixture and the molar volume of the component in an ideal mixture (cm^3/mole). It can be defined as;

$$\overline{V_1^E} = \overline{V}_1 - V_1^0 \tag{8}$$

$$\overline{V_2^E} = \overline{V}_2 - V_2^0 \tag{9}$$

where; $\overline{v}_1^E$ and $\overline{v}_2^E$ are the excess partial molar volume of component 1 and 2, respectively.

Apparent molar volume is one of the solution thermodynamic properties which can measure the amount of solute is required to bring the solvent volume up to the solution volume. Hence, the apparent molar volume (cm^3/mole) is defined as;

$$V_{\varphi,1} = V_1^0 - \frac{V_m^E}{x_1} \tag{10}$$

$$V_{\varphi,2} = V_1^0 - \frac{V_m^E}{x_1} \tag{11}$$

where; $V_{\varphi\text{-}1}$ and $V_{\varphi\text{-}2}$ are the apparent molar volume of component 1 and 2, respectively.

4. Results and discussion

4.1. Density of pure ionic liquids

The density of pure [EMIM][ESO_4], [EMIM][HSO_4], [BMIM][OAc] and [BMIM][NtF_2] ionic liquid at the temperature range from 293.15 to 343.15 K are presented in **Table 1**. Densities of IL's used in this work and commonly used ILs are given in **Figure 2**. Density of all IL's decreases as in the order of; [BMIM][NTF_2] (this work) < [EMIM][TOS] < [BMIM][PF_6] < [EMIM][HSO_4]

S. No	Name	293.15	298.15	303.15	308.15	313.15	318.15	323.15	328.15	333.15	338.15	343.15
1	[EMIM][SCN] [10]	NA	1.1168	NA	1.1107	NA	1.1047	NA	1.0927	NA	NA	NA
2	[BMIM][BF_4] [5]	NA	1.2076	1.2041	1.2005	1.1970	1.1934	1.1899	NA	1.1754	NA	NA
3	[HMIM][BF_4] [5, 10]	NA	1.1488	1.1453	1.1418	1.1384	1.1350	1.1316	NA	NA	NA	NA
4	[OMIM][BF_4] [11]	NA	1.1018	NA	NA	NA	NA	NA	NA	NA	NA	NA
5	[BMIM][PF_6] [12]	NA	1.3697	1.3635	1.3592	1.3555	1.3520	1.3474	NA	NA	NA	NA
6	[EMIM][TOS] [13]	NA	1.3895	1.3853	1.3811	1.3769	1.3727	1.3686	NA	NA	NA	NA
7	[BMIM][TOS] [13]	NA	1.3016	1.2976	1.2937	1.2897	1.2858	1.2819	NA	1.14997	1.14667	1.14347
8	[MMIM][MSO_4] [14]	NA	1.3415	1.3341	1.3248	1.3206	NA	NA	NA	NA	NA	NA
9	[EMIM][$EtSO_4$] [15]	1.2424 1.2402*	1.2394 1.2368*	1.2363 1.2334*	1.2333 1.2300*	1.2302 1.2266*	1.2272 1.2232*	1.2241 1.2199*	1.2211 1.2165*	1.2181 1.2132*	1.2151 1.2099*	1.2120 1.2066*
10	[BMIM][MSO_4] [5]	NA	1.2107	1.2074	1.2041	1.2008	1.1975	1.1942	NA	NA	NA	NA
11	[EMIM][HSO_4]*	1.3691	1.3660	1.3629	1.3599	1.3567	1.3537	1.3508	1.3477	1.3448	1.3418	1.3388
12	[EMIM][OAc]*	1.0555	1.0525	1.0495	1.0465	1.0435	1.0405	1.0375	1.0346	1.0316	1.0287	1.0257
13	[BMIM][NtF2]*	1.4406	1.4358	1.4310	1.4262	1.4215	1.4167	1.4120	1.4073	1.4026	1.3979	1.3933

Table 1. Density as function of temperature for pure ionic liquids.

(this work) < [MMIM][MSO_4] < [BMIM][TOS] < [HMIM][PF_6] < [OMIM][PF_6] < [EMIM][ESO_4] (this work) < [BMIM][BF_4] < [HMIM][BF_4] < [EMIM][SCN] < [BMIM][OAc] (this work) < Water at 298.15 K. Densities of all the studied ionic liquids slightly decreases with increasing temperatures from 293.15 to 343.15 K. It is observed that temperature effect on densities of studied ionic liquids are very small and it may be neglected. The density of ILs' decrease as in the order of; [BMIM][NtF_2] < [EMIM][HSO_4] < [EMIM][ESO_4] < [BMIM][OAc] (**Figure 1**). Since the densities of pure ionic liquids play an important role to estimate the volumetric behavior of individual IL's with other IL's in the binary mixtures for the whole composition at different temperatures. It is noted that the length of alkyl-chain in cation as well as the variety of

http://dx.doi.org/10.5772/intechopen.77016

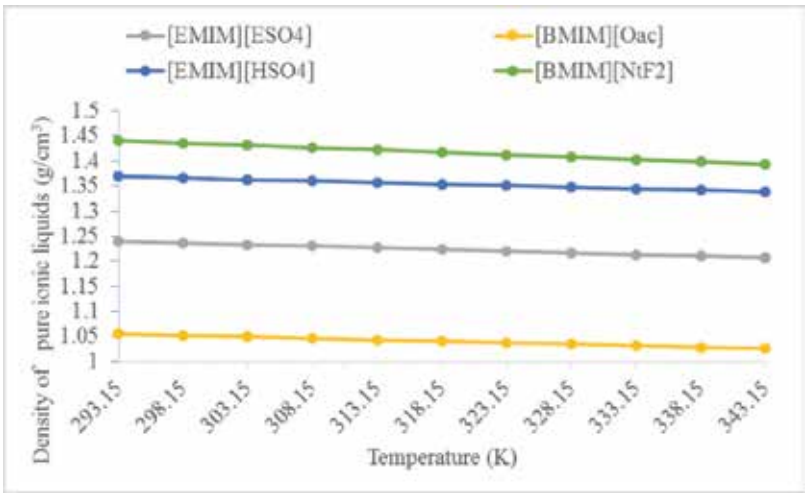

Figure 2. Density of investigated ionic liquids in this work at different temperature.

anion has great impact on density of IL's. Generally, density of pure IL's decreases due to the following reasons; (i) increasing length of the alkyl chain and (ii) increasing volume of the anions [1].

4.2. Isobaric expansivity

The study of temperature and pressure dependence of isobaric expansivity of [EMIM][ESO_4], [EMIM][HSO_4], [BMIM][OAc] and [BMIM][NtF_2] ionic liquids. The ILs do not expanded appreciably at the temperature range from 293.15 to 343.15 K. Isothermal expansivity of all studied ILs are presented in **Table 2**. [BMIM][OAc] gave 5.77×10^{-4}, 4.94×10^{-4} for [BMIM][NtF_2], 4.09×10^{-4} for [EMIM][ESO_4] and 2.95×10^{-4} for [EMIM][HSO_4].

4.3. Excess molar volume

Experimental densities for different binary mixtures of [EMIM][ESO_4] + [BMIM][OAc], [EMIM][ESO_4] + [BMIM][NtF_2] and [EMIM][ESO_4] + [BMIM][HSO_4] as a function of composition at T = 293.15–343.15 K were used to estimate excess molar volume. Excess molar volumes for the binary mixtures of [EMIM][ESO_4] + [BMIM][OAc], [EMIM][ESO_4] + [BMIM][NtF_2] and [EMIM][ESO_4] + [BMIM][HSO_4] from 293.15 to 343.15 K versus the mole fraction of [EMIM][ESO_4] are shown in **Figures 3–5**.

Generally, V^E can be considered arising from three types of interactions between two components in the mixtures: (i) physical interaction mainly consisting of dispersion forces or weak dipole-dipole interactions and making a positive contribution. (ii) Chemical or specific interactions which include charge transfer, formation of hydrogen bonds and other complex forming interactions resulting in negative contribution, and (iii) the structural contributions arising from geometrical fitting of one component into another due to difference in molar volumes resulting in negative excess molar volume [16].

S. no	Name	α (1/K)	
		This work	Literature
1	[EMIM][SCN] [8]	NA	7.23×10^{-4}
2	[BMIM][BF_4] [5]	NA	5.84×10^{-4}
3	[HMIM][BF_4] [5, 8]	NA	6.14×10^{-4}
4	[BMIM][PF_6] [10]	NA	6.63×10^{-4}
5	[EMIM][TOS] [11]	NA	5.80×10^{-4}
6	[BMIM][TOS] [11]	NA	6.19×10^{-4}
7	[MMIM][MSO_4] [12]	NA	10.52×10^{-4}
8	[BMIM][MSO_4]	2.95×10^{-4}	NA
9	[EMIM][$EtSO_4$] [13]	4.09×10^{-4}	4.88×10^{-4}
10	[BMIM][OAc]	5.77×10^{-4}	NA
11	[EMIM][NtF_2]	4.94×10^{-4}	NA

Table 2. Observed and literature values of isobaric thermal expansivities.

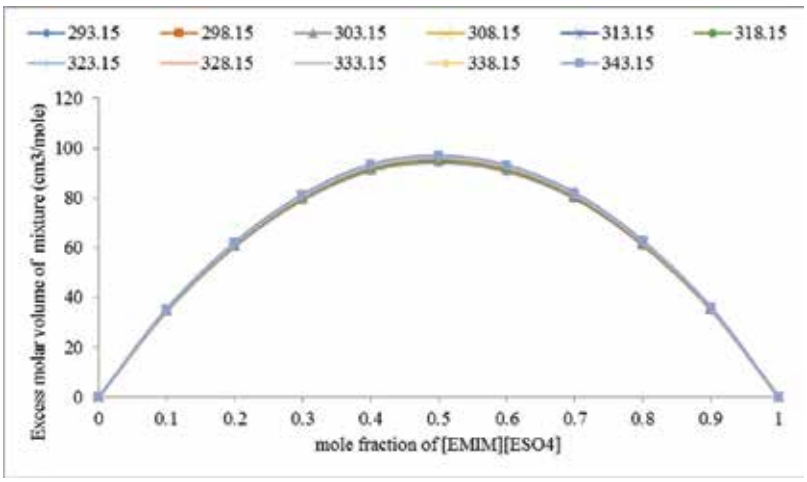

Figure 3. Excess molar volume of binary mixture of [EMIM][ESO_4] + [BMIM][OAc] at different temperature.

Excess molar volumes are positive over the whole composition range for [EMIM][ESO_4] + [BMIM][OAc] and [EMIM][ESO_4] + [BMIM][NtF_2]. [EMIM][ESO_4] + [BMIM][HSO_4] also has positive values at temperature from 293.15 to 343.15 K. But, [EMIM][ESO_4] + [BMIM][HSO_4] has a negative values at 308.15 and 313.15 K which is indicated that alkyl group substitution at anions has a significant role in the formation of hydrogen bond with other IL's at different temperature. The rise in temperature does not show any considerable effect on the excess molar volume of all the studied mixed IL's systems. But [EMIM][ESO_4] + [EMIM][HOS_4] system has shown negative deviation from 0 to 3.5 at 308.15 K and 0 to 6.5 mole fraction of [EMIM][ESO_4]

http://dx.doi.org/10.5772/intechopen.77016

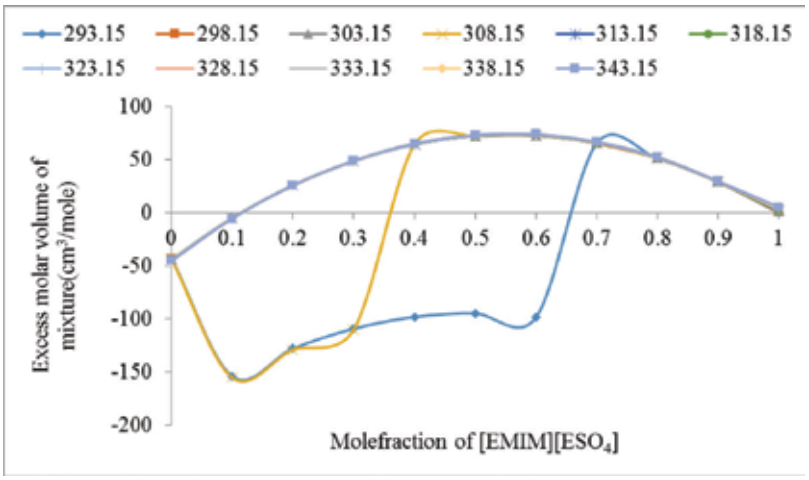

Figure 4. Excess molar volume of binary mixture of [EMIM][ESO_4] + [EMIM][HSO_4] at different temperature.

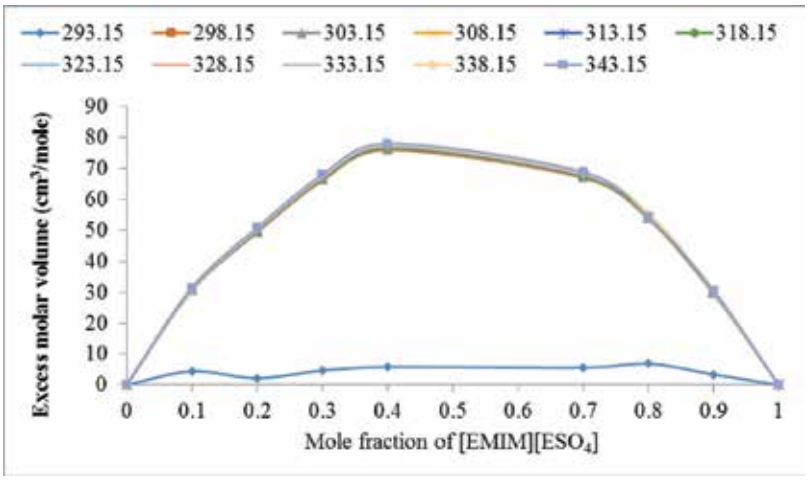

Figure 5. Excess molar volume of binary mixture of [EMIM][ESO_4] + [BMIM][NtF_2] at different temperature.

in [EMIM][HSO_4]. It may be due to the formation of hydrogen bond and also because of interactions. It is also observed that the sign of the excess molar volume and shape of the curve of excess molar volume as a function of [EMIM][ESO_4] is mainly depends on nature and changes of ion's in IL's.

4.4. Partial molar volume

Figures 6–8 shows the partial molar volume of [EMIM][ESO_4] in [EMIM][HSO_4], [BMIM][OAc] and [BMIM][NtF_2] at T (293.15–343.15) K. The values of partial molar volume of all studied system shows negative deviation for the mole fractions of [EMIM][ESO_4] at different temperatures, except [EMIM][ESO_4] + [EMIM][HSO_4] system. [EMIM][ESO_4] + [EMIM][HSO_4]

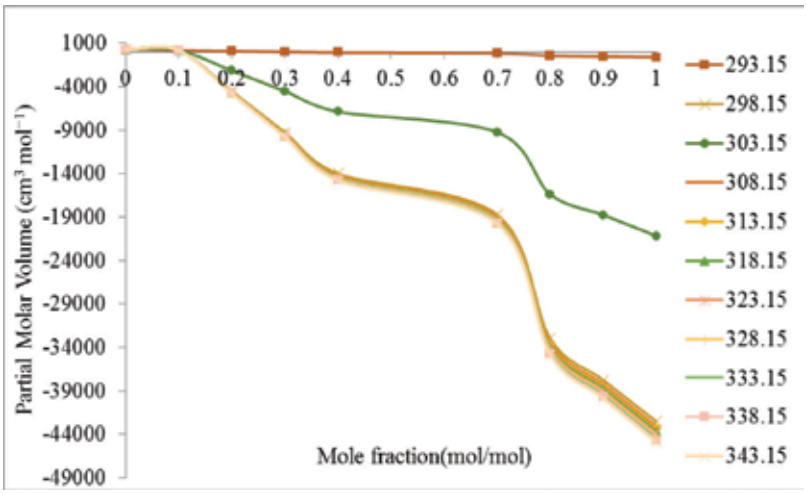

Figure 6. Partial molar volume of [EMIM][ESO_4] in [BMIM][NtF_2] at different temperature.

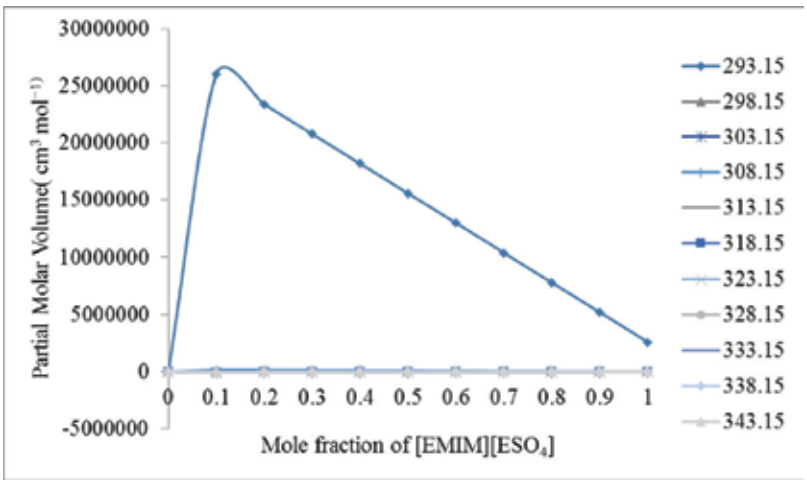

Figure 7. Partial molar volume of [EMIM][ESO_4] in [EMIM][HSO_4] at different temperature.

has positive deviation due to very strong physical interaction between [EMIM][ESO_4] and [BMIM][OAc]/[BMIM][NtF_2]. Physical interaction mainly consisting of dispersion forces or weak dipole-dipole interaction, and weak ion-dipole interaction make a positive deviation. The partial molar volume of [EMIM][ESO_4] with [EMIM][OAc] and [BMIM][NtF_2] mixtures are more negative than [EMIM][ESO_4] + [EMIM][HSO4] mixtures, which imply that there are stronger ion-dipole interactions. On the other hand, packing effect, charge transfer, hydrogen bond formation, other complex interaction, geometrical fitting one component into other due to difference in molar volume make a negative deviation. [EMIM][ESO_4] + [EMIM][HSO_4]

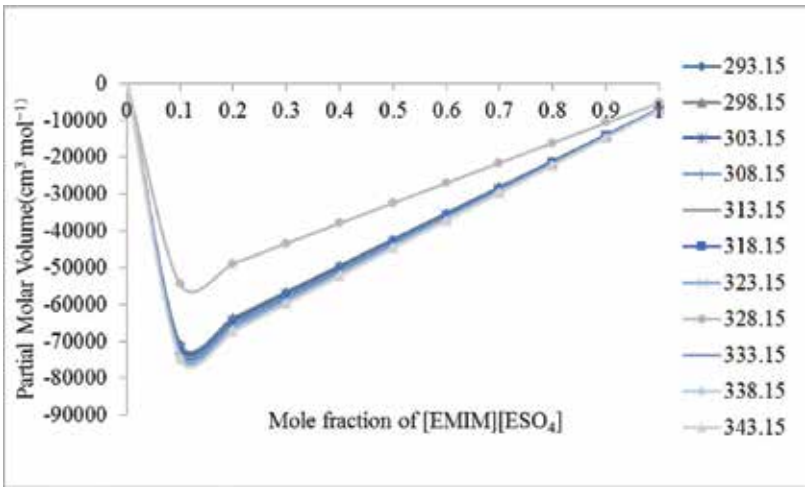

Figure 8. Partial molar volume of [EMIM][ESO_4] in [BMIM][OAc] at different temperature.

system has positive deviation due to very strong physical interaction between these two IL's at molecular level. Usually, physical interaction is dispersion forces or weak dipole-dipole interaction.

4.5. Excess partial molar volume

The excess partial molar volume of [EMIM][ESO_4] in [EMIM][HSO_4],[BMIM][OAc] and [BMIM][NtF_2] at T (293.15–343.15) K are presented in **Figures 9–11**. [EMIM][ESO_4] + [BMIM][NtF_2] and [EMIM][ESO_4] + [BMIM][OAc] shows negative deviation which indicates that

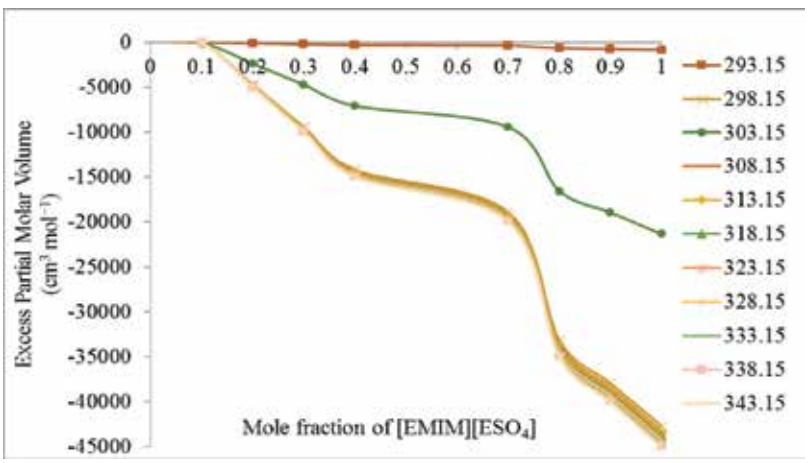

Figure 9. Excess partial molar volume of [EMIM][ESO_4] in [BMIM][NtF_2] at different temperature.

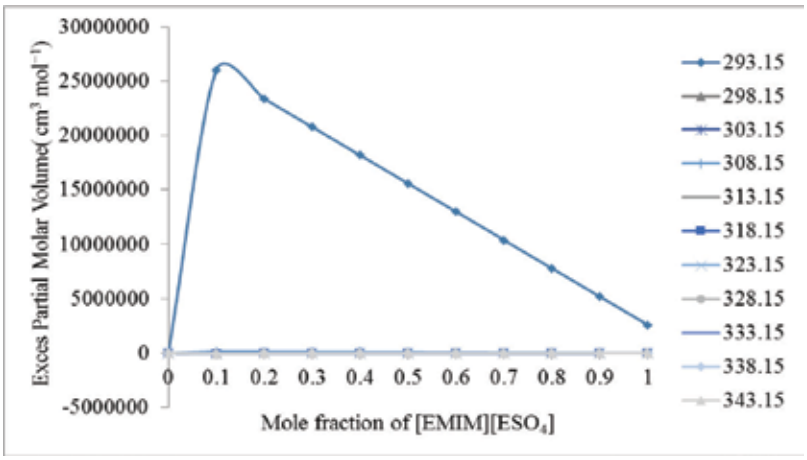

Figure 10. Excess partial molar volume of [EMIM][ESO_4] in [EMIM][HSO_4] at different temperature.

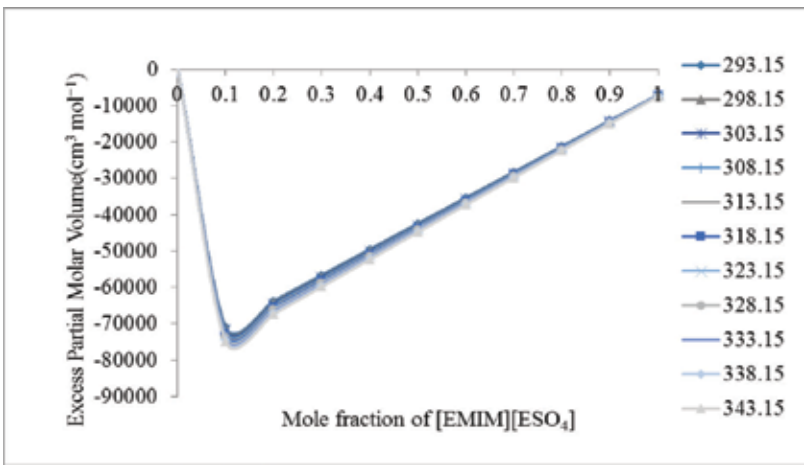

Figure 11. Excess partial molar volume of [EMIM][ESO_4] in [EMIM][OAc] at different temperature.

there is very strong packing effect. The packing effect caused by a large difference in molecular size and configuration between two IL's, charge transfer, hydrogen bond formation and the ion-dipole attractions are even more dominant in IL's mixtures as function of compositions at T (293.15–343.15) K.

4.6. Apparent molar volume

[EMIM][ESO_4] in [BMIM][NtF_2] has positive deviation up to 0.7 mole fraction of [EMIM][ESO_4] due to strong dipole-dipole interaction, dispersion, induction and dipolar forces acting in between these two IL's for entire temperature range (**Figure 12**). The apparent

http://dx.doi.org/10.5772/intechopen.77016

molar volume of [EMIM][ESO_4] in [EMIM][HSO_4] shows positive deviation as function of the composition from 293.15 to 333.15 K which implies that there is strong packing effect due to similar size of cation in both IL's (**Figure 13**). [EMIM][ESO4] + [BMIM][OAc] gave negative apparent molar volume which means that there is very strong hydrogen bond formation and charge-charge interaction between one and another at molecular level (**Figure 14**).

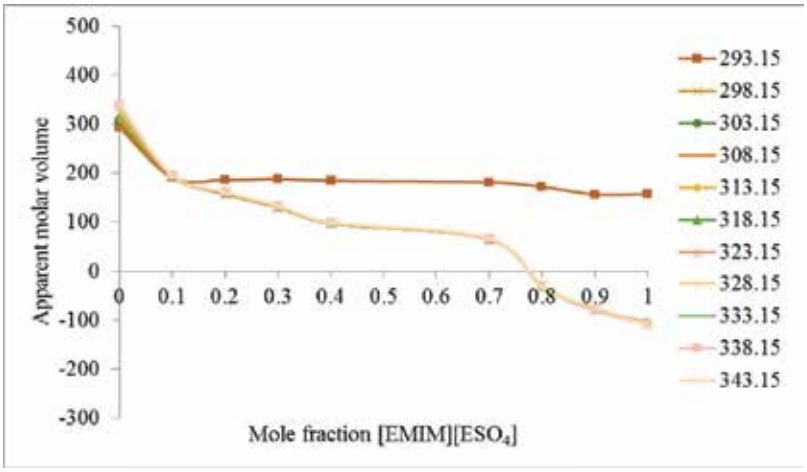

Figure 12. Apparent molar volume of [EMIM][ESO_4] in [BMIM][NtF_2] at different temperature.

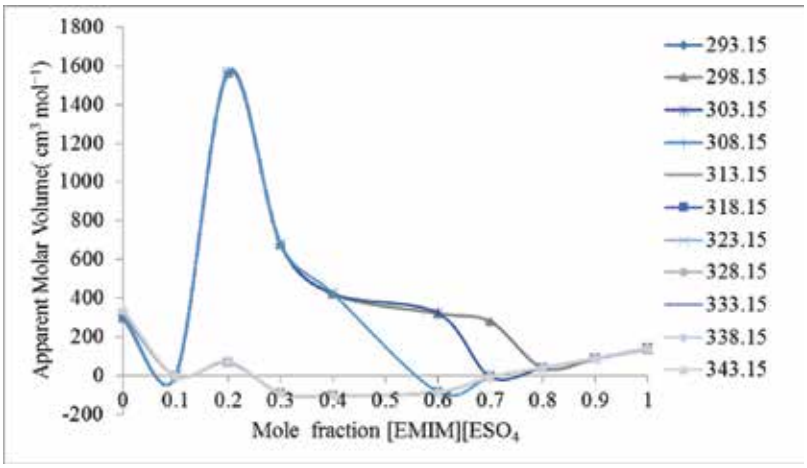

Figure 13. Apparent molar volume of [EMIM][ESO_4] in [EMIM][HSO_4] at different temperature.

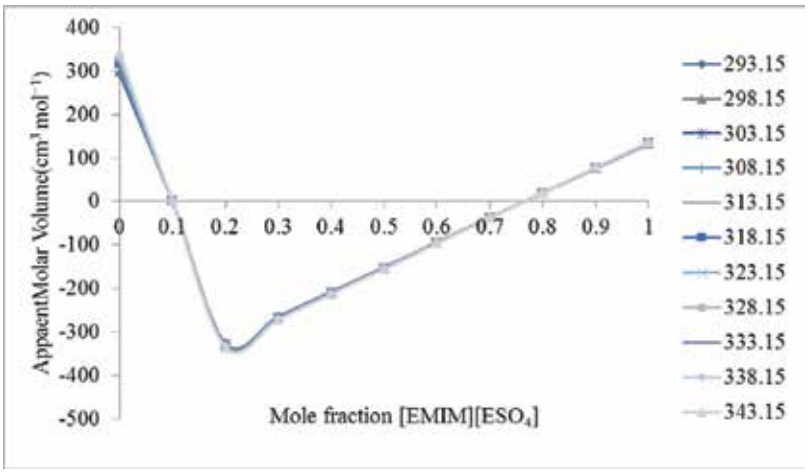

Figure 14. Apparent molar volume of [EMIM][ESO_4] in [EMIM][OAc] at different temperature.

5. Conclusions

Densities for the binary mixtures of [EMIM][ESO_4] + [EMIM][HSO_4], [EMIM][ESO_4] + [BMIM][OAc], [EMIM][ESO_4] + [BMIM][NtF_2] has been measured at 293.15–343.15 K with an interval of 5 K. Isobaric expansivity of all studied IL's have been calculated for temperature ranges from 293.15 to 343.15 K. The corresponding excess molar volume, partial molar volume; excess partial molar volumes; and apparent molar volume have also been calculated. The volumetric behavior of this binary system have been discussed in terms of ion-dipole interaction, packing effect, dipole-dipole interaction, hydrogen bond formation, geometrical fitting of one component into other, charge transfer, electron-electron interaction, and other complex forming interactions. In these mixtures, the forces (that is: dispersion, induction and dipolar forces) between pairs of unlike molecules are less than the forces between like molecules due to the difference in shape and size of the constituent molecules.

Acknowledgements

The authors wish to acknowledge the Department of Science and Technology-SERB (YSS/2015/DO1546), Government of India and SSN trust for funding the work and also Department of Chemical Engineering for supporting the work.

Author details

Achsah Rajendran Startha Christabel, Danish John Paul Mark Reji and Anantharaj Ramalingam*

*Address all correspondence to: anantharajr@ssn.edu.in

Department of Chemical Engineering, SSN College of Engineering, Chennai, India

References

[1] Yanfang G, Tengfang W, Dahong Y, Changjun P, Honglai L, Ying H. Densities and viscosities of the ionic liquid [C4mim][PF6]+N,N-dimethylformamide binary mixtures at 293.15 K to 318.15 K. Chinese Journal of Chemical Engineering. 2008;**16**(2):256-262

[2] Freire MG, Carvalho PJ, Fernandes AM, Marrucho IM, Queimada AJ, Coutinho JAP. Surface tensions of imidazolium based ionic liquids: Anion, cation, temperature and water effect. Journal of Colloid and Interface Science. 2007;**314**:621-630

[3] Freire MG, Ventura SPM, Santos LMNBF, Marrucho IM, Coutinho JAP. Evaluation of COSMO-RS for the prediction of LLE and VLE of water and ionic liquids binary systems. Fluid Phase Equilibria. 2008;**268**:74-84

[4] Ghatee MH, Zolghadr AR. Surface tension measurements of imidazolium-based ionic liquids at liquid–vapor equilibrium. Fluid Phase Equilibria. 2008;**263**:168-175

[5] García-Miaja G, Troncoso J, Romaní L. Excess properties for binary systems ionic liquid + ethanol: Experimental results and theoretical description using the ERAS model. Fluid Phase Equilibria. 2008;**274**:59-67

[6] Dománska U, Marciniak A. Phase behaviour of 1-hexyloxymethyl-3-methyl-imidazolium and 1,3-dihexyloxymethyl-imidazolium based ionic liquids with alcohols, water, ketones and hydrocarbons: The effect of cation and anion on solubility. Fluid Phase Equilibria. 2007;**260**:9-18

[7] Sanmamed YA, Gonźalez-Salgado D, Troncoso J, Cerdeirĩna CA, Roman L. Viscosity-induced errors in the density determination of room temperature ionic liquids using vibrating tube densitometry. Fluid Phase Equilibria. 2007;**252**:96-102

[8] Instruction Manual for Anton Paar DMA 4100 M; DMA 4500 M; DMA 50000 M

[9] Patil PP, Patil SR, Borse AU, Hunndiwale DG, Density. Excess molar volume and apparent molar volume of binary liquid mixtures. Rasayan Journal of Chemistry. 2011;**4**(3):599-604

[10] Domańska U, Krolikowska M, Krolikowski M. Phase behaviour and physico-chemical properties of the binary systems {1-ethyl-3-methylimidazolium thiocyanate, or 1-ethyl-3-methylimidazolium tosylate + water, or + an alcohol}. Fluid Phase Equilibria. 2010;**294**:72-83

[11] Singh T, Kumar A. Physical and excess properties of a room temperature ionic liquid (1-methyl-3-octylimidazolium tetrafluoroborate) with n-alkoxyethanols (C1Em, m = 1 to 3) at T = (298.15 to 318.15) K. The Journal of Chemical Thermodynamics. 2008;**40**:417-423

[12] Zhong Y, Wang H, Diao K. Densities and excess volumes of binary mixtures of the ionic liquid 1-butyl-3-methylimidazolium hexafluorophosphate with aromatic compound at T = (298.15 to 313.15) K. The Journal of Chemical Thermodynamics. 2007;**39**:291-296

[13] Domanska U, Królikowski M. Phase equilibria study of the binary systems (1-butyl-3-methylimidazolium tosylate ionic liquid + water, or organic solvent). The Journal of Chemical Thermodynamics. 2010;**42**:355-362

[14] Shekaari H, Mousavi SS. Volumetric properties of ionic liquid 1,3-dimethylimidazolium methyl sulfate + molecular solvents at T = (298.15-328.15) K. Fluid Phase Equilibria. 2010;**291**:201-207

[15] Wang S, Jacquemin J, Husson P, Hardacre C, Costa Gomes MF. Liquid–liquid miscibility and volumetric properties of aqueous solutions of ionic liquids as a function of temperature. The Journal of Chemical Thermodynamics. 2009;**41**:1206-1214

[16] Wankhede NN, Wankhede DS, Lande MK, Arbad BR. Molecular interactions in (2,4,6-trimethyl-1,3,5-trioxane + *n*-alkyl acetates) at *T* = (298.15, 303.15, and 308.15) K. The Journal of Chemical Thermodynamics. 2006;**38**(12):1664-1668

Chapter 8

Azeotropy: A Limiting Factor in Separation Operations in Chemical Engineering - Analysis, Experimental Techniques, Modeling and Simulation on Binary Solutions of Ester-Alkane

Raúl Rios, Adriel Sosa, Luis Fernández and Juan Ortega

Additional information is available at the end of the chapter

http://dx.doi.org/10.5772/intechopen.75786

Abstract

The presence of azeotropic points in the vapor-liquid equilibria of some solutions is a limiting factor in separation operations by distillation. Knowledge of azeotropy is based on understanding its origins and behavior in relation to the different variables that modulate phase equilibria, and can be used to control the appearance of these singular points. This work studies the phenomenon of azeotropy and presents a practical view based on the study of ester-alkane binary solutions. After considering the principles of vapor-liquid thermodynamics and the special cases of azeotropic points, a detailed description is given of the experimental techniques used to determine these points and also for their thermodynamic verification. Two different but complementary modeling approaches are proposed: the correlation of experimental data and the prediction of azeotropic variables. The first is required to achieve a rigorous design of apparatus and installations, while the second is useful in preliminary design stages. Finally, alternatives to the separation process are studied by simulation. For a practical perspective on these aspects, each section is accompanied by data for ester-alkane solutions, and references are made to applications in the chemical, food and pharmaceutical industries.

Keywords: azeotropy, modeling, experimentation, simulation, ester, alkane

1. Introduction

In general, the matter that makes up the Earth and everything living on it has a heterogeneous nature in relation to the different states (solid, liquid and gas). In the case of liquid solutions, the development of separation technologies is associated with the chemical industry [1, 2], which is a driving force behind it. Any transformation process of matter requires preliminary and/or subsequent steps, which change the composition of the solutions involved. One objective may be to purify the products generated in a reactor, for example, by removing the presence of inert compounds, contaminants, by-products or excess reagents, and even to produce solutions with specific compositions, different to those obtained in the reactor. So, many processes in the chemical industry are essentially combinations of physical separation processes that do not require a chemical reaction.

There are a variety of separation processes known to date [3], but the performance of distillation [4] make it the most important and most used operation in the chemical industry. However, not all solutions can be separated into their simple components by classical multi-step distillation (rectification) techniques. Because of this, advanced methods aimed at resolving the limitations of distillation in relation to specific problems have been developed. Two of the most important complications in the correction of solutions are: (1) the presence of azeotropes and, (2) the proximity of the boiling points of the components in the dissolution (close boiling point). Similar strategies are followed to separate solutions with either of these scenarios, and the main differences between them lie in certain technical details of the design. Some examples are recorded in **Table 1**. Most of the procedures described try to modify the system either by changing the operating conditions (such as in *pressure-swing-distillation*), or by adding an extractant (*entrainer*), although the latter can present some reactivity with some of the components present. Other techniques combine the rectification with other operations based on different physical principles, such as pervaporation or liquid-liquid extraction.

Although important from a practical perspective the problems posed by a "close boiling point" (CBP) do not require complicated theorization. This phenomenon tends to occur in dissolutions involving chemically similar compounds (of the same chemical nature), with a behavior close to ideality. Azeotropy, however, is a complex phenomenon with different modes of presentation for which the complexity increases exponentially with the number of compounds in solution. Many authors have attempted to write about azeotropy [5, 6], while others have focused on making experimental measurements with different solutions and/or compiling the results [7, 8]. However, the current literature is still scarce. It is especially important to clarify the physical causes of the azeotropes, influenced by the situation and their repercussions on process design (with the sequence: experimentation, E-modeling, M-simulation, S), particularly from a practical perspective.

For many years, our research group has conducted experiments on azeotropic systems (see [9–12]), mainly on solutions containing esters, alkanols and alkanes. Experimental developments have also been proposed to determine vapor-liquid equilibria (VLE) [13, 14], and theoretical approaches to model experimental thermodynamic data [14–17] and to assess their quality [18, 19]. In this chapter, the azeotropy is studied from different perspectives which governs the design of some

Enhanced distillation	Particular cases	Mixtures	Entrainer
Azeotropic distillation	Minimum boiling point	Not found	Not found
	pressure-swing	THF + water Methyl ethanoate + methanol Water + ethanol	Non-available Non-available Non-available
	Boundaries bending	Hydrochloric acid + water Nitric acid + water	Sulfuric acid Sulfuric acid
	Liquid-liquid extraction	Ethanol + water Butanol + water Hydrocarbon + water Pyridine + water	Benzene, toluene Self-entraining Self-entraining Benzene
	Pervaporation	Ethanol + water Toluene + heptane	Cellulose acetate membrane
Extractive distillation	With volatile solvent	Not found	Not found
	With heavy solvent	Isoprene + pentane	Furfural, acetonitrile
	With salt	Ethanol + water	Acetate-based salts
Reactive distillation	Reactive entrainer without catalyzer	m-xylene + p-xylene Ethanol + water	Tert-butylbenzene Ethylene glycol
	Reactive entrainer catalyzed-promoted	Methyl ethanoate + isobutanol	o-xylene + ionic liquid

Table 1. Advanced distillation techniques with industrial examples and details of the entrainer used.

engineering operations, and more specifically those cited above (E-M-S), actions that the authors have pursued in recent works [20, 21]. Initially, the phenomenon of azeotropy is considered, supported by the basic thermodynamic formulation, in an attempt to understand its origin and sensitivity to changes in the system conditions. The experimental methods available to measure azeotropic points are exposed, their strengths and limitations are discussed, and reference is made to tools [18, 19] to determine data quality. Regarding the modeling, different strategies are used to characterize VLE diagrams and to estimate the presence of azeotropes, with a critical analysis to predict the appearance of singular points. Finally, the information compiled is used in several examples to design azeotropic separation processes, taking into consideration different conditions of ester and alkane solutions.

2. Azeotropy: description of the phenomenon and thermodynamic representation

Etymologically, the term "azeotrope," coined by the chemists J. Wade and R.W. Merriman [22], comes from the Greek combination of three words "a" (without), "zein" (boiling) and "trope" (change), in other words, to boil without change, referring to a solution for which the variables (p,T,x) remain unchanged, which is the main characteristic of this phenomenon. These authors described the phenomenon of azeotropy when studying the VLE of the

mixture of water + ethanol at atmospheric pressure. They found that at a given composition of liquid solution the mixture cannot separate as the distilled vapor (with composition y) has the same composition as the remaining liquid (with composition x). Thermodynamic formalism establishes the equality $\mathbf{x} = \mathbf{y}$, between the compositions vector of the liquid phase, $\mathbf{x} = [x_1, x_2, \ldots, x_n]$ and the corresponding vapor phase, $\mathbf{y} = [y_1, y_2, \ldots, y_n]$ of a system with n-components, to indicate the presence of an azeotrope. The previous identity implies that the solution behaves, in relation to the distillation process, as a pure product, giving rise to an unusual situation. The behavior is a result of changes in the structure of the final dissolution (in singular conditions), with a different reorganization compared to the original one of pure products. Changes occur in all non-ideal solutions, although not all of them are azeotropic. We may, therefore, ask, "what is the difference? In the case of azeotropes the average interactions that affect the molecules of different compounds in solution are equivalent, causing the volatilities are the same: All components have the same ability to change into the vapor phase, resulting in both phases (líquid and vapor) having the same composition.

VLE thermodynamics states that the partial pressure of each component, p_i, of a mixture in VLE, is determined by a modified version of Raoult's law:

$$p_i = y_i p = \frac{x_i \gamma_i p_i^o}{\Phi_i} \tag{1}$$

where p is the total pressure of the system, x_i and y_i, the compositions of compound i in the liquid and vapor phase, respectively, $\gamma_i = \gamma_i(x_i, p, T)$ is the activity coefficient of this compound in the liquid phase, $p_i^o = p_i^o(T)$ the vapor pressure of this component, and $\Phi_i = \Phi_i(y, p, T)$, related to the fugacity coefficient of pure compound i in solution $\widehat{\phi}_i$, and as saturated vapor ϕ_i^o according to the equation,

$$ln\Phi_i = ln\left(\frac{\widehat{\phi}_i}{\phi_i^o}\right) + \left[\frac{-v_i^o(p - p_i^o)}{RT}\right] \tag{2}$$

The azeotropic condition established previously, $\mathbf{x} = \mathbf{y}$, combined with Eq. (1), gives place to the following relationship for azeotropic pressure:

$$p = \gamma_i p_i^o / \Phi_i \tag{3}$$

which must be obeyed for all components of the system. Equation (4) implies the following identity between all components of the mixture:

$$\frac{\gamma_1 p_1^o}{\Phi_1} = \frac{\gamma_2 p_2^o}{\Phi_2} = \ldots \frac{\gamma_i p_i^o}{\Phi_i} = \ldots = \frac{\gamma_n p_n^o}{\Phi_n} \tag{4}$$

This equation is important because it can be used as a starting point for several considerations. For example, at low and moderate pressures $\Phi_i \approx 1$ and often at high pressures its value would not vary significantly for different compounds and it is acceptable to assume that $\Phi_i/\Phi_j \approx 1$. Therefore, from Eq. (4) it can be deduced that the presence of an azeotrope is due to γ_i and to p_i^o, in other words, for there to be an azeotrope in the VLE equations.

http://dx.doi.org/10.5772/intechopen.75786

$$\gamma_i(T,p,x_i) = p/p_i^o \text{ and } \gamma_j(T,p,x_j) = p/p_j^o \tag{5}$$

must have a real-valued solution. The γ's are a measurement of the non-ideal nature of the liquid phase owing to the interactional effects in the mixing process and depend upon each specific solution, they cannot be known a priori, but are modeled mathematically. The vapor pressures play an important role and depend only upon the equilibrium temperature which, in turn, depends upon the total pressure of the system studied, see **Figure 1**. For Eq. (4) to be rigorously applied, the parameter Φ_i is required; this is calculated from expressions found in any textbook on the Thermodynamics of Solutions [23]. Its more general expression is:

$$\ln\Phi_i = \left[B_{ii}(p - p_i^o) + (1/2)p\sum_j\sum_k y_j y_k(2\delta_{ji} - \delta_{jk})\right]/RT \tag{6}$$

where $\delta_{ji} = 2B_{ji}\text{-}B_{jj}\text{-}B_{ii}$, and the δ_{jk} are easy to deduce; the virial coefficients of the pure compounds B_{ii} and mixtures B_{ji} can be calculated by a correlation process. Adaptation of Eq. (4) to binaries gives:

$$\ln\frac{\gamma_1}{\gamma_2} = \ln\frac{p_2^o}{p_1^o} + B_{11}(p - p_1^o) - B_{22}(p - p_2^o) + p\delta_{12}(y_1 - y_2) \tag{7}$$

There is a clear dependence between the quotients of the activity coefficients and the vapor pressures. Bancroft [24] introduced a rule which, at least graphically is intuitive, that the appearance

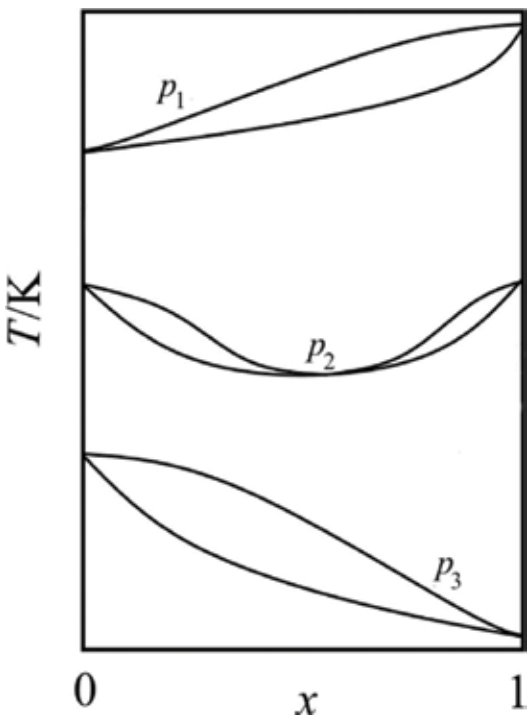

Figure 1. Isobaric-VLE of a binary at different pressures.

of an azeotrope in a homogeneous solution is dependent on the equality of the vapor pressures at a given temperature, ignoring the final summands of Eq. (7). The point of intersection of the vapor pressures is called the *Bancroft point*; although absence of this point does not imply that there is no azeotrope. We insist that one of the most important aspects is to determine the structural behavior of the solution, because the formation of these singular states that identify the azeotropic condition with a pure compound, as mentioned previously, is of significance in the applicability of specific fluids (as occurs in other phase equilibria). This is why it is interesting to define the formation of azeotropes knowing the existence of interactions between different molecules, which can be of attractive nature (favoring the mixing process), or repulsive (impeding it). In the first case, the solution presents a negative deviation of Raoult's law $\gamma_i < 1$, and according to Eq.(4) the p_i^o will be higher than in an ideal solution as would also be the equilibrium temperatures, **Figure 2(a)**. If the net interactional effect is repulsive, $\gamma_i >> 1$, p_i^o would be lower to balance out the total pressure. Now, the equilibrium temperatures also diminish creating an azeotrope of minimum temperature, **Figure 2 (b)**. Occasionally, the effects of the interactions of a solution are not entirely attractive or repulsive, but their sign varies depending on the state (T,p,x) of the system. In these cases, Eqs. (4) and (5) are satisfied in different regions of the equilibrium plots, and present more than one azeotrope (polyazeotropy), see **Figure 2(c)**. When the solution is affected by strong repulsive effects, the liquid phase becomes unstable and separates into two immiscible liquid phases (liquid-liquid equilibrium, LLE) [25]. High values of the activity coefficients associated with this repulsion favor the formation of azeotropes at a minimum temperature. Sometimes, both phenomena (immiscibility and azeotropy) occur in the same conditions (p,T,x,y), **Figure 2(d)**, giving rise to systems in LLE, VLLE. The types of azeotropes indicated in **Figure 2** for binary solutions also occur in multicomponent systems, although the behavior of the solution is more complex. To illustrate this, **Figure 3** shows the residues, see [3], of some examples of ternaries. The presence of an azeotrope in one of the binaries, **Figure 3(a)**, divides the diagram into two distillation regions by a line that joins the stable node with the unstable node. None of the distillation processes occurring in either of the regions could pass from one to the other, because as they move closer to the region boundary, it will tend to fall to the azeotropic point (stable node). The presence of two azeotropic points would not necessarily change the behavior unless this corresponded to some kind of stable node. Hence, if the azeotrope corresponds to a maximum temperature, it can become an unstable node, **Figure 3(b)**, altering the separation regions.

Ternary azeotropes (those produced in the presence of three solution components) do not necessarily correspond to the minimum points of the diagram; occasionally, **Figure 3(c)**, they

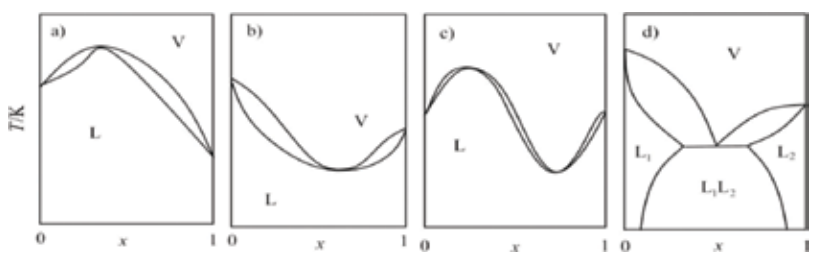

Figure 2. Azeotrope types. (a) Maximum temperature, (b) minimum temperature, (c) polyazeotrope, and (d) non-homogeneous azeotrope. V, vapor phase, L, homogeneous liquid phase, and L_1 and L_2 liquid phases of immiscible system.

http://dx.doi.org/10.5772/intechopen.75786

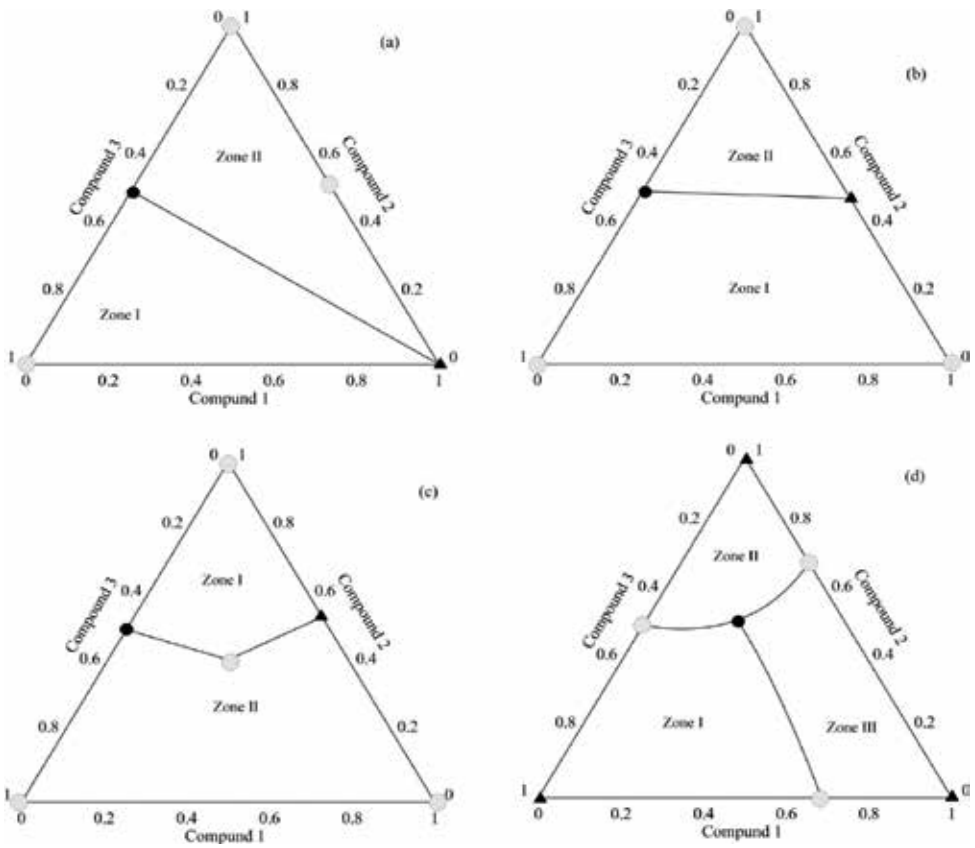

Figure 3. Examples of ternary VLE of azeotropic systems. (●) stable node, (▲) unstable node, (●) saddle-point, (——) separating line. (a) One binary azeotrope, (b) two binary azeotropes, (c) two binary azeotropes and one ternary, (d) minimum temperature ternary azeotrope.

are presented as a saddle-point. However, when they do correspond to the minimum temperature, they also become the stable node for any distillation region. In these cases, the remaining azeotropes also become saddle-points, **Figure 3(d)**.

3. Characterization of azeotropes. Results for ester + alkane solutions

3.1. Experimental techniques for the determination of azeotropes. Details and recommendation

In the experimental characterization of an azeotrope the following parameters or properties must also be specified: (a) composition, (b) boiling point at a given pressure, and (c) the differences between the boiling points of the azeotrope and the most volatile component (positive azeotrope) or that of the component of the lowest boiling point (negative azeotrope). It is usual to specify values for the variables of (a) and (b) to characterize the azeotrope, although the result that establishes (c) should also be given in each case.

Azeotropic points are experimentally determined by several procedures that can be grouped into two categories: direct and indirect. Direct measurements are applied to determine the azeotropic composition inside the apparatus, with the greatest accuracy possible. Experimentalists frequently make mistakes when verifying the precision of the azeotropic coordinates, as the starting products do not always have the desired purity, which distorts the values of the state variables. The commonest example concerns the presence of moisture in the components of a binary system, resulting in the formation of binary or ternary azeotropes with the water; this can even give rise to the appearance of unexpected azeotropes in some systems. Hence, azeotropic experimentation must be rigorous and include a careful rectification procedure. The precise variables of azeotropes can be obtained in a differential ebulliometer [26], such as the one shown in **Figure 4**, with different regions for boiling and condensation, both working to rectify the study mixture, although the temperature on reaching equilibrium must be the same at a given pressure. A recent design for a differential ebulliometer has been proposed by Raal et al. [27].

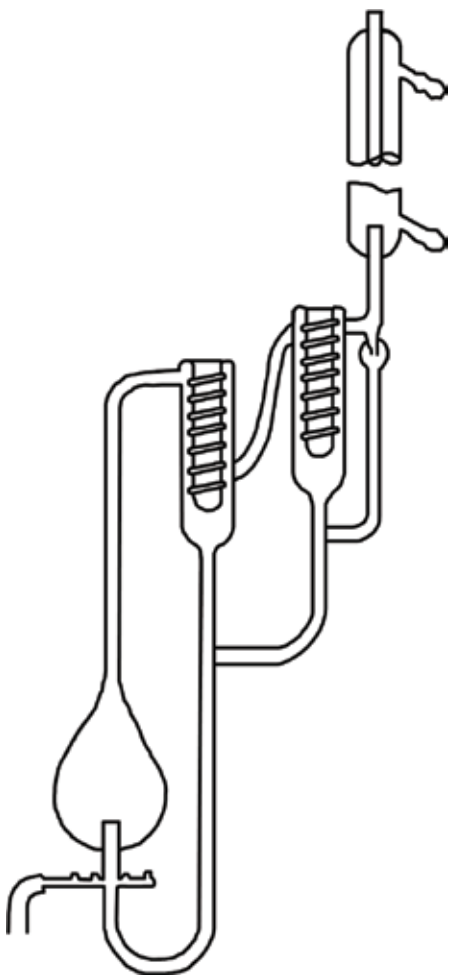

Figure 4. Differential ebulliometer [26].

http://dx.doi.org/10.5772/intechopen.75786

Several studies are described in the literature [28–30] in which the authors use small or medium-scale installations with distillation columns with a high number of equilibrium phases, operating at total reflux and isobaric conditions. These columns can reach a very similar composition to that of the azeotrope in the reflux, after reaching a steady state. **Figure 4** shows a diagram of an installation **Figure 5**. Packed-tower used for the direct determination of azeotropic points showing details of the installation and auxiliary apparatus. On right, data representations and flow control of these characteristics. To collect the purest fraction possible of an azeotrope a differential ebulliometer is placed adjacent to a distillation column. The pure azeotrope is, therefore, determined in the differential ebulliometer and the difference between the boiling points of the reference compound and that of the azeotrope, with the purpose of estimating the latter.

Figure 5 shows a diagram of the experimental apparatus used in our laboratory to directly measure azeotropic points using a distillation column. This experimental design is useful to characterize the azeotropic points relative to pressure, and to determine the separate regions in systems. The former is carried out by adjusting the pressure of the system to reach a stable temperature at the head of the column, to then take samples of the reflux for analysis. In the case of ternary systems, different starting compositions are used, with the purpose of conducting the experiment in the separate regions. The main drawback of this experimental technique is that the data obtained are not useful for the modeling process, as discrete points are obtained. In any

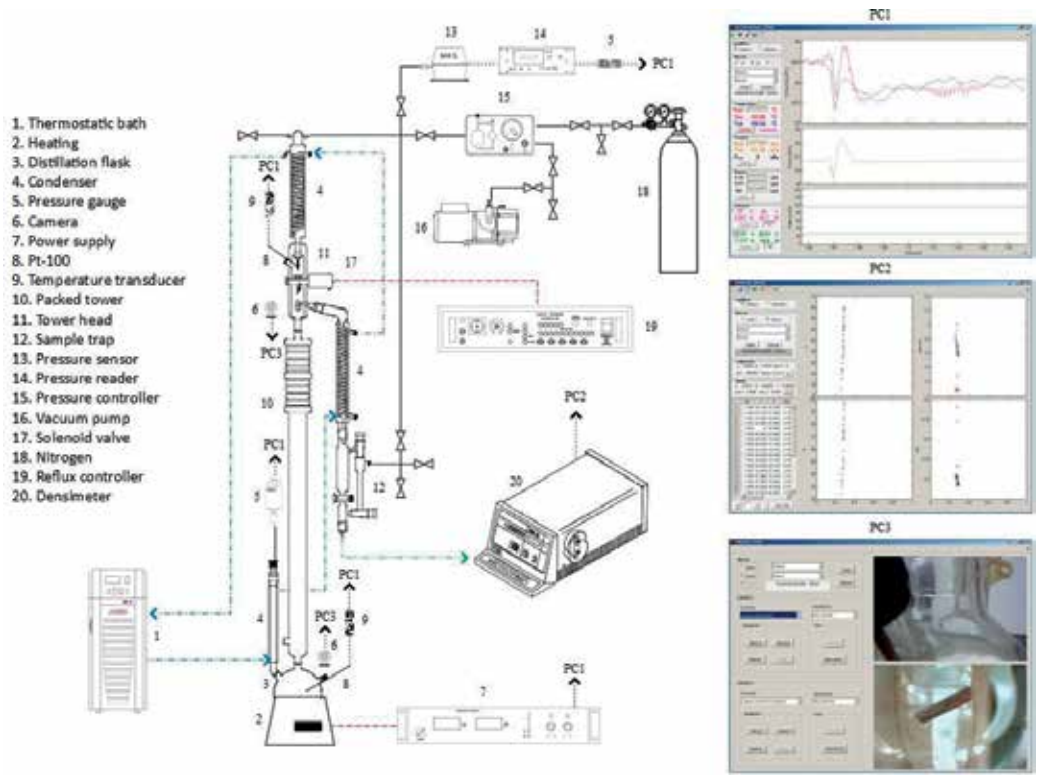

Figure 5. Packed-tower used for the direct determination of azeotropic points showing details of the installation and auxiliary apparatus. On right, data representations and flow control.

case, the azeotropes measured must only be used to complement data available in the complete VLE diagrams.

The indirect technique to determine the coordinates of the azeotropic points consists in interpolating from data determined for the VLE diagram. This is the most widespread procedure [13–15, 26], and the standard one recommended for azeotropes as it describes the entire VLE in given conditions of pressure and temperature. Likewise, an example of the experimental installation to determine VLE data is shown in **Figure 6**, with a small ebulliometer [13, 14] used in our laboratory equipped with a Cotrell pump and a small rectification zone, with temperature differences as specified previously. The samples for binary systems are studied by densimetry/refractometry for ternary systems by gas chromatography. Optimal functioning is achieved by automating the system with suitable software that can carefully control the different variables.

One advantage of the system is that it can obtain a large quantity of data to produce an precise characterization of the VLE. The combination of this technique with the direct method is optimum: the indirect method is used to determine the VLE diagrams of the system in discrete conditions and this information is complemented by azeotropic data at different pressures.

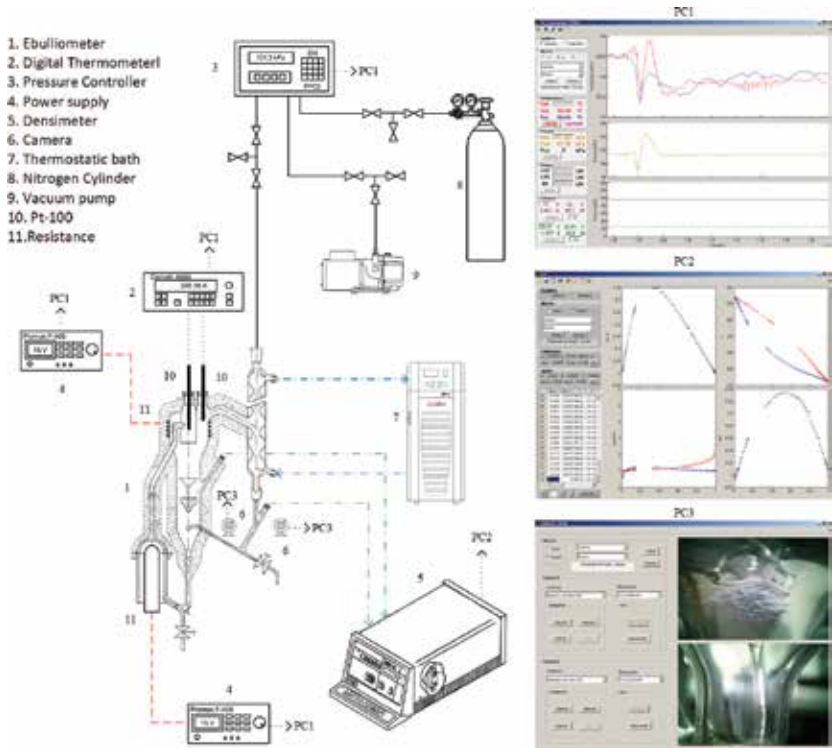

Figure 6. Experimental installation for the experimental determination of VLE, ebulliometer and details of auxiliary equipment.

http://dx.doi.org/10.5772/intechopen.75786

3.2. Verification of experimental data

The high quality of the starting products and the improvement in the instrumentation and control systems combined with standardization of the experimental protocols, increase the probability of obtaining quality data. In any case, it is important to turn to mathematical-thermodynamic procedures that certify the quality of those dat, as these have important repercussions on subsequent operations.

There is a widespread tendency in thermodynamics to establish relationships that verify the scientific coherence between the variables measured, in other words, that establish the *thermodynamic consistency* of the data. Although there are several ways to do this [31, 32], they are of limited scope. In other words, the verification of data must be applied to VLE data before determining the azeotropic coordinates (indirect method). A strategy to check the consistency is based on the following rules:

1. Experimental VLE data are analyzed in graphical form showing the variables measured (x, y, T, p) and those calculated with the thermodynamic formulation, γ_i and g^E. The coherence of these quantities must be illustrated in graphs, otherwise the location of the azeotropes can change. In azeotropic systems, the plot of (y-x) *vs.* x is important as the intersection of the distribution of points with the x-axis indicates the presence of an azeotrope. In binaries, the coordinates of this point coincide with the minimum or maximum temperature (or maximum or minimum pressures).

2. The experimental data must be modeled to solve most of the consistency tests. Recommendations for this are provided in Section 3 of this chapter.

3. A combination of several consistency tests must be used to confirm the quality of the data and their coherence. The tests as the Areas-test [33] and the Fredenslund-test [34] are recommended, together with a third procedure, although they cannot be used in some cases of azeotropy, such as those appearing in partially miscible systems, **Figure 1(d)**, or polyazeotropes, **Figure 1(c)**. Alternatively, a method proposed by the authors [19], with a more rigorous thermodynamic formulation, could be used.

4. It is also worth mentioning here a method that should be avoided. The method of Herington [35] produces incorrect results by assuming false hypotheses [36] in certain cases. In general, no Area-test should be used as the sole test as they are insensitive to pressure errors [37]. The composition/resolution-test [38], or any other test aimed at exactly obeying thermodynamic relations should also be avoided as they are very limiting.

When applying the consistency test to azeotropic systems some peculiarities must be taken into account. As an example, a brief description is included below of the application of two tests commonly used to analyze VLE data.

- Area-test (Redlich-Kister [33] or other): the method is based on solving the integral,

$$A = \int_{x_1=0}^{x_1=1} \ln \frac{\gamma_1}{\gamma_2} dx_1 \tag{8}$$

which should produce a result close to zero. As mentioned above, the activity coefficients at the azeotropic points are identified with the quotient of the vapor pressures, which provides an additional verification of the data.

- Fredenslund-test [34]: in this case the inconsistency is quantified by the residue generated by this model when reproducing the vapor phase of the VLE system, determining the quality from the difference:

$$\delta y = \left| y_{\text{exp}} - y_{\text{cal}} \right| \tag{9}$$

According to this formation, the coordinates of the azeotropic point are only verified with data from the liquid phase:

$$\delta y_1 = \left| x_{1,\text{exp}} - \frac{x_{1,\text{exp}}\gamma_1 p_1^{\text{o}}}{x_{2,\text{exp}}\gamma_2 p_2^{\text{o}} + x_{1,\text{exp}}\gamma_1 p_1^{\text{o}}} \right| = x_{1,\text{exp}} x_{2,\text{exp}} \left| \frac{\gamma_2 p_2^{\text{o}} - \gamma_1 p_1^{\text{o}}}{\gamma_2 p_2^{\text{o}} + x_{1,\text{exp}}\left(\gamma_1 p_1^{\text{o}} - \gamma_2 p_2^{\text{o}}\right)} \right| \tag{10}$$

which should have a value less than 0.01.

In the two cases presented here, the quality of the azeotropic data is linked to the determination of their coordinates by the indirect method. Hence, the azeotropes are verified in the same way as the rest of the data from the VLE series. In order to obtain a procedure that verify the data obtained by the direct method, it is convenient to recur to the test proposed by ours [19], which has the following general expression for a VLE binary (assuming an ideal vapor phase, see [19]):

$$\frac{y_1 - x_1}{y_1(1 - y_1)} = \left(\frac{1}{p} - \frac{v^{\text{E}}}{RT}\right) dp + \left(\frac{h^{\text{E}}}{RT^2} - \sum_{\text{i}=1}^{2} x_{\text{i}} \frac{\partial \ln p_{\text{i}}^{\text{o}}}{\partial T}\right) dT \tag{11}$$

and imposing the condition of azeotropy:

$$\frac{dT}{dp} = -\frac{\left(\frac{1}{p} - \frac{v^{\text{E}}}{RT}\right)}{\left(\frac{h^{\text{E}}}{RT^2} - \sum_{\text{i}=1}^{2} x_{\text{i}} \frac{\partial \ln p_{\text{i}}^{\text{o}}}{\partial T}\right)} \tag{12}$$

Integration of Eq. (12), must be carried out numerically as it corresponds to a differential equation of non-separable variables that relates the azeotropic temperature with the pressure of the system. Estimation of the difference between the temperature obtained by Eq. (12) and the experimental temperature is sufficient to verify thermodynamic consistency.

3.3. Azeotropy in ester-alkane solutions

3.3.1. Preliminary analysis

The energetic and volumetric effects of the mixing process of esters and alkanes, due to inter/intra molecular interactions, present net positive values for g^{E} function, with activity coefficients greater

http://dx.doi.org/10.5772/intechopen.75786

			C_5H_{12}	C_6H_{14}	C_7H_{16}	C_8H_{18}	C_9H_{20}	$C_{10}H_{22}$
			Pentane	**Hexane**	**Heptane**	**Octane**	**Nonane**	**Decane**
			T_b^o **= 309.30 K**	T_b^o **= 341.88 K**	T_b^o **= 371.60 K**	T_b^o **= 398.82 K**	T_b^o **= 423.97 K**	T_b^o **= 447.30 K**
$C_2H_4O_2$	Methyl methanoate	T_b^o = 304.80 K	$^{E}(0.558,293.90)^{39}$ $^{D}(0.575,294.15)^{7}$ $^{D}(0.574,294.85)^{7}$	$^{E}(0.832,302.62)^{43}$ $^{E}(0.849,302.65)^{57}$ $^{E}Z^{7}$	$^{E}(0.992,304.69)^{45}$ $^{E}Z^{12}$	$^{E}Z^{12}$	$^{E}Z^{12}$	$^{E}Z^{50}$
$C_3H_6O_2$	Ethyl methanoate	T_b^o = 327.50 K	$^{E}(0.218,306.50)^{39}$ $^{D}(0.215,307.15)^{7}$ $^{D}Z^{7}$	$^{E}(0.703,323.32)^{43}$ $^{E}(0.709,323.21)^{51}$ $^{D}(0.669,324.90)^{7}$	$^{E}(0.988,327.30)^{7}$ $^{D}(0.973,329.75)^{7}$ $^{E}Z^{51}$	$^{E}Z^{12}$ $^{E}Z^{51}$	$^{E}Z^{12}$ $^{E}Z^{51}$	$^{E}Z^{50}$ $^{E}Z^{51}$
	Methyl ethanoate	T_b^o = 330.02 K	$^{E}(0.203,307.28)^{17}$ $^{D}(0.295,305.65)^{7}$	$^{E}(0.683,325.44)^{17}$ $^{D}(0.703,322.65)^{7}$ $^{D}(0.665,324.80)^{52}$	$^{E}(0.962,329.93)^{17}$ $^{E}(0.934,329.6)^{45}$	$^{E}Z^{17}$	$^{E}Z^{17}$	$^{E}Z^{17}$
$C_4H_8O_2$	Ethyl ethanoate	T_b^o =350.26 K	$^{E}Z^{40}$	$^{E}(0.339,338.15)^{40}$ $^{E}(0.343,338.00)^{46}$ $^{E}(0.343,338.30)^{53}$	$^{E}(0.834,349.99)^{40}$ $^{D}(0.947,350.05)^{7}$	$^{E}Z^{40}$ $^{E}Z^{7}$ $^{E}Z^{56}$	$^{E}Z^{40}$ $^{E}Z^{7}$	$^{E}Z^{40}$ $^{E}Z^{7}$
	Methyl propanoate	T_b^o =352.90 K	$^{E}Z^{14}$	$^{E}(0.279,339.38)^{47}$ $^{E}(0.216,339.95)^{7}$	$^{E}(0.844,351.86)^{14}$ $^{E}(0.929,352.75)^{7}$	$^{E}Z^{47}$	$^{E}Z^{14}$	$^{E}Z^{42}$
	Propyl methanoate	T_b^o =354.00 K	$^{E}Z^{39}$	$^{E}(0.283,339.10)^{43}$ $^{E}(0.295,336.75)^{7}$	$^{E}(0.763,352.20)^{12}$ $^{E}(0.736,351.35)^{7}$ $^{E}(0.786,352.20)^{55}$	$^{E}Z^{12}$ $^{E}Z^{55}$	$^{E}Z^{12}$ $^{E}Z^{55}$	$^{E}Z^{50}$
$C_5H_{10}O_2$.	Ethyl propanoate	T_b^o = 372.20 K	$^{E}Z^{14}$	$^{E}Z^{47}$ $^{D}Z^{7}$	$^{E}(0.481,366.61)^{14}$ $^{E}(0.465,366.15)^{7}$	$^{E}Z^{47}$	$^{E}Z^{14}$	$^{E}Z^{42}$
	Propyl ethanoate	T_b^o = 374.69 K	$^{E}Z^{41}$	$^{E}Z^{41}$ $^{D}Z^{7}$	$^{E}(0.423,366.99)^{41}$ $^{D}(0.421,366.75)^{29}$ $^{E}(0.423,366.90)^{48}$	$^{E}(0.973,374.31)^{41}$ $^{D}Z^{7}$	$^{E}Z^{41}$ $^{E}Z^{48}$	$^{E}Z^{41}$
	Methyl butanoate	T_b^o = 375.90 K	$^{E}Z^{42}$	$^{E}Z^{47}$	$^{E}(0.404,367.65)^{49}$ $^{D}(0.346,368.25)^{7}$ $^{E}(0.398,368.22)^{45}$	$^{E}(0.974,375.59)^{47}$ $^{D}Z^{7}$	$^{E}Z^{49}$	$^{E}Z^{42}$
	Butyl methanoate	T_b^o = 379.30 K	$^{E}Z^{39}$	$^{E}Z^{43}$	$^{E}(0.297,368.80)^{12}$ $^{D}(0.346,367.15)^{7}$	$^{E}(0.872,379.10)^{12}$	$^{E}Z^{12}$	$^{E}Z^{50}$
$C_6H_{12}O_2$	Ethyl butanoate	T_b^o = 394.60 K	$^{E}Z^{42}$	$^{E}Z^{47,54}$	$^{E}Z^{7,49}$	$^{E}(0.637,392.06)^{47}$ $^{D}(0.646,391.65)^{7}$	$^{E}Z^{49}$	$^{E}Z^{42}$

			C_5H_{12}	C_6H_{14}	C_7H_{16}	C_8H_{18}	C_9H_{20}	$C_{10}H_{22}$
			Pentane	**Hexane**	**Heptane**	**Octane**	**Nonane**	**Decane**
			T_b^o = **309.30 K**	T_b^o = **341.88 K**	T_b^o = **371.60 K**	T_b^o = **398.82 K**	T_b^o = **423.97 K**	T_b^o = **447.30 K**
	Propyl propanoate	T_b^o = 395.60 K	$^{E}Z^{42}$	$^{E}Z^{42}$	$^{E}Z^{42}$ $^{E}Z^{48}$	$^{E}(0.581,392.88)^{42}$ $^{D}(0.586,391.95)$ [7]	$^{E}Z^{42,48}$	$^{E}Z^{42}$
	Butyl ethanoate	T_b^o = 399.20 K	$^{E}Z^{20}$	$^{E}Z^{20,44}$	$^{E}Z^{20}$	$^{E}(0.553,394.00)^{20}$ $^{D}(0.486,393.65)$ [7]	$^{E}Z^{20}$	$^{E}Z^{20}$
$C_7H_{14}O_2$	Propyl butanoate	T_b^o = 416.20 K	$^{E}Z^{42}$	$^{E}Z^{42}$	$^{E}Z^{48,42}$	$^{E}Z^{42}$	$^{E}(0.713,415.16)^{42}$ $^{E}(0.726,414.40)^{48}$	$^{E}Z^{42}$
	Butyl propanoate	T_b^o = 419.65 K	$^{E}Z^{42}$	$^{E}Z^{42}$	$^{E}Z^{42}$	$^{E}Z^{42}$	$^{E}(0.628,417.12)^{42}$	$^{E}Z^{42}$
$C_8H_{16}O_2$	Butyl butanoate	T_b^o = 438.61 K	$^{E}Z^{42}$	$^{E}Z^{42}$	$^{E}Z^{42}$	$^{E}Z^{42}$	$^{E}Z^{42}$	$^{E}(0.790,438.29)^{42}$

Table 2. Experimental azeotropic coordinates of binary solutions of (an ester + an alkane) at p = 101.32 kPa, (x_{aze},T_{aze}/K). Type of technique: E = ebulliometry, D = Distillation, Z = zeotropic system.

than one. This is demonstrated in previous studies [12, 14, 17], together with the presence of minimum boiling point azeotropic points for these solutions; we begin with systems at standard pressure. **Table 2** gives the azeotropic coordinates at p = 101.32 kPa available in the literature for alkyl (methyl to butyl) alkanoate (methanoate to butanoate) + alkane (pentane to decane). The esters are arranged according to molecular weight, grouping together the different isomers with similar vapor pressures. Five systems (ethyl methanoate + pentane, methyl methanoate + hexane or heptane, and propyl ethanoate or methyl butanoate + octane) present different results depending of the consulted reference: most of the studies do not report azeotropy but others do.

In most cases, isomeric esters with the same molecular formula have azeotropes with the same alkanes, although this rule is not obeyed by the propyl ethanoate + octane system. An increase in the number of carbons in the ester produces an increase in the appearance of azeotropic points with a lower number of alkanes, resulting from a reduction in the activity coefficients and decreased net effects of the interactions. In esters of greater molecular weight, azeotropes are formed with hydrocarbons of similar vapor pressure as the esters, but with different boiling points for the last esters in the series. For example, propyl butanoate forms azeotropes with nonane, δT_b^o<8 K, but no with octane, δT_b^o<17 K, or with decane, δT_b^o<31 K. In a more extreme case, methyl methanoate forms an azeotrope with hexane, where δT_b^o>37 K. The same phenomenon is described if a hydrocarbon is taken as a reference and the ester is changed. This means that the temperature differences that produce the azeotropy tend to decrease as described in **Figure 7**. The azeotropes arise in solutions of compounds with similar boiling

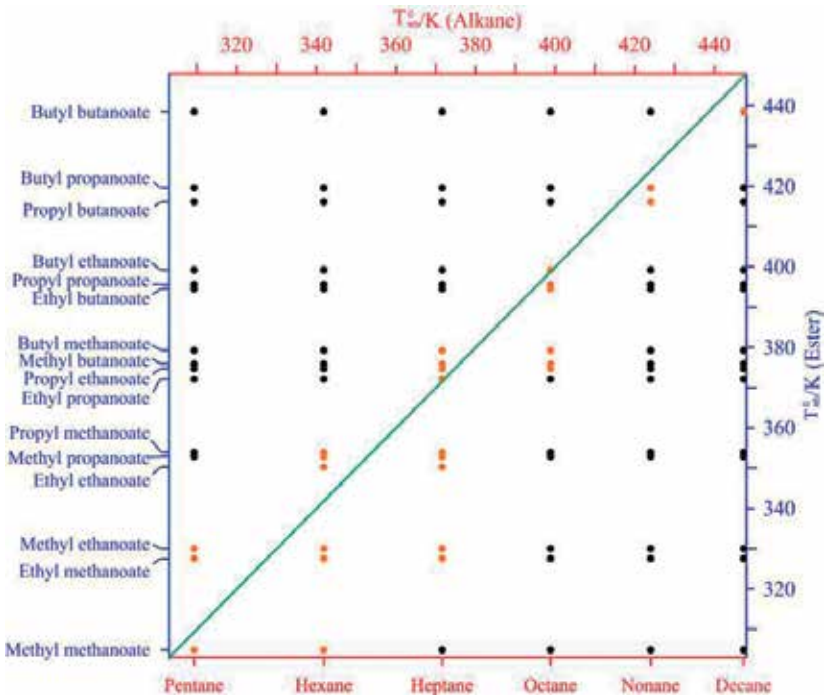

Figure 7. Azeotropes-diagram for ester + alkane mixtures: (●) zeotropic and (●) azeotropic.

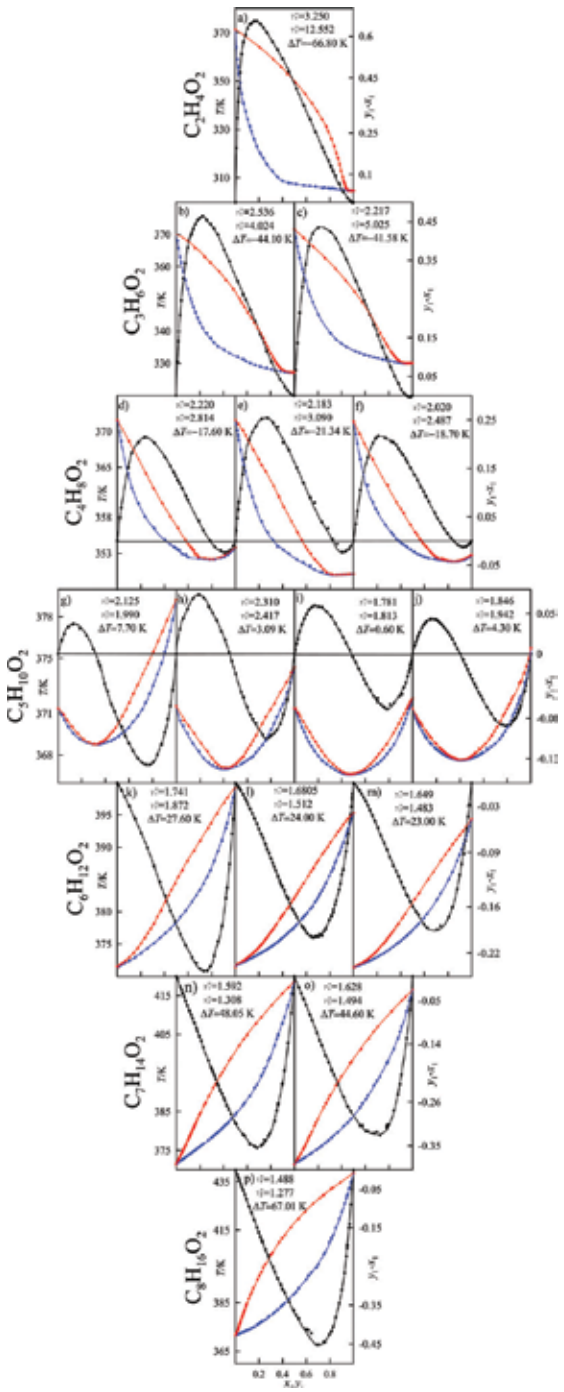

Figure 8. Representation of the VLE of alkyl alkanoate + heptane at 101.32 kPa. Labels indicate the differences of boiling points and the activity coefficients at infinity dilution. (●) *T vs. x*, (●) *T vs. y*, (●) *y-x vs. x*. (a) methyl methanoate, (b) ethyl methanoate, (c) methyl ethanoate, (d) Propyl methanoate, (e) ethyl ethanoate, (f) methyl propanoate, (g) butyl methanoate, (h) propyl ethanoate, (i) ethyl propanoate, (j) methyl butanoate, (k) butyl ethanoate, (l) propyl propanoate, (m) ethyl butanoate, (n) butyl propanoate, (o) propyl butanoate and (p) butyl butanoate.

points arranged near to the diagonal, from the bottom left corner (methyl methanoate + pentane) to the top right (butyl butanoate + decane).

The distance from the azeotropic points to the diagonal becomes shorter as the boiling points of the products increase, and it is deduced that the probability that an ester forms an azeotrope with a given alkane varies with the molecular weight of that ester, although this is reflected in the VLE diagram of the system. **Figure 8** shows the VLE curves of the solutions composed of the different esters and heptane. The difference between the liquid and vapor curves, which shows the volatility, is greater in systems with a smaller ester. This difference only significantly decreases with an increase in the molecular weight of the ester, but does not significantly change with the isomers. This is a result of a decrease in the non-ideality of the liquid phase ($\gamma \approx 1$) in solutions of the larger esters. This change makes it possible to find azeotropes in esters with four carbons, but not in esters with six carbons, in spite of similar differences between the boiling point of the esters and heptane. In ester solutions with five carbons, important differences are observed between isomers, and the azeotrope is found in the equimolar composition in the ethyl propanoate + heptane solution, and in the other cases slightly displaced toward greater alkane compositions. In other words, when the vapor pressures of the compounds are very similar, slight differences in the activity of compounds (e.g., those derived from small steric effects caused by isomerism), have significant repercussions on the equilibrium diagrams. For example, the non-ideality of the solution produces a flat region in the diagram of the solution with methyl methanoate. This does not appear in the mixture with butyl butanoate, which has a practically ideal nature.

Taking all this into consideration, it is important to study the behavior of the azeotropic phenomenon within the families of esters. **Figures 9** and **10** show the matrix with diagrams of *y vs. x* for solutions of (an alkyl ethanoate + an alkane) and (an methyl alkanoate + an alkane), respectively. In both cases, the presence of azeotropic situations can be observed to shift from the mixtures of more volatile compounds to the less volatile ones, with the last azeotrope appearing in the solution of butyl ethanoate + octane in **Figure 9**, and in the solution of methyl butanoate + heptane in **Figure 10**. The increased chain length of the alkyl ester, **Figure 9**, systematically displaces the azeotrope to regions with a smaller ester

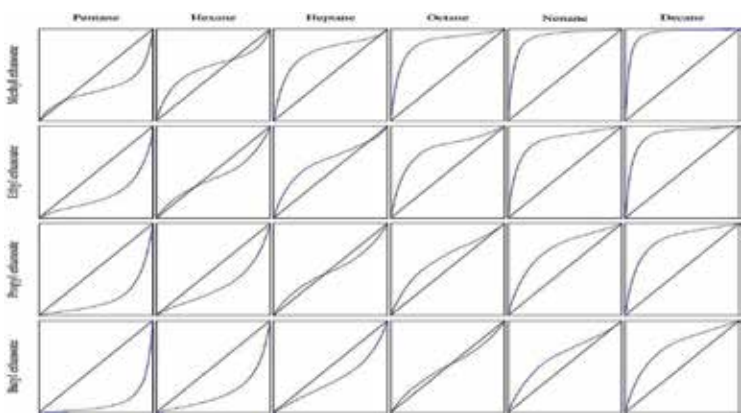

Figure 9. Plot of *y vs. x* (—), for the VLE at 101.32 kPa of binaries (an alkyl ethanoate + an alkane).

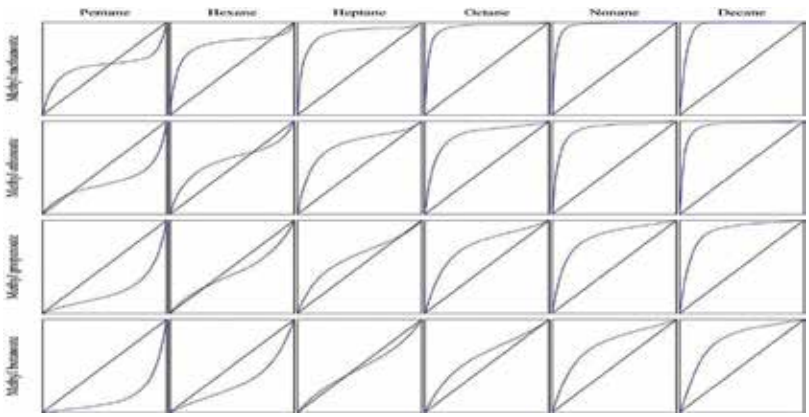

Figure 10. Plot of y *vs.* x (—), for the VLE at 101.32 kPa of binaries (methyl alkanoates + alkanes).

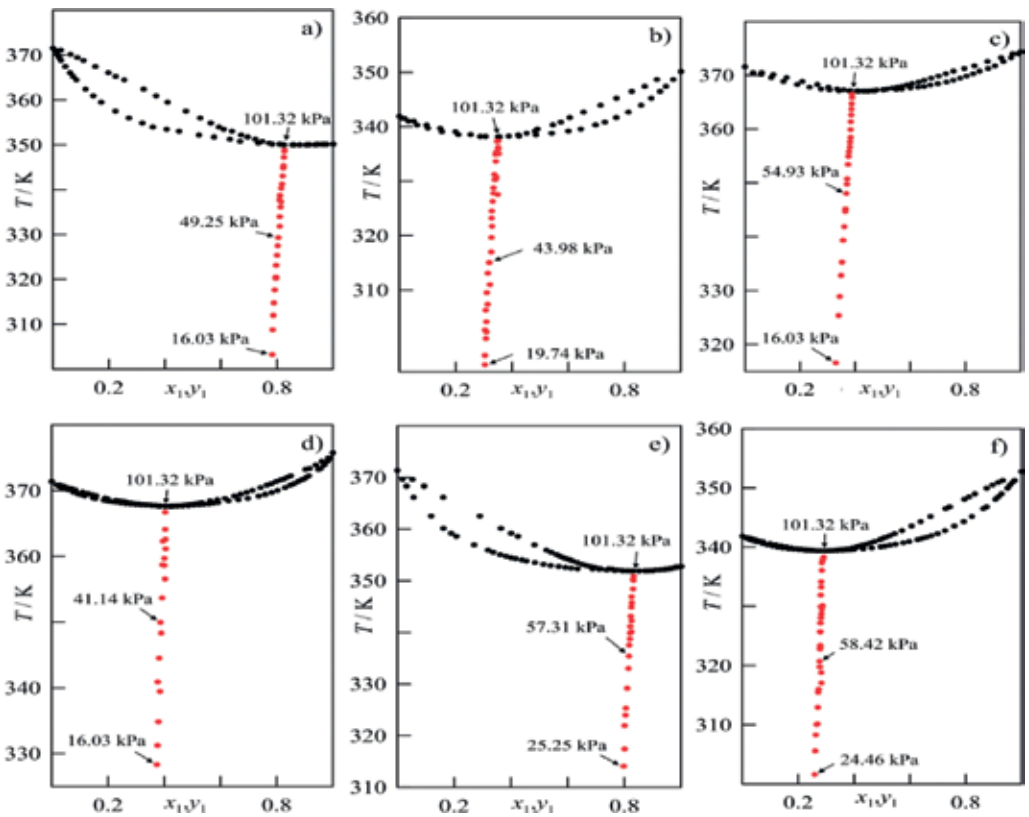

Figure 11. Sensitivity of the azeotropic coordinates to pressure in ester + alkane solutions. (a) Ethyl ethanoate + heptane, (b) ethyl ethanoate + hexane, (c) propyl ethanoate + heptane, (d) methyl butanoate + heptane, (e) methyl propanoate + heptane, (f) methyl propanoate + hexane.

composition. This effect can also be observed with increased alkanoic chain length of the ester, **Figure 10**. By contrast, increases in the size of the alkane cause a shift toward a higher ester composition in both cases.

3.3.2. Changes in azeotropes with pressure

The pressure of the system is a determining factor in the azeotropes formation, so it is important to determine how this magnitude affects the presence of azeotropic points. **Figure 11** shows the case of several azeotropic points determined by distillation for a set of ester + alkane systems, following indications described previously. In all cases, the composition of the azeotrope shifts toward greater alkane compositions as the pressure is reduced. The main reason for this is that the vapor pressure of the ester diminishes more slowly than that of the alkane, which increases the volatility of the hydrocarbon. The slope corresponding to the change in azeotropic composition is similar since the slope of the vapor pressure does not vary greatly between compounds from the same family. In spite of this, the methyl butanoate + heptane system, **Figure 11(d)**, presents a gentler slope, since the differences in vapor pressure between both compounds do not change significantly with temperature.

4. Modeling of azeotropic systems. Correlation and prediction

4.1. Correlation of vapor-liquid equilibria according to the gamma-phi approximation

The modeling of systems presenting azeotropes is not different from that used for any other system in vapor-liquid equilibrium. In order to do this, the following models must be defined:

1. One for the vapor pressure, $p_{\mathrm{i}}^{\mathrm{o}} = p_{\mathrm{i}}^{\mathrm{o}}(T)$.
2. One for *phi* $\Phi_{\mathrm{i}} = \Phi_{\mathrm{i}}(\mathbf{y}, p, T)$.
3. A model for the activity coefficients: $\gamma_{\mathrm{i}} = \gamma_{\mathrm{i}}(\mathbf{x}, p, T)$.

The relationship between vapor pressures and temperature is established by Clapeyron's equation [23], although it is standard practice to use other empirical equations such as those of Wagner or Antoine [25]. The parameter Φ_{i}, defined in Eq. (2), depends on the fugacity coefficient of compound i as saturated vapor phase and in solution. For the calculation, state equations can be used that may be different depending on if they are applied to the liquid or vapor phase.

The activity coefficients are inherent to the formation of the solution and are related to the interactions occurring therein. The phenomenological description of the fluid material is still not precise, although there are some models for which the formulation takes into account the molecular interactions that generate the macroscopic properties. In practice, depending on the theory of the model chosen, some experimental data are required for their accurate representation. For the *gamma-phi* method, models are written for the function of Gibbs excess energy as $g^{\mathrm{E}} = \mathrm{g}^{\mathrm{E}}(\mathrm{x}, p, T)$, and the dependence on γ_{i} is related to its partial molar properties [23]:

$$\gamma_i = \exp\left\{ \left[g^E + \left(\frac{\partial g^E}{\partial x_i} \right)_{p,T,x_{j\neq i}} - \sum x_k \left(\frac{\partial g^E}{\partial x_k} \right)_{p,T,x_{j\neq k}} \right] \Big/ RT \right\} \tag{13}$$

The model most used to date is NRTL [57]:

$$g^E = RT \sum_i x_i \frac{\sum_j \tau_{ji} G_{ji} x_j}{\sum_k G_{ki} x_k} \quad \text{where} \quad G_{ji} = \exp\left(-\alpha_{ji}\tau_{ji}\right) \quad \text{and} \quad \tau_{ji} = f(\mathbf{x}, T) \tag{14}$$

Our research group has used a polynomial model [14–17], with the general expression:

$$g^E_{n,N} = \sum_{i_1 i_2 \ldots i_{n-1} \in C(n,n-1)} g^{E(i_1 - i_2 - i_3 \ldots - i_{n-1})}_{n-1,N} + Z_n \cdot P_N \tag{15}$$

Where n is the number of components present, N the maximum interaction order, $g^{E(i_1-i_2-i_3\ldots-i_{n-1})}_{n-1,N}$ the excess Gibbs function of all the subsystems of inferior order that are present in the system and the product $Z_n \cdot P_N$ is a polynomial made up of multiple products of $(z_1 z_2 \ldots z_n)$ and a polynomial in z_i:

$$Z_n = z_1 z_2 \ldots\ldots z_n = T_n = \frac{\prod_{i=2}^{n} k^{ij} \prod_{i=1}^{n} x_i}{\left[x_1 + \sum_{j=2}^{n} k^{ij} x_j \right]^n}, \quad P_N = \sum_{j=0}^{N} P_j z_n^j \tag{16}$$

For a binary or ternary solution, the model (Eq. (15)) can be written, respectively, as:

$$g^{E(i\text{-}j)} = z_i z_j \sum_{k=0}^{N-2} g_k^{(i-j)} z_i^k \tag{17}$$

$$g^E_{3,4} = g^{E(1\text{-}2)}_{2,4} + g^{E(1\text{-}3)}_{2,4} + g^{E(2\text{-}3)}_{2,4} + z_1 z_2 z_3 (C_0 + C_1 z_1 + C_2 z_2) \tag{18}$$

with the possibility of extending this rule to any number of components. This model has been used to represent the behavior of many binary and ternary systems and has provided excellent results when used in combined correlation procedures of all the properties. This combined modeling method, adapted to suit to each case, was applied to binaries composed of esters and alkanes [10–17, 39–56]. The two following models: NRTL [57] and the Eq. (17) were used. Several of the systems modeled present azeotropy, so the results obtained are described briefly below. In many cases, the two models reproduce the VLE diagram with similar errors. An example is that shown in **Figure 12(a)** for the solution methyl methanoate + pentane, with iso-101.32 VLE data [39]. Slight differences can be observed in the azeotropic coordinates (T_{az}/K; x_{az}) calculated by each model [the proposed model (17) estimates the coordinates to be (293.8; 0.54), while the NRTL model gives (293.7; 0.57)]. However, Eq. (17) is better at predicting the remaining properties and, therefore, guarantees a better global capacity of representation (see details in [39, 41]). Occasionally, the NRTL model does not adequately represent the VLE behavior of azeotropic systems, especially when the parameters are obtained in a combined correlation process as

http://dx.doi.org/10.5772/intechopen.75786

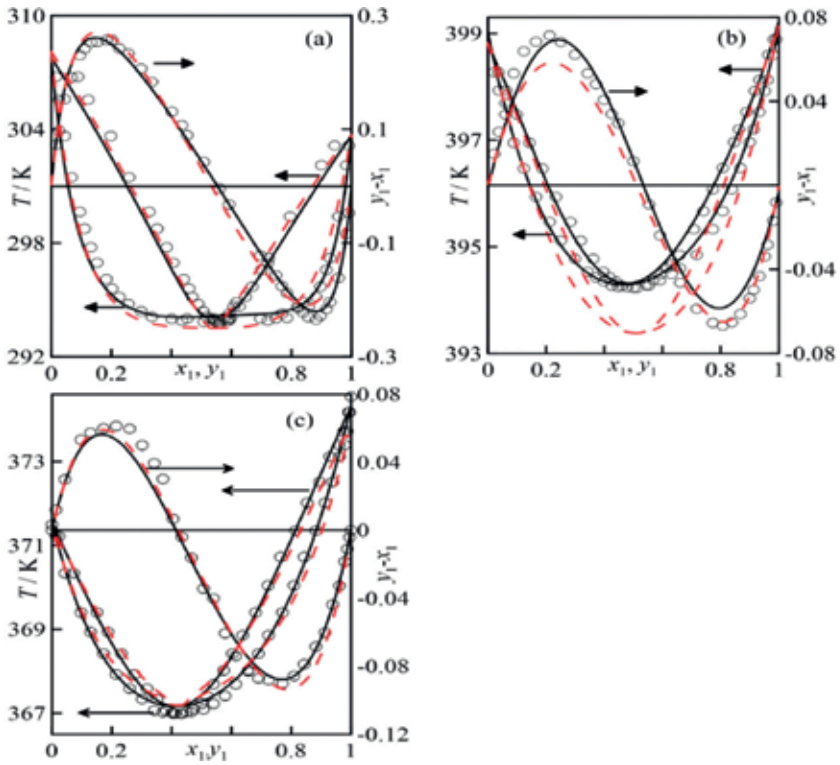

Figure 12. Modeling examples of azeotropic systems using correlative models for: (a) methyl methanoate(1) + pentane(2), (b) butyl ethanoate(1) + octane (2), (c) propyl ethanoate(1) + heptane(2). (——) Eq. (17), (– – –) NRTL, Eq. (14).

recommended here (see [58, 59]). For example the solution butyl ethanoate + octane [20], and reproduced in **Figure 12(b)**, for which NRTL estimates T_{az} = 393.4 K, while model (17) gives T_{az} = 394.1 K, close to the experimental value of $T_{az,exp}$ = 394.0 K.

In some cases, a considerable amount of data is modeled together. When these extend over a broad range of pressures and temperatures the ability of both models to accurately reproduce the azeotropic coordinates, or any other property, diminishes. In other words, the resolution capacity in the calculation of coordinates, at a given p, becomes smaller as the range of estimation increases. This case was studied [60] for the solution propyl ethanoate + heptane, where VLE data were available for temperatures between 273 and 373 K. Estimations for the two models, for iso-101.32 kPa VLE, are shown in **Figure 12(c)**, which shows that the azeotropic temperature calculated for the two models (367.17 K with our model and 367.19 K with NRTL) is slightly higher than the experimental value (367.0 K). These results are considered here to be positive. In conclusion, from observations made from the modeling described in numerous articles [10–17, 39–41], the model (17) appears to be recommendable to correlate VLE data and hence, to estimate azeotropic conditions. Either model can be used for the individual correlation of VLE data, although the modeling obtained should not be used to extrapolate azeotropic coordinates to conditions different from the experimental conditions.

4.2. The prediction of azeotropes by activity coefficients. Application to ester + alkane solutions

When experimental VLE data are not available, azeotropic points are estimated using predictive procedures. In the field of chemical engineering, the UNIFAC model by Gmehling et al. [61] (referenced as UNIFAC-DM), mainly designed for phase equilibria and some derived properties, is well known. Nonetheless, advances in the molecular sciences have helped to understand the intrinsic behavior of fluids in greater depth, with more solid phenomenological bases. This is the case of the quantum chemistry-based COSMO-RS model [62], which is able to estimate a significant number of properties of solutions. This chapter compares the results obtained after applying the two models to ester-alkane binaries, enabling us to establish certain criteria for their use.

Figure 13 represents the relative errors obtained with each of models in the estimation of azeotropic points of ester-alkane systems. The plot is constructed with color gradient according to the magnitude of the error (white cells indicate non-azeotrope). The error measurement is evaluated as:

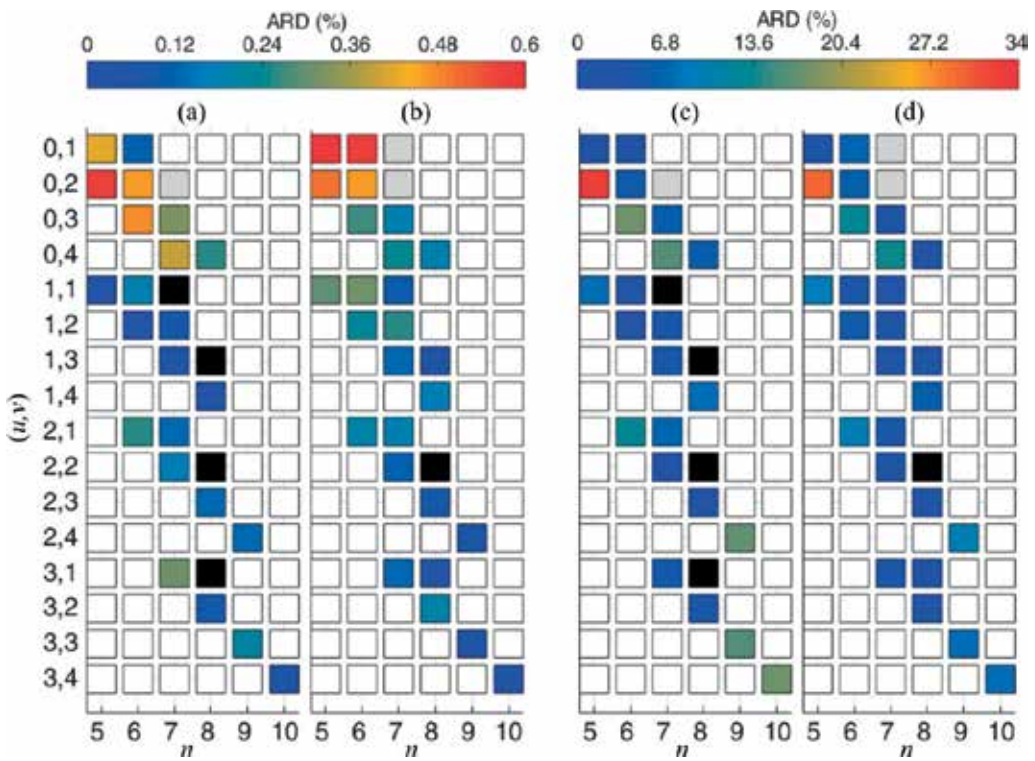

Figure 13. Matrices of estimated ARD for azeotropic coordinates of ester + alkane: $C_{u\text{-}1}H_{2u+1}COOC_vH_{2v+1} + C_nH_{2n+2}$. Errors in composition with UNIFAC-DM (a) and COSMO-RS (b); and in temperature using UNIFAC-DM (c) and COSMO-RS (d). ■ Model fails to estimate the azeotrope; ■ Model wrongly considers the system as azeotropic.

http://dx.doi.org/10.5772/intechopen.75786

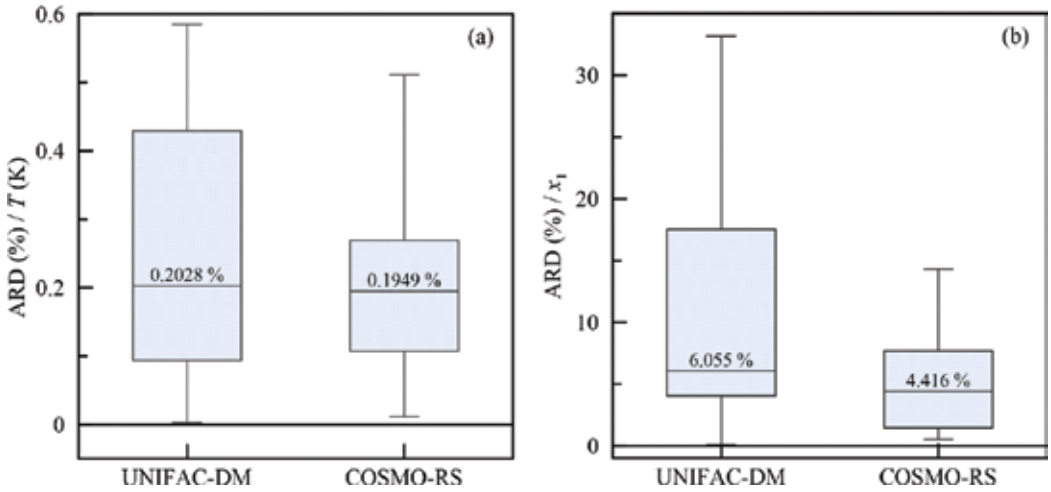

Figure 14. Plot of boxs and whiskers of ARD distribution on the estimation of temperature (a) and composition (b) of the azeotropes obtained with the models UNIFAC-DM and COSMO-RS.

$$ARD_f = \left| f_{\text{exp}} - f_{\text{est}} \right| \cdot 100 / f_{\text{exp}} \quad \text{where } f \equiv x_{\text{az}} \text{ or } T_{\text{az}}/\text{K} \tag{19}$$

colored according to the scale shown in **Figure 13**. In general, an acceptable description is observed for both models for the azeotropic systems studied, although both are less effective at estimating the composition, max(ARD_x) = 33%, than the equilibrium temperature of the azeotrope, max(ARD_T) = 0.6%. However, there are some differences in the qualitative description produced by both models. Hence, UNIFAC-DM does not estimate an azeotrope in the systems methyl ethanoate + heptane, propyl ethanoate + octane and methyl butanoate + octane, but considers the system ethyl methanoate + heptane to be azeotropic, which is regarded as zeotropic in the literature. With regards to the COSMO-RS model [61], all the systems described in the literature as azeotropic qualified to be so by the model, with the exception of methyl methanoate + heptane and ethyl methanoate + heptane, which are qualifies as azeotropic (see **Figure 13**) when experimentally they are not obtained at the pressure studied. In summary, estimation of the azeotropic coordinates is slightly more accurate when using the COSMO-RS model than the UNIFAC-DM model, as can be observed in the box-and-whiskers diagrams of **Figure 14**. Although both models give a similar mean error, the errors presented by estimations obtained with COSMO-RS have a significantly smaller interquartile range than those obtained with UNIFAC-DM; in other words, they have less dispersion. The same pattern can be observed in the estimation of compositions but with the additional factor that the mean error with the COSMO-RS model is also smaller.

In the preliminary design of separation equipment or *screening* procedures involving ester + alkane systems it is recommended to use COSMO-RS rather than UNIFAC-DM to predict the azeotrope. This is not because of the quantitative difference between the estimations, but because of the qualitative improvement obtained with the former model in several of the cases

studied here. Without ignoring these observations, if experimental data are available the model that best represents the real behavior of each system must be chosen in each case.

5. The use of advanced separation techniques in ester + alkane solutions

Advanced distillation techniques for the separation of azeotropic systems are described in detail in **Table 1**. This section shows some simulated cases of the use of these techniques for the treatment of azeotropic solutions of esters and alkanes. This was carried out using the commercial software Aspen Plus v.8.8 [63], using *RadFrac* blocks for distillation columns.

5.1. Separation of the binary propyl ethanoate + heptane by pressure-swing-distillation

A complete modeling using a multiobjective correlation procedure [60] to represent Gibbs excess function, g^E/RT, with the proposed model (17), was carried out for the binary propyl ethanoate + heptane in a previous work using extensive experimental data, with iso-*T* [64] and iso-*p* [4] VLE data as well as other properties (h^E, v^E, c_p^E [65]). The resulting model is dependent on the different intensive variables and can estimate VLE in different conditions of pressure and temperature to those used in the combined correlation process with a high degree of reliability. This work compares the degree of representation with those obtained by NRTL and UNIFAC-DM, although the authors' observations are not included here (they are not relevant to this chapter as both models are implemented in ASPEN). Hence, simulation of the separation of the binary is proposed by means of a distillation train with two towers, see diagram in **Figure 15**, operating at different pressure conditions; the first at atmospheric pressure (p = 101.32 kPa) and the second at high vacuum (p = 7 Pa).

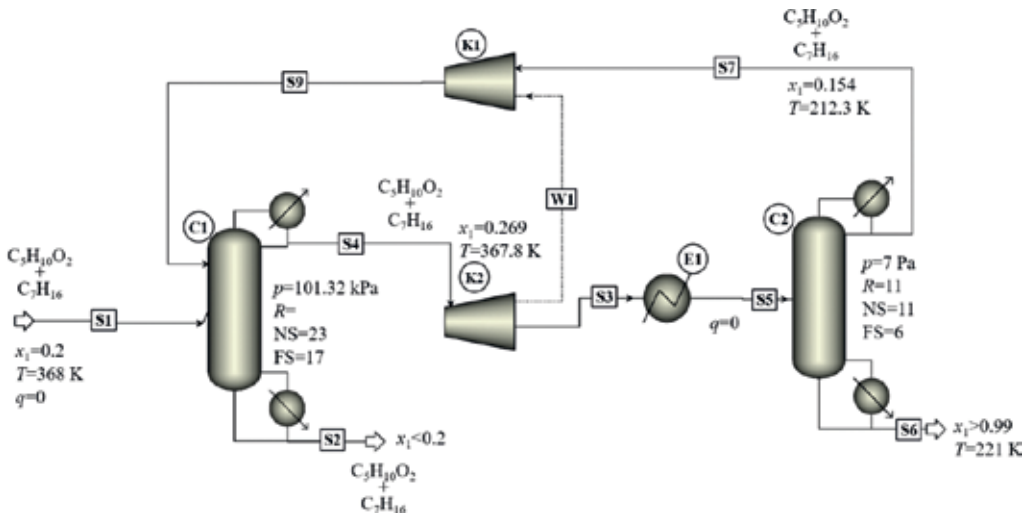

Figure 15. Simulation-scheme to separate the binary propyl ethanoate + heptane by a *pressure-swing distillation process.*

The pressure in the second column is extremely low, which is difficult to get in practice, but is established here to emphasize the characteristics of *pressure-swing-distillation* operation. As can be observed in **Figure 16**, the difference in pressure between the columns significantly displaces the coordinates of the azeotropic point, as estimated by Eq. (17). So, in the first column there is a partial separation of the solution, with the alkane, of high purity, collected in the bottom. The composition obtained in the head of the atmospheric column that feeds the second tower, **Figure 15**, was established between the azeotropic composition at each pressure, in order to optimize the number of stages.

The influence of the model used on the design was studied [21], and the most significant discrepancy that arises when changing the model occurs in the composition and temperature profiles in the inside of the column as shown in **Figure 17**, where important differences can be found. Use of the proposed model can therefore, guarantee reproduction of the real behavior of the apparatus.

5.2. Separation of the binary ethyl butanoate + octane by extractive distillation

In the previous case, it was proposed to reduce the pressure in order to separate the azeotropic solution. Alternatively, an extractant (*entrainer*) can be used to displace or destroy the azeotrope. This can be illustrated by separating the azeotropic solution ethyl butanoate(1) + octane(2) ($x_{1,az}$ = 0.63, T_{az} = 392 K a p = 101 kPa). For the preliminary design of this type of process a suitable *entrainer* must be chosen. In the absence of experimental data, theoretical models are chosen to establish the feasibility of the process. As possible *entrainers* for the binary selected, two compounds were chosen from the same families (ester and alkane) but with some structural differences, with greater molecular weights and, therefore, higher boiling points: (1) decane (2) butyl

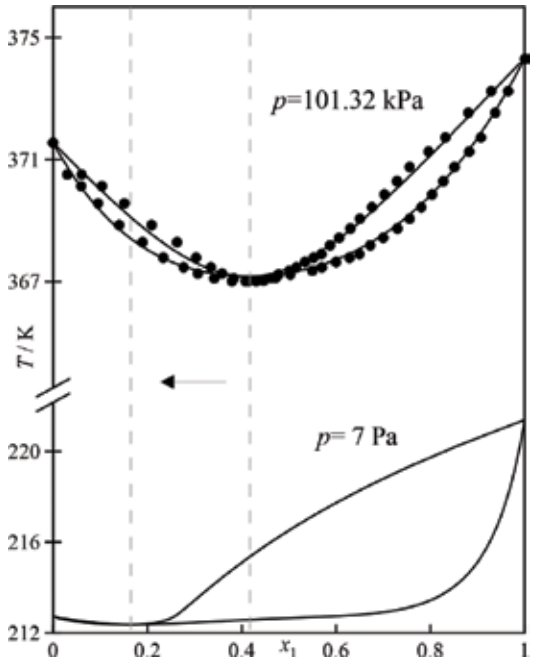

Figure 16. Representation of *T vs. x,y* of propyl ethanoate(1) + heptane(2). (●) Experimental values, (——), Eqs. (8–10).

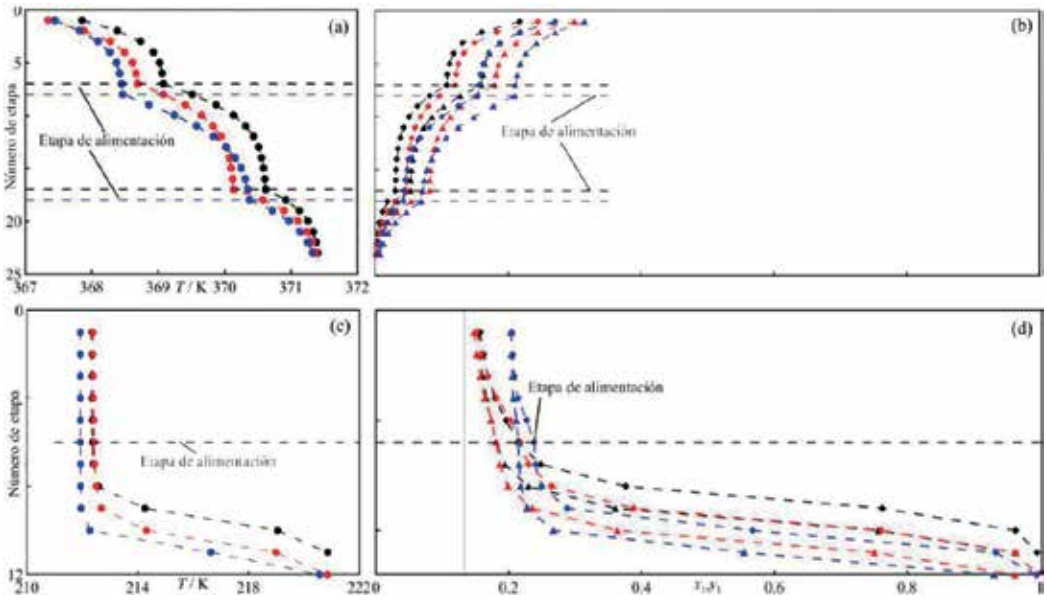

Figure 17. Profiles of temperature (a) and composition (b) for the first and second tower, obtained with Eqs. (17) (– – –), NRTL (– – –), and UNIFAC (– – –). (●)*T*/K, (▲) liquid phase composition, *x*; (¯) vapor phase composition, *y*.

butanoate. Taking into consideration the comments made in Section 3.2 of this chapter, the results obtained by UNIFAC-DM and COSMO-RS are compared being the representation of this azeotropic system more accurate with the former model. On the other hand, the ester + alkane binaries resulting from combining compounds of the mixture with potential solvents give rise to zeotropic systems of high relative volatility, with both models producing good estimations.

The final selection of one solvent or the other is based on the dynamics of the ternary system formed in the column, from analysis of the residual curves, **Figure 18**. The results obtained show that decane is the best option, since the residual curves rapidly veer toward the line $x_1 = 0$, facilitating the subsequent separation. Introduction of the solvent in the process and the

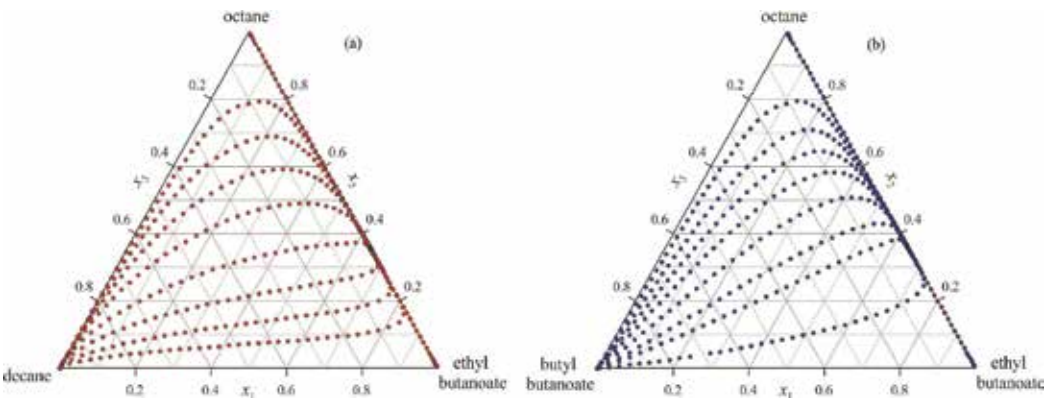

Figure 18. Residue curve map for best solvent selection for extractive distillation operation using different entrainers. (a) Decane, (b) butyl butanoate. Curves obtained with UNIFAC-DM.

http://dx.doi.org/10.5772/intechopen.75786

need to use two columns (separation and recovery) increases the number of design criteria. Therefore, six variables have been taken to configure the first column: number of steps, reflux ratio, solvent/feed ratio, feed stage, solvent stage, and temperature of the solvent. To obtain the best conditions for the planned operation a sensitivity analysis was carried out in relation to different variables, the results of which are summarized in **Figure 19**. The solvent-feed ratio is the design variable with the most impact on the compositions of ethyl butanoate in the head and octane in the bottom, together with the energy consumption of the process. The reflux ratio largely determines the decane contents in the head.

Maximization of the ethyl butanoate composition in the head and minimization of the composition of solvent (decane) in the head, together with maximization of octane in the bottoms and the energy consumption are the main goals that must be found in the design of the extractive distillation column. The final configuration generated by the simulator is shown in **Figure 20**.

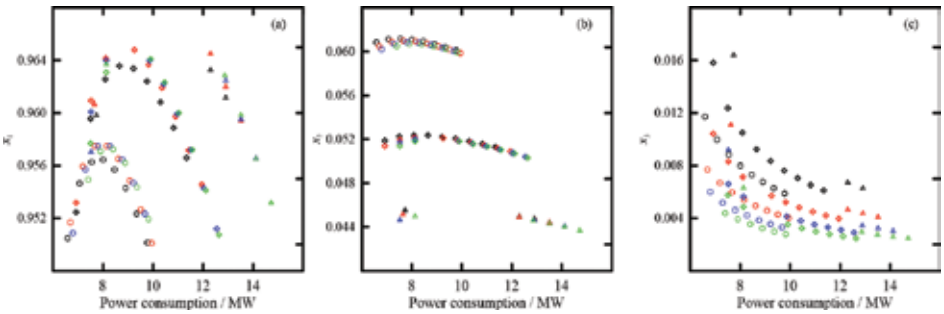

Figure 19. Sensitivity analysis curves for the following conditions: N = 30, F-S = 20 and S-Stage = 7. (o) S/F = 5; (%) S/F = 6; (1) S/F = 7. (—) R = 1; (—) R = 1.33; (—) R = 1.66; (—) R = 2. (a) Top composition of ethyl butanoate; (b) bottom composition of octane; and (c) top composition of decane.

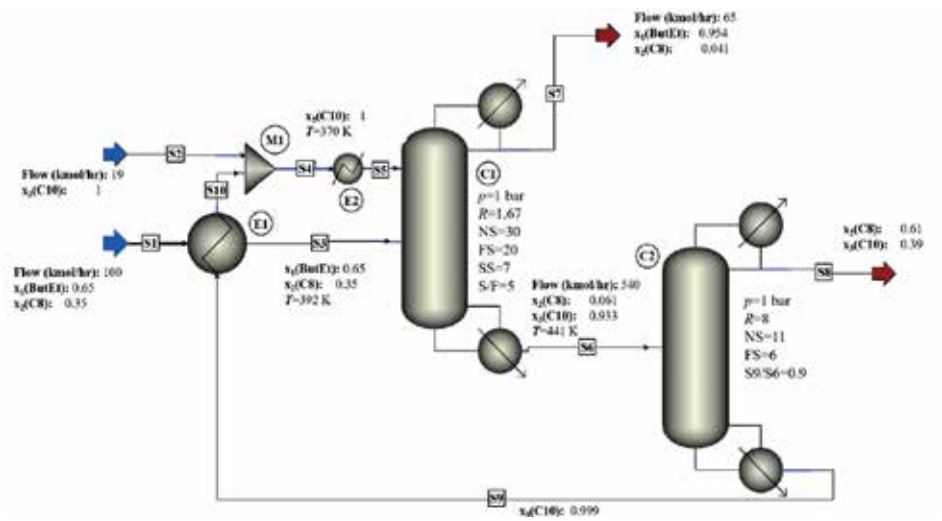

Figure 20. Simulation-scheme to separate the binary ethyl butanoate + octane by extractive distillation.

6. Conclusions

The different theoretical and practical settings related to azeotropy within the context of chemical engineering, have been described taking into account the experience of our research group in this area. The relationship between the presence of azeotropes, the non-ideality of the solution and the difference in vapor pressures of the pure compounds has been exposed. This information, together with some additional knowledge about the compounds involved in a solution, can be used to estimate the appearance of the azeotrope.

The combination of direct and indirect measuring techniques, together with suitable treatment of the results, is an excellent way to generate experimental data on which to base the studies. On the other hand, the polynomial equation proposed and used here would seem to be the best option to model the systems, provided that the parameters are optimized using all the experimental data available by means of a combined correlation procedure.

For the prediction of azeotropes, COSMO-RS method produces the best results, although in some cases the quantitative values produced by UNIFAC-DM approximate real values. Simulation of a process by *pressure-swing-distillation* and another by *extractive-distillation* allow verify the impact of the modeling and selection of the design parameters on the results of the separation operation.

Acknowledgements

This work was supported by MINECO from Spanish Government, Grant CTQ2015-68428-P. One of us (AS) is grateful to the ACIISI (from Canaries government, No. 2015010110) for the support received.

Nomenclature

ARD_f	relative deviations in absolute value ($\equiv \left\|f_{\exp} - f_{\text{est}}\right\| \cdot 100/f_{\exp}$)
B_{ii}, B_{ij}, $m^3\ mol^{-1}$	second Virial coefficient for pure component "i" and ij-pair for mixtures
C_n	ternary parameters for molar Gibbs excess model in Eq. (18)
FS	feed stage in distillation column
g^E, $J{\cdot}mol^{-1}$	excess molar Gibbs function
$g^E_{n,N}$	excess molar Gibbs function given by Eq. (15)
$g_k^{(i\text{-}j)}$	coefficients for molar Gibbs excess energy model in Eq. (17) for binary i-j
G_{ij}	interaction parameters of NRTL model

h^{E}, J·mol^{-1}	excess enthalpy
L	liquid phase
NS	number of stages in distillation column
p, kPa	pressure
p_i, kPa	partial pressure of i-th component
p_i^{o}, kPa	vapor pressure of pure component i
P_N / P_j	polynomial of order N / Coefficient of polynomial P_N
R or R	gas constant Pa·m^3 mol^{-1} / Reflux ratio in distillation column
SS	solvent feed stage in extractive distillation column
S/F	solvent-To-Feed ratio in extractive distillation column
T, K	system temperature
u	number of carbons in alkyl substituent of esters
v^{E}, m^3 mol^{-1}	molar excess volume
V	vapor phase
x_i	molar fraction of i-th component in the solution
y_i	generic thermodynamic quantity/vapor composition of i-th component
z_i	active fraction of i-th component
Z_n	product of active fractions up to nth-component
Sub/Supercripts	
est	denotes a property estimated by a model
exp	denotes an experimentally determined property
aze	relative to azeotropic conditions
Greek letters	
α_{ij}	non-randomness parameter of NRTL model
δ_{ij}	function of second Virial coefficients in the mixture ($\equiv 2B_{ij} - B_{ii} - B_{jj}$)
γ_i	activity coefficient of i-th component
Φ_i	ratio between fugacity coefficient of component "i" in solution and as saturated vapor
τ_{ij}	τ-function of NRTL model
v	number of carbons in alkanols

Author details

Raúl Rios, Adriel Sosa, Luis Fernández and Juan Ortega*

*Address all correspondence to: juan.ortega@ulpgc.es

Laboratorio de Termodinámica y Fisicoquímica de Fluidos (ITI-IDeTIC), Parque Científico-Tecnológico, Universidad de Las Palmas de Gran Canaria, Canary Islands, Spain

References

[1] Grayson M, Kirk RE, Othmer DF. Kirk-Othmer Encyclopedia of Chemical Technology. New York: Wiley; 1984. p. 22950. DOI: 10.1002/0471238961

[2] Ullmann F. Ullmann's Encyclopedia of Industrial Chemistry. 7th ed. Weinheim: Wiley-VCH. DOI: 10.1002/14356007

[3] Green DW, Perry RH. Perry's Chemical Engineers' Handbook. Vol. 1973. NY: McGraw-Hill; 1973. p. 2240

[4] Robinson CS. The Elements of Fractional Distillation. NY: McGraw-Hill; 1922. p. 216

[5] Malesiński W. Azeotropy and Other Theoretical Problems of Vapour-Liquid Equilibrium. New York: Interscience Publishers; 1965. p. 221

[6] Swietoslawski W. Azeotropy and Polyazeotropy. New York: Pergamon Press; 1963. p. 226

[7] Gmehling J, Menke J, Krafczyk J, Fischer K. Azeotropic Data, Part I and Part II. Weinheim: VCH-Publishers; 1994. p. 1992

[8] Horsley LH. Azeotropic Data I-III, ACS. Washington: ACS; 1973. DOI: 10.1021/ba-1973-0116

[9] Blanco AM, Ortega J. Densities and vapor-liquid equilibrium values for binary Mistures composed of methanol+an ethyl ester at 141.3 kPa with application of an extended correlation equation for isobaric VLE data. Journal of Chemical & Engineering Data. 1998;**43**: 638-645. DOI: 10.1021/je980012o

[10] Ortega J, Hernandez P. Thermodynamic study of binary mixtures containing an isobutylalkanol and an alkyl (ethyl to butyl) alkanoate (methanoate to butanoate), contributing with experimental values of excess molar enthalpies and volumes, and isobaric vapor-liquid equlibria. Journal of Chemical & Engineering Data. 1999;**44**:757-771. DOI: 10.1021/je990004n

[11] Ortega J, Espiau F, Postigo M. Vapor-liquid equilibria at 101.32 kPa and excess properties of binary mixtures of butyl esters+ tert-butyl alcohol. Journal of Chemical & Engineering Data. 2005;**50**:444-454. DOI: 10.1021/je0497350

[12] Ortega J, Fernández L, Sabater G. Solutions of alkyl methanoates and alkanes: Simultaneous modeling of phase equilibria and mixing properties. Estimation of behavior by UNIFAC with recalculation of parameters. Fluid Phase Equilibria. 2015;**402**:38-49. DOI: 10.1016/j.fluid.2015.05.031

[13] Ortega J, Peña J, de Afonso C. Isobaric vapor-liquid equilibria of ethyl acetate + ethanol mixtures at 760 ± 0.5 mmHg. Journal of Chemical & Engineering Data. 1986;**31**:339-342. DOI: 10.1021/je00045a023

[14] Rios R, Ortega J, Fernandez L, de la Nuez I, Wisniak J. Improvements in the experimentation and the representation of thermodynamic properties (iso-p VLE and y^E) of alkyl propanoate+alkane binaries. Journal of Chemical & Engineering Data. 2014;**59**:125-142. DOI: 10.1021/je4009415

[15] Ortega J, Espiau F. A new correlation method for vapor-liquid equilibria and excess enthalpies for nonideal solutions using a genetic algorithm. Application to ethanol+an n-alkane mixtures. Industrial and Engineering Chemistry Research. 2003;**42**(20):4978-4992. DOI: 10.1021/ie030327j

[16] Ortega J, Espiau F, Wisniak J. New parametric model to correlate the Gibbs excess function and other thermodynamic properties of multicomponent systems. Application to binary systems. Industrial and Engineering Chemistry Research. 2010;**49**:406-421. DOI: 10.1021/ie900898t

[17] Fernández L, Pérez E, Ortega J, Canosa J, Wisniak J. Multiproperty modeling for a set of binary systems. Evaluation of a model to correlate simultaneously several mixing properties of methyl ethanoate+alkanes and new experimental data. Fluid Phase Equilibria. 2013; **341**:105-123. DOI: 10.1016/j.fluid.2012.12.027

[18] Wisniak J, Ortega J, Fernández L. A fresh look at the thermodynamic consistency of vapour-liquid equilibria data. The Journal of Chemical Thermodynamics. 2017;**105**:385-395. DOI: 10.1016/j.jct.2016.10.038

[19] Fernández L, Ortega J, Wisniak J. A rigorous method to evaluate the consistency of experimental data in phase equilibria. Application to VLE and VLLE. AIChE Journal. 2017;**63**:5125-5148. DOI: 10.1002/aic.15876

[20] Pérez E, Ortega J, Fernández L, Wisniak J, Canosa J. Contributions to the modeling and behavior of solutions containing ethanoates and hydrocarbons. New experimental data for binaries of butyl ester with alkanes (C_5 to C_{10}). Fluid Phase Equilibria. 2016;**412**:79-93. DOI: 10.1016/j.fluid.2015.12.013

[21] Sosa A, Fernández L, Ortega J, Pérez E. La modelización termodinámica en la simulación de un proceso de rectificación. Revista Academia Canaria Ciencias. 2016;**XXVIII**:7-31

[22] Wade J, Merriman RW. Influence of water on the boiling point of ethyl alcohol at pressures above and below the atmospheric pressure. Journal of the Chemical Society, Transactions. 1911;**99**:997-1011. DOI: 10.1039/ct9119900997

[23] Smith JM, Van Ness HC, Abbott MM. Introduction to Chemical Engineering Thermodynamics. 7th ed. New York: McGraw-Hill, Inc; 2004. p. 817

[24] Bancroft WD. The Phase Rule. New York; 1897

[25] Prausnitz JM, Lichtenthaler RN, de Azevedo EG. Molecular Thermodynamics of Fluid-Phase Equilibria. New York: Prentice Hall; 1998. p. 864

[26] Hála E, Pick J, Fried V, Vilím O. Vapor-Liquid Equilibrium. 2nd ed. Oxford: Pergamon Press; 1967. p. 599

[27] Raal JD, Gadodia V, Ramjugernath D, Jalari R. New developments in differential ebulliometry: Experimental and theoretical. Journal of Molecular Liquids. 2006;**125**:45-57. DOI: 10.1016/j.molliq.2005.11.015

[28] Chen GH, Wang Q, Zhang LZ, Bao JB, Han SJ. Study and applications of binary and ternary azeotropes. Thermochimica Acta. 1995;**253**:295-305. DOI: 10.1016/0040-6031(94)02078-3

[29] Gmehling J, Bölts R. Azeotropic data for binary and ternary systems at moderate pressures. Journal of Chemical & Engineering Data. 1996;**41**:202-209. DOI: 10.1021/je950228f

[30] Rogalski M, Malanowski S. Ebulliometers modified for the accurate determination of vapour-liquid equilibrium. Fluid Phase Equilibria. 1980;**5**:97-112. DOI: 10.1016/0378-3812(80)80046-x

[31] Wisniak J, Apelblat A, Segura H. An assessment of thermodynamic consistency tests for vapor-liquid equilibrium data. Physics and Chemistry of Liquids. 1980;**35**:1-58. DOI: 10.1080/00319109708030571

[32] Van Ness HC. Thermodynamics in the treatment of (vapor+liquid) equilibria. The Journal of Chemical Thermodynamics. 1995;**27**:113-134. DOI: 10.1006/jcht.1995.0011

[33] Redlich O, Kister AT. Thermodynamics of nonelectrolyte solutions-xyt relations in a binary system. Industrial and Engineering Chemistry. 1948;**40**:341-345. DOI: 10.1021/ie50458a035

[34] Fredenslund P, Gmehling J, Rasmussen P. Vapor-Liquid Equilibria Using UNIFAC: A Group-Contribution Method. Amsterdam/New York: Elsevier; 1977. p. 379

[35] Herington EFG. A method for testing thermodynamic consistency. Journal Institute of Petroleum. 1951;**37**:457-459

[36] Wisniak J. The Herington test for thermodynamic consistency. Industrial and Engineering Chemistry Research. 1994;**33**:177-180. DOI: 10.1021/ie00025a025

[37] Van Ness HC, Byer SM, Gibbs RE. Vapor-liquid equilibrium: Part I. An appraisal of data reduction methods. AICHE Journal. 1973;**19**:238-244. DOI:10.1002/aic.690190206

[38] Van Ness HC. Precise testing of binary vapour-liquid equilibrium data by the Gibbs-Duhem equation. Chemical Engineering Science. 1959;**11**:118-124. DOI:10.1016/0009-2509(59)80006-3

[39] Fernández L, Ortega J, Sabater G, Espiau F. Experimentation and thermodynamic representations of binaries containing compounds of low boiling points: Pentane and alkylmethanoates. Fluid Phase Equilibria. 2014;**363**:167-179. DOI: 10.1016/j.fluid.2013.11.026

[40] Fernández L, Perez E, Ortega J, Canosa J, Wisniak J. Measurements of the excess properties and vapor-liquid equilibria at 101.32 kpa for mixtures of ethyl ethanoate+alkanes (from C_5 to C_{10}). Journal of Chemical & Engineering Data. 2010;**55**:5519-5533. DOI: 10.1021/je100832h

[41] Fernández L, Ortega J, Pérez E, Toledo F, Canosa J. Multiproperty correlation of experimental data of the binaries propyl ethanoate+alkanes (pentane to decane). New experimental information for vapor liquid equilibrium and mixing properties. Journal of Chemical & Engineering Data. 2013;**58**:686-706. DOI: 10.1021/je3011979

[42] Unpublished data measured in our laboratory

[43] Ortega J, Sabater G, de la Nuez I, Quintana J. Isobaric vapor-liquid equilibrium data and excess properties of binary systems comprised of alkyl methanoates +hexane. Journal of Chemical & Engineering Data. 2007;**52**:215-225. DOI: 10.1021/je060355j

[44] Feng L-C, Chou C-H, Tang M, Chen Y-P. Vapor-liquid equilibria of binary mixtures 2-butanol+butyl acetate, hexane+butyl acetate, and cyclohexane+2-butanol at 101.3 kPa. Journal of Chemical & Engineering Data. 1998;**43**:658-661. DOI: 10.1021/je9800205

[45] Ortega J, Espiau F, Tojo J, Canosa J, Rodriguez A. Isobaric vapor-liquid equilibria and excess properties for the binary systems of methyl esters+heptane. Journal of Chemical & Engineering Data. 2003;**48**:1183-1190. DOI: 10.1021/je030117d

[46] Acosta J, Arce A, Martinez-Ageitos J, Rodil E, Soto A. Vapor-liquid equilibrium of the ternary system ethyl acetate+hexane+acetone at 101.32 kPa. Journal of Chemical & Engineering Data. 2002;**47**:849-854. DOI: 10.1021/je0102917

[47] Rios R, Ortega J, Fernández L, Sosa A. Strategy for the management of thermodynamic data with application to practical cases of systems formed by esters and alkanes through: Experimental information, checking-modeling and simulation. Industrial and Engineering Chemistry Research. 2018;**57**:3410-3429. DOI: 10.2021/acs.iecr.7b04918

[48] Ortega J, González C, Galván S. Vapor-liquid equilibria for binary systems composed of a propyl ester (ethanoate, propanoate, butanoate)+an alkane (C_7, C_9). Journal of Chemical & Engineering Data. 2001;**46**:904-912. DOI: 10.1021/je000358a

[49] Rios R, Ortega J, Fernández L. Measurements and correlations of the isobaric vapor-liquid equilibria of binary mixtures and excess properties for mixtures containing an alkyl (methyl, ethyl) butanoate with an alkane (heptane, nonane) at 101.3 kPa. Journal of Chemical & Engineering Data. 2012;**57**:3210-3224. DOI: 10.1021/je300799f

[50] Sabater G, Ortega J. Excess properties and isobaric vapor–liquid equilibria for four binary systems of alkyl (methyl to butyl) methanoates with decane. Fluid Phase Equilibria. 2010; **291**:18-31. DOI: 10.1016/j.fluid.2009.12.003

[51] Ortega J, Espiau F, Dieppa R. Measurement and correlation of isobaric vapour-liquid equilibrium data and excess properties of ethyl methanoate with alkanes (hexane to decane). Fluid Phase Equilibria. 2004;**215**:175-186. DOI: 10.1016/j.fluid.2003.08.003

[52] Gorbunova LV, Lutugina NV, Malenko YI. Relations between the boiling points and composition in binary systems formed by acetic acid, ethyl acetate, methyl ethyl ketone and hexane. Zhurnal Prikladnoi Khimii (Leningrad). 1965;**38**:374-377

[53] Marrufo B, Rigby B, Pla-Franco J, Loras S. Solvent effects on vapor liquid equilibria of the binary system 1-hexene+n-hexane. Journal of Chemical & Engineering Data. 2012;**57**: 3721-3729. DOI: 10.1021/je3009599

[54] Galvan S, Ortega J, Susial P, Peña JA. Isobaric vapor-liquid equilibria for propyl methanoate+n-alkanes (C_7, C_8, C_9) or n-alkanols (C_2, C_3, C_4). Journal of Chemical Engineering of Japan. 1994;**27**:529-534. DOI: 10.1252/jcej.27.529

[55] Chen Z, Hu W. Isobaric vapor-liquid equilibriums of octane-ethyl acetate and octane-isopropyl acetate systems. Chinese Journal of Chemical Engineering. 1995;**3**:180-186

[56] Ogorodnikov SK, Kogan VB, Nemtsov MS. Separation of C(5) hydrocarbons by azeotropic and extractive distillation: IV liquid-vapor equilibrium in systems of hydrocarbons and methyl formate. Zhurnal Prikladnoi Khimii (Leningrad). 1961;**34**:581-584

[57] Renon H, Prausnitz J. Local composition in thermodynamic excess function for liquid mixtures. AICHE Journal. 1968;**14**:135-142. DOI: 10.1002/aic.690140124

[58] Nocedal J, Wright SJ. Numerical Optimization. 2nd ed. Berlín: Springer; 2006. p. 664. DOI: 10.1007/978-0-387-40065-5

[59] Deb K. Multi-Objective Optimization Using Evolutionary Algorithms. New York: Wiley; 2001. p. 518

[60] Fernández L, Sosa A, Ortega J. Multiobjective correlation of properties of binary systems usingan evolutionary algorithm. Practical examples to analyze the impact of a trade-off decision on the simulation of rectification operations. Trends in Chemical Engineering. 2018, in press

[61] Gmehling J, Li J, Schiller M. A modified UNIFAC model. 2. Present parameter matrix and results for different thermodynamic properties. Industrial and Engineering Chemistry Research. 1993;**32**:178-183. DOI: 10.1021/ie00013a024

[62] Klamt A. Conductor-like screening model for real solvents: A new approach to the quantitative calculation of solvation phenomena. The Journal of Physical Chemistry. 1995;**99**: 2224-2235. DOI: 10.1021/j100007a062

[63] Aspen Technologies Inc. Aspen Physical Properties System. Cambridge: Aspen Technologies Inc; 2004

[64] Negadi L, Belabbaci A, Kaci AA, Jose J. Isothermal vapor-liquid equilibria and excess enthalpies of (propyl ethanoate+heptanes), (propyl ethanoate+cyclohexane) and (propyl ethanoate+1-hexene). Journal of Chemical & Engineering Data. 2007;**52**:47-55. DOI: 10.1021/je060184i

[65] Jimenez E, Romaní L, Wilhelm E, Roux-Desgranges G, Grolier J-PE. Excess heat capacities and excess volumes of (an n-alkyl alkanoate+heptane or decane or toluene). The Journal of Chemical Thermodynamics. 1994;**26**:817-827. DOI: 10.1006/jcht.1994.1098

Edited by Omar M. Basha and Badie I. Morsi

This book covers a wide variety of topics related to the application of experimental methods, in addition to the pedagogy of chemical engineering laboratory unit operations. The purpose of this book is to create a platform for the exchange of different experimental techniques, approaches and lessons, in addition to new ideas and strategies in teaching laboratory unit operations to undergraduate chemical engineering students. It is recommended for instructors and students of chemical engineering and natural sciences who are interested in reading about different experimental setups and techniques, covering a wide range of scales, which can be widely applied to many areas of chemical engineering interest.

Published in London, UK

IntechOpen

ISBN 978-1-83881-700-8